STUDIES IN FLOTATION RATE DISTRIBUTION OF PARTICULATE SPECIES AND OPTIMAL DESIGN OF FLOTATION CIRCUITS

A Thesis Submitted
In Partial Fulfilment of the Requirements
for the Degree of
DOCTOR OF PHILOSOPHY

By

SURYA PRATAP MEHROTRA

to the

DEPARTMENT OF METALLURGICAL ENGINEERING

INDIAN INSTITUTE OF TECHNOLOGY KANPUR

SEPTEMBER, 1973

CERTIFICATE

Certified that this work on " Studies in Flotation Rate Distribution of Particulate Species and Optimal Design of Flotation Circuits", has been carried out under my supervision and that it has not been submitted elsewhere for a degree.

(P. C. Kapur)
Associate Professor
Department of Metallurgical Engineering
Indian Institute of Technology,
Kanpur-208016

ACKNOWLEDGEMENTS

The author is highly indebted to Professor P.C. Kapur under whom this work destined to successful completion. His lively interest, inspiring guidance and illuminating discussions have gone a long way in shaping this dissertation in its present form.

The author would like to thank his friends Messers N.B. Ballal, Nirbhay Singh, K.N. Rao and S. Mazumdar for their cooperation in various ways.

Finally he would also thank Mr. J.K. Misra for elegant typing and Mr. A.K. Bhargava for excellent drawings.

TABLE OF CONTENTS

LIST OF TABLES

LIST OF FIGURES

LIST OF SYMBOLS

a	diameter of an air bubble
$A(a)$	function of bubble size a and the hydrodynamic conditions in the pulp
b_n	unknown parameters in equation (A-2)
B	proportionality constant
c_j	constant in empirical expression relating $\bar{t}$ to L
C	concentration of solid particulate species in pulp
C_i	concentration of i-th species in pulp
C_∞	terminal concentration
d_j	algebraic sum of successful steps in direction j
d_p	predefined limiting value of pulp density
$D(K,L)$	detachment rate constant of particles $[K,L]$
Dp	pulp density in a cell
D_s	density of solid
e_j	step-size for variable X_j
$E(t)$	residence time distribution of particles
E	objective function defined in equation (5.21)
E_j	functional value at j-th vertex in complex method of optimization
E_{max}	maximum functional value in complex method
E_{min}	minimum functional value in complex method
E_{new}	functional value at new trial point in random search technique
E_{old}	functional value at initial base point in random search technique

ΔE_j	defined in equation (B-15)
$\bar{E}$	objective function defined in equation (5.34
E'	objective function defined in equation (7.10)
$f(x_i,t)$	function of x_i and t defined in equation (A-3)
$F(x_i)$	defined in equation (5.15)
F_j	j-th number in the series of Fibonacci numbers
F_{ji}	total feed rate of j-th species in i-th cell
$F_u(x_i)$	unknown function of x_i in equation (A-3)
$F'(x)$	defined in equation (5.36)
$F''(x)$	defined in equation (7.8)
$\bar{F}(x)$	defined in equation (5.14)
g	predefined limiting value of grade of concentrate
G	grade of concentrate
G_F	grade of feed ore
$G_s(L,t)$	cumulative grade of solid species of size L in pulp at time t
$\bar{G}$	grade of a particle
H	hold-up of air in cell
H_i	defined in equation (8.19)
$\bar{H}(Ka)$	defined in equation (4.42)
I_1	prescribed numbers of successive unsuccessful trials in random search
I_2	prescribed maximum number of successful trials with same ΔX_i
I_3	total number of trials in random search

k	number of vertices in complex method of optimization
k'	specific flotation rate constant defined in equation (2.3)
K	specific attachment rate constant
$\bar{K}$	function of degree of hydration defined in equation (2.27)
K^o	defined in equation (6.12)
Ka	Overall specific flotation rate constant
Ka_j	Overall specific flotation rate constant for j-th species
l_j	defined in equation (B-6)
L	diameter of the particle
L_1	diameter of the smallest particle in the pulp
L_2	diameter of the largest particle in the pulp
L_{max}	diameter of the largest particle which will remain attached to a bubble
$\bar{L}_j$	interval of search at j-th stage of computation in Fibonacci search technique
$m(a,t,\tau)$	mass of particles attached on the bubble of specification $[a,t,\tau]$
$m(K,L,a,t,\tau)$	mass of particles $[K,L]$ on the bubble of specification $[a,t,\tau]$
m'	some positive number defined in equation (B-14)
$\bar{m}(a)$	time invariant potential bubble capacity
$\bar{m}(a,t,\tau)$	instantaneous potential bubble capacity
$M_1(S,L,\bar{G})$	mass of particles with attributes $[S,L,\bar{G}]$
$M_2(K,L,\bar{G})$	mass of particles with attributes $[K,L,\bar{G}]$
$m_b(K,L,t)$	mass of particles $[K,L]$ attached on air phase at time t

$M_b(K,L,a,t,\tau)$ mass of particles $[K,L]$ on bubbles of specification $[a,t,\tau]$

$M_c(K,L,t)$ mass of particles $[K,L]$ in concentrate at time t

$M_c(Ka,L,t)$ mass of particles $[Ka,L]$ in concentrate at time t

$M_C(Ka)$ mass flow rate of particles with overall flotation rate constant Ka in concentrate stream

$M_C(L)$ mass flow rate of particles of size L in concentrate stream

$M_{C,1}$ mass flow rate in concentrate stream in rougher cell

$M_{C,2}$ mass flow rate in concentrate stream in cleaner cell

M_{Cj} mass flow rate of j-th species in concentrate stream

M_{Cjk} concentrate flow rate of j-th species from k-th cell

$M_f(t)$ fraction of floatable material remaining in the cell at time t

M_F mass flow rate of solid species in feed

$M_F(Ka,L)$ mass flow rate in feed of particles with attributes $[Ka,L]$

M_{Fj} mass flow rate of j-th species in new feed

$M_s(t)$ mass of particles in pulp at time t

$M_s(Ka)$ mass of particles $[Ka]$ in feed material

$M_s(Ka,L)$ mass of particles $[Ka,L]$ in feed material

$M_s(Ka,t)$ mass of particles $[Ka]$ in pulp at time t

$M_s(L,t)$ mass of particles of size L in pulp at time t

M_T mass flow rate of solid species in tailings stream

$M_T(Ka)$ mass flow rate of particles with overall flotation rate constant Ka in tailings stream

$M_T(Ka,L)$ mass flow rate of particles $[Ka,L]$ in tailings stream

$M_T(Ka,L,t)$	mass flow rate of particles $[Ka,L]$ in tailings stream t time after introduction of a tracer impulse
$M_T(L)$	mass flow rate of particles of size L in tailings stream
M_{T_j}	mass flow rate of j-th species in tailings stream
$M_{T_{jk}}$	tailings flow rate of j-th species from k-th cell
M_∞	mass fraction of non-floatables in original feed
$M'(x)$	defined in equation (A-2)
$M'_s(t)$	mass fraction of particles in pulp at time t
$\bar{M}_s(K)$	mass of particles with specific attachment rate constant K, in feed material
$\bar{M}_s(K,L)$	mass of particles $[K,L]$ in feed material
$\bar{M}_s(K,L,t)$	mass of particles $[K,L]$ in pulp at time t
$M^o_s(K^o)$	frequency function in K^o
$\bar{M}(t)$	defined in equation (5.7)
n	order of quadrature formula used for discretizing integral
n_c	number of cells in flotation circuit
n_i	order of reaction with respect to i-th species in equation (2.3)
n_s	number of species in pulp
n'	number of trials to be made in Fibonacci search technique
$\bar{n}$	overall order of reaction in equation (2.4)
N	number of data points
$N_b(a)$	steady state number of bubbles of size a in pulp
$N_b(a,t,\tau)$	number of bubbles of specification $[a,t,\tau]$

$N_f(a,t,\tau)\delta(t-\tau)$ rate of number of bubble of size a fed at time t

P_f price of feed ore

P_G increase in price of the concentrate for every one percent improvement in the grade

P_a probability of adhesion

P_c probability of collision

P_d probability of detachment

P_e probability of a particle being retained and lifted through liquid

P_f probability of particle being retained in froth

P_o overall probability of flotation

P_r probability of particle being retained by bubble

P_n Jacobi polynomial

q mass of solids in froth product

Q flow rate of air

$r(a,t,\tau)$ net rate of attachment of all particles on bubble $[a,t,\tau]$

$r(K,L,a,t,\tau)$ net rate of attachment of particles $[K,L]$ on bubble $[a,t,\tau]$

$r_a(K,L)$ rate of attachment of particles $[K,L]$ on a bubble $[a,t,\tau]$

r_c collision diameter of a bubble

$r_d(K,L)$ rate of detachment of particles $[K,L]$ from bubble $[a,t,\tau]$

r' random number

$\bar{r}'$ parameter defined in Table 5.2

$R(Ka)$ cumulative apparent flotation rate distribution

$R_F(Ka,L)$	cumulative apparent flotation rate distribution of particles of size L in a continuously operated cell
R_c	percentage overall recovery
$R_F(Ka,L)$	cumulative apparent flotation rate distribution of particles of size L in a continuously operated cell
$R'(Ka)$	defined in equation (5.32)
$\bar{R}(K)$	cumulative particle bubble attachment rate distribution
R^*	defined in equation (6.11)
$R^o(K^o)$	defined in equation (6.16)
$R^{\neq}$	defined in equation (6.24)
s	scaling factor
S	particle surface characteristic index
S_o	ratio of total available bubble surface to bubble surface occupied by solid particle in unit time
t	flotation time
$\bar{t}$	mean residence time of particles in pulp
$\bar{t}'$	predefined upper limit for mean residence time of particles
T	mean residence time of air bubbles in cell
$\bar{T}$	defined in equation (4.52)
u_j	set of independent vectors
$\bar{u}_j$	set of orthogonal vectors
V(K,L)	mass of valuable mineral with attribute K in feed of size L
v_i	volume of i-th flotation cell
$V_s(Ka,L)$	mass of valuable mineral with overall rate constant Ka in feed of size L
$V_s(L,T)$	mass of valuable mineral remaining in suspension of particles of size L at time t

V_T	total volume of all flotation cells in circuit
w_i	i-th weight of Lobatto quadrature formula
w_i'	i-th weight of Legendre quadrature formula
$\bar{w}'$	weighting factor
$\bar{w}_{ji}$	fraction of j-th species in tailings of i-th cell
x	transformation variable
x_i	i-th abscissa of Lobatto quadrature formula
x_i'	i-th abscissa of Legendre quadrature formula
$\bar{x}$	defined in equation (7.20)
X_i	independent variable in objective function defined in equation (B-1)
X_i^j	value of X_i at j-th stage of computation in univariant search technique
X_{ib}	i-th coordinate of the best vertex in old complex
X_{iC}	modified coordinates of centroid in complex method defined in equation (B-19)
X_{ij}	i-th coordinate of the j-th vertex
X_{iL}	lower limit of X_i
X_i^L	upper limit of X_i
X_{iN}	i-th coordinate of the new trial point
$X_{iN'}$	modified new trial point defined in equation (B-18)
X_{iR}	i-th coordinate of the worst point to be rejected
$X_{i,New}$	new trial point in random search technique
$X_{i,old}$	initial base point in random search technique
ΔX_i	defined in equation (B-23)

α	parameter in particle residence time distribution function in equation (2.23)
α_{ji}	defined in equation (8.4)
α'	unknown parameter in equation (A-2)
$\bar{\alpha}$	acceleration factor
$\bar{\alpha}'$	reflection factor
β	parameter in particle residence time distribution function in equation (2.23)
β_{ki}	split fraction of concentrate flow from k to i-th cell
β_{io}	fraction of concentrate output from i-th cell
β'	unknown parameter in equation (A-2)
$\bar{\beta}$	deceleration factor
ϵ	hydrodynamic parameter
μ	unknown parameter defined in equation (A-2)
ν	unknown parameter defined in equation (A-2)
ϕ	weighted mean bubble size defined in equation (4.19)
$\psi(t)$	time dependent weighted mean bubble size defined in equation (4.20)
ξ	a parameter defined in equation (4.27)
ξ_j	j-th direction of search in Rosenbrock technique of optimization
σ^2	variance of particle residence time distribution
τ	time of introduction of a bubble in pulp
λ	inverse of mean residence time of air bubble defined in equation (4.12)
η	function of particle size defined in equation (6.12)
$\bar{\eta}$	function of particle size and aeration rate defined in equation (6.15)

θ	defined in equation (6.25)
δ_{fi}	fraction of feed going to i-th cell
δ_{ki}	split fraction of tailings flow from k to i-th cell
δ_{io}	fraction of tailings output from i-th cell
$\mathcal{f}_j$	fraction of valuable mineral in j-th species
Δ_j	determinant defined in equation (8.30)
χ	contribution of surface hydration to the probability of adhesion
γ	amount of solid on unit bubble surface

SYNOPSIS

The first part of the present study which deals with some quantitative aspects of flotation kinetics has been subdivided as: (1) a phenomenological model for flotation kinetics; (2) an algorithm for estimation of flotation rate distribution; (3) the effect of process variables on the flotation rate distributions; and (4) the effect of process variables on the flotation rate distribution in a continuous operation. The second par deals with (5) the optimal synthesis and design of a flotation circuit.

1. A Phenomenological Model for Flotation Kinetics:

A phenomenological model for flotation kinetics has been derived which provides an explicit relationship between the apparent rate constant and the specific rate constant for particle-bubble attachment subprocess. In first instance a general formulation of the kinetics has been constructed in terms of a set of non-linear differential equations. Mathematical conditions for the free flotation case under which flotation process can be described by a simple first order rate equation are stipulated. A simplified method for analysis of kinetics in terms of grade of the concentrate has been proposed in which flotation kinetics is concurrently analyzed for total mass

recovery and mass of valuable mineral.

2. Estimation of Flotation Rate Distribution By Numerical Inversion of the Laplace Transform:

The problem of estimation of the rate distribution function in apparent rate constant in first order flotation rate equation is equivalent to the inversion of the Laplace transform. A reliable method for estimating the flotation rate constant distribution in cumulative mode by the numerical inversion of the Laplace transform has been developed. The proposed algorithm has been tested for synthetic data generated from different distribution functions. The effects of errors in the data, number of data points, initial guess in the optimization step and non-floatables on the accuracy of the proposed algorithm have also been studied.

3. The Effect of Process Variables on the Flotation Rate Distributions:

The computed cumulative distributions in apparent rate constant, as a whole, have been examined for appropriate relationships between cumulative distribution and aeration rate, particle size and pulp density. The distribution function is found to remain unaltered, but the argument of the function, the apparent rate constant, is rescaled with change in the rate of aeration and particle size. The scaling factor increases /

rapidly with the rate of aeration and exhibits a characteristic maximum for intermediate particle size. The calculated distributions are independent of initial pulp density when dilute, but show marked divergence for concentrated pulp. A partial proof for the validity of the model proposed in part 1 has been given.

4. The Effect of Particle Size and Feed Rate on the Flotation Rate Distribution in a Continuous Cell:

An algorithm for estimating the flotation rate distribution in a continuously operated cell has been developed and using the tabulated data given in the literature, the effects of particle size and feed rate on the flotation rate distribution have been examined. The distributions are found to be independent of slurry flow rate and the effect of particle size is similar to that in the semi-batch process. The estimated rate distributions have been employed to predict the kinetics of cleaner cell whose feed comprises of the rougher concentrate. Similar results have been obtained for the gangue component.

5. Optimal-Suboptimal Synthesis and Design of Flotation Circuits:

A preliminary investigation of the feasibility of synthesizing and designing optimal and suboptimal flotation circuits by optimization of a number of appropriate objective functions of recovery and grade and profit has been carried out. In this approach, the optimal structure and design parameters are

extracted simultaneously from a generalized circuit by direct search. First, a flotation circuit with two cells and feed comprising of two species of known overall rate constant is synthesized and designed and the results are compared with the real optimum circuit for this case, obtained by using the trial and error technique. The approach is then extended to a flotation circuit with four cells and for batteries of cells for a feed comprising of valuable, gangue and middlings.

CHAPTER I

INTRODUCTION

Froth flotation of particulate solids, suspended in water, by means of air bubbles is perhaps the most important technique available at present for separation of valuable minerals from associated gangue impurities. The commercial exploitation of froth flotation can be traced back to first decade of the twentieth century.[1] Probably no other process in the history of mineral beneficiation has been responsible for such increased mineral production as froth flotation. At present, many low grade and finely grained complex ores, which were previously considered worthless, are mined only because they can be economically enriched to concentrates by the flotation process.

In view of the importance of the flotation process, attempts are continuously being made to obtain better understanding of the underlying kinetic mechanisms and physical phenomena which may lead to:

(1) Development of the process strategy for ores which, at present, cannot be beneficiated by flotation.

(2) Modification of the existing processes, so that as the mineral rich ores are depleted these processes may be adopted to low quality ores.

(3) Improvement in the efficiency of the existing processes for improvement in the quality of the product, the plant throughput and the operating cost.

Once the basic process has been evolved, any further improvement in its efficiency is in general possible only by optimization and automatic control of the process. This, however, requires a reasonably accurate mathematical kinetic model which should be able to predict the performance of the unit operation under varying operating conditions. Because of the large tonnage of ores treated, even a marginal improvement in the process efficiency can have significant economical impact. Thus, the importance of a quantitative understanding of flotation as a rate process is obvious.

At present, it is not possible to derive the flotation kinetic model from first principles, although some attempts have been made recently in this direction. A feasible and useful approach is to develop a kinetic model which is in agreement with overall flotation kinetics and then to study systematically the effects of various process variables on the specific rate parameters appearing in the model. However, the number of variables which have an appreciable effect on the flotation behaviour is very large. An exhaustive list of the variables has been given by Rose[2], and Sutherland and Wark[3], but as suggested by Arbiter and Harris[4], this problem can be somewhat simplified by grouping together the variables

pertaining to (1) ore and mineral properties; (2) nature of reagent treatment; and (3) aggregate of flotation machine characteristics. Since the flotation kinetics depends on nonlinear interactions of the variables, this classification is, strictly speaking, not mutually exclusive. Group 1 includes particle size, shape and density, and mineral composition and distribution etc. whereas variables related to adsorption or reaction of chemical reagents, e.g. collector, frother and modifier etc. at the surface of mineral particle and air bubbles constitute group 2. In group 3, the most important variables are the number of bubbles and their size distribution, and the complex hydrodynamic environment prevailing in the cell.

Although a large number of studies on flotation kinetics have been reported, a majority of these are experimental and empirical in nature and a comprehensive model, which can interpret the existing kinetic data satisfactorily and further predict the performance of the process under varying operating conditions, is yet to be evolved. In the present study an attempt has been made to study some aspects of flotation kinetics leading to development of a more meaningful kinetic model based on the distributed particle-bubble attachment rate constant. The resulting model has been reduced to distributed apparent flotation kinetics, which has been highly successful for the analysis of the existing kinetic data, under free flotation constraints. A method for numerical inversion of the

Laplace transform has been proposed which is suitable for estimation of the apparent flotation rate distribution. The effects of some of the process variables on flotation kinetics have been studied and some of the results are interpreted on the basis of the new kinetic model. Finally, optimal synthesis and design of the industrial flotation circuits has been carried out. These objectives are discussed in more detail in Chapter 3.

CHAPTER 2

LITERATURE REVIEW

There exists considerable literature on flotation processes. For convenience, it can be divided into five broad categories: literature pertaining to 1) physical chemistry of flotation; 2) kinetics of the process; 3) design of flotation cell and various other technological aspects; 4) optimization of the flotation circuit and process variables; and 5) automatic control of the process. It is beyond the scope of this study to review all these areas; only, literature pertaining to second and fourth categories is discussed under the titles of flotation kinetics and optimization.

A. FLOTATION KINETICS:

The mathematical description of flotation as a rate process was first given by Gracia-Zuniga[5] who, on the basis of experimental data in a semi-batch process, reported that the material remaining in the pulp decays exponentially with time t, i.e.

$$M_s'(t) = \exp\,[-Ka\ t] \qquad (2.1)$$

where $M_s'(t)$ is fraction of material remaining in suspension at time t and Ka is apparent or overall flotation rate constant.

This empirical equation means that a plot of ln ($M_s'(t)$) versus t should be a straight line with slope equal to minus Ka. Since then several kinetic equations and models have been proposed. In this review, these models have been discussed in more or less the same order in which they were evolved and this is reflected in the degree of sophistication in models which tends to increase as we go from one model to the next.

A.1 Kinetic Models Based on Chemical Kinetic Analogy:

Starting from the premise that the rate of flotation can be expressed as a first order chemical reaction, Beloglazov[6] proposed a differential equation for a semi-batch flotation process, similar to that of Gracia-Zuniga[5], which can be written as

$$\frac{dC(t)}{dt} = - Ka\ C(t) \qquad (2.2)$$

where C is the concentration of solid particulate species in pulp. The first order kinetic form of the rate expression in equation (2.2) probably led Grunder and Kadur[7], and later, Plaksin, Klassen and Berger[8] to adopt the law of mass action in chemical kinetics for their kinetic equations for flotation process. Superficially, the chemical kinetic analogy seems quite reasonable if one considers the formation of bubble particles aggregate as the rate controlling step, similar to the chemical reactions governed by interaction between atoms, molecules or ions. According to this view point, a general

equation for the kinetics of the semi-batch process can be postulated as[4],

$$\frac{dC(t)}{dt} = -k' \prod_{i=1}^{n_s} C_i^{n_i}(t) \qquad (2.3)$$

where, as defined earlier, C refers to the concentration of flotation material, C_i is the concentration of a particular constituent i in the pulp, k' is specific flotation rate constant, n_i is the order of reaction with respect to i-th species and n_s is the number of species in the pulp taking part in aggregation step. If one assumes that there are only two constituents in the pulp, namely, solid particles and air bubbles, and if the air supply is constant, merger of all constant terms with k' reduces equation (2.3) to

$$\frac{dC(t)}{dt} = - Ka\, C^{\bar{n}} \qquad (2.4)$$

where $\bar{n}$ is the overall order of reaction. Schuhmann[9] pointed out that for $\bar{n} = 1$, the rate constant in equation (2.4) has the same dimensional significance as the specific reaction rate constant for a first order chemical reaction. Mika[10] has, however, correctly pointed out that the analogy between flotation and chemical reaction rate equations arises from the use of the terms, such as rate constant and order of reaction, and these parameters, as such, have no physical significance in flotation phenomena except when $\bar{n} = 1$.

There has been some controversy in the literature concerning the value of $\bar{n}$ in equation (2.4). Gracia-Zuniga[5], Beloglazov[6], Grunder and Kadur[7], Schuhmann[9], Sutherland[11], Volkova[12], Morris[13], Brown and Smith[14], Jowett and Safvi[15], Modi and Fuerstenau[16], Imaizumi and Inoue[17], and Chi and Young[18] postulated $\bar{n}$ to be unity, whereas Arbiter[19], Bennett, Chapman and Dell[20], Hukki[21], Mitrofanov[22,23] and Suwanasing and Salman[24] proposed a value of two. Bogdanov and coworkers[25,26], Horst[27,28], deBruyn and Modi[29], and Volin and Swami[30] assigned various other values. Plaksin et al[8] asserted that it would be incorrect to assume a constant value for $\bar{n}$ during the entire period of flotation because conditions and forms of the mineralized bubbles undergo change during the process. Krokhin[31] and Kakovskii[32] divided the whole process into several stages and described each stage by a different equation. Examination of systems that exhibit non-first order kinetics led Pogorely[33], and Tomlinson and Fleming[34] to introduce the concept of free and inhibited flotation. In the case of free flotation, which requires dilute pulp and high aeration rate, the bubbles are only sparsely coated with mineral particles and at no stage there is a deficiency of the bubble surface. Now it is likely that the conditions and forms of mineralized bubbles remain constant and, therefore, the first order kinetic equation describes the process during the entire period of flotation. In the case of inhibited flotation, bubble rising

through the pulp becomes effectively saturated with the particles and reaches the surface with a load of particles determined either by its surface capacity to accommodate particles or its lifting power. A generalized equation which includes both these cases was given by Pogorely[33]

$$\frac{dq}{dt} = S_o \gamma \left[1-\exp\left(-\frac{Ka\ C\ T}{\gamma}\right)\right] \qquad (2.5)$$

where q is mass of solids in froth product, S_o is the ratio of total available bubble surface to bubble surface occupied by solid particles in unit time, γ is the amount of particulate solids on unit bubble surface area, and T is the average holding time of bubbles in pulp. For low concentration of solids in pulp, equation (2.5) reduces to a first order process while in the case of high concentration, the equation tends to zero order.

A.2 Effect of Non-Floatable Components:

An assumption implicit in the foregone discussion is that the feed solids are homogeneous. The experimental data when plotted according to $\bar{n}$-th order rate law, however, frequently failed to verify the proposed rate expression. Morris[35] modified the first order rate equation by incorporating an additional parameter C_∞ as follows:

$$\frac{dC}{dt} = - Ka\ (C - C_\infty) \qquad (2.6)$$

He did not provide any physical interpretation of C_∞ but computed it from experimental data. Bushell[36], however, recognized C_∞ as the terminal concentration, representing the material that would not float even after an infinite time, and observed that C_∞ was a nonlinear function of particle size. Similar observations have also been reported by Cooper[37]. On the other hand, the work of Jowett and Safvi[15] strongly indicates that C_∞ is merely an empirical parameter, whose actual behaviour does not correspond to the true terminal concentration and, moreover, instead of being a strictly mineralogical variable it apparently represents the hydrodynamic nature of the test cell as well as the flotation chemistry.

A.3 Probabilistic and Stochastic Kinetic Models:

According to Schuhmann[9] the kinetics of first order homogeneous reaction is applicable to flotation, and the overall probability of flotation of a solid particle may be expressed in terms of probabilities of collision (P_c), adhesion (P_a) and particles being retained by bubble (P_r). Thus, if individual probabilities are independent of each other, the overall probability (P_o) of flotation is

$$P_o = P_c P_a P_r \qquad (2.7)$$

Similar approach was adopted by Bogdanov et al[26,38-40]. A modification to equation (2.7) has been proposed by Tomlinson and Fleming[34]

$$P_o = P_c P_a P_e P_f \qquad (2.8)$$

where P_e is probability of a particle being retained and lifted through the liquid and P_f refers to the probability of a particle being retained in the froth. Strictly speaking, the hypothesis of statistically independent events, implicit in equations (2.7) and (2.8) is not valid. For example the probability of particle-bubble attachment depends on the number of particles already present on the surface. For a battery of continuously operated cells arranged in series, Kelsall[41] showed that the mass of material, M_T, leaving in tailings after passing in n_c cells in series is given by

$$M_T = M_F (1 - P_o)^{n_c} \qquad (2.9)$$

where M_F is mass flow rate of particulate solids in feed. Kelsall also proposed a graphical method for evaluation of P_o. Davis[42] has applied this approach to industrial plants floating lead and zinc concentrates. However, as pointed out by Woodburn[43] the main objection to this model is that it fails to take into account the increase in residence time per cell down a consequitive cell bank which results in gradual increase in probability of flotation.

Bodzinoy[44] has been among the first authors to develop a stochastic model for flotation. He showed that the flotation can be described as a so called 'simple death process' which reduces to the first order kinetics in the mean. Recently,

Katz and Shinnar[45] have considered flotation as a random phenomena belonging to the family of the Markov processes.[46]

A.4 Two Phase Model:

A kinetic model of the flotation process, which recognizes that the cell contents are partitioned between pulp and froth and that there exists a mutual traffic of material between these two phases, was proposed by Arbiter and Harris[4] and further extended by Harris and Rimmer[47]. The basic assumption in this model is that both pulp and froth phases are perfectly mixed, and first order kinetics is applicable for individual transfer step. This model was experimentally verified by Harris, Jowett and Ghosh[48] for continuous flotation of coal at steady state. Bogdanov et al[49] and Bull[50] have also supporte this approach. Later, Ball, Kapur and Fuerstenau[51] introduced distributed flotation rate constant into this model.

Several authors such as Niemi[52], Woodburn and Loveday[53], and Imaizumi and Inoue[54] pointed out that for sufficiently fast rate of froth removal the rate of return of material from froth to pulp is negligible and, therefore, under such conditions two phase model is not necessary. This point, however, has been criticized by Maksimov and Khainman[55] who observed that even for high concentration yields and with the use of reagents which ensured a stable froth, the probability of particles remaining in the froth was much smaller than unity, and the

rate of return of particles increased rapidly with particle size. Bushell[36] assumed that the rate of re-entry of particles to the pulp was proportional to the rate of transfer of material from pulp to froth. One of the basic assumptions of the two phase model, that the froth phase is perfectly mixed is really questionable. Cooper's[37] concept of horizontally homogeneous, but vertically distributed froth phase seems physically more reasonable.

A.5 Kinetic Models Based on Mechanistic Approach:

Models included in this category are based on one or more sub-mechanisms involved in the process. Although these models lead to result far too complex to be of any industrial utility, they, nontheless, attempt to provide valuable insight into the likely mechanism of the process.

Mineral particles are transferred from pulp to froth through any of the following four mechanisms: (1) attachment of the mineral particles with the air bubbles in the pulp followed by the transfer of bubble to the froth; (2) selective precipitation of the gas dissolved in water on the surface of mineral particles; (3) mechanical straying of the mineral particles into the froth column; and (4) attachment of mineral particles to the bottom of the froth column by the agitation of the pulp. It has been observed by many investigators that the third and fourth mechanisms of mineral transfer from pulp to froth are not significant in many systems and the major fraction of the material is transferred in the form of bubble-particle aggregates.[4]

Taggart[56] proposed the hypothesis of bubble-particle aggregate formation due to precipitation of gas on the hydrophobic surface of mineral particles from supersaturated gas solution. This, however, was criticized by Bogdanov and Filanovski[57], and Gaudin[58], who postulated that the direct encounter between particles and bubbles is more plausible for the formation of bubble particle aggregate. The direct encounter hypothesis has been supported by Malozemoff and Ramsey[59], Plante and Sutherland[60], Spedden and Hannan[61], Whelan and Brown[62], Kirchberg and Topfer[63], and Imaizumi and Inoue[54]. Klassen[64] proposed an intermediate mechanism in which a large bubble coalesces with a micro bubble precipitated and attached to the mineral surface. The conditions under which gas precipitation on the mineral surface becomes important have been reviewed by Smith et al[65], and Klassen[66]. It should be pointed out that the phenomenon of mineralization of bubbles by precipitation of gases raises a number of fundamental questions, the answer to which may be of great importance in flotation practice. For example, in the flotation of very fine particles, owing to their small mass, particles are normally swept away with bubble stream lines and undergo collision with great difficulty. In the case of coarse particles also, formation of several clusters of small bubbles by precipitation of gas may enhance the rate of flotation.

The formation of bubble mineral particle aggregates by direct encounter, which is the most frequent mechanism under normal flotation conditions, involves several sequential stages, viz., adsorption of reagents on the surface of particles and bubbles, collision between bubbles and particles, attachment, partial detachment of particles from the bubbles due to gravitational and inertial forces, and froth unstability etc. The kinetic models developed on the basis of mechanistic approach incorporate one or more of these steps.

First such model was proposed by Sutherland[11]. He assumed that water is non viscous and incompressible, the bubbles and particles are both rigid spheres and incompressible, and the inertia of particle is negligible, and calculated the probability of interception from streamline flow around spheres. The collision radius, r_c, of the bubble for a particle of diameter L, as obtained by him, is

$$r_c = 2\sqrt{3\,a\,L} \qquad (2.10)$$

where a is the diameter of the air bubble. Photographic observations by Spedden and Hannan[61], however, showed that the larger particle deforms the bubble appreciably during collision. This deficiency was removed by Philippoff[67] and Evans,[68] who independently postulated a bounce theory in which the role of inertial forces is emphasized. Further modifications to the theory have been proposed by Whelan and Brown[62]. On the

other hand the empirical correlations reported by Langmuir[69], Herne[70], Ranz and Wong[71], on collision of particles seem to be consistent with the results of Sutherland. Using a similar approach, Bogdanov and his collaborators[38-40] have calculated the probabilities of collision and adhesion. Recently, Flint and Howarth[72] evaluated the collision efficiency of a particle with a bubble from considerations of particle trajectory as a function of particle size and hydrodynamic conditions prevailing in the cell. Although this study provides a qualitative understanding of the collision phenomena, its extension in quantitative sense, to a system of swarms of particles and bubbles in turbulent medium is not available at present.

A rate equation based on analogy between adsorption and mineralization of air bubbles was derived by Matveenko[73]. A detailed analysis of bubble particle interaction for small and medium size particles (< 100 μ), based on physico-chemical aspects, has been made by Derjaguin and Dukhin[74]. The mechanism of bubble particle attachment has also been studied by Eigeles[75,76], Volkova[77,78], Morris[79], Zaidenberg[80] and Glembotskii et al[81]. A more detailed and structurally complex phenomenological model for flotation kinetics has been proposed by Mika and Fuerstenau[82] wherein each elementary rate process is formulated in terms of linear first order differential equations for individual discrete size particles and bubble species. Although this model clearly identifies and elucidates the basic

steps in interphase transfer of particles, its practical utility remains to be demonstrated because it involves a number of unknown parameters which are at present not amenable to theoretical or experimental estimates. Recently, Woodburn, King and Colborn[83] have proposed a kinetic model for a continuous flotation cell in which the rate constant is derived as a function of particle size, its mineralogy and the tailings flow rate. The final expression is product of three probabilities pertaining to events of Collision P_c, adhesion P_a and disengagement P_d as follows:

$$P_c = B \exp\left(-\frac{\theta}{L^2}\right) \qquad (2.11)$$

$$P_a = \frac{\kappa \theta^2}{L} \qquad (2.12)$$

$$P_d = \left(\frac{L}{L_{max}}\right)^{1.5} \quad \text{for } L \leq L_{max}$$

$$= 1 \quad \text{for } L > L_{max} \qquad (2.13)$$

where B is a proportionality constant, θ is a hydrodynamic parameter, L is particle size, κ refers to contribution of surface hydration to the probability of adhesion, and L_{max} is maximum particle size which will remain attached to a bubble. It should be noted that in the derivation of these probabilities, a number of simplifications and crude approximations had to be made and at best, these represent a first tentative attempt in this direction.

A.6 Kinetic Models with Distributed Apparent Flotation Rate Constant:

In the literature cited above, it is assumed that the rate constant is single valued. It is, however, more likely that the feed material comprises of several different species with different values of the rate constant associated with each of these species as well as with surface and composition heterogeneity within a species. Thus, it is more rational to associate a distributed rather than a single valued rate constant with the feed material. The over simplified probabilistic model of Kelsall[41] reflected this fact in that there are at least two species of floatable particles, an easily recoverable fraction having a high probability of flotation, and a low probability fraction which floats with difficulty.

Pogorely[84], and Imaizumi and Inoue[54] were among the first authors to formally introduce the concept of variable and distributed rate constant. The latter postulated that the rate of removal of solid from pulp to froth is a time invariant first order process but the particulate species are distributed with respect to the overall specific flotation rate constant. Thus, if M_s (Ka, t) is mass of solid particulate species with attribute overall rate constant Ka, remaining in the cell at time t, the rate of removal of solids of this specification from the pulp is

$$\frac{dM_s(Ka, t)}{dt} = - Ka\ M_s(Ka, t), \quad 0 \leq Ka \leq \infty \qquad (2.14)$$

Solution to this equation is

$$M_s(Ka, t) = M_s(Ka) \exp [-Ka\ t] \qquad (2.15)$$

where,

$$M_s(Ka) = M_s(Ka, 0) \qquad (2.16)$$

Therefore, the total material remaining in the pulp at time t is,

$$M_s(t) = \int_0^\infty M_s(Ka) \exp [-Ka\ t]\ dKa \qquad (2.17)$$

If $M_s(t = 0)$ is normalized, $M_s(Ka)$ becomes a true density function, and, explicitly, $M_s(Ka)\ dKa$ represents the mass fraction of particles with overall rate constant in range Ka to Ka + dKa in the feed material. The main difficulty in this model lies in evaluation of $M_s(Ka)$ given noisy experimental data $M_s(t)$. If $M_s(Ka)$ is a discrete density function, equation (2.17) becomes,

$$M_s(t) = M_s(Ka_1) \exp [-Ka_1\ t] + M_s(Ka_2) \exp [-Ka_2\ t] + \ldots + M_s(Ka_{n_s}) \exp [-Ka_{n_s}\ t] \qquad (2.18)$$

where

$$\sum_{i=1}^{n_s} M_s\ (Ka_i) = 1 \qquad (2.19)$$

Imaizumi and Inoue[54] proposed a method for evaluating Ka_i and corresponding $M_s(Ka_i)$ by considering asymptotes on the log $(M_s(t))$ versus t plots. Similar approach has also been taken by Huber-Panu[85]. Unfortunately, the number of species n_s is not known a priori and must be assumed arbitrarily. Complete identification of the discrete distribution from noisy data is a very difficult task.. A more commonly used method of determining the density function consists of assuming a functional form for $M_s(Ka)$ in equation (2.17), and then determining the parameters of the distribution from the experimental data. Thus, Woodburn and Loveday[53], and Inoue and Imaizumi[86] assumed a gamma distribution and evaluated the parameters by graphical methods. Loveday[87], however, observed that a better fit to experimental data is obtained with incomplete gamma distribution. Ball, Kapur and Fuerstenau[51] also used gamma distribution for $M_s(Ka)$ and carried out the analysis of the flotation kinetics using the moments of the distribution. Harris and Chakravarti[88] suggested a bimodal gamma distribution for $M_s(Ka)$. Kinetic equation by Huber-Panu[89], however, starts with a rectangular distribution of rate constant. When $M_s(Ka)$ is assumed to be an incomplete or a bimodal gamma distribution, greater flexibility and enhanced agreement is to be expected because now $M_s(Ka)$ is expressed in terms of three or more adjustable parameters instead of two in the case of gamma distribution. Recently, Black and Faulkner[90] have arbitrarily

assigned values to n_s and Ka_i and evaluated $M_s(Ka_i)$ in equation (2.18) by linear regression techniques. This is essentially a curve fitting exercise and provides no insight into the structure of the distribution. A large number of different equations can fit the data quite accurately and therefore, evaluation of rate constant distribution from equation (2.18) in this manner is rather meaningless. Methods for analyzing kinetic data assuming distributed rate constant models have also been discussed by Woodburn, King, Buchalter and Piper[91], Huber-Panu[92], Tille and Panou[93], and Cuttris[94].

Harris and Chakravarti[88] correctly pointed out that in equation (2.17), $M_s(t)$ is the laplace transform of $M_s(Ka)$ and, therefore, $M_s(Ka)$ is inverse of the Laplace transform. Hence, the problem of evaluating flotation rate distribution, $M_s(Ka)$, is the problem of inversion of the Laplace transform. In the case of experimental data $M_s(t)$, this inverse must be computed by numerical means. Unfortunately, numerical inversion of the Laplace transform is not an easy task and success is not always assured, especially, in presence of experimental errors. This is because Laplace inverse is a very unstable operator which implies that arbitrarily small variations in $M_s(t)$ may cause arbitrarily large changes in $M_s(Ka)$ as highlighted by Krylov and Skoblya[95], and, Bellman Kalaba and Lockett[96]. Although in the literature a number of algorithms are available for numerical inversion of the exact data, they invariably become ineffective

in the case of noise corrupted data. Some of these algorithms are discussed in Appendix A. In Chapter 5, we shall present a simple and robust method for the numerical inversion of the Laplace transform.

It should be understood that although $M_s(Ka)$ is a frequency function, it is not an exclusively internal coordinate or attribute of the particles. In other words, the apparent rate constant, Ka, depends, as pointed out by Harris and Chakravarti[88], on numerous factors only a few of which, such as size, degree of liberation and distribution of valuable mineral in a particle, its surface characteristics and conditioning etc. are specific attributes of the particles. Other factors that contribute to the structure of the apparent flotation rate constant are aeration rate, population, size, and residence time distributions of bubbles, as well as, complex hydrodynamics and physicochemical conditions prevailing in the pulp. Ka incorporates in some complicated fashion a number of elementary interphase transfer steps such as particle bubble attachment and detachment rate, and escape of particle ladden bubbles from pulp to froth.

Work of Zaidenberg, Lisvoskii and Burovoi[97] is noteworthy in this connection. They have attempted an analysis of flotation kinetics using a multivariate distribution of the particle entities in particle size, degree of liberation in individual size fraction, and floatability for a given size and mineral composition. However, the main drawback of their model is that

invariably neither the conditional distribution in mineralogy for a given size nor the floatability as a function of particle size and mineralogy is known. However, recent results of Woodburn, King and Colborn[83] have shown that even a limited extension of first order treatment on the lines suggested by Zaidenberg et al offers significant advantages for simulation and control of the flotation circuit. Recently, King[98] has further extended and applied this multivariate distribution model for analysis of kinetics for a flotation circuit.

A.7 Kinetics of Flotation in a Continuously Operated Flotation Cell:

Most of the models discussed till now were developed for semi-batch flotation operation. Although these can be easily extended to steady state continuous case, the analysis based on semi-batch system, as such, has been criticized by many investigators on the ground that both the mineral and reagent concentrations undergo continuous change with time, thereby, possibly enhancing the complexity of the system. Further, most of the information has to be collected in a rather short time which may lead to erroneous results. The merits and demerits of both semi-batch and continuous operations for development of flotation kinetic models have been discussed by Arbiter and Harris[4], Woodburn et al[91], Brown and Smith[14], and deBruyn and Modi[29].

The basic difference between semi-batch and continuous operations is that in the latter case the residence time of all elements in the system is distributed. If in a continuous steady state cell with spatially homogeneous pulp the residence time distribution of solids is E(t) dt, i.e., the fraction of solids in tailings exit that has spent time t to t + dt in pulp, the tailings mass flow rate of particles of size L with overall rate constant Ka is[53]

$$M_T(Ka, L) = \int_0^\infty M_F(Ka,L)\, E(t)\, \exp\,[-Ka\ t]\ dt \qquad (2.20)$$

where M_F (Ka,L) is mass flow rate in feed of particles of size L and overall rate constant Ka. In distributed rate model the overall flow rate of particles of size L in tailings, $M_T(L)$, and concentrate streams, $M_C(L)$, are, respectively,

$$M_T(L) = \int_0^\infty \int_0^\infty M_F(Ka,L)\, E(t)\, \exp\,[-Ka\ t]\ dt\ dKa \qquad (2.21)$$

and

$$M_C(L) = \int_0^\infty M_F(Ka,L)\ dKa - M_T(L) \qquad (2.22)$$

Many investigators have postulated that a continuously operated sub-aeration flotation cell is close to a perfect mixer[53,87,91,99-101] and therefore, E(t) is an exponential distribution function. However, Niemi[52] showed that although the residence time of liquid phase can be assumed to be that of a perfect mixer, in the case of solid particles, particularly of large particles, the assumption of perfect mixing requires some modifications.

He further reported that even if solid particles were apparently ideally mixed, their mean residence time was different from that of the liquid phase.

Bogdanov, Hainman and Maximov[40] have attempted to explain the observations of Bogdanov, Kizivalter and Khainman[104], and Zakhvatkin et al[105] that the time of flotation required for a given recovery is reduced with increase in throughput. They deduced that with increase in throughput the flotation time is improved due to changes in the hydrodynamic regime of the pulp. However, analysis of the data of Woodburn et al [83] in Chapter 7 of the present work shows that the throughput rate has negligible influence on the apparent flotation rate constant. Bogdanov Hainman and Maximov[40] derived a rate equation for an ideal case where there is no mixing and cell behaves as a plug flow reactor. In such a case flotation is predicted to be independent of the flow rate. Loveday[87] reported that reduction in the mixing coefficient is likely to give improved grades at a constant recovery level, results which are also well known in the theory of continuous polymer reactors.

In a significant contribution which includes valuable and extensive experimental data, Woodburn et al[83] have shown that the residence time distribution is adequately characterized by the gamma distribution

$$E(t) = \frac{\beta^{\alpha+1} t^{\alpha}}{\Gamma(\alpha+1)} \exp[-\beta t] \qquad (2.23)$$

where the parameters α and β are functions of slurry flow rate and particle size and mass, and are related to mean and variance of the distribution by

$$\bar{t} = \frac{\alpha+1}{\beta} \qquad (2.24)$$

$$\sigma^2 = \frac{\alpha+1}{\beta^2} \qquad (2.25)$$

The additional parameter α, which was found to be quite small, takes into account the deviation from perfect mixing behaviour ($\alpha = 0$). Substitution of equations (2.23) and (2.21) into (2.22) leads to the following expression for recovery.

$$M_C(L) = \int_0^\infty M_F(Ka,L) \left[1 - \frac{\beta^{\alpha+1}}{(Ka+\beta)^{\alpha+1}}\right] dKa \qquad (2.26)$$

A.8 Effect of Process Variables on Flotation Kinetics:

(i) Effect of Particle Size: Particle size is one of the most important parameters and has been studied extensively, among others, by Kidd and Wall,[106] Sutherland[3], Chuan and Zimmerman[107], Morris[35], Gaudin, Schuhmann and Schlechten[108], Bogdanov and Khainman[25], Eigeles and Leviush[109], Brown and Smith[14,110] deBruyn and Modi[29], Bennett et al [20], Krokhin[111], Mackenzie and Matheson[112], Huber-Panu and coworkers[113-115], Tomlinson and Fleming[34], Imaizumi and Inoue[54], Heinrich and Walter[116], Mika[10], Ek[117], Tewari and Biswas[118], Suwanasing and Salman[24], Woodburn et al [83], and Clement et al[119]. From these studies, it may be concluded that regardless of the mineral, collector or flotation machine,

there is a definite trend with regard to variation in the recovery as a function of particle size, and there exists an intermediate size or size range at which the recovery is optimum. This size depends on the mineral to be floated and the hydrodynamic conditions in the flotation machine. Both fine and coarse particles float with difficulty, and in the latter case practically no flotation occurs above a limiting size.

The explanation for low recoveries of very fine particles is attributed to low probabilities of collision because these have a tendency to follow the stream lines. On the other hand, the probability of detachment increases with particle size because of disruptive and inertial forces that come into play. These opposing influences of the particle size give rise to a critical intermediate size at which the flotation rate is optimum. Combining the probabilities of collision, adhesion and detachment given in equations (2.11), (2.12), and (2.13) Woodburn et al[83] have, recently, proposed an expression for the overall rate constant Ka as a function of particle size, L, and hydrodynamic parameter, ϵ, as follows:

$$Ka = \bar{k}(\bar{G}) \frac{\epsilon^2}{L} \left[\exp\left(-\frac{\epsilon}{L^2}\right)\right] \left[1-\left(\frac{L}{L_{max}}\right)^{1.5}\right] \qquad (2.27)$$

where $\bar{k}(\bar{G})$ is a function of the degree of hydration of a particle of grade $\bar{G}$ and it depends on the mineralogy of the particles and its surface treatment with the surfactants.

(ii) Effect of Aeration Rate: The effect of aeration rate on flotation kinetics has been studied by Huber-Panu et al[114,120], Inoue and Imaizumi[86], Tewari and Biswas[118], Lynch[121], Edwards[122], Burdon[123], and Bennett et al[20]. The first three groups of investigators reported that the overall flotation rate increased with the enhanced rate of aeration. Mathematical model proposed by King[124] also supports this observation. Edwards, however, observed that although the flotation kinetics was very sensitive to the rate of aeration, the efficiency of separation remained more or less unchanged. Bennett et al pointed out that the enhanced aeration rate could lead to increase in flotation rate only if the distribution of bubble size does not change because the maximum flotation rate is achieved with largest number of small bubbles. Lynch, however, did not find a significant correlation between flotation kinetics and aeration rate.

(iii) Effect of Pulp Density: The effect of pulp density on flotation rate has been investigated by Newton and Ipsen[125], Gutsalyuk[126], Klassen[127], Burdon[123], Imaizumi and Inoue[54], deBruyn and Modi[29], and Loveday[87]. They observed that except for highly concentrated suspensions the average or instantaneous flotation rate is independent of pulp density, which is in conformity with the first order kinetics in free flotation regime. In the case of concentrated pulps the flotation depends primarily on the capacity of the carrier air phase to

lift the particles from pulp into froth rather than on the particle bubble attachment rate constant, and therefore, flotation rate constant is no longer independent of the pulp density. Now the specific rate constant in term of per unit mass should decrease with increasing concentration of solid particles in the pulp, as shown in Chapter 6 of this study.

(iv) Effect of Reagents:

Collectors: Both the structure of the collector molecules and its concentration affect the flotation rate by influencing the particle-bubble attachment rate. In general, the adhesion of particle to bubble improves with increase in the length of hydrocarbon chain in the collector molecule. The effect of collector concentration on the flotation kinetics has been studied by Beloglazov[6], Schuhmann[9], Inoue and Imaizumi[86], and Lynch[121]. These studies show that both the recovery and flotation rate increase with concentration of collector in the pulp. However, this is usually accomplished with loss of selectivity. In order to maximize recovery, most industrial flotation circuits are operated at saturated collector dosage.

Frothers: In addition to providing stability to air bubble, the function of the frother is to decrease the bubble size and bubble velocity. Studies by Grunder et al[128], and Bennett et al[20] have shown that increase in the amount of frother tends to increase the number of bubbles by reducing their average size, and the flotation rate is enhanced. Lynch[121], however,

attributed the increased flotation rate with frother addition to enhanced rate of water transfer from pulp to froth.

It may be pointed out here that the effect of reagents on flotation kinetics has not been discussed here in detail because in order to do justice to this topic it will be necessary to treat individual mineral systems, which cover a vast area.

B. OPTIMIZATION OF FLOTATION OPERATION:

Once the kinetic behaviour of a single flotation cell is known in terms of its process variables, it is then possible in theory, to optimize the process efficiency and automatically control the process[129-131]. The problem of optimization, considered so far essentially consists of defining a suitable objective function, followed by determination of the values of these process variables such that the objective function is optimal. The problems associated with the formulation of the meaningful objective function, appropriate to flotation process, have been concisely stated by Nixon and Moir[132]. Jowett and Ghosh[133] optimized the performance of a flotation circuit consisting of a sequence of cells with series tailings throughput and parallel froth withdrawal. Their profit function (objective) was defined as the difference between the selling price of the concentrate and the production cost which included the cost of the raw material and the cost of operation.

Sergeev and Smirnov[134] also used a similar objective function in which, however, the number of cells connected in series was predefined. Recently, Woodburn et al[91] have proposed a simpler objective function where the recovery of concentrates was maximized such that the grade of the product was always better than a minimum acceptable grade value.

In industrial flotation practice due to various reasons the separation of valuable mineral from the associated gangue is seldom complete and in order to improve the process efficiency it is a normal practice to employ a number of flotation cells or banks of flotation cells. The basic drawback of all the above mentioned approaches is that the configuration, i.e., the number of cells and/or their linkages is assumed a priori. In general, a flotation circuit is comprised of many flotation cells, performing rougher, cleaner and scavanger functions and it is quite tedious to enumerate all possible meaningful configurations. A particular configuration which is optimal for a given type of ore under certain process conditions may not be optimal for other ores. In general, there is no justification for assuming a configuration and then optimizing the process variables, since the assumed configuration may not be the best possible. Thus, the problem of optimization should be conceived of comprising the following two steps: (1) synthesis of flotation circuit, that is, how the various cells are interconnected such that the optimal process

efficiency is embedded in the derived circuit, and (2) determination of the values of the process parameters of this configuration.

Each flotation cell can be considered as a separate reactor unit. Recently, systematic strategies have been developed for synthesis of the chemical reactor units for optimum efficiency which are relevant to the flotation problem. These are briefly reviewed in the following section.

Synthesis of Reactor Units:

Except for the isolated treatments of the heat exchange networks and multicomponent distillation separation sequences, the development of formal systematic approaches to synthesis in the design of chemical processes dates back to 1968 only. The subject is still in considerable flux. The chief difficulty encountered during the process structure synthesis lies in the large number of possible configurations for the typical industrial processing tasks. Examination in turn of each of these configurations is not only tedious but occassionally it is not possible to enumerate all possible configurations. Conventional optimization techniques designed to handle discrete variables (representing equipment connections) are generally applicable to fairly small size problems only.

Rudd[135] proposed an approach to process system synthesis which is based on decomposition of the main problem into a

sequence of subproblems until the level of available technology is reached. This approach has been applied by Nishida et al[136], and Kobayaski et al[137] for optimal synthesis of heat exchangers, by Menzies et al[138] for synthesis of energy recovery networks, and by Umeda and Ichikawa[139] for synthesis of generalized systems. Masso and Rudd[140] further modified the decomposition approach by introducing the use of heuristic problem solving techniques. The combined heuristic design decomposition approach to process analysis has been applied for synthesis of chemical processes by Siirola, Powers and Rudd[141] and Nishimura and Hiraizumi[142] etc. It may,however, be pointed out that the final configuration depends heavily on heuristic rules which are used at the various decomposition stages. As Masso and Rudd correctly pointed out, really satisfactory rules are yet to be developed. Therefore, solution to practical problems by this technique is fairly limited at this stage.

A synthesis technique, known as 'Evolutionary synthesis', has been suggested by King, Gantz and Barnes[143], and Ichikawa and Fan[144]. This technique is based on synthesis of new process by modification of previously generated techniques. A somewhat more theoretical approach to the evolutionary synthesis was taken by McGalliard and Westerberg[145] who applied Lasdon's[146] dual feasible decomposition method for process optimization. The strategy for optimal design of chemical processes from the view point of statistical design theory has been studied by

Watanabe, Nishimura and Matsubara[147]. The branch and bound techniques of problem solving have also been shown to provide guidance in solving the design problems. As shown by Lee, Masso and Rudd[148], the design problem is branched to simpler design problems which bound the original problem. The main difficulty, however, comes in formulating the alternate problem, solution of which bounds the solution of the original design problem. Umeda, Hirai and Ichikawa[149] have attempted to apply well known optimization and mathematical programming techniques to the synthesis of chemical processes. In their approach all possible configurations are imbedded into a generalized configuration by defining all the interconnections which might exist between various reactor units. Split fractions with values zero to one are assigned to all such interconnections and the solution to the synthesis problem is obtained by determining optimal split fraction (0 or 1) for each linkage along with the optimal design parameters. Values of one or zero indicate whether a pair of equipment are connected or not. This approach has been criticized by Hendry, Rudd and Seader[150] on the grounds that the parametric space for most of the industrial situations becomes so large that it is difficult to ensure a global optimum in the resulting mix integer optimization problem. Recently, this problem has been taken care of to some extent in some systems by a multilevel technique[151] which partitions the integrated problem into smaller

independent subproblems which can be solved with ease. To coordinate the solutions of subproblems and determine the overall system an adjustment problem is required to be carried out.

CHAPTER 3

OUTLINE OF WORK

The present work can be divided into two parts. In the first part some aspects of flotation kinetics have been studied whereas the second part deals with the synthesis and design of a flotation circuit.

Part I: FLOTATION KINETICS:

This can be further subdivided as follows:

(1) A Phenomenological Model for Flotation Kinetics:

From the literature review given in the previous chapter it is evident that the kinetic models based on distributed apparent flotation rate constant lack justification for the first-order kinetics with respect to the species with a given rate constant. A phenomenological model for flotation kinetics has been derived which is perhaps more meaningful in so far as the model provides an explicit relationship between the apparent rate constant and the specific rate constant for particle bubble attachment subprocess which, from the flotation mechanism point of view, is a more pertinent attribute. Concurrently the effect of bubble population is incorporated. Mathematical conditions for the free flotation case under which flotation process can be described by a simple first order rate equation given by equation (2.17) are stipulated.

(ii) Estimation of Flotation Rate Distribution by Numerical Inversion the Laplace Transform:

The problem of determining the density function $M_s(Ka)$ in equation (2.17) has been solved, so far by assuming a priori a specific frequency function (usually, the gamma function) and then evaluating the parameters of the distribution from experimental data by some graphical technique. These graphical methods are quite tedious and the results depend, to some extent, on the personal judgment of the computer. Although recently, Woodburn et al[91] have used numerical methods for estimating the parameters, a more fundamental objection, however, lies in the rather arbitrary assumption of the form of the distribution function for $M_s(Ka)$. Harris and Chakravarti[88] have correctly pointed out that in equation (2.17) $M_s(t)$ is the Laplace transform of $M_s(Ka)$, therefore, $M_s(Ka)$ is inverse of the Laplace transform. A numerical method for estimating the rate constant distribution in cumulative mode by inversion of the Laplace transform has been developed. The method has been tested for synthetic data generated from different distributions. Effects of errors in data, number of data points, initial guesses in the optimization step and non-floatables have been studied. This method of inversion of the Laplace transform has been found to be especially suitable for noise corrupted data which is inevitable in flotation experiments.

(iii) The Effects of Aeration Rate, Particle Size and Pulp Density on the Flotation Rate Distributions:

In the literature cited above, the effects of process variables on flotation kinetics were determined either in terms of the rate constants in some empirical kinetic expressions or by monitoring the instantaneous flotation rates. Perhaps the only exception is the study of Inoue and Imaizumi[86] who studied the effects of the aeration rate on the distribution as a whole. In this part of the work, using the numerical inversion technique, developed in part (ii), cumulative apparent flotation rate distributions have been evaluated for kinetic data available in literature. Appropriate relationships between the estimated distribution functions and the aeration rate, particle size and pulp density, respectively, are examined and a partial proof for the validity of the model, developed in part (i) is provided.

(iv) The Effects of Particle Size and Feed Rate on the Flotation Rate Distributions in a Continuous Cell:

First a reliable method, similar to the numerical inversion of the Laplace transform, for computation of $M_F(Ka,L)$ in expression for mass flow rate of particles of size L in concentrate stream in the steady state, given in equation (2.26), is developed. This method is again not restricted to any a priori assumption concerning the mathematical form of the distribution function. Using the tabulated data of

Woodburn et al[83] the effects of particle size and feed rate on rate distribution have been examined. The estimated rate distribution is then employed to predict the kinetics of a cleaner cell whose feed comprises of the rougher concentrate. The analysis has been extended to gangue component for which data is also available.

Part II: OPTIMAL AND SUBOPTIMAL SYNTHESIS AND DESIGN OF FLOTATION CIRCUITS:

The integral synthesis approach proposed by Umeda, Hirai and Ichikawa[149], has been applied for synthesis and design of an optimal or suboptimal multicell flotation circuit, using appropriate objective functions of recovery, grade and profit. For illustration purpose a flotation circuit with two cells and feed comprising of two species is considered. The validity of the method is checked by comparing the results with the real optimal circuit obtained by examining each configuration separately. The approach is then extended to a more realistic flotation circuit with four cells and for batteries of flotation cells with a three species feed comprising valuable, gangue and middlings.

PART I

CHAPTER 4

A PHENOMENOLOGICAL MODEL FOR FLOTATION KINETICS

The model developed in the present work takes into account the two distinct states of particles in pulp, namely, free particles suspended in water phase and particles attached to air bubbles. In first instance a general formulation explicitly incorporating the important particle-bubble attachment subprocess is constructed which is then reduced to the expression in equation (2.17) under clearly defined conditions. In this manner it will be possible to identify the relationship that exists between the apparent rate constant Ka and the specific rate constant, K, for particle bubble attachment subprocess, in terms of a weighted mean of the bubble population size distribution.

MATHEMATICAL MODEL FOR FLOTATION KINETICS:

The model is based on a number of restrictions and assumptions as follows, some of which are only approximately true, but nevertheless, have frequently been invoked in the analysis of flotation kinetics.

1. The bubble population and size distribution in pulp is time invariant[52] i.e. steady state exists. The residence time of the bubbles conforms to that of a perfect mixer[53,87,91,99-103].

Thus, the escape probability of a bubble from pulp to froth is a function of air hold up and aeration rate only (both assumed to be constant), independent of the pulp density and particle load on the bubble. The latter stipulation is perhaps strictly valid for the free flotation case only[34]. The gas phase dispersion does not change[40], i.e., bubbles neither coalesce nor break-up during their sojourn in the pulp.[3]

2. The net rate of attachment of particles to bubbles in pulp is a first order rate process with respect to mass of particles in suspension, but the particles are distributed in specific attachment rate constant[82] which is assumed to be independent of bubble size and population in the pulp[152]. The rate constant for detachment of particles from bubble is a function - albeit in some inverse sense - of the attachment rate constant as well as the particle size. In particular, attachment and detachment rate constants are independent of the aeration rate in the highly turbulent regime.

3. Auxiliary interphase particle transfer process, such as direct entrainment from pulp to froth and its reverse, are of second order significance and can be neglected[4,51]. Inclusion of these processes will add to complexity of the kinetic formulation, but will not materially alter the basic frame work of the model.

4. The model presented here refers to a semi-batch process with fast froth removal rate, however, it can be extended to the continuous mode of operation, including network of cells, with appropriate modifications for particle residence time and tailings flow rate as suggested by Woodburn et al [83].

Let $[a,t,\tau]$ be specifications of an air bubble of size a in the pulp at time t from start of the flotation process which was introduced in the pulp at time τ ($t \geq \tau$), and $m(K,L,a,t,\tau)$ be mass of particles of size L with specific attachment rate constant K on the bubbles of specification $[a,t,\tau]$. The total mass of particles adhering to the bubble $[a,t,\tau]$ is

$$m(a,t,\tau) = \int_{L_1}^{L_2} \int_{0}^{\infty} m(K,L,a,t,\tau)\, dK\, dL \qquad (4.1)$$

where L_1 and L_2 refer to the smallest and largest particle sizes, respectively. It is recognized that the capacity of a bubble to accommodate more particles on its surface is an exceedingly complicated function of its size, and, the mass and size distribution of particles already present on the surface which would naturally change with time. This difficulty leads to the concept of an instantaneous potential bubble capacity $\bar{m}(a,t,\tau)$, defined such that the rate of attachment of particles of attribute $[K,L]$ on the bubble $[a,t,\tau]$ is

$$r_a(K,L) = A(a) \left[1 - \frac{m(a,t,\tau)}{\bar{m}(a,t,\tau)}\right] K \bar{M}_s(K,L,t) \qquad (4.2)$$

where $r_a(K,L)$ is the rate of attachment of particles $[K,L]$ on a bubble $[a,t,\tau]$, $\bar{M}_s(K,L,t)$ is mass of particles $[K,L]$ in free suspension at time t, and A(a) is a function of the bubble size and hydrodynamic conditions, including the intensity of mixing, of the pulp. Equation (4.2) is similar to the relationship suggested by Sastry and Fuerstenau[152] with the difference that the bubble size is incorporated in the form of a general, but unknown function A(a) and $\bar{m}$ is a function of time. Similarly, the rate of detachment of particles $[K,L]$ from bubble $[a,t,\tau]$ to free suspension state is proportional to the mass of particles on the surface as follows:

$$r_d(K,L) = D(K,L)\, m(K,L,a,t,\tau) \tag{4.3}$$

where $r_d(K,L)$ is the rate of detachment of particles $[K,L]$ and D(K,L) is the detachment rate constant. The net rate of attachment of particles $[K,L]$ on the bubble $[a,t,\tau]$ is

$$\begin{aligned} r(K,L,a,t,\tau) &= \frac{dm(K,L,a,t,\tau)}{dt} \\ &= r_a(K,L) - r_d(K,L) \\ &= A(a)\left[1 - \frac{m(a,t,\tau)}{\bar{m}(a,t,\tau)}\right] K \bar{M}_s(K,L,t) \\ &\quad - D(K,L)\, m(K,L,a,t,\tau) \end{aligned} \tag{4.4}$$

and the net rate of attachment of all particulate entities on bubble $[a,t,\tau]$ is,

$$r(a,t,\tau) = \int_{L_1}^{L_2} \int_{0}^{\infty} r(K,L,a,t,\tau)\, dK\, dL \tag{4.5}$$

Substitution of equation (4.4) into (4.5) gives

$$r(a,t,\tau) = A(a)\left[1-\frac{m(a,t,\tau)}{\bar{m}(a,t,\tau)}\right]\int_{L_1}^{L_2}\int_{o}^{\infty} K\,\bar{N}_s(K,L,t)\,dK\,dL$$

$$-\int_{L_1}^{L_2}\int_{o}^{\infty} D(K,L)\,m(K,L,a,t,\tau)\,dK\,dL \qquad (4.6)$$

Let $N_b(a,t,\tau)$ be the number of bubbles of specification $[a,t,\tau]$ in the pulp. The mass of particles $[K,L]$ on these bubbles is

$$M_b(K,L,a,t,\tau) = N_b(a,t,\tau)\,m(K,L,a,t,\tau) \qquad (4.7)$$

Therefore, the mass of particles $[K,L]$ on bubbles of all sizes and ages, i.e., on the air phase in the pulp, is

$$M_b(K,L,t) = \int_{o}^{\infty}\int_{o}^{t} N_b(a,t,\tau)\,m(K,L,a,t,\tau)\,d\tau\,da \qquad (4.8)$$

Moreover,

$$m(K,L,a,t,t) = 0 \qquad (4.9)$$

Differentiation of equation (4.8) with respect to time followed by substitution of equation (4.4) results in

$$\frac{dM_b(K,L,t)}{dt} = \int_{o}^{\infty}\int_{o}^{t} N_b(a,t,\tau)\,r(K,L,a,t,\tau)\,d\tau\,da$$

$$+\int_{o}^{\infty}\int_{o}^{t}\frac{dN_b(a,t,\tau)}{dt}\,m(K,L,a,t,\tau)\,d\tau\,da \qquad (4.10)$$

Now the net rate of change of the number of bubbles $[a,t,\tau]$ is

$$\frac{dN_b(a,t,\tau)}{dt} = -\lambda N_b(a,t,\tau) + N_f(a,t,\tau)\,\delta(t-\tau),$$

$$0 \leq \tau < t \qquad (4.11)$$

where λ is inverse of the mean bubble residence time T. Hence

$$\lambda = \frac{1}{T} = \frac{Q}{H} \qquad (4.12)$$

where Q is feed rate of air and H is hold up of air in the perfectly mixed cell. $N_f(a,t,\tau)\,\delta(t-\tau)$ is the rate of number of bubbles of size a fed at time t, and $\delta(t-\tau)$ is the delta function. But

$$N_f(a,t,\tau)\,\delta(t-\tau) = 0, \qquad \tau \neq t$$

$$= N_f(a), \quad \tau = t \qquad (4.13)$$

Combining equations (4.10) and (4.11)

$$\frac{dM_b(K,L,t)}{dt} = \int_0^\infty \int_0^t N_b(a,t,\tau)\, r(K,L,a,t,\tau)\, d\tau\, da$$

$$- \lambda \int_0^\infty \int_0^t N_b(a,t,\tau)\, m(K,L,a,t,\tau)\, d\tau\, da$$

$$+ \int_0^\infty \int_0^t N_f(a,t,\tau)\,\delta(t-\tau)\, m(K,L,a,t,\tau)\, d\tau\, da \qquad (4.14)$$

In view of equations (4.9) and (4.13) the last double integral term vanishes. Further, substitution of equation (4.8) into equation (4.14) results in

$$\frac{dM_b(K,L,t)}{dt} = -\lambda M_b(K,L,t) + \int_0^\infty \int_0^t N_b(a,t,\tau)$$

$$r(K,L,a,t,\tau)\, d\tau\, da \qquad (4.15)$$

The double integral term in this equation will be recognized as the net rate of change of mass of solid particles [K,L] in suspension, viz.,

$$\frac{d\bar{M}_s(K,L,t)}{dt} = -\int_0^\infty \int_0^t N_b(a,t,\tau)\, r(K,L,a,t,\tau)\, d\tau\, da \qquad (4.16)$$

Substitution for $r(K,L,a,t,\tau)$ from equation (4.4) leads to

$$\frac{d\bar{M}_s(K,L,t)}{dt} = -K\bar{M}_s(K,L,t) \int_0^\infty \int_0^t A(a)\, N_b(a,t,\tau)\, d\tau\, da$$

$$+ K\bar{M}_s(K,L,t) \int_0^\infty \int_0^t \frac{m(a,t,\tau)}{\bar{m}(a,t,\tau)}$$

$$A(a)\, N_b(a,t,\tau)\, d\tau\, da + \int_0^\infty \int_0^t D(K,L)$$

$$m(K,L,a,t,\tau)\, N_b(a,t,\tau)\, d\tau\, da \qquad (4.17)$$

Substitution of equation (4.8) gives

$$\frac{d\bar{M}_s(K,L,t)}{dt} = -K\bar{M}_s(K,L,t)\, \phi \left[1 - \frac{\Psi(t)}{\phi}\right] + D(K,L)M_b(K,L,t) \qquad (4.18)$$

where ϕ is a weighted mean bubble size defined as

$$\phi = \int_0^\infty \int_0^t A(a)\, N_b(a,t,\tau)\, d\tau\, da$$

$$= \int_0^\infty A(a)\, N_b(a)\, da \qquad (4.19)$$

where $N_b(a)$ is the steady state number of bubbles of size a in the pulp and $\Psi(t)$ is a time dependent weighted mean bubble size defined as

$$\Psi(t) = \int_0^\infty \int_0^t \frac{m(a,t,\tau)}{\bar{m}(a,t,\tau)} A(a)\, N_b(a,t,\tau)\, d\tau\, da \qquad (4.20)$$

By definition

$$\frac{m(a,t,\tau)}{\bar{m}(a,t,\tau)} \leq 1 \qquad (4.21)$$

It then follows that

$$\Psi(t) \leq \phi \quad \text{for } t \geq 0 \qquad (4.22)$$

Combining equations (4.16) and (4.18) with (4.15)

$$\frac{dM_b(K,L,t)}{dt} = K\bar{M}_s(K,L,t)\,\phi\left[1-\frac{\Psi(t)}{\phi}\right] - D(K,L)\,M_b(K,L,t) - \lambda M_b(K,L,t) \qquad (4.23)$$

Since froth removal is assumed to be very fast and mass of the solids is conserved

$$\frac{d}{dt}\left[\bar{M}_s(K,L,t) + M_b(K,L,t) + M_c(K,L,t)\right] = 0 \qquad (4.24)$$

where $M_c(K,L,t)$ is mass of particles $[K,L]$ in the concentrate. Substitution of equations (4.18) and (4.23) into (4.24) results in

$$\frac{dM_c(K,L,t)}{dt} = \lambda M_b\,(K,L,t) \qquad (4.25)$$

Equations (4.18), (4.23) and (4.25) then formally describe the flotation kinetics. However, even approximate characterization of $\Psi(t)$ by experimental means or from theoretical considerations on the basis of our current understanding of the physical mechanisms of the flotation subprocesses, presents formidable problems. But it is of passing interest to note that some simplification in the model is possible, if it is assumed that $\bar{m}(a,t,\tau)$ is time invariant, i.e.,

$$\bar{m}(a,t,\tau) = \bar{m}(a) \tag{4.26}$$

and both $A(a)$ and $\bar{m}(a)$ increase with increasing bubble size in such a manner that

$$\frac{A(a)}{\bar{m}(a)} = \xi \tag{4.27}$$

where ξ is some unknown parameter independent of bubble size. With these assumptions equation (4.20) can be rewritten as

$$\Psi(t) = \xi \int_0^\infty \int_0^t m(a,t,\tau)\, N_b(a,t,\tau)\, d\tau\, da$$

$$= \xi\, M_b(t) \tag{4.28}$$

Substitution of equation (4.28) into (4.18) and (4.23) leads to following two equations

$$\frac{d\bar{M}_s(K,L,t)}{dt} = -K\bar{M}_s(K,L,t)\, \phi \left[1 - \frac{\xi}{\phi} M_b(t)\right]$$

$$+ D(K,L)\, M_b(K,L,t) \tag{4.29}$$

and

$$\frac{dM_b(K,L,t)}{dt} = K\bar{M}_s(K,L,t)\,\phi\,\left[1-\frac{\xi}{\phi}\cdot M_b(t)\right] - D(K,L)\,M_b(K,L,t) - \lambda M_b(K,L,t) \qquad (4.30)$$

and as before

$$\frac{dM_c(K,L,t)}{dt} = \lambda M_b(K,L,t) \qquad (4.31)$$

The term in square bracket in equations (4.29) and (4.30) explicitly, but only approximately, accounts for the fact that the capacity of bubble phase to accommodate more particles is limited by the amount of particles already present in its surface.

Free Flotation Case:

The potential application of equations (4.18), (4.23) and (4.25) is in the important free flotation case which is frequently encountered in practice[34,91]. Free flotation, which implies that the bubbles are not over loaded, should result when one or more of the following conditions are met. The aeration rate Q is very large, which happens to be invariably true, and D(K,L) is relatively significant in relationship to K. These stipulations concurrently justify the quasi-steady state assumption for $M_b(K,L,t)$, that is

$$\frac{dM_b(K,L,t)}{dt} \longrightarrow 0 \quad \text{as } M_b(K,L,t) \rightarrow 0 \qquad (4.32)$$

Moreover, from the definition of free flotation, it immediately follows that $m/\bar{m} \rightarrow 0$. Therefore, in equation (4.20)

$$\psi(t) \rightarrow 0 \tag{4.33}$$

Substitution of equations (4.32) and (4.33) into (4.23) results in

$$M_b(K,L,t) = \frac{\phi K \bar{M}_s(K,L,t)}{D(K,L) + \lambda} \tag{4.34}$$

Substitution of equations (4.33) and (4.34) into (4.18) and (4.25) and rearrangement of terms results in following two equations

$$\frac{d\bar{M}_s(K,L,t)}{dt} = -Ka\ \bar{M}_s(K,L,t) \tag{4.35}$$

and

$$\frac{dM_c(K,L,t)}{dt} = Ka\ \bar{M}_s(K,L,t) \tag{4.36}$$

where the apparent flotation rate constant is

$$Ka = \frac{\lambda \phi K}{D(K,L) + \lambda} \tag{4.37}$$

Integration of equation (4.35) gives

$$\bar{M}_s(K,L,t) = \bar{M}_s(K,L) \exp\left[-Ka\ t\right] \tag{4.38}$$

where

$$\bar{M}_s(K,L) = \bar{M}_s(K,L,0)$$

Total amount of particulate species of size L, remaining in the pulp is

$$M_s(L,t) = \int_0^\infty \bar{M}_s(K,L) \exp[-Ka\ t]\ dK \qquad (4.39)$$

or

$$M_s(L,t) = \int_0^\infty M_s(Ka,L) \exp[-Ka\ t]\ dKa \qquad (4.40)$$

Here a change of scale from K to Ka has been made so that

$$M_s(Ka,L) = \bar{M}_s(\bar{H}(Ka),L)\ \frac{d\bar{H}(Ka)}{dKa} \qquad (4.41)$$

where $\bar{H}(Ka)$ is a solution to equation (4.37) i.e.

$$K = \bar{H}(Ka) \qquad (4.42)$$

Equation (4.40) is evidently equivalent to equation (2.17) for single size species, and equation (4.37) describes the relationship that exists between the apparent flotation rate constant Ka and the first order attachment rate constant K. This relationship is important not only for the insight it provides into the structure of apparent rate constant in terms of ϕ, λ, K and D but, in theory, it also permits evaluation of $\bar{M}_s(K,L)$ within a constant of proportionality from $M_s(Ka,L)$ since the latter can be computed from experimental data. Further reduction in equation (4.37) is possible when free flotation results from stipulation of very large aeration rate. Thus, when $\lambda >> D(K,L)$, a simple relationship exists between Ka and K

$$Ka = \phi K \qquad (4.43)$$

This equation should be useful for determining the effect of aeration rate on the flotation rate distribution. Moreover, integrating equation (4.40) over entire particle size range gives

$$M_s(t) = \int_0^\infty M_s(L,t)\, dL$$

$$= \int_0^\infty \int_0^\infty M_s(Ka,L) \exp\left[-Ka\ t\right] dKa\ dL$$

$$= \int_0^\infty M_s(Ka) \exp\left[-Ka\ t\right] dKa \qquad (4.44)$$

Thus, we find that in case of dispersed size particulate feed, first order flotation kinetics with distributed apparent flotation rate constant is valid only if the mean residence time of the bubbles is very small.

Recovery and Grade:

Recovery and grade are the two most important aspects of the flotation process. Although, the analysis presented thus far deals with recovery only as given by

$$M_c(L,t) = \int_0^\infty M_c(Ka,L,t)\, dKa \qquad (4.45)$$

it should be noted that the flotation experiments conducted for determination of the distribution $M_s(Ka,L)$ in equation (4.40) by some numerical technique (a suitable algorithm will be presented in the next chapter) can be extended to compute the distribution $V_s(Ka,L)$ also, where $V_s(Ka,L)\, dKa$ is mass of

valuable mineral embedded in the feed of size L which floats with apparent rate constant in range Ka to Ka + dKa. Thus, if we conduct flotation experiments and determine, in addition to $M_s(L,t)$, the mass of valuable mineral $V_s(L,t)$ remaining in cell at time t, Laplace inversion of

$$V_s(L,t) = \int_0^\infty V_s(Ka,L) \exp[-Ka\ t]\ dKa \qquad (4.46)$$

will give $V_s(Ka,L)$. The cumulative grade of the material in pulp is

$$0 \leq G_s(L,t) = \frac{V_s(L,t)}{M_s(L,t)} \leq 1 \qquad (4.47)$$

or

$$G_s(L,t)\ M_s(L,t) = V_s(L,t) \qquad (4.48)$$

Application of Borel's theorem[153] for inversion of the Laplace transform gives

$$V_s(Ka,L) = \int_0^{Ka} G_s(Ka',L)\ M_s(Ka-Ka',L)\ dKa' \qquad (4.49)$$

$G_s(Ka,L)$ will be recognized as the impulse response function in sample space and it relates the two feed distributions $M_s(Ka,L)$ and $V_s(Ka,L)$. $G_s(Ka,L)$ may be calculated by the Laplace inversion of $\frac{V_s(L,t)}{M_s(L,t)}$ experimental data or directly from equation (4.49) by well known techniques.[154]

DISCUSSION AND CONCLUSIONS:

It should be stressed that the approach adopted in our analysis is not unique. One can formulate alternate kinetic model in terms of multivariate distributions which includes the grade of the individual entities, as done by Zaidenberg et al[97]. Our procedure, however, seems to possess inherent advantage of simplicity and practical utility. The analysis of flotation kinetics can be carried out by computing two parallel mathematical streams, one for total mass recovery and other for mass of valuable mineral keeping in mind the fact that these two computations refer to the same particulate entities whose common attribute is Ka or K but the dependent variable is particle mass or its valuable mineral content. In this connection, consider a multivariate distribution as follows:

$$M_1(S,L,\bar{G})\, dS\, dL\, d\bar{G} \qquad (4.50)$$

which is the mass of particles with attribute surface affinity or reactivity including its hydrophobicity ranging from S to S + dS, particle size from L to L + dL and grade (fraction of valuable mineral) in range $\bar{G}$ to $\bar{G}$ + $d\bar{G}$. Here S is an index of particle surface characteristics such as fractional area of the valuable mineral on surface, adsorption of flotation reagents and geometry of particles (in particular high energy

surface locations) which, in turn, may or may not depend on L and $\bar{G}$. Now the particle-bubble attachment rate constant, K, can be expressed as a function of S, L and $\bar{G}$

$$K = K(S,L,\bar{G}) \tag{4.51}$$

Actually K is perhaps a function of particle mass also which is, however, taken care of by inclusion of terms L and $\bar{G}$. It is now possible to convert the density function $M_1(S,L,\bar{G})$ into an alternate trivariate density function $M_2(K,L,\bar{G})$. It is assumed that equation (4.51) can be solved for S as a function of $K,L,\bar{G}$ and, one to one transformation is possible. Let the solution to equation (4.51) be

$$S = \bar{T}(K,L,\bar{G}) \tag{4.52}$$

It then follows that a trivariate distribution in attribute K, L and $\bar{G}$ is

$$M_1(\bar{T}(K,L,\bar{G}),L,\bar{G}) \left[\frac{\partial \bar{T}(K,L,\bar{G})}{\partial K} \right] dK\ dL\ d\bar{G} \tag{4.53}$$

which can be written in simpler notation as

$$M_2(K,L,\bar{G})\ dK\ dL\ d\bar{G} \tag{4.54}$$

Therefore,

$$M_2(K,L) = \int_0^1 M_2(K,L,\bar{G})\ d\bar{G} \tag{4.55}$$

and

$$V(K,L) = \int_0^1 M_2(K,L,\bar{G})\ \bar{G}\ d\bar{G} \tag{4.56}$$

These two distributions are then the points of departure for the kinetic model described here and result in tractable mathematical forms and concurrently provide the desired information with respect to both grade and recovery for a given particle size.

The kinetic model presented here is based on rather simplified formulations of particle bubble attachment detachment rates in equation (4.4). Detailed investigations of particle-bubble aggregation, adherence and detachment subprocesses lead to more complicated relationships which, nontheless, continue to suffer from various assumptions and extreme simplifications. In fact, rigorous derivation of these rates from first principles and explicit solution to the resulting equations is not yet possible.

The following results emerge from the kinetic analysis:

1. The particle-bubble attachment (interception and adherence lumped together)rate constant K is related to the apparent rate constant by equation (4.37).

2. The role of bubble population can be incorporated by a weighted mean $\emptyset$ as in equations (4.18), and (4.23).

3. First order flotation kinetics with respect to distributed K is possible if quasi-steady state assumption in equation (4.30) is made.

4. First order kinetics for all size particles require that the residence time of bubbles be very small.

5. The problem of grade can be simplified considerably by two parallel analyses in total mass and mass of valuable mineral which are related to cumulative grade by equation (4.47).

CHAPTER 5

ESTIMATE OF THE FLOTATION RATE DISTRIBUTIONS

As pointed out earlier also, one of the most important problems in the flotation kinetics analysis is that of evaluation of the flotation rate constant distribution in equation (2.17) which is reproduced here.

$$M_s(t) = \int_0^\infty M_s(Ka) \exp\left[-Ka\ t\right] dKa \qquad (5.1)$$

In this chapter a relatively straight forward method for reliable computation of rate distribution from $M_s(t)$ data, which exploits the structural features of the problem, is presented. The inversion is carried out in term of cumulative distribution rather than the frequency function. The algorithm consists of discretizing the appropriately transformed integral in equation (5.1) by the Lobatto quadrature[155,156] and then carrying out optimization of the resulting constrained variables. First, the general method is developed and then its applications under different conditions of numerically generated data with suitable amount of errors are presented. It may be pointed out that the validity of any estimation method can be established only if one can extract back the distribution that is used to generate the numerical data. The closeness of fit between experimental and computed $M_s(t)$ is an unreliable, even misleading, criterion for this purpose because the Laplace

transform is inherently a very stable operator and consequently $M_s(t)$ is quite insensitive to reasonable variations in $M_s(Ka)$.

NUMERICAL INVERSION OF THE LAPLACE TRANSFORM:

After numerous attempts it was established that success is more readily assured if inversion is carried out in the cumulative distribution mode. This is because the cumulative form of the distribution function is inherently smoother and less sensitive to the influence of errors. Moreover, this mode provides a number of constraints which considerably shorten the region of search in the optimization step and prevent wild fluctuations which tend to occur in the hitherto proposed methods for numerical inversion of the Laplace transform in presence of errors. Let R(Ka) be the normalized cumulative distribution function, hence

$$R(Ka) = \int_{Ka}^{\infty} M_s(Ka') \, dKa' \qquad (5.2)$$

where

$$R(0) = \int_{0}^{\infty} M_s(Ka') \, dKa' = 1 \qquad (5.3)$$

and

$$M_s(Ka) = - \frac{\partial R(Ka)}{\partial Ka} \qquad (5.4)$$

Substitution of equation (5.4) into (5.1) leads to

$$M_s(t) = - \int_{0}^{\infty} \frac{\partial R(Ka)}{\partial Ka} \exp [-Ka\ t] \, dKa \qquad (5.5)$$

Integrating by parts we obtain

$$\bar{M}(t) = \int_0^\infty R(Ka) \exp [-Ka\ t]\ dKa \qquad (5.6)$$

where

$$\bar{M}(t) = \frac{1-M_s(t)}{t} \qquad (5.7)$$

Equation (5.6) is the cumulative distribution analog of equation (5.1) and it is required to extract R(Ka) by inversion of the Laplace transform. By definition of the Laplace transform

$$\bar{M}\left(\frac{t}{s}\right) = \int_0^\infty R(Ka) \exp \left[-\frac{Ka\ t}{s}\right] dKa \qquad (5.8)$$

where s is an adjustable scaling factor, (s > 0). Define a transformation variable x as

$$x = 2 \exp \left[-\frac{Ka}{s}\right] - 1 \qquad (5.9)$$

Therefore,

$$Ka = s \ln \left[\frac{2}{x+1}\right] \qquad (5.10)$$

and

$$dKa = -\left[\frac{s}{x+1}\right] dx \qquad (5.11)$$

Substitution of equations (5.10) and (5.11) into (5.8) gives

$$\bar{M}\left(\frac{t}{s}\right) = \frac{s}{2^t} \int_{-1}^{1} R\left(s \ln \left[\frac{2}{x+1}\right]\right) [x+1]^{t-1}\ dx \qquad (5.12)$$

The limits of the integral are now suitable for a n-point Lobatto quadrature formula for discretization of the integral term. Therefore,

$$\frac{\bar{M}(\frac{t}{s})}{s} = \frac{1}{2^t}\left\{\left[2\,\frac{\bar{F}(1)+\bar{F}(-1)}{n(n-1)}\right] + \sum_{i=2}^{n-1} w_i\ \bar{F}(x_i)\right\} \quad (5.13)$$

where w_i and x_i are i-th weight and abscissa, respectively, of the Lobatto quadrature formula (both are tabulated in the literature[156]) and

$$\bar{F}(x_i) = F(x_i)\ [x_i+1]^{t-1} \quad (5.14)$$

where

$$F(x_i) = R(s \ln [\frac{2}{x_i+1}]) \quad (5.15)$$

When $Ka = 0$

$$X_n = 1 \quad (5.16)$$

and

$$\bar{F}(1) = 2^{t-1} \quad (5.17)$$

Similarly, when $Ka = \infty$

$$x_1 = -1 \quad (5.18)$$

and

$$\bar{F}(-1) = 0 \quad (5.19)$$

On substituting equations (5.17) and (5.19), equation (5.13) is simplified as

$$\frac{\bar{M}\,(\frac{t}{s})}{s} = \frac{1}{n(n-1)} + \frac{1}{2^t}\sum_{i=2}^{n-1} w_i\ F(x_i)\ [x_i+1]^{t-1} \quad (5.20)$$

In equation (5.20), the only unknowns are $F(x_i)$, $i = 2,3,\ldots, n-1$. Equation (5.20) can be solved for $F(x_i)$, and hence for $R(Ka_i)$ since x_i and Ka_i are related by equation (5.9), using some optimization techniques. A least squares objective function of the following form was found to be quite suitable for this purpose.

$$E = \sum_{j=1}^{N} \left\{ \frac{M_s(t_j)}{s} - \frac{1}{n(n-1)} - \frac{1}{2t_j} \sum_{i=2}^{n-1} w_i F(x_i)[x_i+1]^{t_{j-1}} \right\}^2 \tag{5.21}$$

where N is the number of data points, $M_s(t_j)$, $j = 1,2,\ldots, N$. The problem is now reduced to minimization of the objective function with appropriate choice of $F(x_i)$.

The unknown variables of the objective function in equation (5.21) are subjected to a number of constraints which arise from the following properties of the cumulative distribution function:

(i) $R(Ka_i) \geq 0, \quad 0 \leq Ka_i \leq \infty$ (5.22)

(ii) $R(Ka)$ is a monotonically non-increasing function of Ka, i.e.

$$1 \geq R(Ka_1) \geq R(Ka_2) \geq \cdots \geq R(Ka_n) \ldots \geq 0. \tag{5.23}$$

when

$$0 \leq Ka_1 \leq Ka_2 \cdots \leq Ka_m \cdots \leq \infty$$

(iii) $R(0) = 1$ and $R(\infty) = 0$ (5.24)

The Lobatto quadrature formula was chosen because it is exact at the two extremes and, therefore, the last constraint is automatically satisfied (equations (5.17) and (5.19)). The second constraint, which is key to the success of the method, drastically narrows down the region of search to that within the confine of two neighbouring points and prevents wild oscillations. This feature can be readily incorporated in many optimization algorithms such as univariant search method, similar to Friedman and Savage[157] method using Fibonacci search technique[157,158], Rosenbrock[159], Random Search[160] methods etc. The optimization techniques used in this, as well as in following chapters are discussed in Appendix B. Essentially same results were obtained when the initial guess was changed or different optimization methods were employed. It was concluded that this step of the inversion algorithm does not present any special difficulties.

Eight point Lobatto quadrature formula was employed to approximate the integral in equation (5.12), the values of weights and abscissas are given in Table 5.1. In some instances this did not cover adequately the abscissa range of interest especially when function R(Ka) varied sharply over a narrow interval of Ka. This difficulty was readily taken care of by suitable adjustment in the scaling factor s in equation (5.9) in order to generate more points in the region of interest. The optimization was usually initiated with s equal to unity, and subsequently the scaling factor was changed if found necessa-

Table 5.1: Abscissas and Weights of 8 Point Lobatto and Legendre Quadrature Formulae.

Lobatto Quadrature		Legendre Quadrature	
Abscissa	Weight	Abscissa	Weight
1.00000000	0.03571428	0.96028986	0.10122854
0.87174015	0.21070422	0.79666678	0.22238103
0.59170018	0.34112270	0.52553241	0.31370666
0.20929922	0.41245880	0.18343464	0.36268378
-0.20929922	0.41245880	-0.18343464	0.36268378
-0.59170018	0.34112270	-0.52553241	0.31370666
-0.87174015	0.21070422	-0.79666678	0.22238103
-1.00000000	0.03571428	-0.96028986	0.10122854

EVALUATION OF THE METHOD:

1. Error Free Data: The proposed method was tested with numerical data $M_s(t)$ generated from the following test distributions.

(i) Triangular distribution

(ii) Rectangular distribution

(iii) Exponential distribution

(iv) Gamma distribution

(v) Bimodal (mixture of two) gamma distribution.

Table 5.2 gives the assumed values of the parameters in these distributions and the explicit forms of function $M_s(t)$ obtained by substitution of these distributions in equation (5.1), which were then used to generate essentially error free numerical data divided in 20 points at well spaced intervals in range $0.01 \leq M_s(t) \leq 1$. Figures 5.1 and 5.2 show that the cumulative distribution estimated by the proposed inversion technique is in reasonably good agreement with the test distribution in every case. Very accurate inversion of triangular and rectangular distribution is not feasible because of abrupt changes in the slopes of these frequency functions. Intuitively distributions with such sharp variations are not expected to be encountered in case of actual minerals. Fig. 5.2 also illustrates the use of scaling factor for generation of additional points on the curve.

Table 5.2: Functional Form of $\bar{M}_s(Ka)$, $M_s(t)$ and the Values of the Parameters Used for Synthetic Generation of Flotation Data

Distribution	$\bar{M}_s(Ka)$	$M_s(t)$	Values of parameters used in generation of data, $M_s(t)$
Triangular	$\frac{2Ka}{\bar{r}\,\bar{Ka}_m^2}$, $Ka \leq \bar{r}\,Ka_m$	$\frac{2}{\bar{r}(1-\bar{r})\,\bar{K}_m^2\,t^2}$, $Ka \leq \bar{r}\,Ka_m$	$\bar{r} = 0.4$
	$\frac{2(Ka_m-Ka)}{\bar{Ka}_m^2(1-\bar{r})}$, $Ka > \bar{r}\,Ka_m$	$1-\exp[-\bar{r}\,Ka_m\,t] - \bar{r}(1-\exp[-Ka_m\,t])$; $Ka > \bar{r}\,Ka_m$	$Ka_m = 20$
Rectangular	$\frac{1}{Ka_m}$, $0 \leq Ka \leq Ka_m$	$\frac{1-\exp[-Ka_m\,t]}{Ka_m\,t}$	$Ka_m = 20$
Exponential	$\bar{\lambda}\exp[-\bar{\lambda}\,Ka]$	$\left(\frac{\bar{\lambda}}{\bar{\lambda}+t}\right)$	$\bar{\lambda} = 1$

contd...

Contd...

Distribution	$\bar{M}_s(Ka)$	$M_s(t)$	Values of parameters used in generation of data, $M_s(t)$
Gamma	$\dfrac{\bar{\lambda}^{\theta_1} Ka^{\theta_1-1} \exp\left[-\bar{\lambda} Ka\right]}{\Gamma^*(\theta_1)}$	$\left(\dfrac{\bar{\lambda}}{\bar{\lambda}+t}\right)^{\theta_1}$	$\theta_1 = 3,\ \bar{\lambda} = 1$
Bimodal Gamma	$\dfrac{\bar{r}\,\bar{\lambda}^{\theta_1} Ka^{\theta_1-1} \exp[-\bar{\lambda} Ka]}{(\theta_1)} + \dfrac{(1-\bar{r})\,\bar{\lambda}^{\theta_2} Ka^{\theta_2-1} \exp\left[-\bar{\lambda} Ka\right]}{\Gamma(\theta_2)}$	$\bar{r}\left(\dfrac{\bar{\lambda}}{\bar{\lambda}+t}\right)^{\theta_1} + (1-\bar{r})\left(\dfrac{\bar{\lambda}}{\bar{\lambda}+t}\right)^{\theta_2}$	$\bar{\lambda} = 1,\ \theta_1 = 1$ $\theta_2 = 3,\ \bar{r} = 0.2$

* $\Gamma(\theta)$ is gamma function defined as

$$\Gamma(\theta) = \int_0^\infty t^{\theta-1} \exp\left[-t\right] dt, \qquad \theta > 0$$

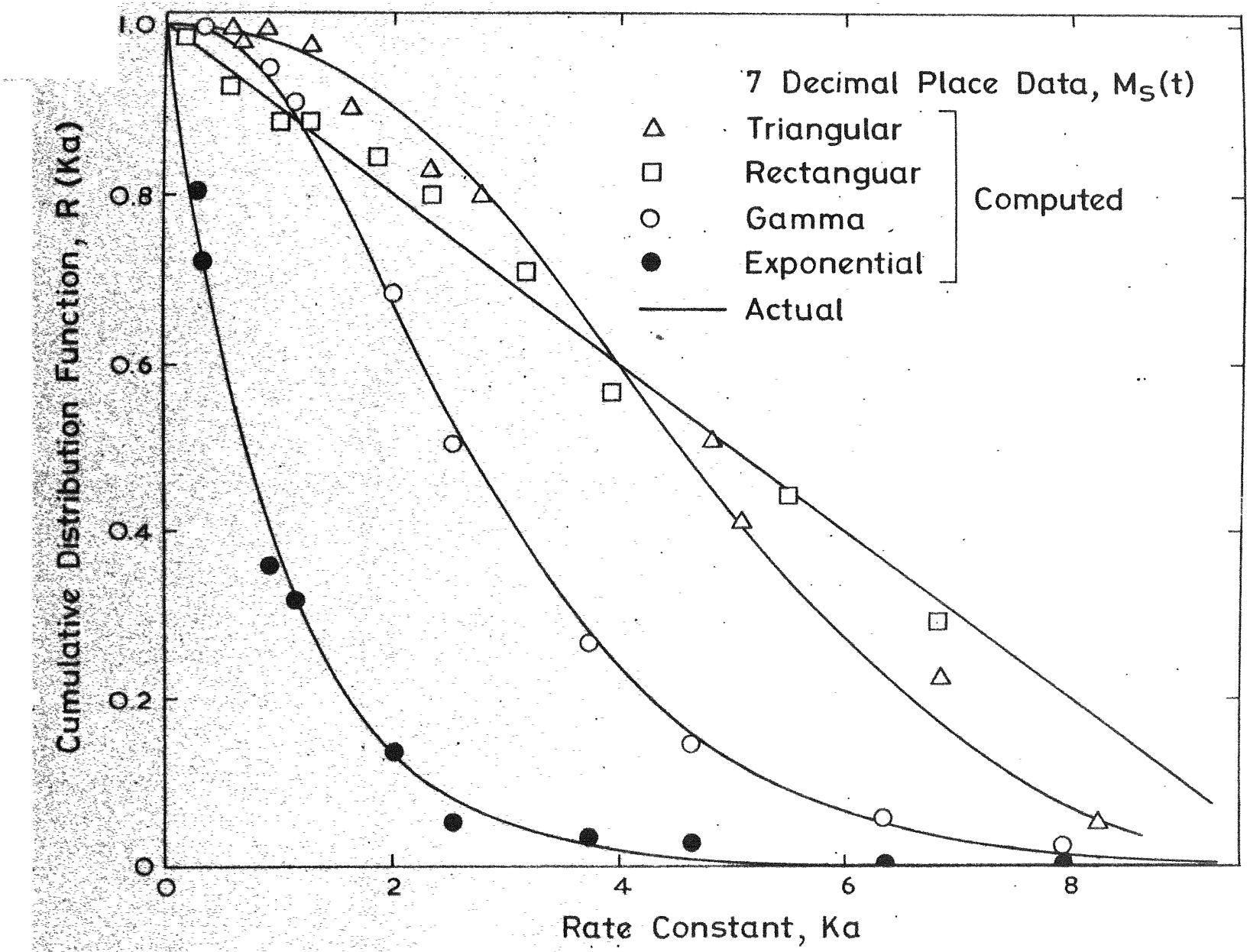

Fig. 5.1 Theoretical and computed triangular, rectangular, gamma and exponential cumulative distributions using 'exact' numerically generated data.

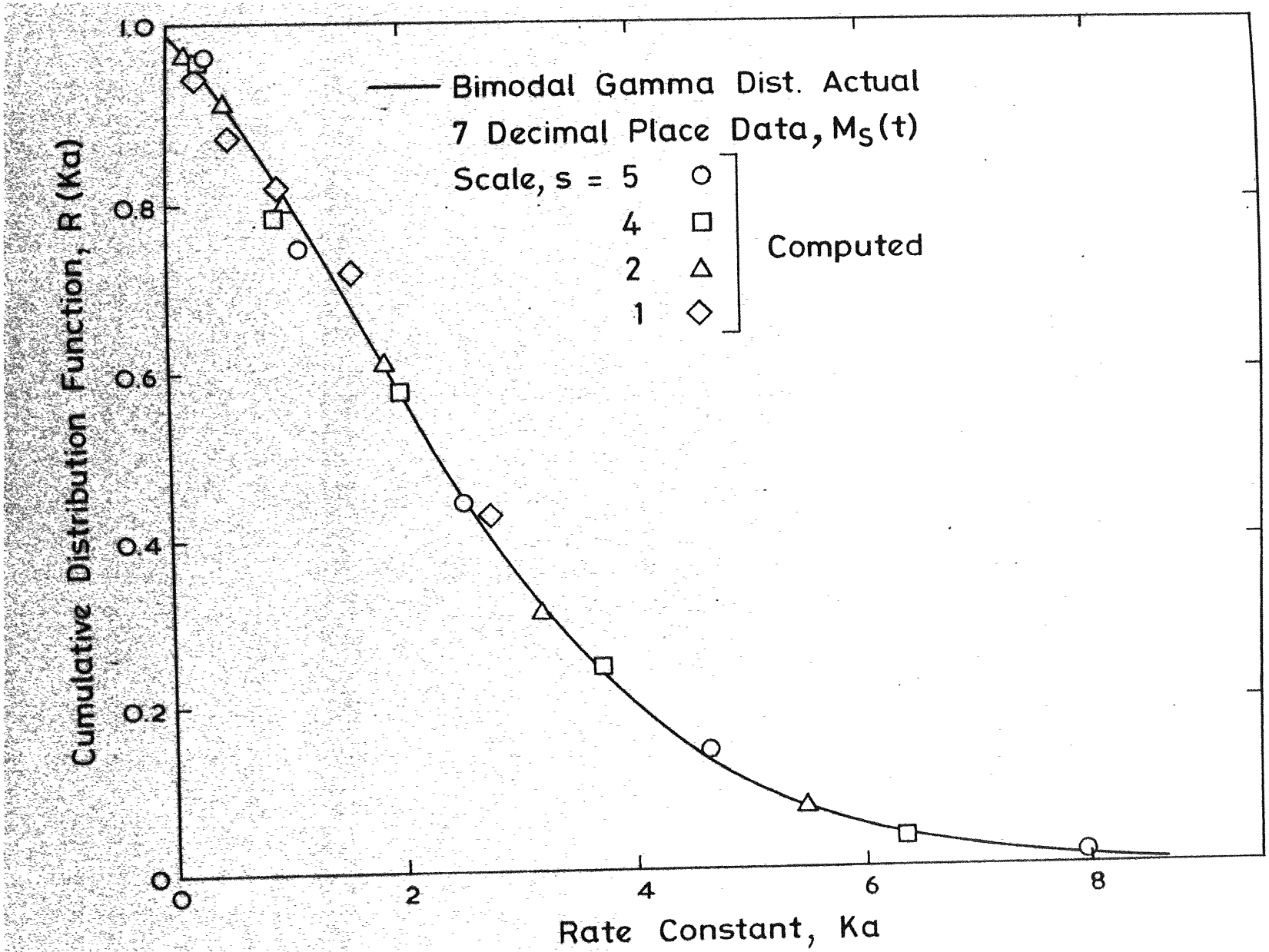

Fig. 5.2 Theoretical and computed cumulative bimodal gamma distribution for different values of scaling factor, s

2. Effect of Errors in the Data:

As mentioned earlier, inversion of the Laplace transform is very sensitive to the accuracy of the data. The effect of errors has been studied for exponential and gamma distributions by rounding off $M_s(t)$ data ($0 < M_s(t) < 1$) beyond 1, 2 and 5 decimal places, using 16 data points at well spaced time intervals. Percentage errors, thus introduced in the $M_s(t)$ data is shown in Fig. 5.3 for the gamma distribution for all three sets of data. It will be seen that with increasing flotation time the data has become progressively degraded. This trend is expected to be in line with actual experimental results as the rate of flotation decreases continuously with time and errors accumulate. Fig. 5.4 shows that, as anticipated, the deviation of calculated distribution from the corresponding theoretical curve increases with increasing error content in $M_s(t)$ but the method is reasonably successful if the data is accurate to two decimal places. It is felt that this degree of accuracy is attainable in a reasonably carefully conducted experiment. Further discussion of the Laplace inversion will be illustrated with two decimal place data only, generated from the gamma distribution. A plot of log $(M_s(t))$ versus t for this distribution is shown in Fig. 5.5. Fig. 5.4 also shows that inversion algorithm is robust in that the test data which were read off directly from the graph in Fig. 5.5 could also be inverted with acceptable precision. The data points shown in

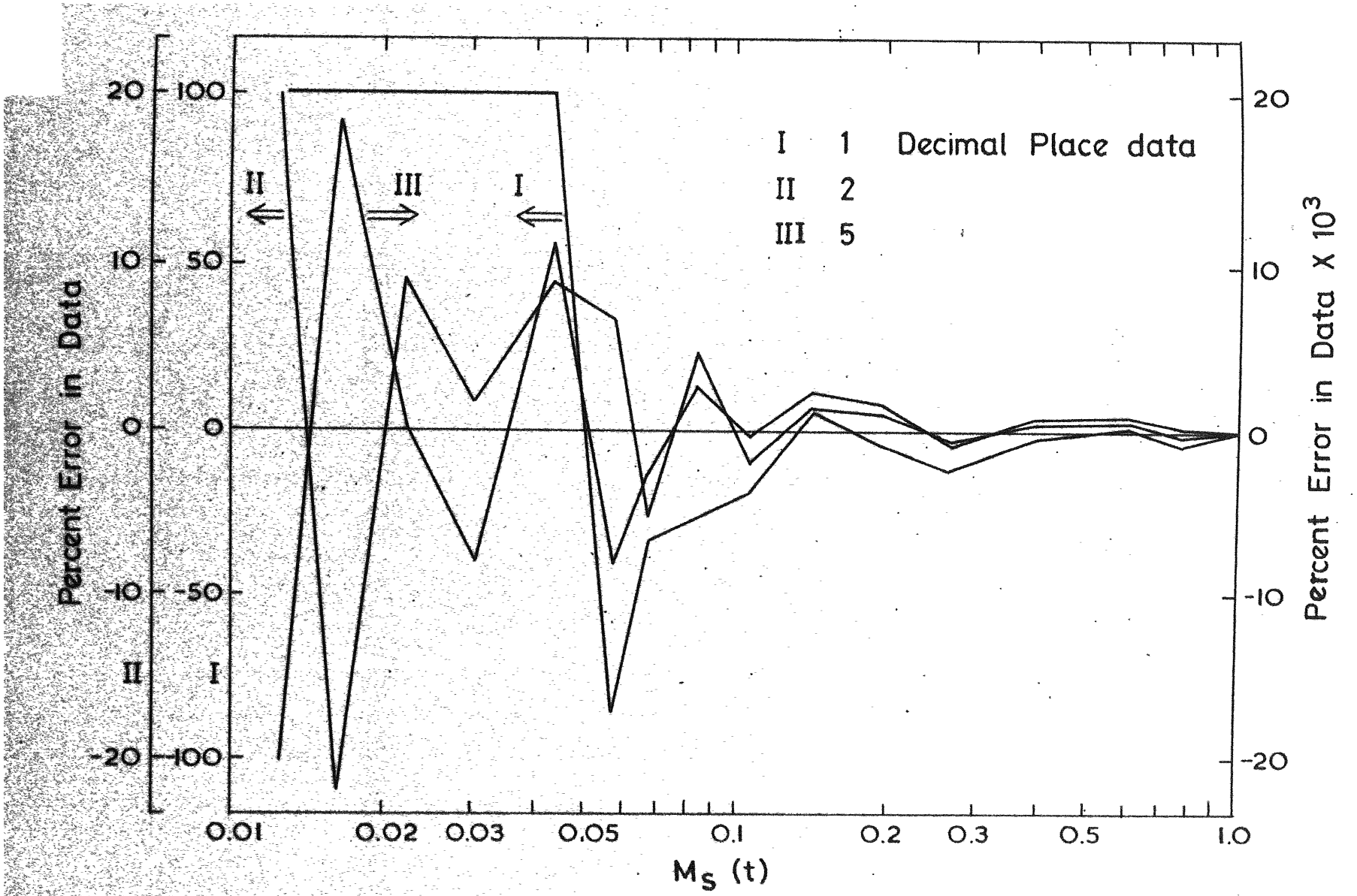

Fig.5.3 Percentage error in synthetic kinetic data accurate to 1,2 and 5 decimal places calculated from the gamma distribution.

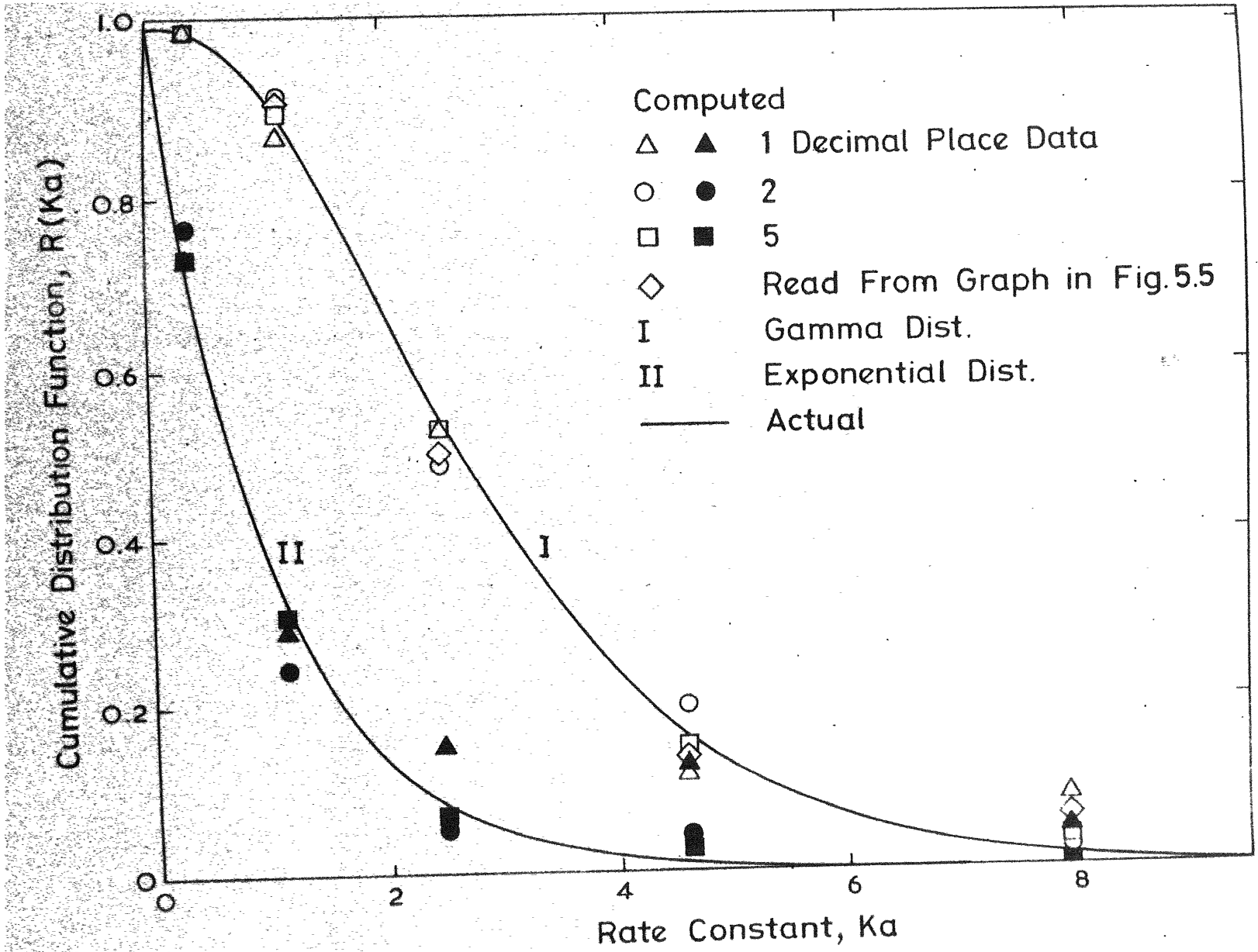

Fig 5.4 Theoretical and computed gamma and exponential distributions illustrating the effect of errors in the data.

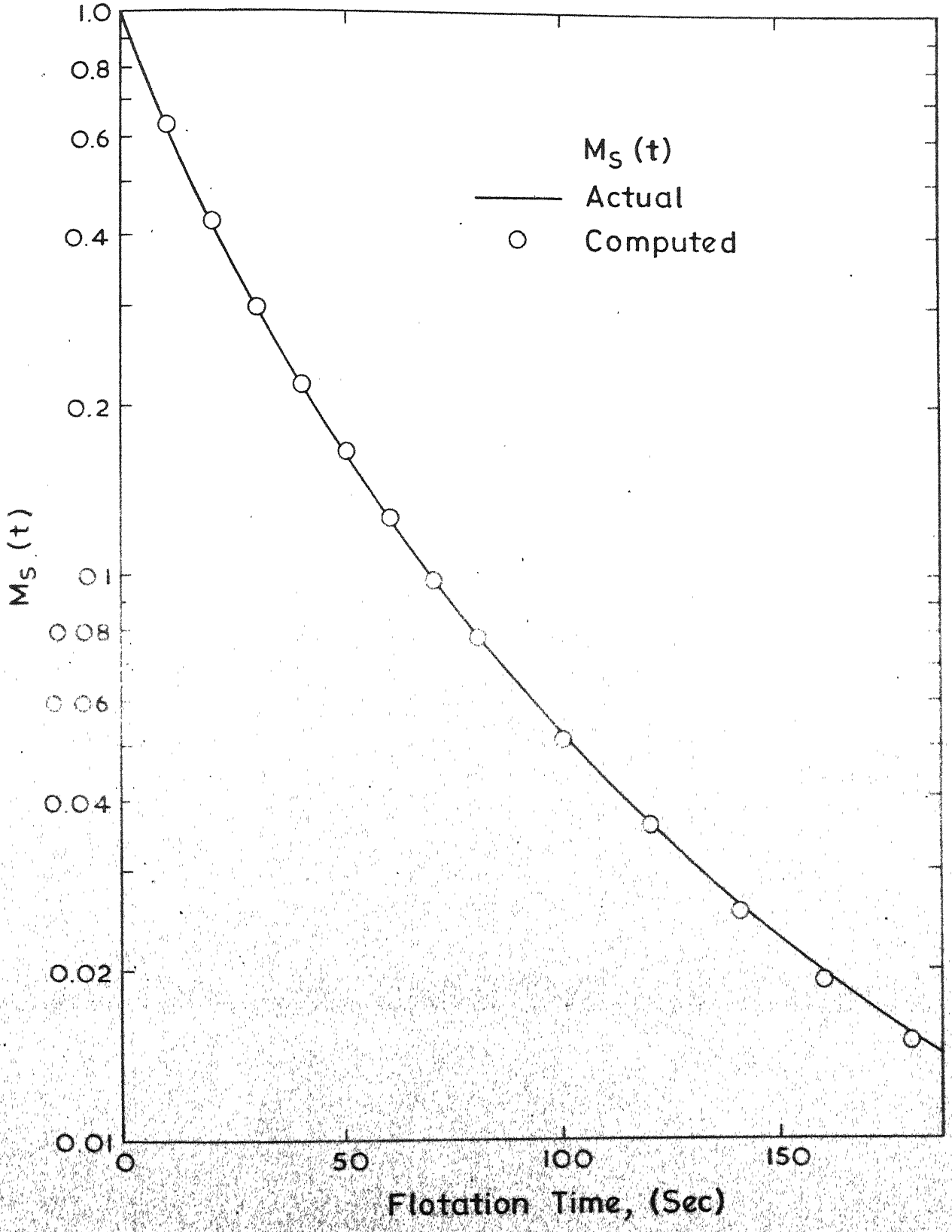

Fig.5.5 Plot of $\log(M_S(t))$ versus time for synthetic data for gamma distribution. Data points are for $M_S(t)$ back calculated from computed gamma distribution in Fig.5.4.

Fig. 5.5 represent $M_s(t)$ values back calculated by substituting the computed gamma function in Fig. 5.4 in equation (5.20) It will be seen that excellent agreement is obtained.

3. Effect of Initial Guess:

It is obvicus that the computational efficiency of the method in optimization step will depend on the choice of the initial guess vector. Fig. 5.6 shows that the widely different starting guesses essentially converged to the optimum value and, therefore, the success of the method does not seem to depend on the choice of the base point. But the search time was found to be strongly correlated with the starting vector.

4. Effect of Number of Data Points:

The effect of number of data points used in inverting the Laplace transform is shown in Fig. 5.7 where the distributions were estimated using 7, 11 and 20 well spaced data points in range of $0.01 < M_s(t) < 1$. It will be seen that the results are quite satisfactory even when only 7 data points were employed. However, it should be emphasized that if relatively small number of data points are used then it is necessary to ensure that the data should be well distributed over the entire range.

5. Effect of Non-Floatables:

The synthetic data employed, thus far, was restricted to floatable species only. In practice one frequently

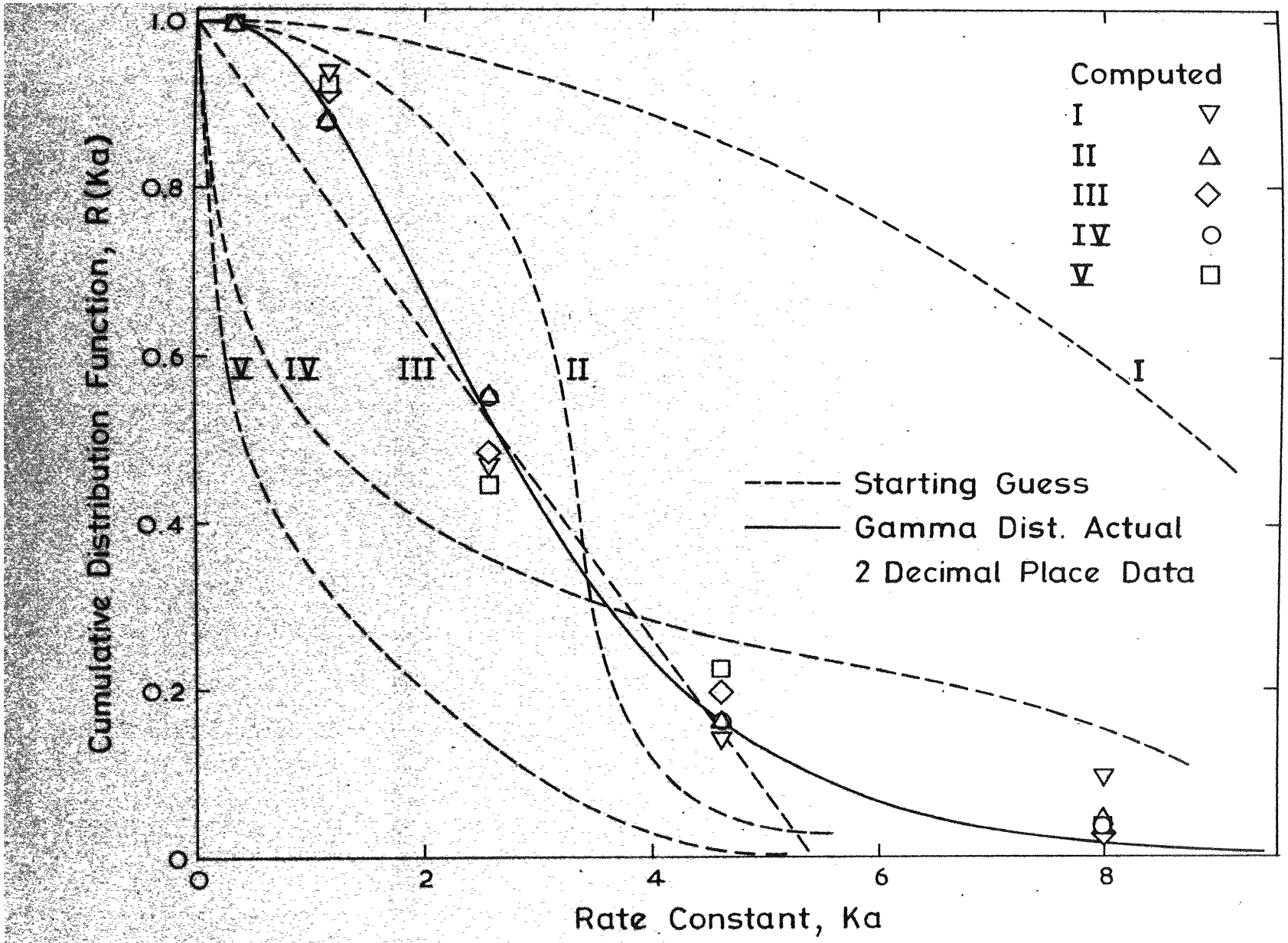

Fig. 5.6 Effect of initial guess in the optimization step on estimation of the flotation rate distribution for the gamma function case.

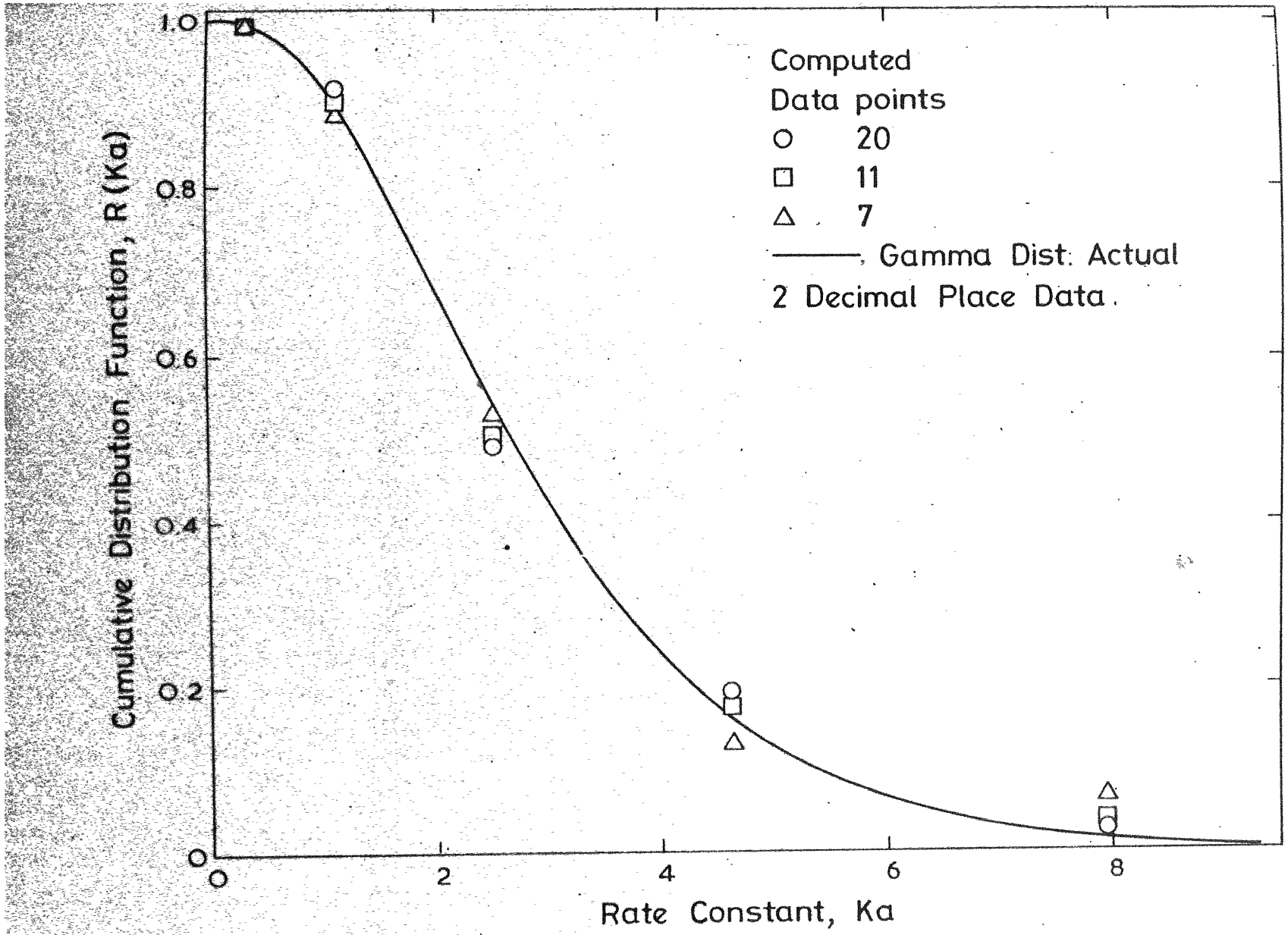

Fig. 5.7 Effect of number of data points in range $M_S(t) = 1$ to 0.01 on computation of flotation rate distribution in case of the gamma distribution.

encounters ores with significant amount of non-floatable component. To examine the applicability of the inversion method for this case, synthetic data with different percentages of non-floatables were generated. Let $M_f(t)$ be the fraction of floatable material remaining in the cell at time t and M_∞ be the fraction of non-floatable in the original feed. The fraction of total material remaining in the cell at time t is given by,

$$M_s(t) = M_f(t)\,[1-M_\infty] + M_\infty \qquad (5.25)$$

where

$$M_s(0) = 1 \qquad (5.26)$$

and

$$M_f(0) = M_s(0)\,[1-M_\infty] \qquad (5.27)$$

$M_s(t)$ data were generated with 10 to 50 percent non floatables. Substitution for $M_f(t)$ in terms of the frequency function $M_s(Ka)$ in equation (5.25) leads to

$$M_s(t) = [1-M_\infty] \int_0^\infty M_s(Ka)\, \exp\,[-Ka\ t\,]\ dKa + M_\infty \qquad (5.28)$$

Substitution of equation (5.4) into (5.28) gives

$$M_s(t) = [1-M_\infty] \int_0^\infty - \frac{\partial R(Ka)}{\partial Ka}\, \exp\,[-Ka\ t]\ dKa + M_\infty \qquad (5.29)$$

Integrating by parts

$$\bar{M}(t) = [1-M_\infty] \int_0^\infty R(Ka)\, \exp\,[-Ka\ t]\ dKa \qquad (5.30)$$

or

$$\bar{M}(t) = \int_0^\infty R'(Ka)\, \exp\,[-Ka\ t]\ dKa \qquad (5.31)$$

where

$$R'(Ka) = [1-M_\infty]\, R(Ka) \tag{5.32}$$

Although equation (5.31) is similar to equation (5.6), it should be noted that now R'(0) is equal to an unknown $[1-M_\infty]$. Thus, one of the end points corresponding to $x_n = 1$ in equation (5.17) is no longer preassigned, and therefore, the Lobatto quadrature cannot be used. Using the transformation in equation (5.9), equation (5.31) is transformed into

$$\bar{M}\left(\frac{t}{s}\right) = \frac{s}{2^t} \int_{-1}^{1} R'\left(s \ln\left[\frac{2}{x+1}\right]\right) [x+1]^{t-1}\, dx \tag{5.33}$$

and discretized using a 8 point Legendre quadrature formula[155]. Now the required objective function corresponding to equation (5.21) becomes

$$\bar{E} = \sum_{j=1}^{N} \left\{ \frac{\bar{M}\left(\frac{t_j}{s}\right)}{s} - \frac{1}{2^{t_j}} \sum_{i=1}^{8} w_i' F'(x_i') [x_i'+1]^{t_j-1} \right\}^2$$

$$= \bar{E}(F_1', F_2', \ldots, F_8') \tag{5.34}$$

subject to constraints

$$0 \le F_1' \le F_2' \cdots \le F_8' \le 1 \tag{5.35}$$

where

$$F'(x_i) = R'\left(s \ln\left[\frac{2}{x_i+1}\right]\right)$$

$$= F_i' \tag{5.36}$$

and w_i' and x_i' are i-th weight and abscissa, respectively, of the 8 point Legendre quadrature formula tabulated in Table 5.1.

Optimization results are shown in Fig. 5.8 and it will be seen that for four cases with M_∞ = 0.1, 0.2, 0.3 and 0.5, the calculated distributions are quite close to the theoretical curves. Since $R'(0)$ is equal to $[1-M_\infty]$, this method automatically gives the amount of non-floatables present in the feed. It should be mentioned that it is also possible to employ Radau's quadrature formula[156] for discretizing the integral which is exact at one of the end points, namely, when $Ka \to \infty$, $R'(Ka) = 0$.

DISCUSSION AND CONCLUSIONS:

The proposed method of estimating the flotation rate distribution by inversion of the Laplace transform has been tested for its reliability using synthetic data based on a number of test distribution functions. It is noteworthy that the method has been shown to actually extract back the distribution function from noisy data, provided the errors are random and unbiased, which has not been demonstrated for earlier methods using graphical or numerical techniques. Moreover, in our approach no a priori assumption is made regarding the form of the distribution function. This has important consequence as shown in Chapter 7. The inversion algorithm is reliable and robust as it can tolerate considerable error in the data which is inevitable in any experimental study. The non-floatables can be estimated also. Estimationof the cumulative distribution rather than the frequency function does not present any difficulty in the sense that the kinetic equations can be reformulated

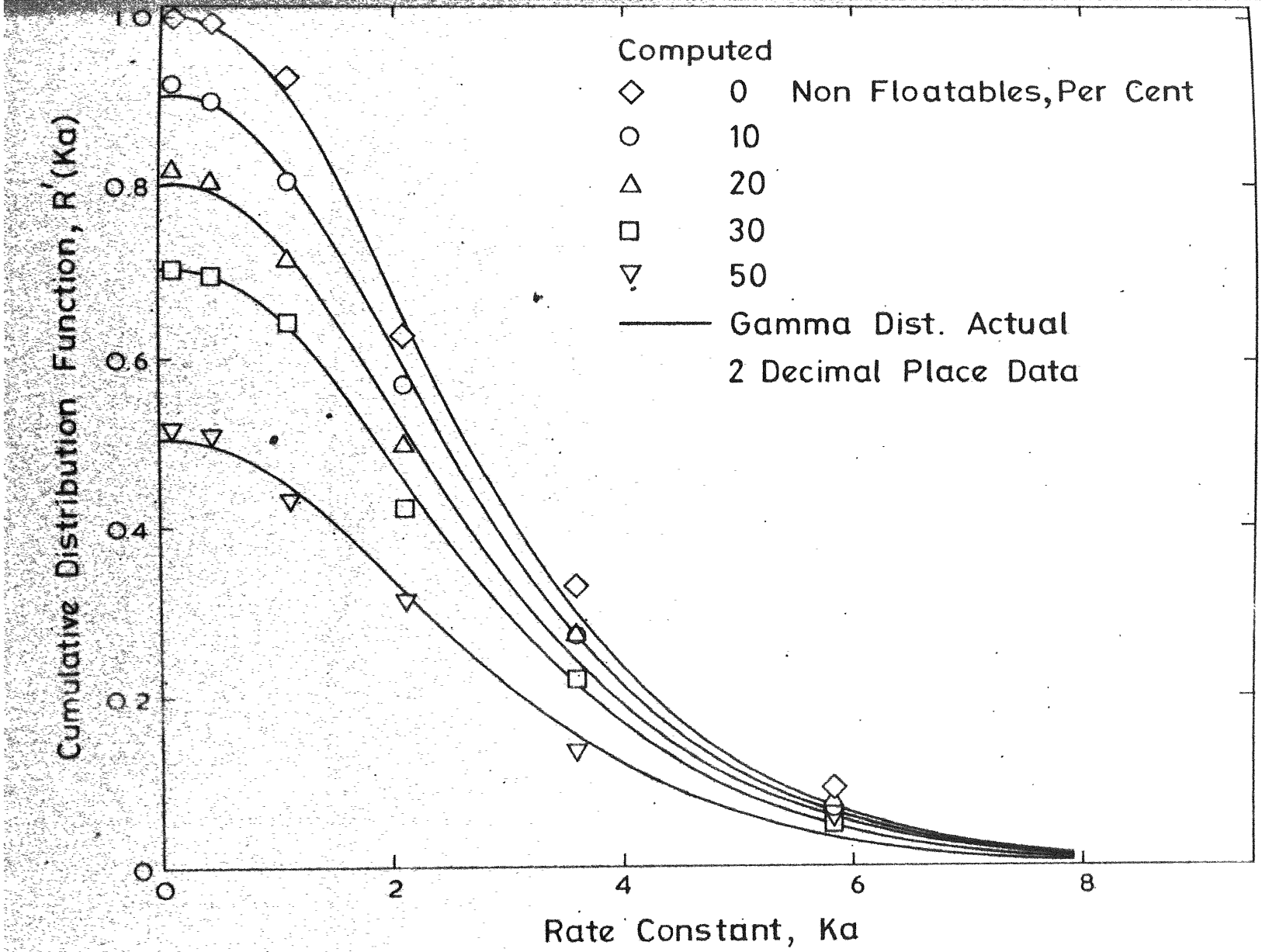

Fig. 5.8 Theoretical and computed cumulative distribution functions for various percentages of non-floatables in synthetic data generated from the gamma distribution.

completely in the cumulative mode. With the availability of the algorithm it is now possible to analyse the structure of the apparent rate constant in terms of particle size, aeration rate, pulp density, flow rate etc. Thus a broad new area for flotation investigation becomes accessible for systematic investigations, some aspects of which are dealt in next two chapters.

CHAPTER 6

THE EFFECTS OF AERATION RATE, PARTICLE SIZE AND PULP DENSITY ON THE FLOTATION RATE DISTRIBUTIONS

As mentioned earlier, most of the studies in past on the effects of process variables on flotation kinetics have been carried out in terms of some average or instantaneous flotation rates or parameters in empirical kinetic expressions, and not in terms of rate constant distribution as a whole. The reason for this can be attributed to the fact that the notion of the rate distributed particulate species is comparatively new and, moreover, till now no satisfactory and reliable method was available for estimation of the apparent flotation rate distribution $M_s(Ka)$ in equation (5.1), given noisy experimental data $M_s(t)$. In this chapter, using some of the numerous experimental data available in the literature, the changes that occur in the flotation rate distribution, as a whole, as a function of aeration rate, particle size and pulp density have been studied. The procedure comprises of the following two steps.

$M_s(t)$ data is employed for computation of the flotation rate distribution by numerical inversion of the Laplace transform in equation (5.1) using the algorithm developed in the preceding chapter. The computed cumulative apparent flotation rate distribution, R(Ka), is then examined for appropriate

relationships between R(Ka) and the aeration rate, particle size and pulp density. In this manner it has been possible to develop useful correlations for the structure of the apparent flotation rate constant Ka in the distributed parameter flotation model and to check the validity of equation (4.43) for the effect of the aeration rate in the phenomenological model developed in Chapter 4.

EFFECT OF AERATION RATE:

Fig. 6.1 shows normalized cumulative distributions in the apparent flotation rate constant Ka for four aeration rates. These were computed from Tewari and Biswas data[118] for four different aeration rates for -140 + 200 mesh (A.S.T.M.) calcite by numerical inversion of the Laplace transform. The data employed for computation of these distributions was read off from the graph and is tabulated in Table 6.1. It will be seen that distributions shift to the right and the flotability increases rapidly with increasing aeration rate.

Under the condition $\gamma >> D(K,L)$, the relationship between apparent flotation rate constant, Ka, and the first order particle to bubble attachment specific rate constant K is given by equation (4.43). The parameter ϕ in this equation, an unspecified function of weighted mean bubble size and hydrodynamic conditions prevailing in the cell, depends primarily on the rate of aeration. The distributions in Fig. 6.1 can now be used to test the validity of this simple relationship.

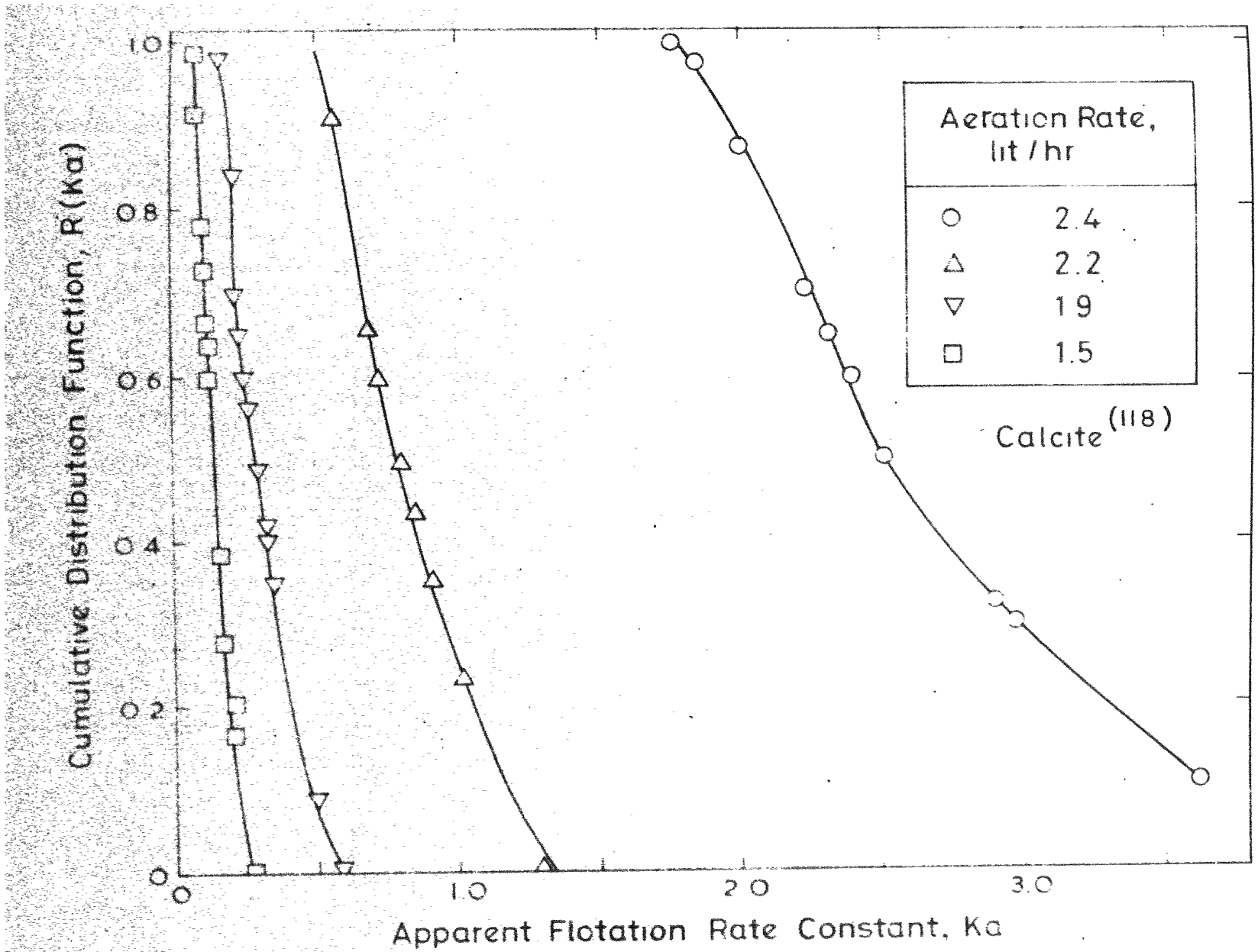

Fig 6.1 Calculated apparent cumulative flotation rate distributions for calcite[118] at four aeration rates.

Table 6.1: Fraction of Calcite Remaining in the Cell at Cumulative Times for Four Aeration Rates[118].

Time (Sec.)	Aeration Rate in litre/min			
	2.4	2.2	1.9	1.5
0	1	1	1	1
6	0.805	0.942	0.980	0.993
15	0.422	0.824	0.945	0.978
30	0.252	0.603	0.876	0.953
45	0.181	0.450	0.795	0.916
60	0.141	0.352	0.705	0.852
75	0.107	0.288	0.624	0.778
90	0.081	0.248	0.544	0.705
105	0.053	0.212	0.485	0.648
120	0.040	0.185	0.440	0.606
135	0.027	0.166	0.410	0.562
150	-	0.146	0.384	0.530
165	-	0.133	0.367	0.500
180	-	0.119	0.350	0.478

By definition, the cumulative rate distribution in attachment rate constant K can be written as

$$\bar{R}(K) = \int_{K}^{\infty} \bar{M}_s(K')\, dK' \tag{6.1}$$

Substituting for K from equation (4.43)

$$\bar{R}(K) = \bar{R}\left(\frac{Ka}{\phi}\right)$$

$$= \int_{Ka}^{\infty} \frac{1}{\phi} \bar{M}_s\left(\frac{Ka}{\phi}\right) dKa \tag{6.2}$$

Equation (4.39) can be rewritten as

$$M_s(t) = \int_{0}^{\infty} \bar{M}_s(K) \exp\left[-Ka\ t\right]\ dK \tag{6.3}$$

Comparison of this equation with (2.17) leads to following equation

$$\bar{M}_s(K)\, dK = M_s(Ka)\, dKa \tag{6.4}$$

Substitution of equation (4.43) results in

$$M_s(Ka) = \frac{1}{\phi} \bar{M}_s(K) \tag{6.5}$$

Combining equations (4.43) and (6.5) with (6.2)

$$\bar{R}\left(\frac{Ka}{\phi}\right) = \int_{Ka}^{\infty} M_s(Ka)\, dKa \tag{6.6}$$

From equations (5.2), (6.2) and (6.6) it follows that

$$R(Ka) = \bar{R}\left(\frac{Ka}{\phi}\right) = \bar{R}(K) \tag{6.7}$$

Since $\bar{R}(K)$ is the cumulative rate distribution in K, it is independent of the aeration rate. In general, the value of the function ϕ is not known, but it can be readily estimated within an uncertainty of a constant of proportionality as follows. Denote the median apparent flotation rate in distribution R(Ka) by Ka(0.5). From equation (6.7)

$$0.5 = R(Ka(0.5)) = \bar{R}\left(\frac{Ka(0.5)}{\phi}\right)$$

$$= \bar{R}(K(0.5)) \qquad (6.8)$$

Hence

$$\frac{Ka(0.5)}{\phi} = K(0.5) \qquad (6.9)$$

But K(0.5) is a constant for a given assembly of conditioned particles. Hence, ϕ is directly proportional to Ka(0.5). Substitution of equation (6.9) in (6.7) gives

$$R(Ka) = \bar{R}\left(\frac{Ka\ K(0.5)}{Ka(0.5)}\right) = \bar{R}(K) \qquad (6.10)$$

The constant K(0.5) may be absorbed in function $\bar{R}$ to give R^* and equation (6.10) becomes

$$R(Ka) = R^*\left(\frac{Ka}{Ka(0.5)}\right) = \bar{R}(K) \qquad (6.11)$$

These relationships along with equation (6.9) imply that for every aeration rate there exists a parameter ϕ, which is proportional to Ka(0.5), such that if the abscissa scale in

plots of R(Ka) versus Ka is divided by the corresponding value of Ka(0.5) the resulting curves for different aeration rates should collapse onto a single similarity distribution R^* equal to $\bar{R}(K)$ which, in turn, is independent of the aeration rate. Fig. 6.2 shows that within limitations of noise in experimental data and computational error in the inversion of the Laplace transform, the similarity distributions R^* as a function of dimensionless similarity variable Ka/Ka(0.5) have indeed collapsed even though Ka(0.5) varied nearly 18 times from 0.14 to 2.5 min^{-1}. It may be concluded that the simple relationship given by equation (4.43) is apparently valid. Fig.6.3 illustrates the rapidly increasing strong dependence of Ka(0.5), (i.e. of $\emptyset$) on the aeration rate. Thus, the rate of aeration can be an important control variable in operation of flotation circuit[118,120,124]. However, in some flotation systems such strong correlation between flotation kinetics and aeration rate has not been found. From the data on bubble size distribution in pulp it is also possible to extract some approximate information on the nature of the function of $\emptyset$ since in view of equation (6.9), there might exist a moment of the bubble size distribution which may be proportional to Ka(0.5).

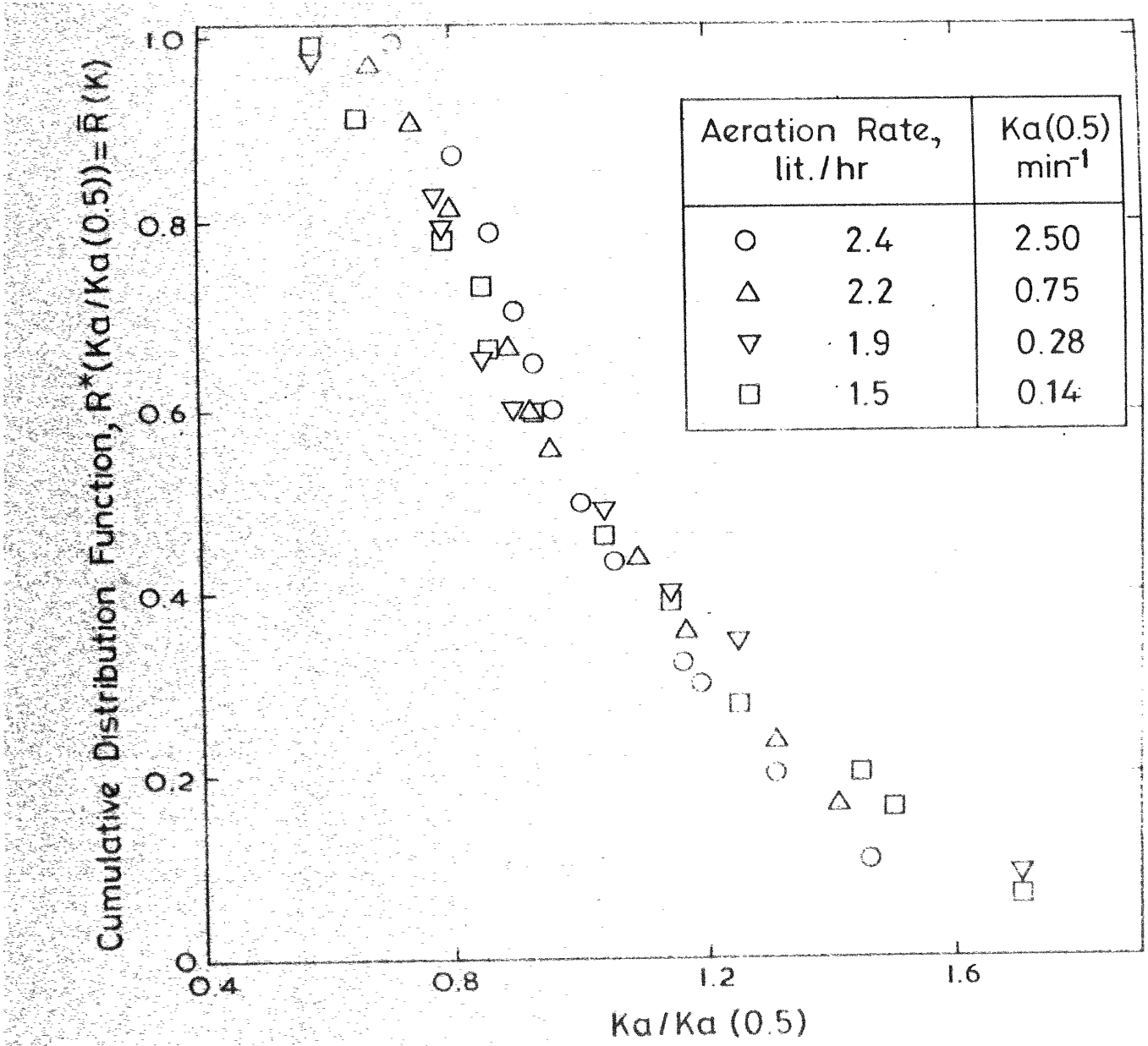

Fig 6.2 Self-similar form of apparent cumulative flotation rate distribution for calcite as a function of dimensionless flotation rate constant Ka / Ka(0.5)

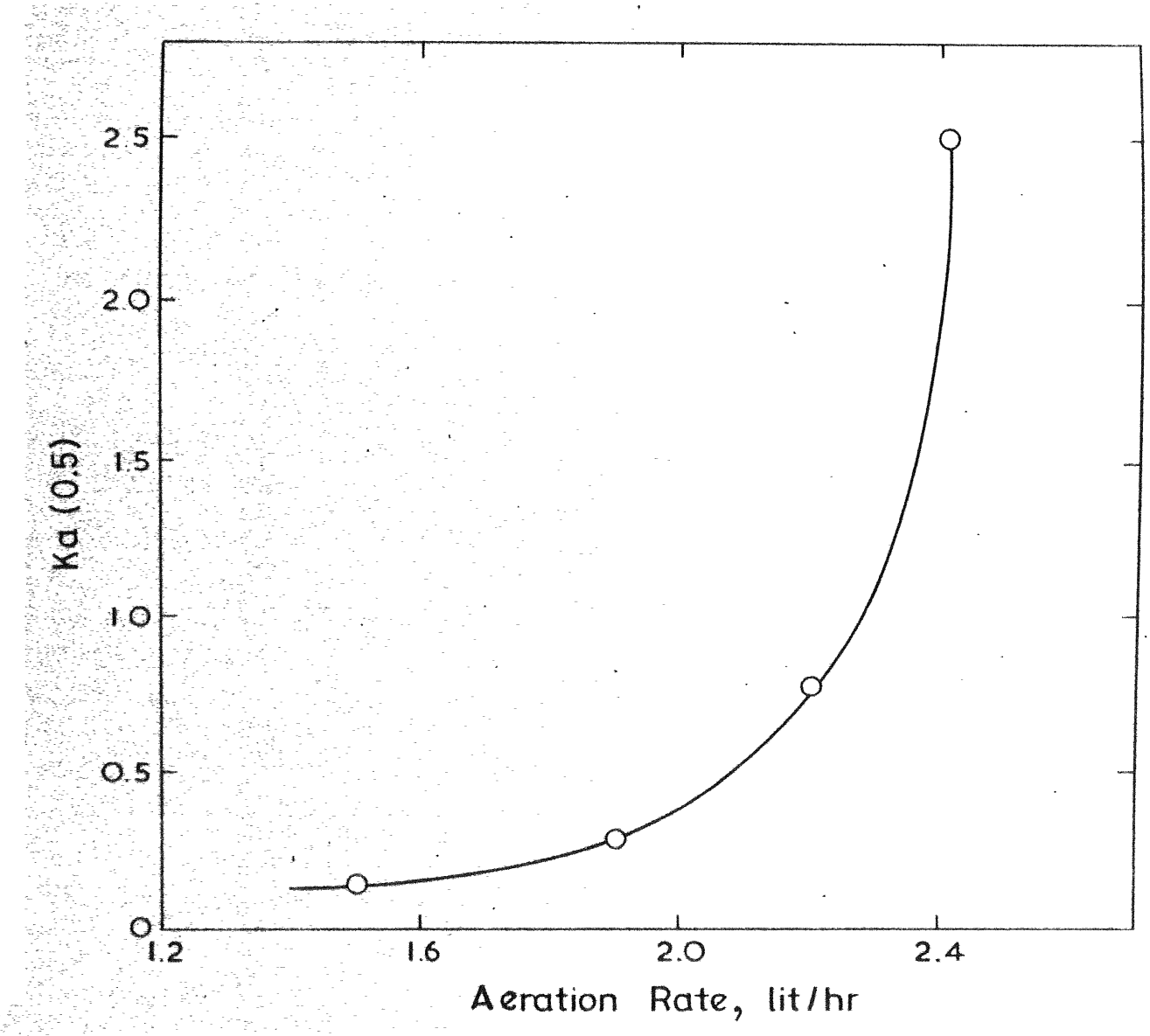

Fig.6.3 Median apparent flotation rate, which is proportional to ϕ in Eq.(6.9), as a function of aeration rate.

EFFECT OF PARTICLE SIZE:

Figs. 6.4, 6.5, 6.6 and 6.7 show the apparent flotation rate distributions computed from Tewari and Biswas data for four size fractions of calcite[118], Tomlinson and Fleming data for five size fractions of apatite[34], and Volin and Swami data for five size fractions of hematite and for six size fractions of magnetite particles[30], respectively. The data employed for computation of these rate constant distributions is reported in Tables 6.2, 6.3, 6.4 and 6.5. In first three cases the originally reported data was in graphical form whereas in the latter two cases it was in tabulated form. In some cases of tabulated data where number of data points was not sufficient graphical interpolation was carried out. Interpolated points have been tabulated along with the reported data points in Table 6.4 and 6.5. We shall now investigate if the approach taken in the previous section can be extended for analysis of the particle size effect also.

It is assumed that the contribution of the particle size in particle to bubble attachment rate constant K may be separated in the following manner

$$K = \eta(L)K^{o} \qquad (6.12)$$

where $\eta(L)$ is a function of particle size only and K^{o}, the reduced rate constant, depends on grade and surface hydrophobicity which is assumed to be independent of particle size. Combining equation (6.12) with (4.43)

$$Ka = \phi\, \eta(L) K^{o} \tag{6.13}$$

When the aeration rate is held constant this equation may be rewritten for convenience as

$$Ka = \bar{\eta}(L)\ K^{o} \tag{6.14}$$

and

$$\bar{\eta}(L) = \phi\, \eta(L) \tag{6.15}$$

Following the arguments, used in derivation of equations (6.1) to (6.11), it is possible to derive a relationship between cumulative rate distribution in terms of Ka and cumulative rate distribution in K^{o}, $R^{o}(K^{o})$. Again by definition

$$R^{o}(K^{o}) = \int_{K^{o}}^{\infty} M_{s}^{o}\ (K^{o})\ dK^{o} \tag{6.16}$$

where M_{s}^{o} is the frequency function in K^{o}. Substitution of equation (6.14) into (6.16) gives

$$R^{o}\left(\frac{Ka}{\bar{\eta}}\right) = \int_{Ka}^{\infty} \frac{1}{\bar{\eta}}\, M_{s}^{o}\ \left(\frac{Ka}{\bar{\eta}}\right)\ dKa \tag{6.17}$$

Let

$$M_{s}(Ka) = \frac{1}{\bar{\eta}}\, M_{s}^{o}\ \left(\frac{Ka}{\bar{\eta}}\right) \tag{6.18}$$

Substitution of equation (6.18) into (6.17) leads to

$$R^{o}\ \left(\frac{Ka}{\bar{\eta}}\right) = \int_{Ka}^{\infty} M_{s}(Ka)\ dKa$$

$$= R(Ka) \tag{6.19}$$

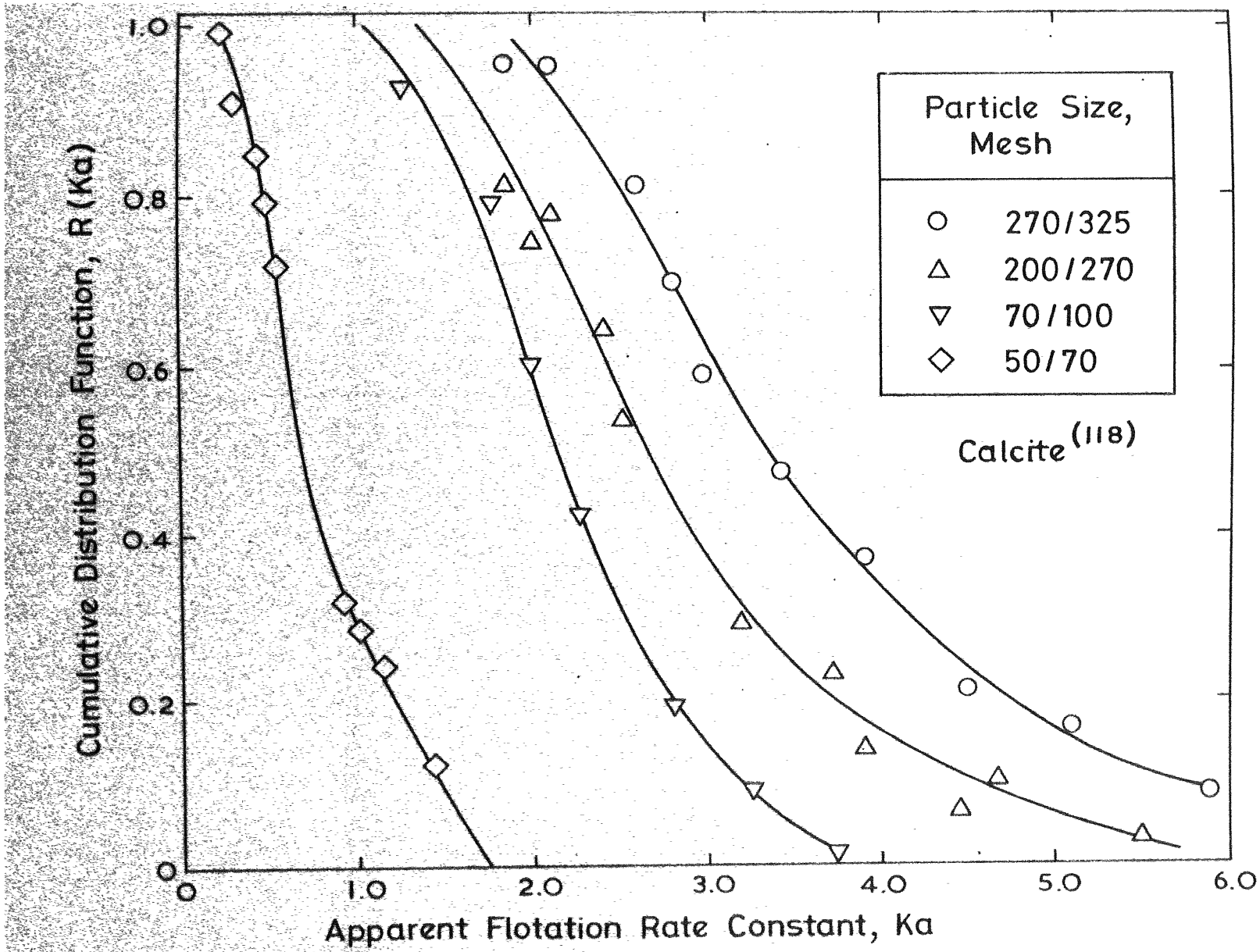

Fig.6.4 Calculated apparent flotation rate distributions for calcite[118] for four particle sizes.

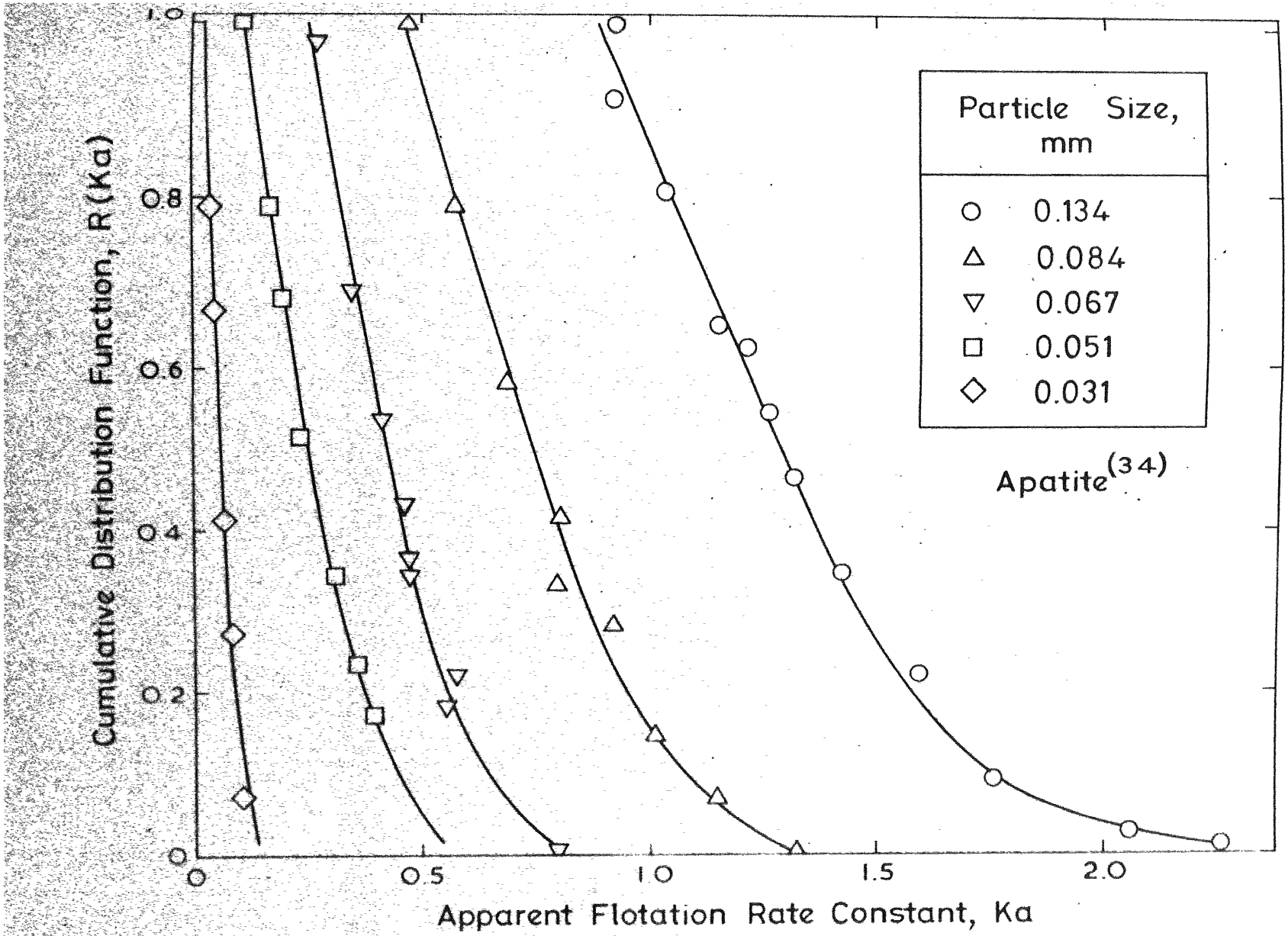

Fig.6.5 Calculated apparent flotation rate distributions for apatite[34] for five particle sizes.

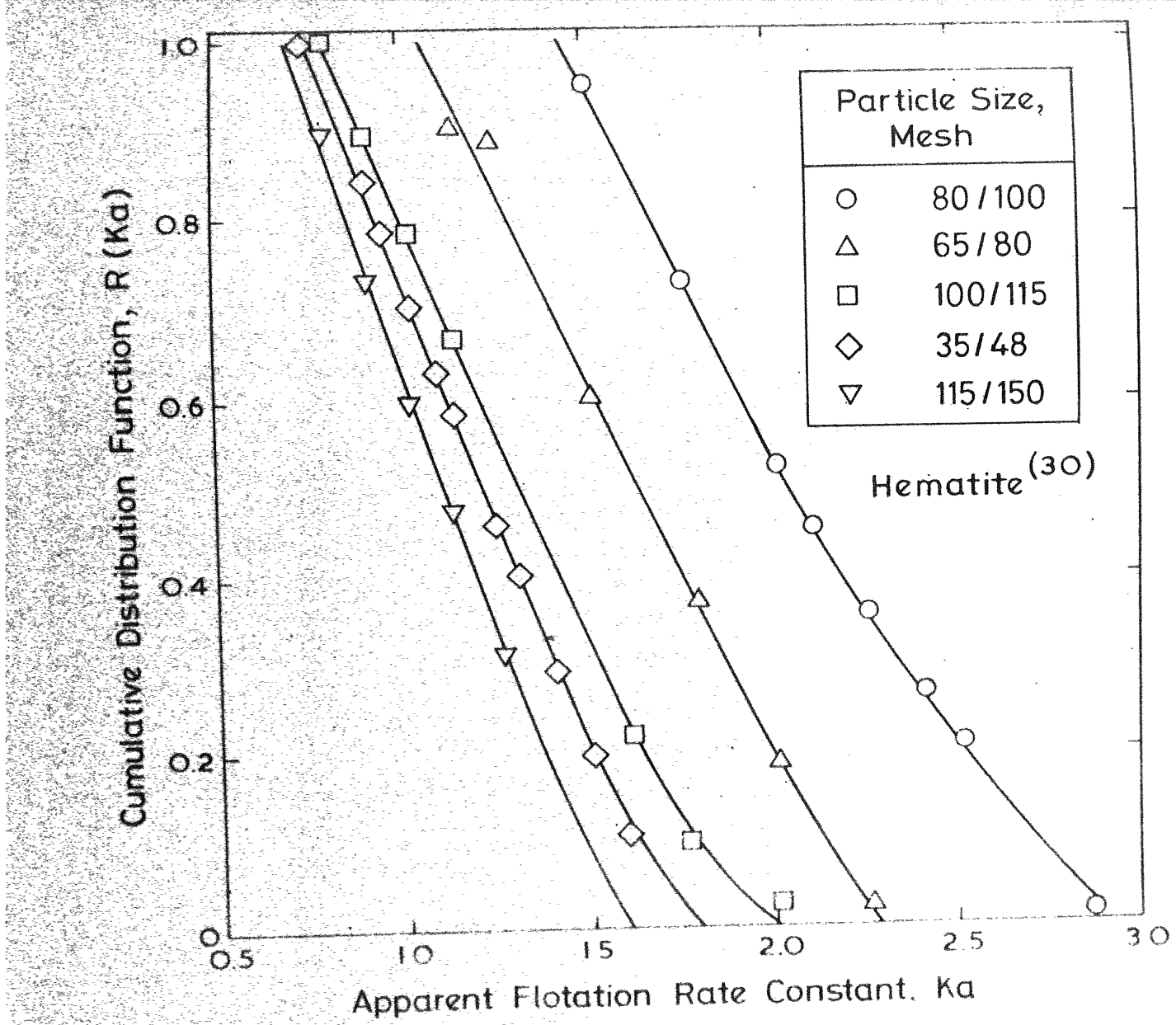

Fig.6.6 Calculated apparent flotation rate distributions for hematite[30] for five particle sizes.

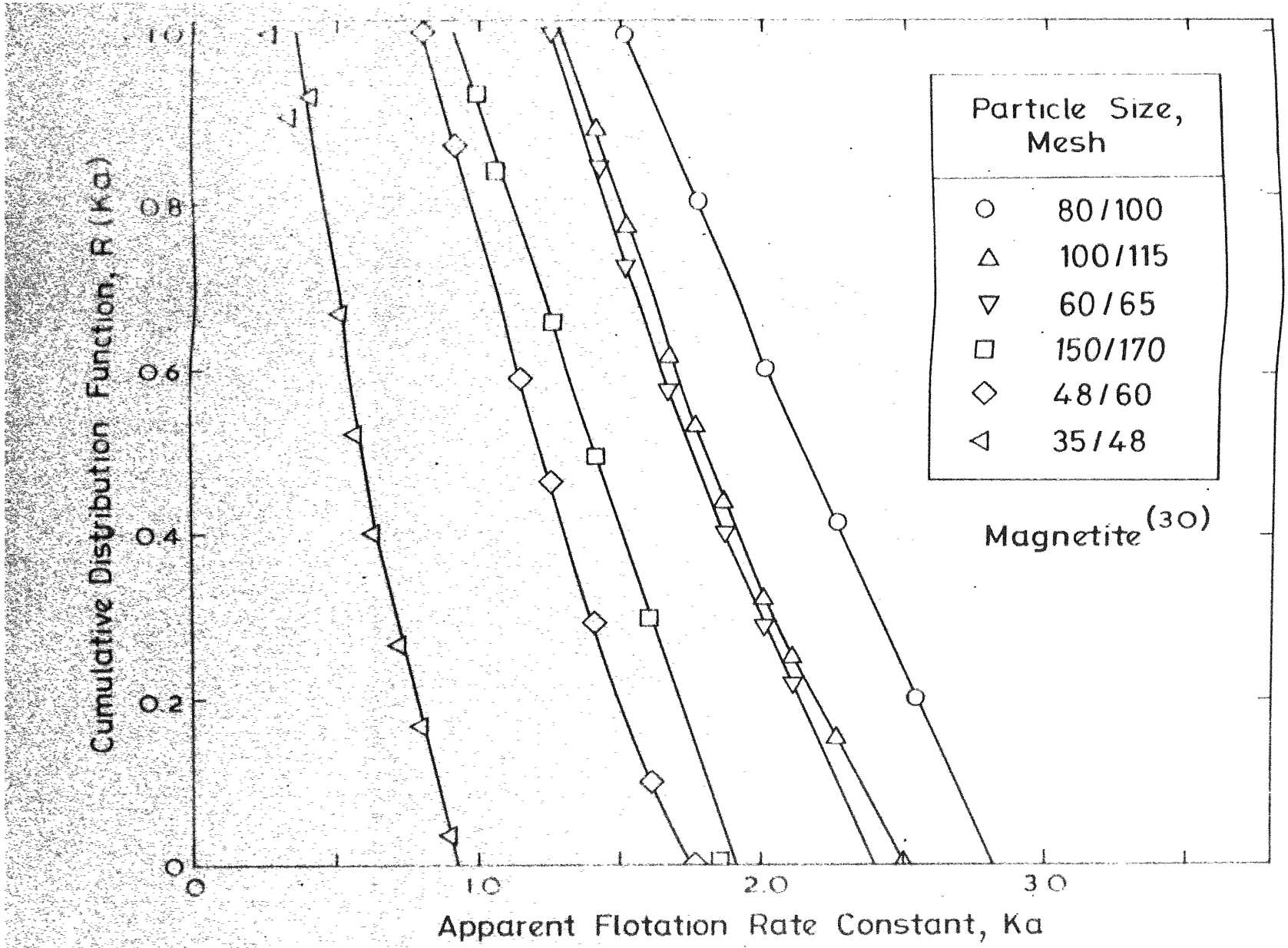

Fig 6.7 Calculated apparent flotation rate distributions for magnetite[30] for six particle sizes

Table 6.2 Fraction of Calcite Remaining in the Cell at Cumulative Times for Four Particle Size Fractions[118].

Time (Sec.)	Particle Size in Mesh			
	-270+325	-200+270	-70+100	-50+70
0	1	1	1	1
6	0.722	0.775	0.829	0.927
12	0.451	0.564	0.658	0.855
18	0.342	0.388	0.447	0.756
24	0.288	0.338	0.356	0.684
30	0.252	0.293	0.290	0.619
45	0.180	0.226	0.211	0.514
60	0.144	0.180	0.168	0.441
75	0.126	0.148	0.132	0.395
90	0.117	0.141	0.118	0.358
105	0.108	0.134	0.108	0.337
120	0.094	0.127	0.095	0.314
135	0.086	0.124	0.082	0.303
150	0.076	0.113	0.066	0.283

Table 6.3: Fraction of Apatite Remaining in the Cell at Cumulative Times for Five Particle Size Fractions[34].

Time (Sec.)	Particle size in microns				
	134	84	67	51	31
0	1	1	1	1	1
10	0.853	0.910	0.945	0.967	0.980
15	0.780	0.865	0.915	0.950	-
20	0.680	0.804	0.880	0.925	0.962
30	0.480	0.680	0.810	0.883	0.940
40	0.350	0.595	0.745	0.845	0.925
50	0.265	0.515	0.690	0.805	0.910
60	0.220	0.450	0.630	0.775	0.890
70	0.180	0.380	0.580	0.740	0.877
80	0.155	0.335	0.530	0.710	0.865
90	0.090	0.300	0.500	0.680	0.850
100	0.080	0.265	0.470	0.650	0.835
110	0.070	0.235	0.440	0.627	0.820
120	0.050	0.220	0.413	0.605	0.800
130		0.190	0.385	0.585	0.785
140		0.175	0.370	0.563	0.775
150		0.160	0.350	0.545	0.760
160		0.140	0.330	0.530	0.750
170		0.125	0.315	0.515	0.735
180		0.115	0.300	0.500	0.725
190		0.100	0.290	0.485	0.720
200		0.085	0.275	0.470	0.705
210		-	0.260	0.460	0.690

Table 6.4: Fraction of Hematite Remaining in the Cell at Cumulative Times for Five Particle Size Fractions[30].

Time (Sec.)	Particle size in mesh				
	35-48	65-80	80-100	100-115	115-150
0	1	1	1	1	1
5	0.901	0.865	0.855	0.901	0.925
10	0.825	0.738	0.722	0.805	0.850
15	0.756	0.606	0.605	0.732	0.779
20	0.670	0.528	0.505	0.638	0.705
25	-	-	0.387	-	-
30	0.546	0.366	0.288	0.492	0.593
40	-	0.248	0.170	-	-
45	0.363	0.185	0.133	0.312	0.402
60	0.244	0.096	0.057	0.146	0.263
75	0.135	0.054	0.024	0.079	0.163
90	0.091	0.031	0.013	0.042	0.100
105	0.065	0.022	-	0.022	0.051
120	0.049			0.013	0.028
135	0.038			0.010	0.020
150	0.023			0.007	0.014

Table 6.5: Fraction of Magnetite Remaining in the Cell at Cumulative Times for Six Particle Size Fractions[30].

Time (Sec.)	Particle size in mesh					
	35–48	48–60	60–65	80–100	100–115	150–170
0	1	1	1	1	1	1
5	0.960	0.928	0.880	0.864	0.900	0.920
10	–	0.850	0.775	0.740	0.790	0.822
15	0.880	0.771	0.664	0.618	0.673	0.730
20	–	–	0.580	0.520	0.562	0.638
25	–	0.630	0.500	0.431	0.465	0.526
30	0.782	0.551	0.424	0.300	0.372	0.466
40	–	–	0.279	0.170	0.235	0.342
45	0.666	0.330	0.212	0.107	0.175	0.293
60	0.542	0.159	0.081	0.025	0.094	0.204
75	0.430	0.040	0.018	–	0.041	0.143
90	0.309	0.011	–	–	0.014	0.091
105	0.168	0.008	–	–	–	0.056
120	0.080	–	–	–	–	0.018

From equations (6.16) and (6.19) it follows that

$$R(Ka) = R^{o}\left(\frac{Ka}{\bar{\eta}}\right) = R^{o}(K^{o}) \qquad (6.20)$$

For median apparent flotation rate constant, equation (6.20) can be written as

$$0.5 = R(Ka(0.5)) = R^{o}\left(\frac{Ka(0.5)}{\bar{\eta}}\right) = R^{o}(K^{o}(0.5)) \qquad (6.21)$$

Hence

$$\frac{Ka(0.5)}{\bar{\eta}} = K^{o}(0.5) \qquad (6.22)$$

Since $K^{o}(0.5)$ is independent of particle size for a given assembly of conditioned particles, it follows then that $\bar{\eta}$ is directly proportional to Ka(0.5). Substitution in equation (6.20) leads to

$$R(Ka) = R^{o}\left(\frac{Ka\ K^{o}(0.5)}{Ka(0.5)}\right) = R^{o}(K^{o}) \qquad (6.23)$$

Absorbing constant $K^{o}(0.5)$ in R^{o} and denoting the resulting distribution by $R^{\neq}$

$$R(Ka) = R^{\neq}\left(\frac{Ka}{Ka(0.5)}\right) = R^{o}(K^{o}) \qquad (6.24)$$

Accordingly, plots of R(Ka) as a function of Ka/Ka(0.5) should collapse onto a single similarity distribution $R^{\neq}$, equal to $R^{o}(K^{o})$, which is independent of the particle size. Figs.6.8, 6.9, 6.10 and 6.11 show that the distributions in Figs.6.4, 6.5,6.6 and 6.7, respectively have indeed collapsed, within error limits, and the validity of equation (6.14) is thus

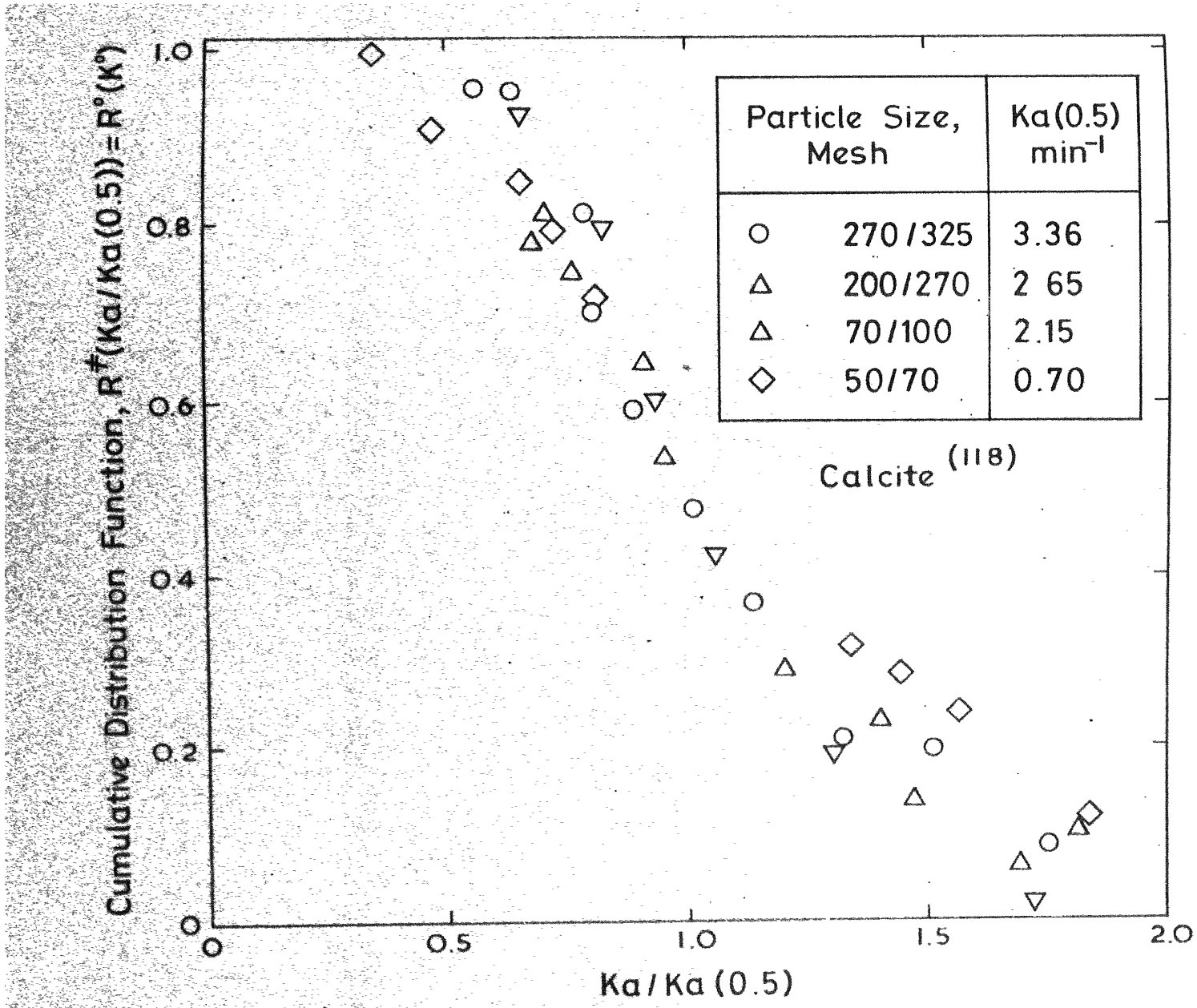

Fig. 6-8 Self-similar form of apparent cumulative flotation rate distribution for calcite as a function of dimensionless flotation rate constant Ka/Ka(0.5).

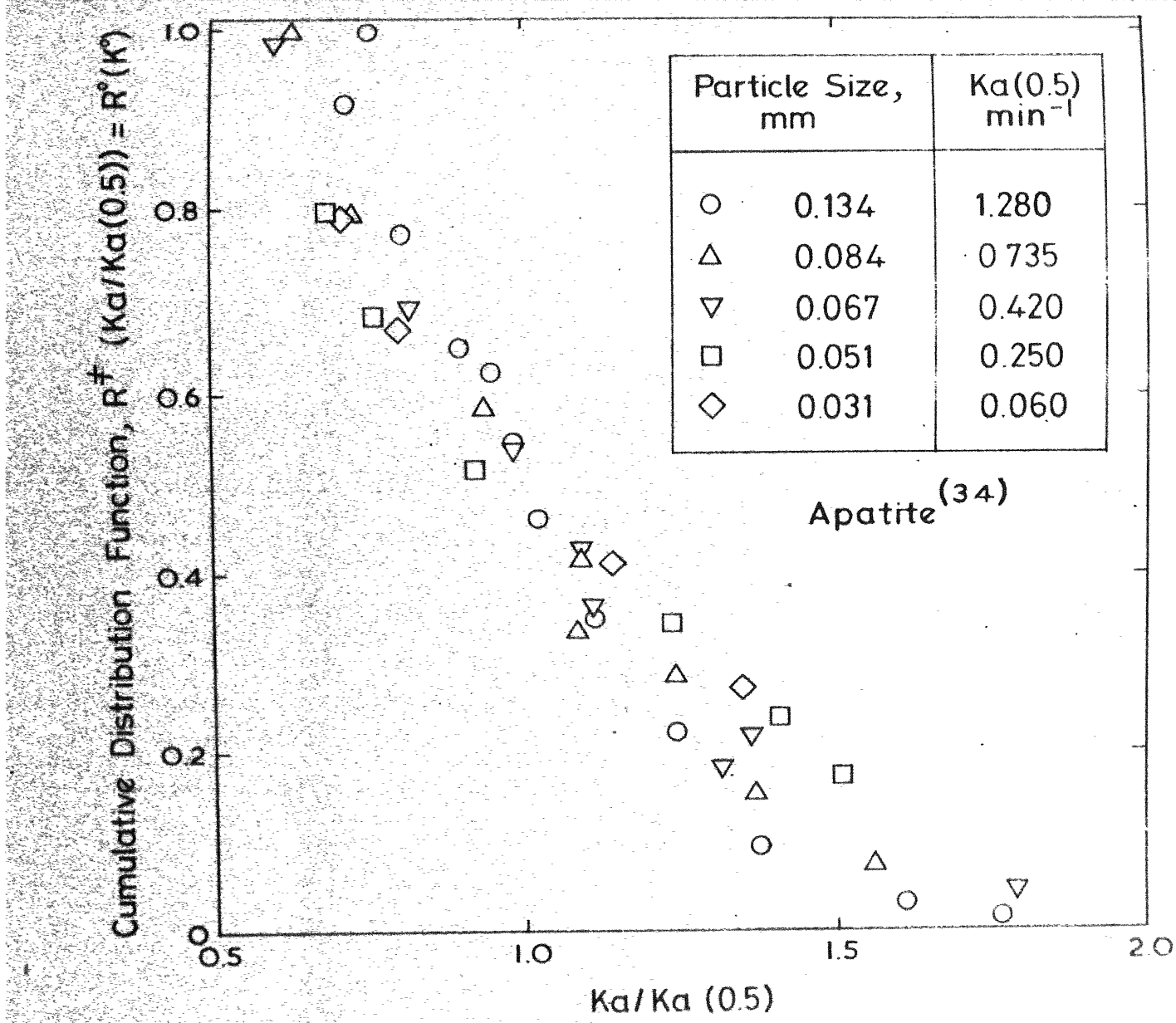

Fig.6.9 Self-similar form of apparent cumulative flotation rate distribution for apatite as a function of dimensionless flotation rate constant Ka/Ka (0.5).

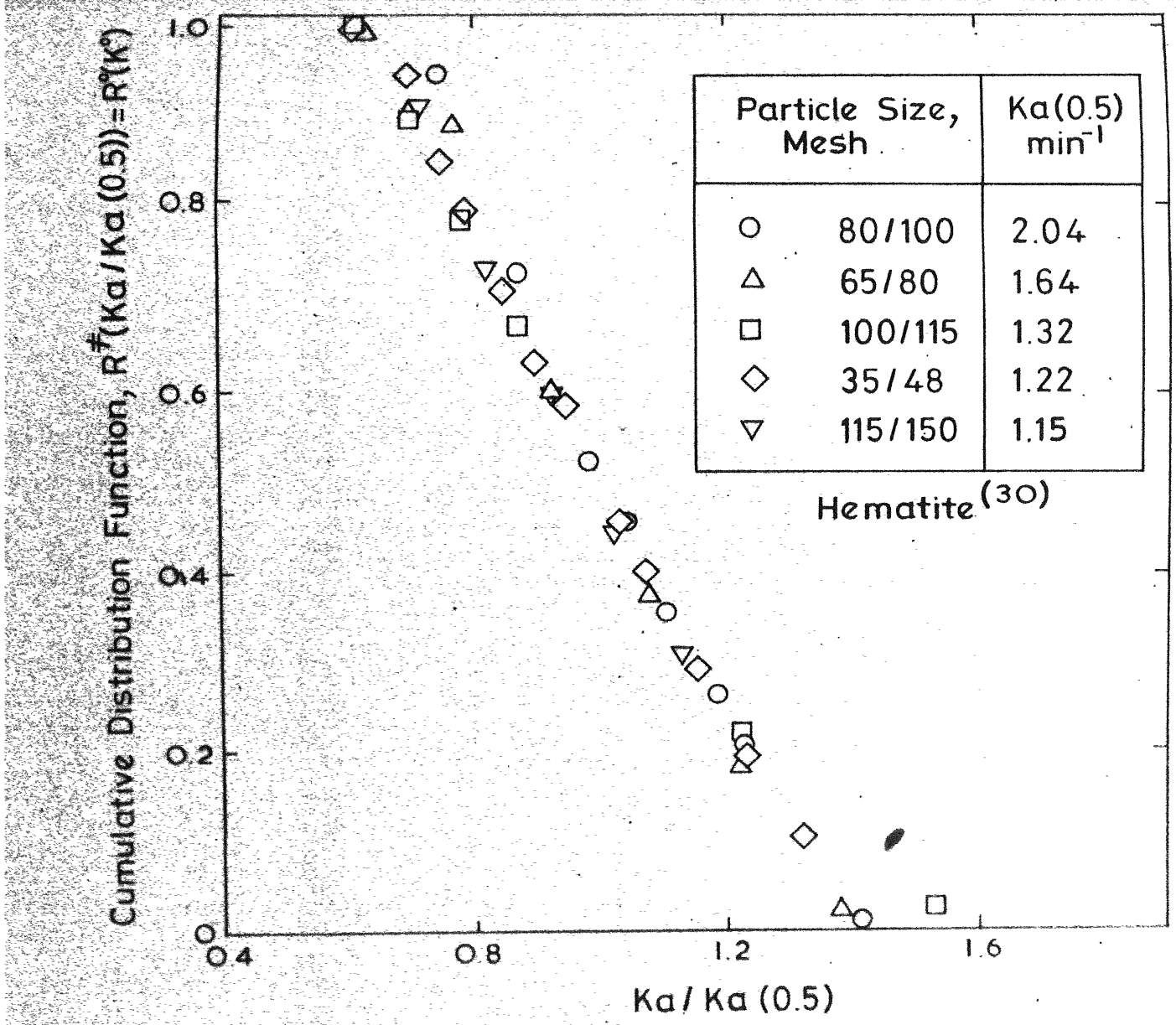

Fig 6.10 Self-similar form of apparent cumulative flotation rate distribution for hematite as a function of dimensionless flotation rate constant Ka/Ka (0.5).

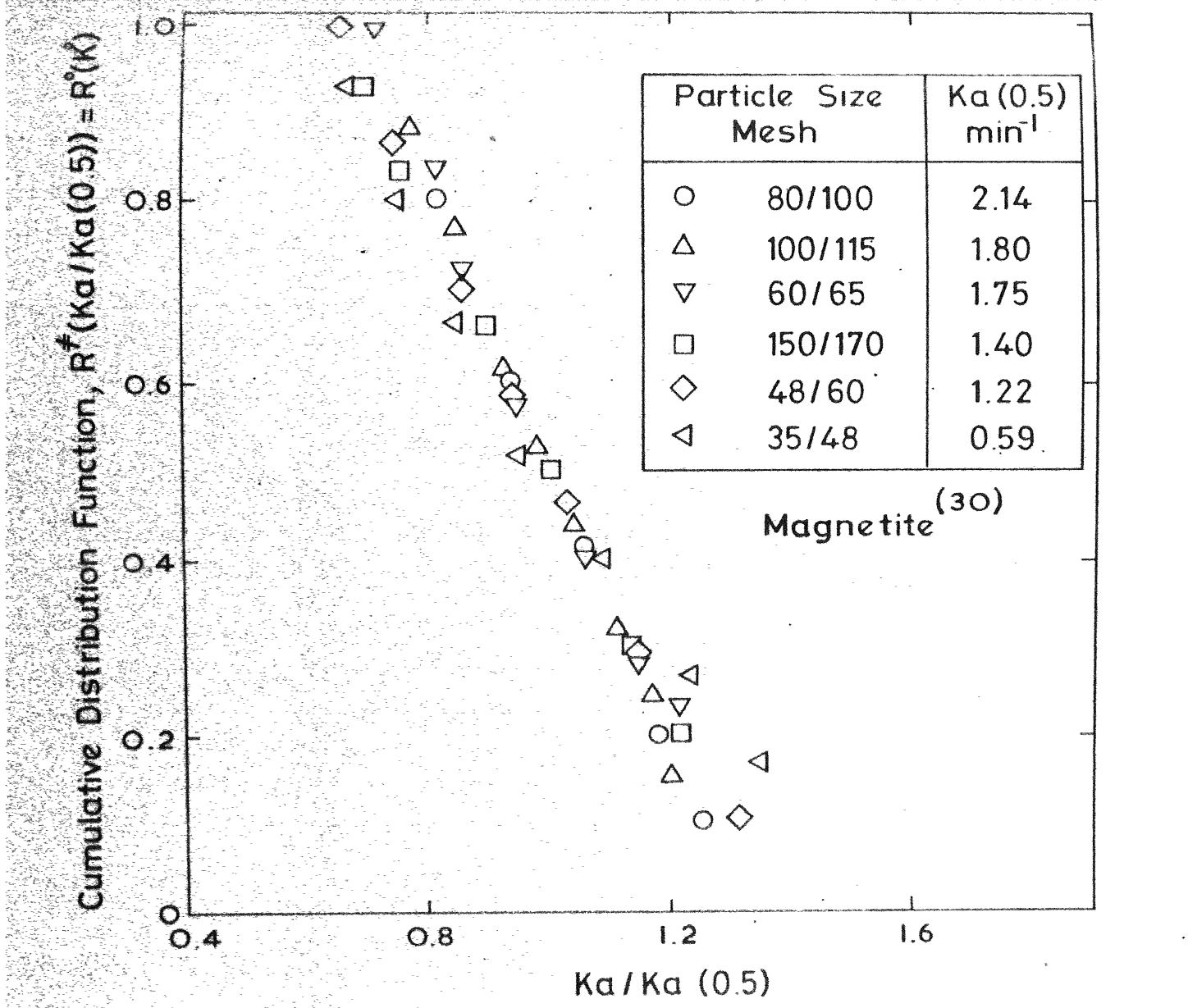

Fig.6.11 Self-similar form of apparent cumulative flotation rate distribution for magnetite as a function of dimensionless flotation rate constant Ka/Ka(0.5)

confirmed. Fig. 6.12 shows the plots of Ka(0.5), which is proportional to $\bar{\eta}$, as a function of the mean particle size. The curves for Volin and Swami[30] data for hematite and magnetite exhibit characteristic peak in the intermediate particle size, in conformity with the well known experimental fact that too large or small particles donot float well. The curves corresponding to Tewari and Biswas data for calcite, and Tomlinson and Fleming data for apatite, however, donot exhibit such maximum flotation rate at some intermediate particle size. This may be attributed to the fact that perhaps the range of particle size examined was not sufficiently extended in these experiments. As pointed out earlier the particle size at which the flotation rate is maximum would strongly depend on the mineral species, its density and surface characteristics, as well as, the hydrodynamic conditions prevailing in the cell. Thus, it is quite likely that for Tewari and Biswas data flotation rate will be maximum at a particle size range $< 50\mu$ whereas for Tomlinson and Fleming data it is maximum at a particle size range $> 134\mu$.

EFFECT OF PULP DENSITY:

Flotation kinetic data of Imaizumi and Inoue[54] for quartz particles in size range 74-105 microns with five initial pulp densities, namely, 7.7, 23, 69, 208 and 460 gm/litre was employed for computation of R(Ka). The data which was read

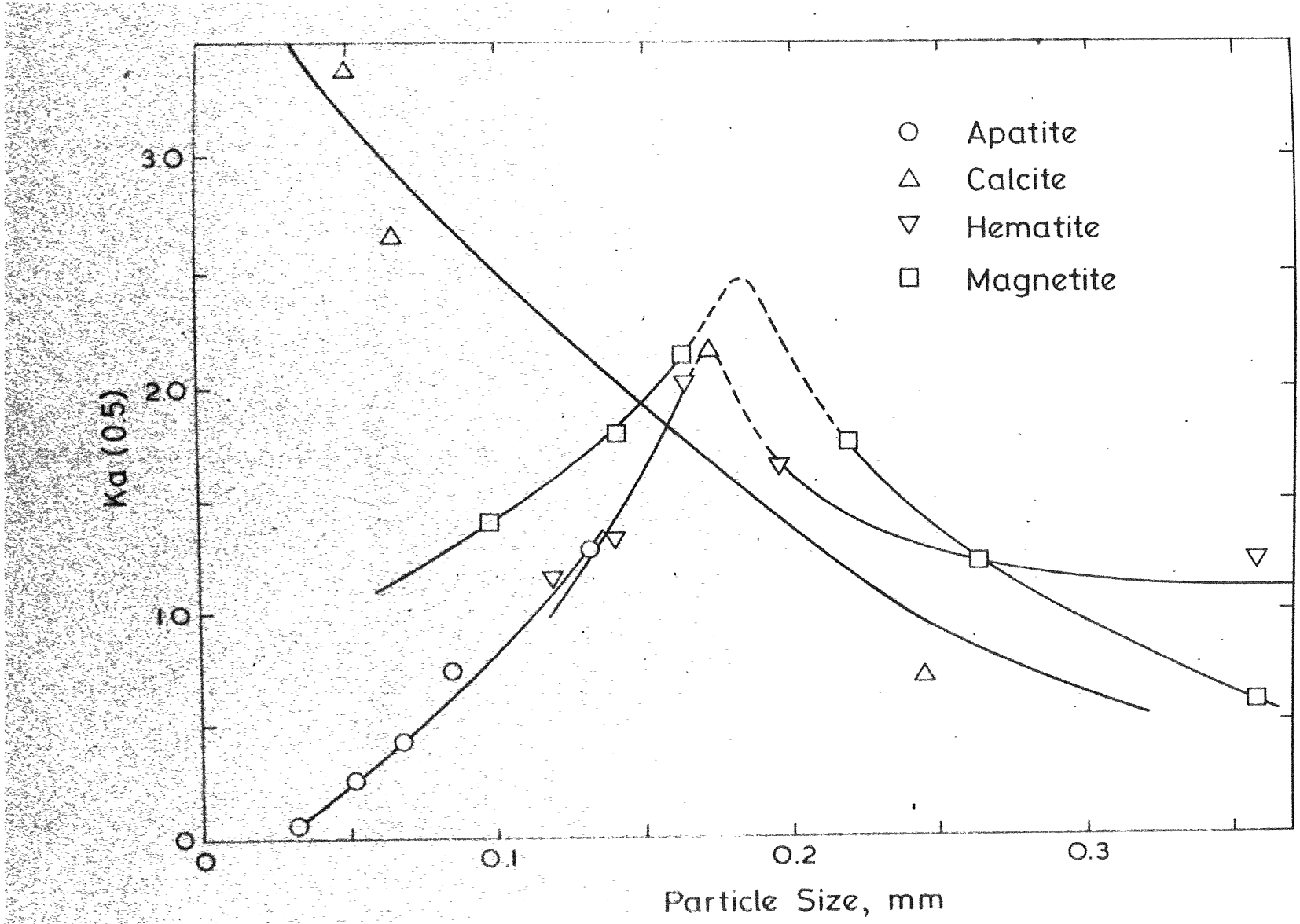

Fig. 6.12 Median apparent cumulative flotation rate constant as a function of the average particle size.

off from the graphs is tabulated in Table 6.6. Fig. 6.13 shows that for three dilute pulps, the apparent flotation rate distributions are, within limits of errors, bunched together and independent of the pulp densities. In case of the two concentrated pulps the free flotation hypothesis, which forms the basis for derivation of equation (2.17), is not likely to be satisfied. The overall rate of flotation now depends primarily on the capacity of the carrier air phase to accommodate and lift the particles from pulp into froth. Consequently, the exact nature of the flotation rate distribution has only a secondary influence on the flotation rate and this is perhaps reflected qualitatively in the steep slopes of these two distributions in Fig. 6.13. The pulp density limit for free flotation would depend, apart from the strong influence of the rate of aeration, on the volume of solid phase rather than its mass and it would differ for different minerals. Loveday[87] had shown that upto 45.7 gm/litre for pyrite-silica mixture the instantaneous average flotation rate is independent of initial pulp density. For the first time, however, Fig.6.13 exhibits this invariance in direct terms of the calculated flotation rate distribution.

DISCUSSION AND CONCLUSIONS:

Flotation data available in literature has been used to compute the apparent flotation rate distributions. These distributions and corresponding apparent flotation rate

Table 6.6: Fraction of Quartz Remaining in Cell at Cumulative Times for Five Initial Pulp Densities[86].

Time (Min.)	Pulp density in gm/litre				
	7.7	23	69	209	460
0	1	1	1	1	1
0.5	0.678	0.654	0.717	0.850	0.967
1.0	0.452	0.371	0.494	0.666	0.889
1.5	0.262	0.262	0.294	0.518	0.833
2.0	0.202	0.158	0.20	0.352	0.750
2.5	0.155	0.127	0.106	0.218	0.667
3.0	0.102	0.088	0.073	0.166	0.589
3.5	0.077	0.065	0.037	0.119	0.500
4.0	0.059	0.050	0.027	0.100	0.433
4.5	0.046	0.035	0.021	0.066	0.367
5.0	0.034	0.026	0.018	0.055	0.317
5.5	0.027	0.019	0.016	0.041	0.283
6.0	0.023	0.016	-	0.030	0.250
7.0	-	-	-	-	0.167
8.0	-	-	-	0.012	0.117

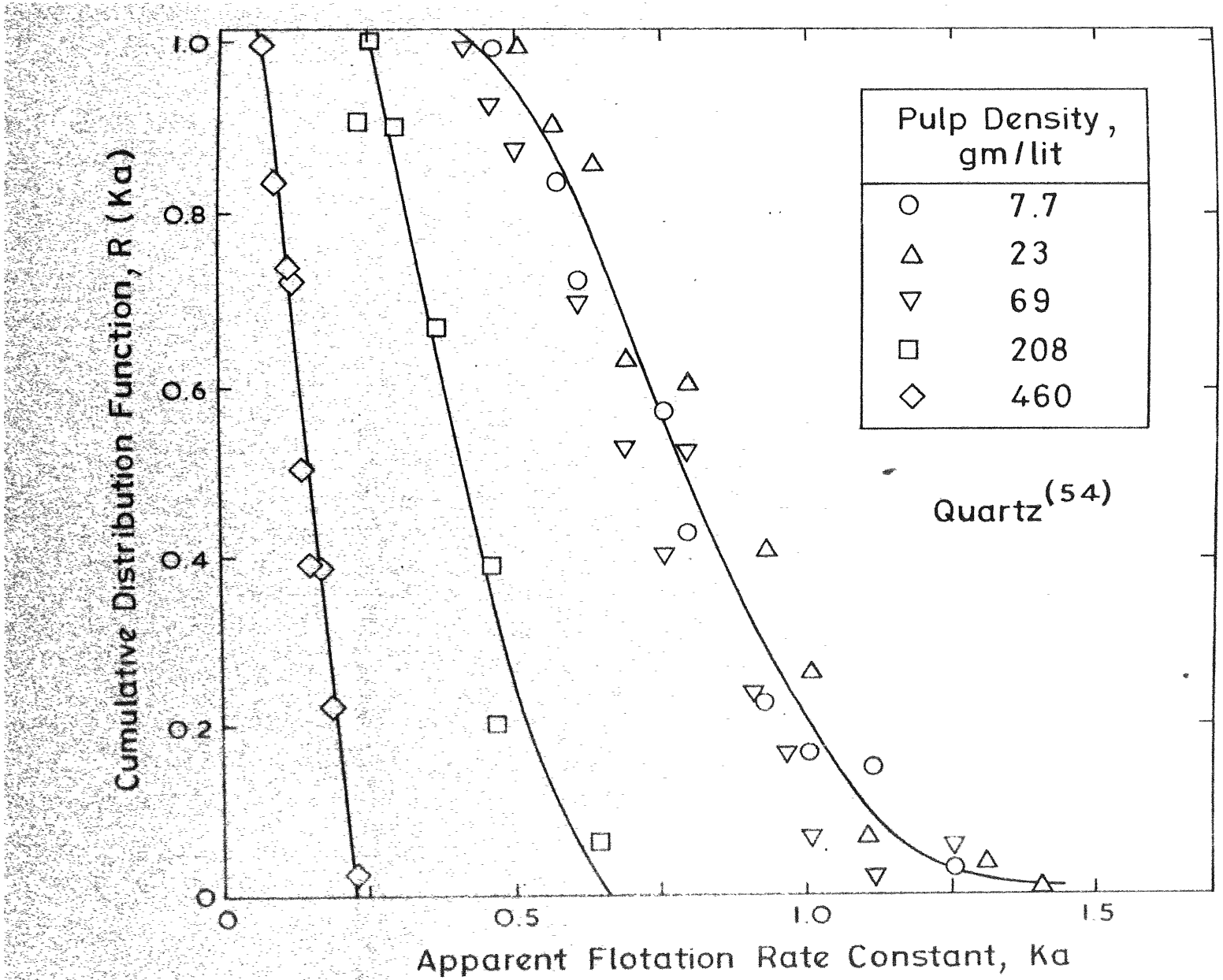

Fig 6.13 Calculated apparent cumulative flotation rate distributions for quartz[54] for five initial pulp densities.

constants have been analyzed as a function of aeration rate, particle size and initial pulp density. It will be noted that the assumed structure of Ka in equation (6.14) is somewhat similar to the model proposed by Woodburn, King and Colborn[83]. In present notation their expression for overall rate constant, given by equation (2.27) can be rewritten as

$$Ka = \theta(\epsilon, L)\ K^{o} \qquad (6.25)$$

where θ is a specific function of particle size and a hydrodynamic parameter ϵ defined in terms of bubble size and relative particle bubble velocity. For a given cell, in first instance, both ϵ and θ are unknown functions of the rate of aeration. Although equation (6.25) bears formal resemblence to equation (6.14), the function θ suggested by Woodburn et al does not permit separation of particle size effect as in equation (6.12). When only one variable is changed, either aeration rate or particle size, both models require self similar distribution in scaled apparent flotation rates as shown in Figs. 6.2, 6.8, 6.9, 6.10 and 6.11. Unfortunately, due to lack of suitable data it has not been possible to discriminate between these two structures of the apparent flotation rate constant.

Woodburn et al[83] have shown that for modelling of continuous flotation cells for design and control of industrial circuits it is necessary to incorporate explicitly the dependence

of apparent flotation rate constant on particle size since the residence time distribution depends on size. In the present approach the distribution as a whole is scrutinized for the effects of both aeration rate and particle size. The principal conclusion is that the nature of the function R(Ka) does not change with these variables, only the argument of the function, Ka, is altered or rescaled as in equations (4.43) and (6.14), and the scaling parameters may be determined from the appropriate data. This is a significant result in so far as it greatly simplifies the description of the distributed particulate species, specially when incorporated into a model of the flotation circuit. Determination of the apparent flotation rate distributions and the scaling parameter for particle size effect from continuous steady state data, which is more meaningful from the practical point of view has been carried out in a similar manner, details of which are given in the following chapter.

Fig. 6.13 shows that the free flotation hypothesis for dilute pulps is justified in context of distributed apparent flotation rate constant and, using the inversion algorithm, it is possible to determine the limiting concentration of solids for free flotation kinetics from suitable experimental data.

CHAPTER 7

THE EFFECTS OF PARTICLE SIZE AND FEED RATE ON THE FLOTATION RATE DISTRIBUTIONS IN A CONTINUOUS CELL

Analysis of flotation kinetic data for a semi-batch flotation operation has been discussed in the previous chapters. The approach applied therein can be easily extended for the analysis of kinetic data for continuously operated cell. In a continuous steady state operation the mass flow rate of solid particulate species in tailings and concentrate streams, as a function of the residence time distribution, is given by equations (2.21) and (2.22). Based on experimental evidence Woodburn et al[83] proposed that the residence time distribution of solid particles in the pulp can be assumed to be a gamma distribution (equation (2.23)) with mean and variance of the distribution, as given by equations (2.24), and (2.25), respectively. Therefore, equations (2.21) and (2.22) can be rewritten as

$$M_T(L) = \int_0^\infty M_F(Ka,L) \left[\frac{\beta^{\alpha+1}}{(Ka+\beta)^{\alpha+1}}\right] dKa \qquad (7.1)$$

and

$$M_C(L) = \int_0^\infty M_F(Ka,L) \left[1- \frac{\beta^{\alpha+1}}{(Ka+\beta)^{\alpha+1}}\right] dKa \qquad (7.2)$$

In a 25 Cu ft continuously operated Denver Cell, using an impulse of irradiated apatite rich tracer, but excluding the

flotation reagents, Woodburn et al[83] have computed the parameters of the residence time distribution for a number of particle size groups and slurry flow rates. The impulse tests were also conducted under flotation conditions to generate data suitable for computation of $M_F(Ka,L)$. Based on earlier works, Woodburn et al initially assumed that $M_F(Ka,L)$ is given by the gamma distribution, but found that, contrary to expectations, the parameters of the distribution for a given size group were not invariant with flow rate.

In this chapter, it is shown that this dependence on flow rate is perhaps more apparent than real and seemingly arises from a restricted choice of the gamma function for characterization of the flotation rate distribution. First a reliable method for computation of $M_F(Ka,L)$ in the steady state expression for recovery in equation (7.2) is presented, which is not restricted to any a priori assumption concerning the mathematical form of the distribution function. Using tabulated data of Woodburn et al it will be then possible to demonstrate that the computed distribution $M_F(Ka,L)$ is independent of throughput, and the apparent flotation rate constant, Ka, is related to particle size L by equation (6.14). The estimated flotation rate distribution is then employed to predict fairly accurately the flotation kinetics of a continuous cleaner cell whose feed comprises the rougher concentrate. The analysis is then extended to the data of Woodburn et al for gangue component.

AN OBJECTIVE FUNCTION FOR ESTIMATION OF FLOTATION RATE DISTRIBUTION

Identification of the flotation rate distribution requires knowledge of the steady state flow $M_T(L)$ or $M_C(L)$, as well as parameters α and β, for many feed slurry flow rates. Discretization of the integral term in equation (7.2), followed by either solution of the resulting algebraic equations or application of the least squares technique should, in theory, provide an estimate of the distribution. It turns out, however, that because of the ill-conditioned nature of the matrix in the discretized form, this estimate may prove to be unreliable, frequently physically meaningless, in presence of even a modest level of errors which is inevitable in any experimental data. A numerical method similar to the one used for inversion of the Laplace transform in Chapter 5 was developed as follows:

Let $R_F(Ka,L)$ be the cumulative retained distribution function which is related to the frequency function by

$$M_F(Ka,L) = -\frac{\partial R_F(Ka,L)}{\partial Ka} \qquad (7.3)$$

Substitution in equation (7.2) results in

$$M_C(L) = \int_0^\infty -\frac{\partial R_F(Ka,L)}{\partial Ka}\left[1-\frac{\beta^{\alpha+1}}{(Ka+\beta)^{\alpha+1}}\right] dKa \qquad (7.4)$$

Integration by parts leads to

$$M_C(L) = (\alpha+1)\,\beta^{\alpha+1}\int_0^\infty \frac{R_F(Ka,L)}{(Ka+\beta)^{\alpha+2}}\,dKa \qquad (7.5)$$

where for convenience $R_F(Ka,L)$ has been normalized by dividing throughout by slurry mass flow rates of particles of size L in feed. Transform the variable Ka to x by

$$Ka = \left[\frac{1-x}{1+x}\right] \frac{1}{s} \tag{7.6}$$

where, as defined earlier, s is a scale parameter ($s > 0$) which can be arbitrarily adjusted to generate estimate of $R_F(Ka,L)$ in any region of interest in range $0 \leq Ka \leq \infty$. Substitution of equation (7.6) into (7.5) results in

$$M_C(L) = \frac{2(\alpha+1)}{s} \beta^{\alpha+1} \int_{-1}^{1} \frac{F''(x)}{\left[\frac{(1-x)}{(1+x)s} + \beta\right]^{\alpha+2}} \frac{dx}{(1+x)^2} \tag{7.7}$$

where

$$F''(x) = R_F\left(\frac{(1-x)}{(1+x)s}, L\right) = R_F(Ka,L) \tag{7.8}$$

Discretization of integral term in equation (7.7) by n-point Lobatto quadrature[155,156] leads to the following expression

$$M_C(L) = \frac{2(\alpha+1)\beta^{\alpha+1}}{s} \left\{ \frac{1}{2n(n-1)\beta^{\alpha+2}} + \sum_{i=2}^{n-1} \left[\frac{F''(x_i)}{\left[\frac{(1-x_i)}{(1+x_i)s} + \beta\right]^{\alpha+2}} \right] \frac{1}{(1+x_i)^2} \right\} w_i \tag{7.9}$$

where x_i and w_i are i-th abscissa and weight, respectively, in n-point Lobatto quadrature formula. For determination of $F''(x)$ (i.e. $R_F(Ka,L)$), the following least squares objective function is found to be quite satisfactory.

$$E' = \sum_{j=1}^{N} \left\{ M_{C,j}(L) - \left[\frac{2(\alpha_j+1)\,\beta_j^{\alpha_j+1}}{s} \right] \left[\frac{1}{2n(n-1)\beta_j^{\alpha_j+2}} \right. \right.$$

$$\left. \left. + \sum_{i=2}^{n-1} \frac{F''(x_i)}{\left[\frac{(1-x_i)}{(1+x_i)s} + \beta_j \right]^{\alpha_j+2}} \right] \frac{w_i}{(1+x_i)^2} \right\}^2 \qquad (7.10)$$

where subscript j denotes the values of recovery and residence time parameters at j-th slurry flow rate, j = 1,2,..., N. The problem is now reduced to minimizing the objective function with appropriate choice of $F''(x)$. The constraints on $R_F(Ka,L)$, which are identical to those defined by equations (5.22),(5.23) and (5.24) and are reproduced below for convenience, considerably simplify the evaluation of $F''(x)$.

(i) $R_F(Ka,L) \geq 0, \quad 0 \leq Ka \leq \infty \qquad (7.11)$

(ii) $R_F(Ka,L)$ is a monotonically non-increasing function of Ka. Therefore,

$$1 \geq R_F(Ka_1,L) \geq R_F(Ka_2,L) \ldots \geq R_F(Ka_m, L) \ldots \geq 0 \qquad (7.12)$$

where

$$0 \leq Ka_1 \leq Ka_2 \ldots \leq Ka_m \ldots \leq \infty$$

(iii) Finally,

$$R_F(0,L) = 1 \qquad (7.13)$$

and

$$R_F(\infty,L) = 0 \qquad (7.14)$$

COMPUTATIONAL ASPECTS:

Again a 8 point (n = 8) Lobatto quadrature was chosen to discretize the integral in equation (7.7). As pointed out earlier, the choice of this formula is dictated by the fact that it is exact at the limits of the integral and the constraints in equations (7.13) and (7.14) are automatically satisfied. Apatite and gangue data for steady state concentrate output as a function of the feed slurry flow rates were taken from Table 6 of Woodburn et al[83]. The number of data points, which for different particle sizes, ranged from 6 to 9, was deemed to be insufficient. In order to smoothen out any scatter in the data and over determine the unknown variables, a third order polynomial was fitted to the data set and additional points were interpolated from this curve. Tables 7.1 and 7.2 give the Woodburn et al data in terms of recovery of apatite and gangue, respectively, as a function of throughput for different particle size groups after smoothening and interpolation. Total number of smoothened and interpolated data points ranged from 11 to 17 for different particle size groups.

From data given in Table 2 of Woodburn et al[83], plots of mean^{-1} and $\text{variance}^{-0.5}$ of particle residence time distribution as a function of feed slurry flow rate for various particle size groups were obtained and are shown in Figs. 7.1 and 7.2, respectively. Using these two figures and equations (2.24) and (2.25) values of parameters α and β in residence time distribution

Table 7.1: Fractional Recoveries of Apatite as a Function of Particle Size Range and Slurry Flow Rate.

Particle size range, micron	Slurry flow rate cu ft/min	Fractional Recovery		
		Experimental	Polynomial Fit	Predicted
37 to 63	5.70	0.585	0.570	0.528
	6.10	–	0.540	–
	6.50	0.486	0.513	0.493
	6.95	–	0.486	–
	7.40	0.475	0.462	0.458
	7.80	–	0.443	–
	8.20	0.415	0.426	0.432
	8.80	–	0.404	–
	9.40	0.394	0.386	0.397
	10.05	–	0.370	–
	10.70	0.357	0.356	0.365
	11.30	–	0.345	–
	11.90	0.360	0.334	0.339
	12.40	–	0.325	–
	12.90	0.284	0.316	0.321
	13.90	–	0.296	–
	14.90	0.276	0.269	0.289
67 to 88	5.70	0.613	0.605	0.597
	6.10	–	0.593	–
	6.50	0.558	0.579	0.562
	6.95	–	0.563	–
	7.40	0.558	0.547	0.537
	7.80	–	0.532	–
	8.20	0.534	0.517	0.500
	8.80	–	0.494	–
	9.40	0.453	0.471	0.464
	10.05	–	0.447	–
	10.70	0.415	0.423	0.429
	11.30	–	0.402	–
	11.90	0.410	0.382	0.402
	12.40	–	0.367	–
	12.90	0.336	0.353	0.362
	13.90	–	0.329	–
	14.90	0.314	0.312	0.332

Contd...

Contd...

Particle size Range, micron	Slurry flow rate cu ft/min	Fractional Recovery		
		Experimental	Polynomial Fit	Predicted
88 to 125	5.70	0.590	0.576	0.546
	6.10	–	0.552	–
	6.50	0.543	0.530	0.511
	6.95	–	0.507	–
	7.40	0.497	0.486	0.477
	7.80	–	0.468	–
	8.20	0.458	0.451	0.450
	8.80	–	0.429	–
	9.40	0.408	0.408	0.414
	10.05	–	0.388	–
	10.70	0.363	0.370	0.381
	11.30	–	0.355	–
	11.90	0.330	0.341	0.356
	12.40	–	0.331	–
	12.90	0.307	0.320	0.337
	13.90	–	0.301	–
	14.90	0.270	0.284	0.301
125 to 177	5.70	0.490	0.488	0.473
	6.10	–	0.472	–
	6.50	0.448	0.455	0.430
	6.95	–	0.436	–
	7.40	0.422	0.416	0.406
	7.80	–	0.399	–
	8.20	0.385	0.382	0.369
	8.80	–	0.356	–
	9.40	0.329	0.331	0.332
	10.05	–	0.305	–
	10.70	0.271	0.281	0.290
	11.30	–	0.260	–
	11.90	0.257	0.242	0.266
	12.40	–	0.229	–
	12.90	0.211	0.218	0.230
	13.90	–	0.202	–
	14.90	0.197	0.197	0.210

Contd...

Contd...

Particle size range, micron	Slurry flow rate, cu ft/min	Fractional Recovery		
		Experimental	Polynomial Fit	Predicted
177 to 250	5.70	0.422	0.409	0.375
	6.10	-	0.369	-
	6.50	0.295	0.337	0.320
	6.95	-	0.309	-
	7.40	0.339	0.288	0.291
	7.80	-	0.274	-
	8.20	0.241	0.262	0.269
	8.80	-	0.245	-
	9.40	0.223	0.226	0.243
	10.05	-	0.196	-
	10.70	0.155	0.153	0.199
> 250	5.70	0.219	0.218	0.177
	6.10	-	0.189	-
	6.50	0.163	0.164	0.138
	6.95	-	0.139	-
	7.40	0.112	0.117	0.117
	7.80	-	0.100	-
	8.20	0.094	0.085	0.107
	8.80	-	0.067	-
	9.40	0.047	0.052	0.067
	10.05	-	0.038	-
	11.70	0.028	0.027	0.050

Table 7.2: Fractional Recoveries of Gangue as a Function of Particle Size Range and Slurry Flow Rate.

Particle size range, micron	Slurry flow rate, cu ft/min	Fractional Recovery		
		Experimental	Polynomial Fit	Predicted
37 to 63	5.70	0.361	0.345	0.308
	6.10	-	0.322	-
	6.50	0.277	0.301	0.279
	6.95	-	0.280	-
	7.40	0.258	0.261	0.253
	7.80	-	0.245	-
	8.20	0.233	0.231	0.234
	8.80	-	0.213	-
	9.40	0.206	0.198	0.209
	10.05	-	0.183	-
	10.70	0.187	0.171	0.188
	11.30	-	0.162	-
	11.90	0.142	0.154	0.172
	12.40	-	0.148	-
	12.90	0.135	0.142	0.161
	13.90	-	0.132	-
	14.90	0.125	0.121	0.142
63 to 88	5.70	0.369	0.363	0.354
	6.10	-	0.343	-
	6.50	0.313	0.325	0.314
	6.95	-	0.306	-
	7.40	0.292	0.288	0.277
	7.80	-	0.273	-
	8.20	0.259	0.259	0.256
	8.80	-	0.240	-
	9.40	0.229	0.223	0.229
	10.05	-	0.206	-
	10.70	0.191	0.192	0.205
	11.30	-	0.180	-
	11.90	0.164	0.170	0.180
	12.40	-	0.162	-
	12.90	0.159	0.156	0.170
	13.90	-	0.145	-
	14.90	0.136	0.136	0.147

Contd...

Contd...

Particle size range, micron	Slurry flow rate, cu ft/min	Fractional Recovery		
		Experimental	Polynomial Fit	Predicted
88 to 125	5.70	0.315	0.315	0.285
	6.10	–	0.294	–
	6.50	0.273	0.275	0.258
	6.95	–	0.256	–
	7.40	0.242	0.238	0.233
	7.80	–	0.224	–
	8.20	0.215	0.211	0.215
	8.80	–	0.194	–
	9.40	0.171	0.180	0.192
	10.05	–	0.167	–
	10.70	0.164	0.156	0.172
	11.30	–	0.148	–
	11.90	0.134	0.141	0.157
	12.40	–	0.136	–
	12.90	0.137	0.132	0.146
	13.90	–	0.125	–
	14.90	0.117	0.118	0.129
125 to 177	5.70	0.256	0.252	0.219
	6.10	–	0.232	–
	6.50	0.210	0.214	0.198
	6.95	–	0.196	–
	7.40	0.175	0.179	0.169
	7.80	–	0.165	–
	8.20	0.153	0.153	0.155
	8.80	–	0.137	–
	9.40	0.127	0.123	0.134
	10.05	–	0.111	–
	10.70	0.104	0.101	0.117
	11.30	–	0.093	–
	11.90	0.087	0.087	0.104
	12.40	–	0.083	–
	12.90	0.075	0.080	0.094
	13.90	–	0.075	–
	14.90	0.075	0.073	0.0901

Contd...

Contd..

Particle size range, micron	Slurry flow rate, cu ft/min	Fractional Recovery		
		Experimental	Polynomial Fit	Predicted
177 to 250	5.70	0.181	0.177	0.146
	6.10	-	0.157	-
	6.50	0.128	0.141	0.130
	6.95	-	0.126	-
	7.40	0.129	0.115	0.116
	7.80	-	0.107	-
	8.20	0.096	0.100	0.106
	8.80	-	0.902	-
	9.40	0.078	0.080	0.094
	10.05	-	0.066	-
	10.70	0.048	0.047	0.078
> 250	5.70	0.064	0.064	0.045
	6.10	-	0.056	-
	6.50	0.049	0.049	0.040
	6.95	-	0.041	-
	7.40	0.032	0.035	0.035
	7.80	-	0.030	-
	8.20	0.030	0.026	0.032
	8.80	-	0.020	-
	9.40	0.013	0.015	0.025
	10.05	-	0.010	-
	10.70	0.006	0.006	0.021

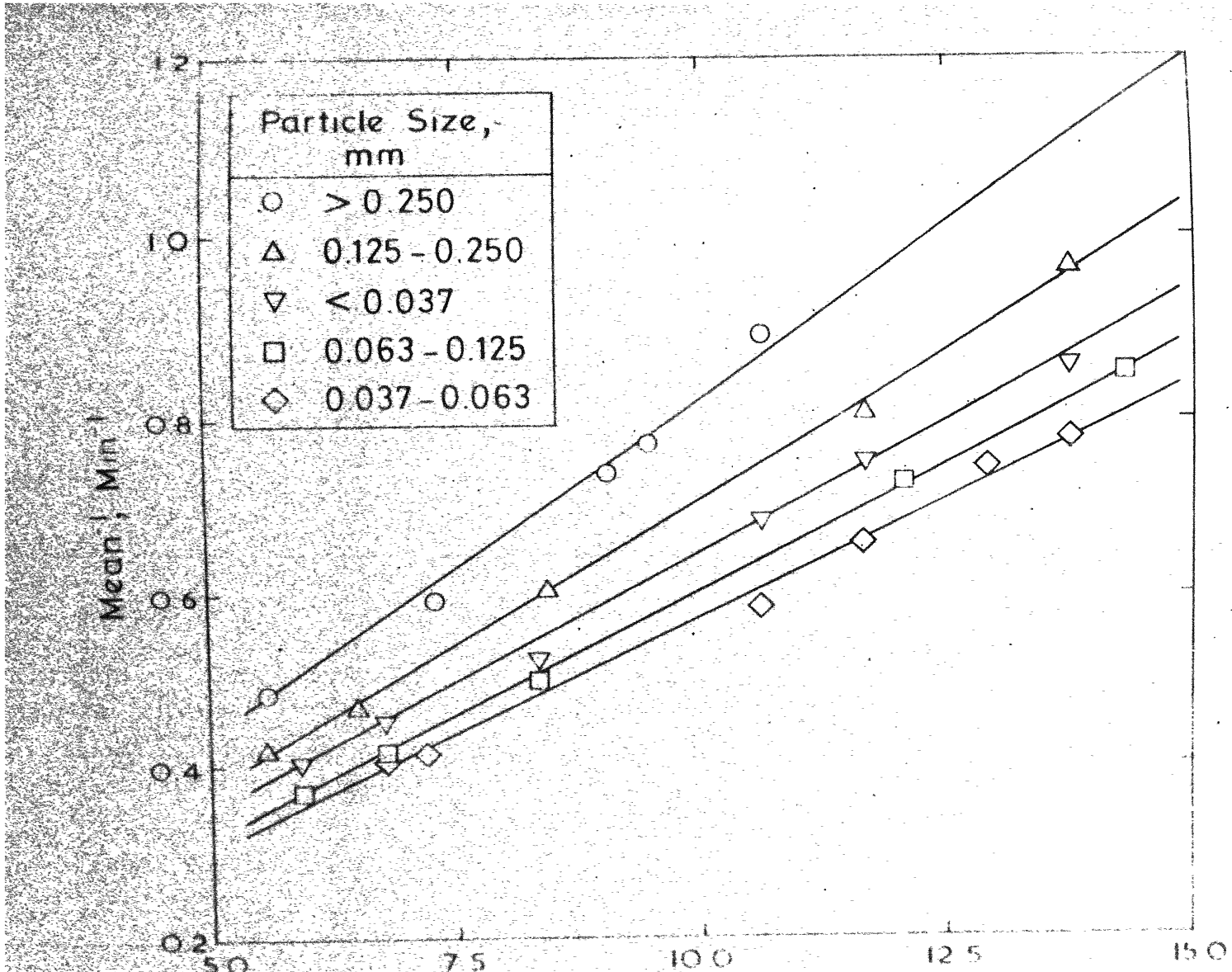

Fig 7.1 Plot of mean^{-1} of the residence time distribution versus slurry flow rate for five particle size groups.

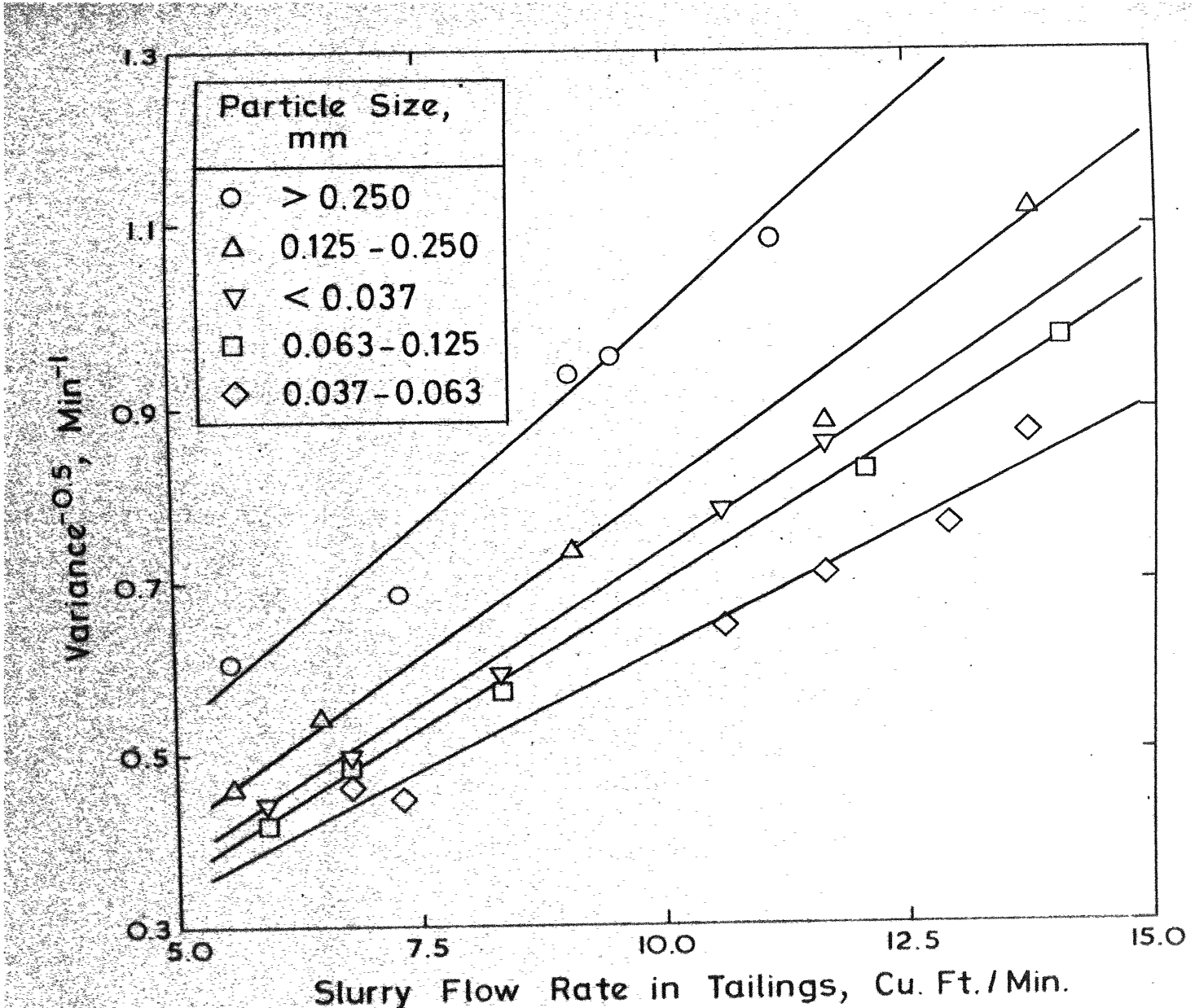

Fig.7.2 Plot of variance$^{-0.5}$ of the residence time distribution versus slurry flow rate for five particle size groups.

could be obtained at any desired slurry flow rate. The values of α, thus obtained, were found to be quite small. This shows that the cell nearly behaves like a perfect mixer. Three optimization algorithms, univariant search using Fibonacci technique[157,158], Rosenbrock[159] and Random Search[160], were tested. Although, Random search turned out to be the most satisfactory, it is possible that a still more efficient method might exist. In order to check against possible realization of local minima, widely different initial guesses were employed. The scaling factor was varied from 1 to 5.

FLOTATION RATE DISTRIBUTION:

Figs. 7.3 and 7.4 show plots of computed cumulative flotation rate distributions, $R_F(Ka,L)$ for apatite and gangue for six particle size groups. These distributions were employed to back calculate fractional recovery as a function of throughput. Figs. 7.5, 7.6, 7.7, 7.8 and 7.9 show the plots of fractional recovery as a function of throughput for apatite and gangue for different particle size groups. It can be seen in these figures that the overall agreement between the calculated recovery values and experimental values is satisfactory.

The validity of the throughput invariant distributions in Figs. 7.3 and 7.4 has been tested in a somewhat more stringent manner by predicting the recovery when the rougher concentrate is refloated in a steady state cleaner cell.

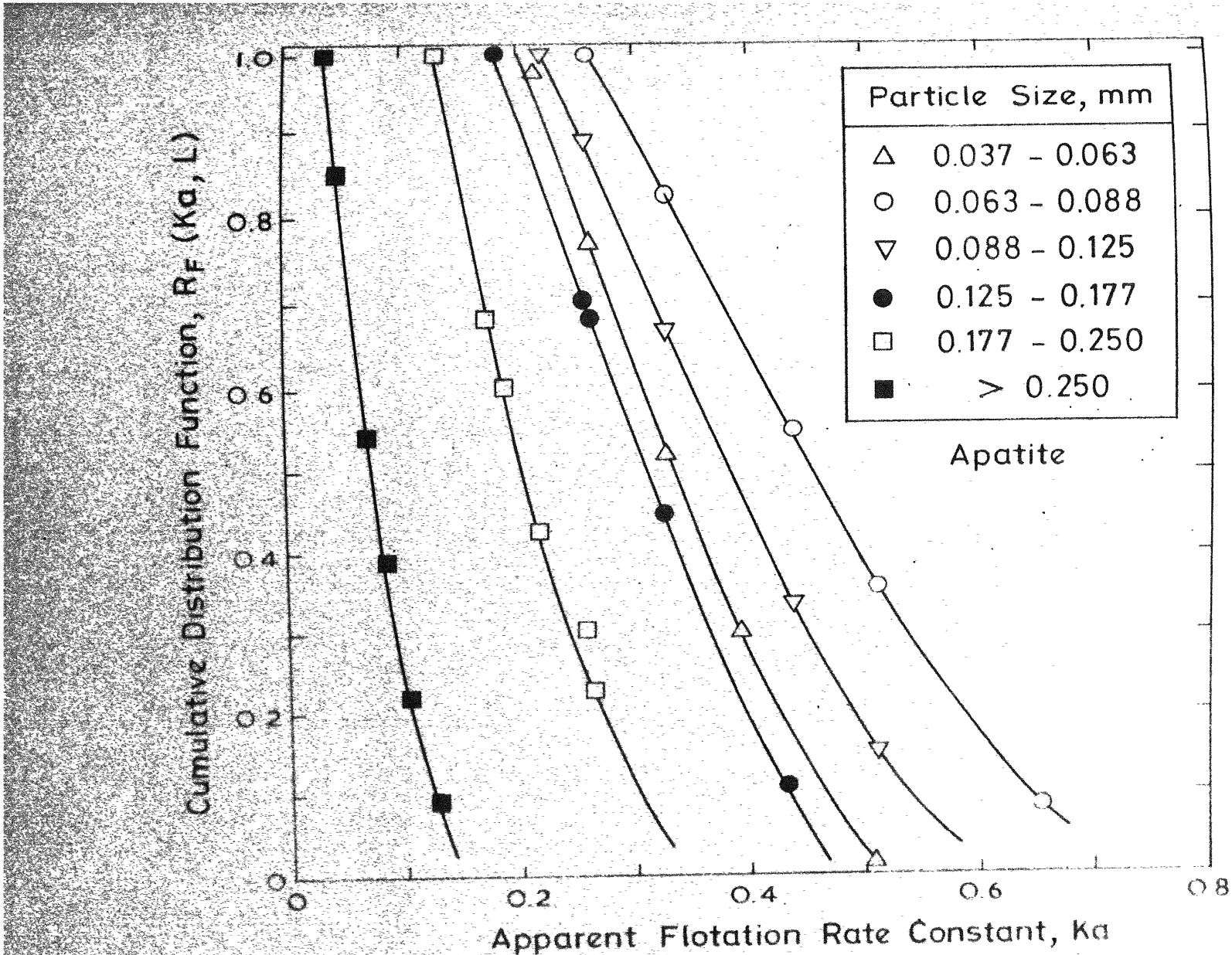

Fig. 7.3 Calculated apparent cumulative flotation rate distributions for apatite of six particle size groups.

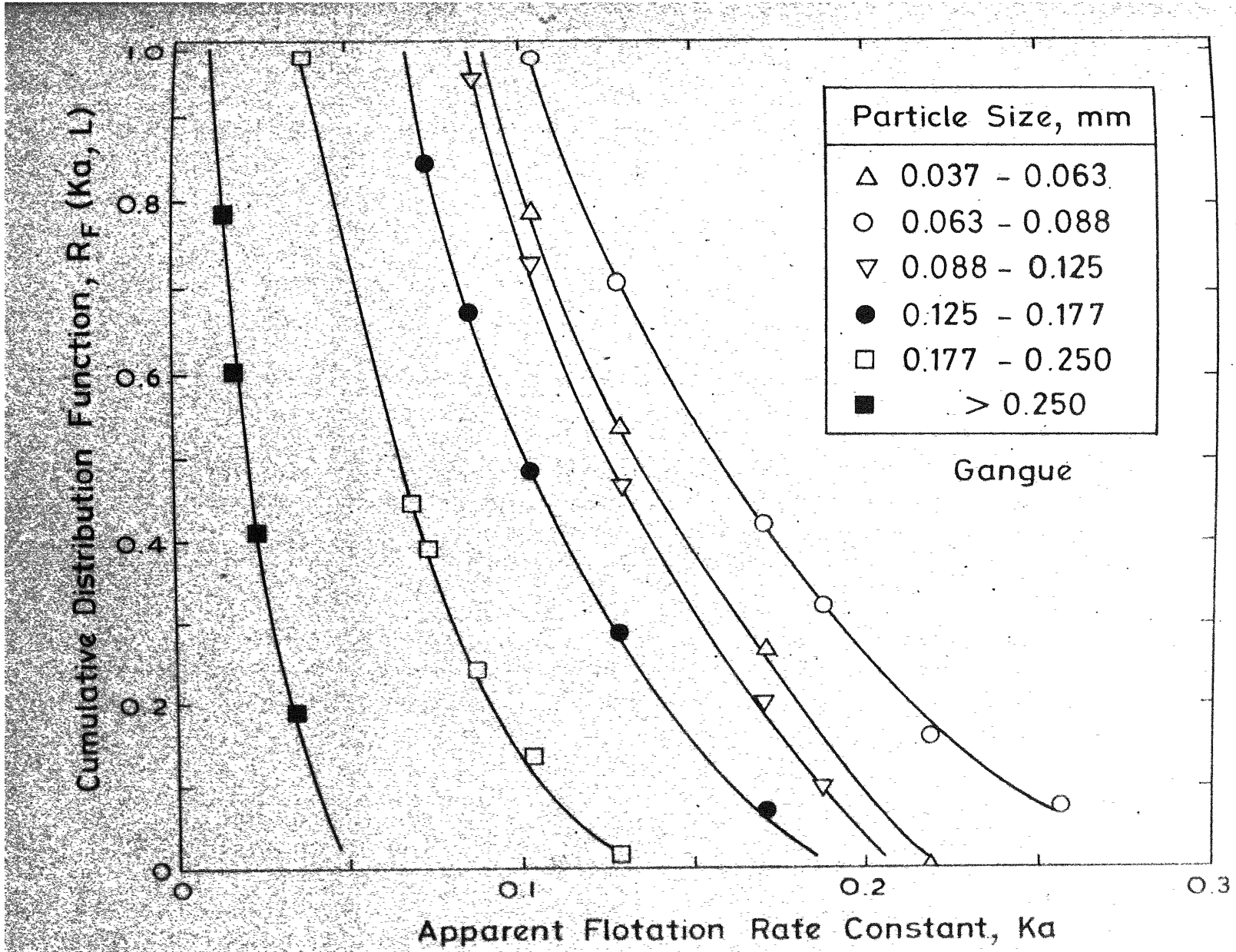

Fig 7.4 Calculated apparent cumulative flotation rate distributions for gangue of six particle size groups.

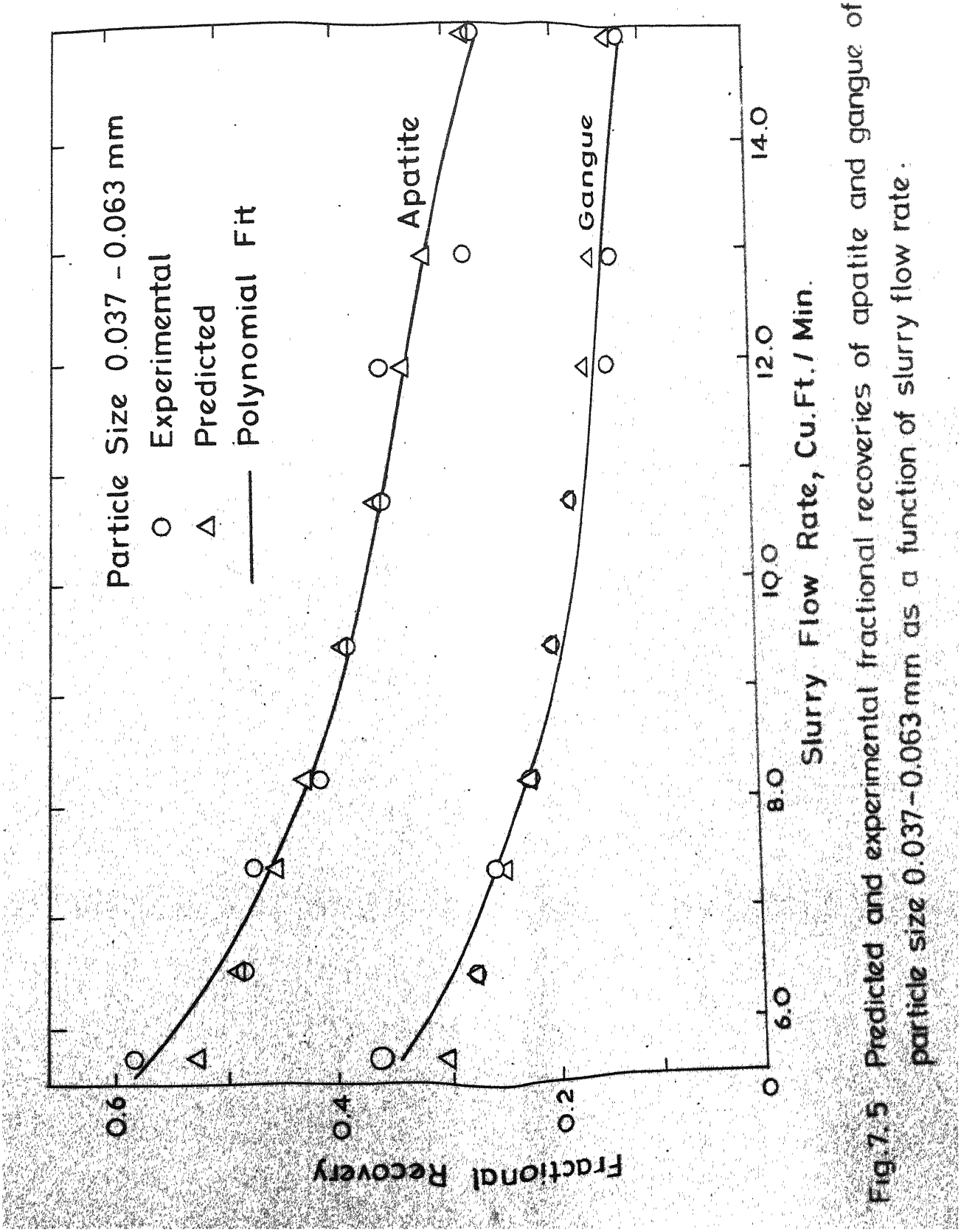

Fig. 7.5 Predicted and experimental fractional recoveries of apatite and gangue of particle size 0.037–0.063 mm as a function of slurry flow rate.

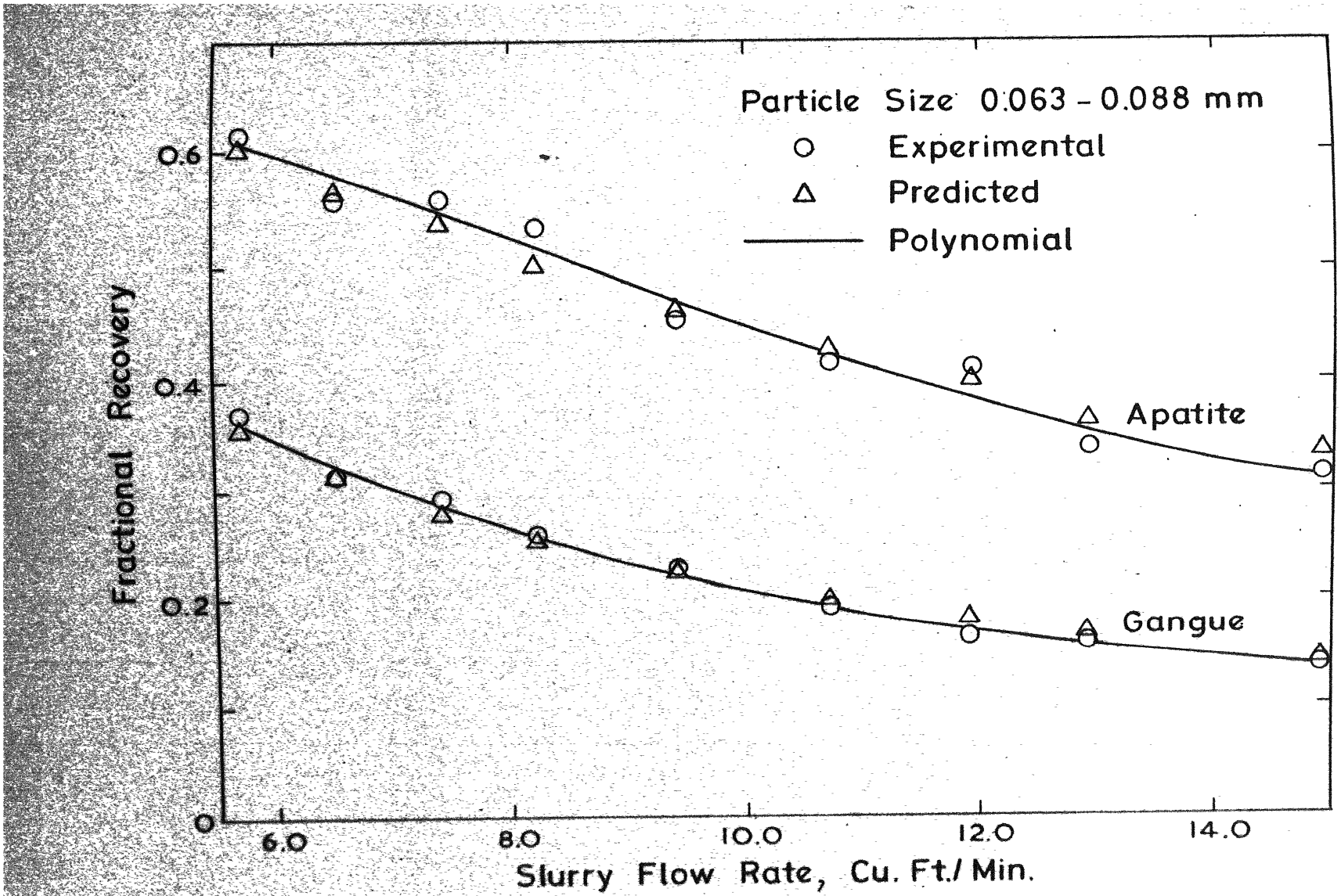

Fig.7.6 Predicted and experimental fractional recoveries of apatite and gangue of particle size 0.063–0 088 mm as a function of slurry flow rate.

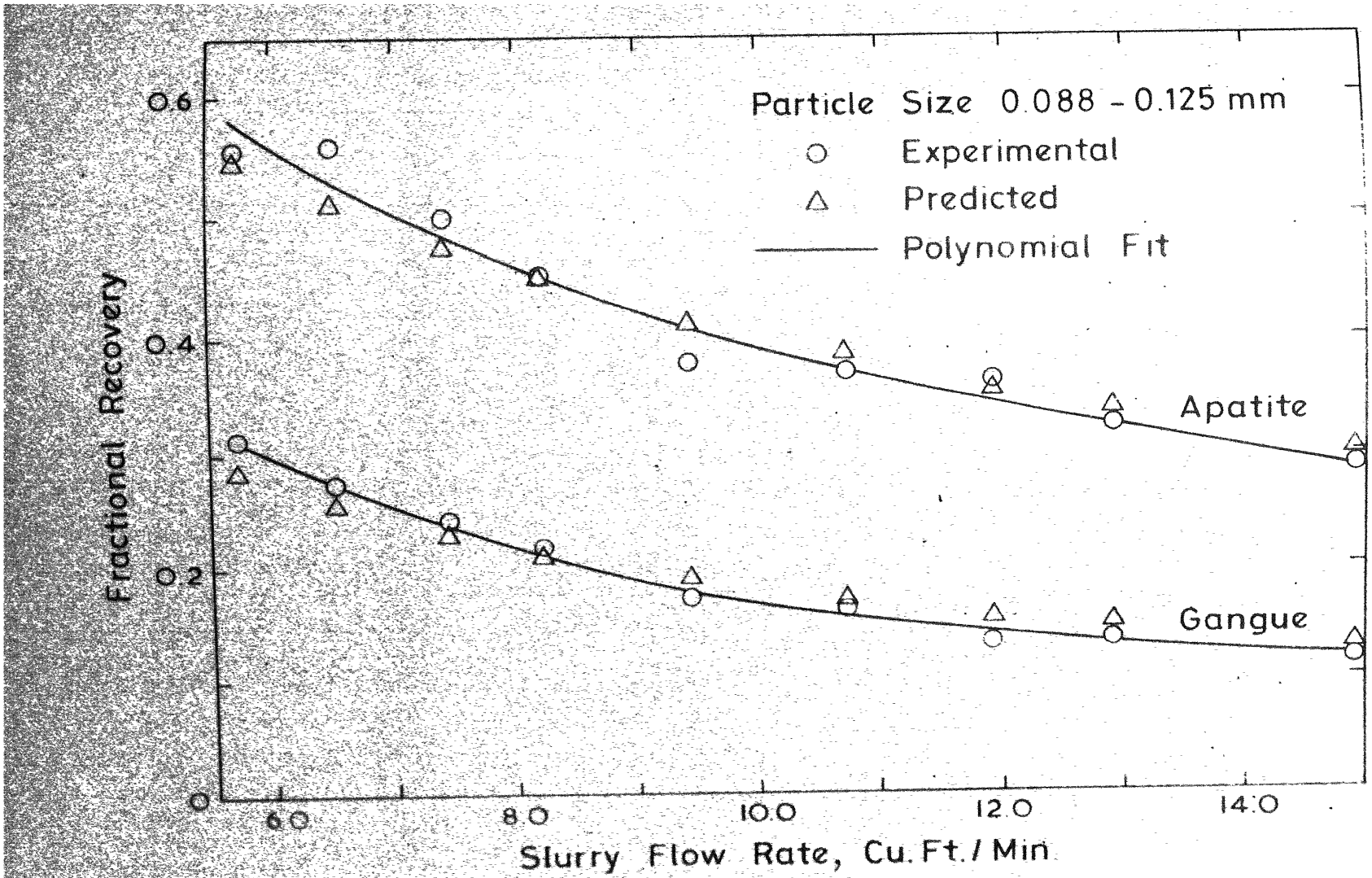

Fig 7.7 Predicted and experimental fractional recoveries of apatite and gangue of particle size 0.089-0.125 mm as a function of slurry flow rate.

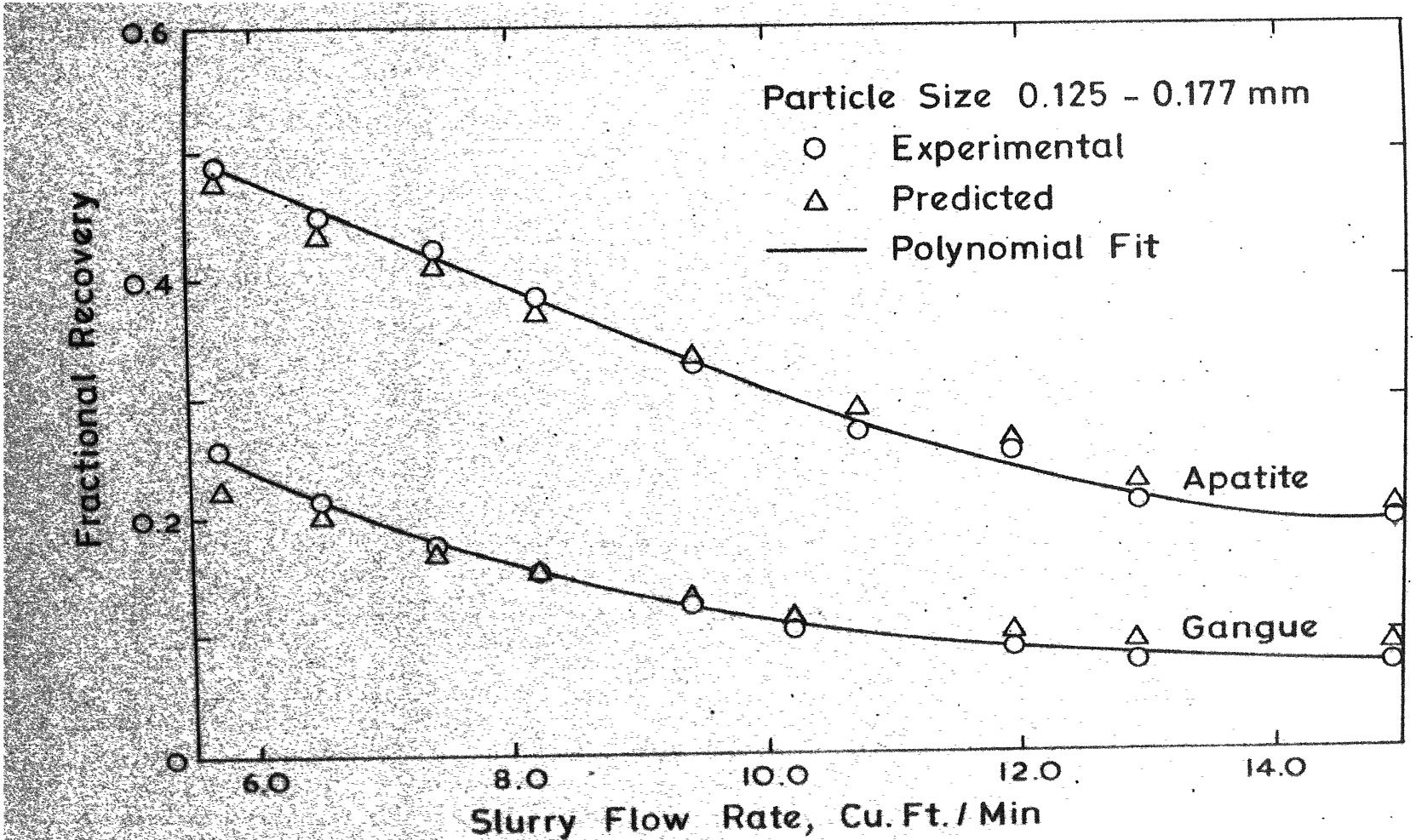

Fig.7.8 Predicted and experimental fractional recoveries of apatite and gangue of particle size 0.125-0.177 mm as a function of slurry flow rate.

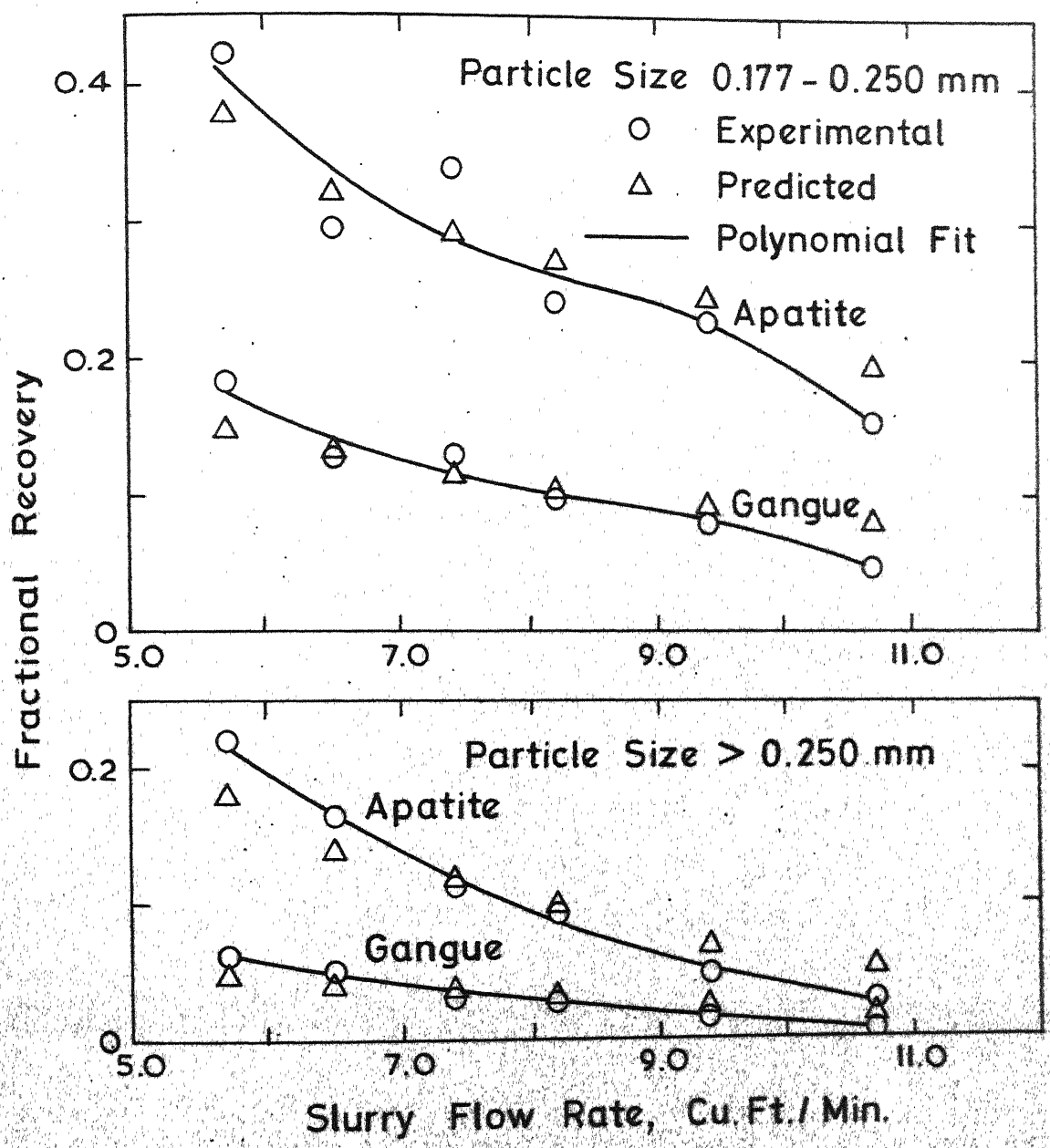

Fig.7.9 Predicted and experimental fractional recoveries of apatite and gangue of particle sizes 0.177-0.250 and > 0.250 mm as a function of slurry flow rate.

Following the argument used to derive equation (7.2), it can be shown that the mass flow rate in concentrate stream of cleaner cell is

$$M_{C,2}(L) = \int_0^\infty M_{C,1}(Ka,L)\left[1-\frac{\beta_2^{\alpha_2+1}}{(Ka+\beta_2)^{\alpha_2+1}}\right] dKa \quad (7.15)$$

where subscript 1 and 2 refer to rougher and cleaner cells, respectively. With changed notations the recovery of particles with attribute $[Ka,L]$, from equation (7.2), can be written as

$$M_{C,1}(Ka,L) = M_F(Ka,L)\left[1-\frac{\beta_1^{\alpha_1+1}}{(Ka+\beta_1)^{\alpha_1+1}}\right] \quad (7.16)$$

Substitution of equation (7.16) followed by substitution of equation (7.3) into (7.15) results in

$$M_{C,2}(L) = \int_0^\infty -\frac{\partial R_F(Ka,L)}{\partial Ka}\left[1-\frac{\beta_1^{\alpha_1+1}}{(Ka+\beta_1)^{\alpha_1+1}}\right]\left[1-\frac{\beta_2^{\alpha_2+1}}{(Ka+\beta_2)^{\alpha_2+1}}\right] dKa \quad (7.17)$$

Integration by parts leads to

$$M_{C,2}(L) = \int_0^\infty R_F(Ka,L)\left[\frac{(\alpha_1+1)\beta_1^{\alpha_1+1}}{(Ka+\beta_1)^{\alpha_1+2}}+\frac{(\alpha_2+1)\beta_2^{\alpha_2+1}}{(Ka+\beta_2)^{\alpha_2+2}}-\frac{\beta_1^{\alpha_1+1}\beta_2^{\alpha_2+1}\{(\alpha_1+1)(Ka+\beta_2)+(\alpha_2+1)(Ka+\beta_1)\}}{(Ka+\beta_1)^{\alpha_1+2}(Ka+\beta_2)^{\alpha_2+2}}\right] dKa \quad (7.18)$$

Change of variable from Ka to x, using equation 7.6 with s = 1 results in following equation,

$$M_{C,2}(L) = 2 \int_{-1}^{1} F''(x) \left[\frac{(\alpha_1+1)\beta_1^{\alpha_1+1}}{(\bar{x}+\beta_1)^{\alpha_1+2}} + \frac{(\alpha_2+1)\beta_2^{\alpha_2+1}}{(\bar{x}+\beta_2)^{\alpha_2+2}} - \frac{\beta_1^{\alpha_1+1}\beta_2^{\alpha_2+1}\{(\alpha_1+1)(\bar{x}+\beta_2) + (\alpha_2+1)(\bar{x}+\beta_1)\}}{(\bar{x}+\beta_1)^{\alpha_1+2}(\bar{x}+\beta_2)^{\alpha_2+2}} \right] \frac{dx}{(1+x)^2} \tag{7.19}$$

where $F''(x)$ is same as defined in equation (7.8) and

$$\bar{x} = \frac{1-x}{1+x} \tag{7.20}$$

Discretization of the integral term in equation (7.19) by 8-point Lobatto quadrature results in

$$M_{C,2}(L) = 2 \sum_{i=2}^{7} F''(x_i) \left[\frac{(\alpha_1+1)\beta_1^{\alpha_1+1}}{(\bar{x}_i+\beta_1)^{\alpha_1+2}} + \frac{(\alpha_2+1)\beta_2^{\alpha_2+1}}{(\bar{x}_i+\beta_2)^{\alpha_2+2}} - \frac{\beta_1^{\alpha_1+1}\beta_2^{\alpha_2+1}\{(\alpha_1+1)(\bar{x}_i+\beta_2) + (\alpha_2+1)(\bar{x}_i+\beta_1)\}}{(\bar{x}_i+\beta_1)^{\alpha_1+2}(\bar{x}_i+\beta_2)^{\alpha_2+2}} \right] \frac{w_i}{(1+x_i)^2} \tag{7.21}$$

Substitution of the numeric values of $F''(x)$, computed earlier in estimation of the flotation rate distribution, in the above equation gives the predicted fractional recovery $(M_{C,2}(L)/M_{C,1}(L)$ in the cleaner cell. Experimental and predicted fractional recovery values as a function of slurry flow rate for apatite

for different particle size groups are shown in Fig. 7.10. Similar plots for gangue are shown in Fig. 7.11. For reasons unknown, predicted recovery values in cleaner for particle size > 0.25 mm in the case of apatite and for particle size 0.177-0.25 mm in the case of gangue show considerable deviation from experimental values. Comparison of Woodburn et al model, based on throughput dependent Ka, with the present throughput invariant first order distributed rate constant approach shows that, on the whole, both lead to comparable results as far as the back calculated rougher recovery is concerned, but in the cleaner float the latter model turns out to be somewhat more accurate. We may therefore conclude that based on the data that has been scrutinized, the simpler kinetic representation is quite adequate atleast for modelling purposes, as compared to the model of Woodburn et al where in order to obtain an acceptable fit, it was found necessary to introduce slurry flow rate in the expression for the flow rate constant.

EFFECT OF PARTICLE SIZE:

The computed flotation rate distributions provide a good opportunity to test the validity of equation (6.14) which was originally proposed for semi-batch flotation operation. When $R_F(Ka,L)$ is equal to 0.5, substitution of equation (6.14) gives

$$0.5 = R_F(Ka(0.5,L)) = R_F(\bar{\eta}(L)K^o(0.5)) \qquad (7.22)$$

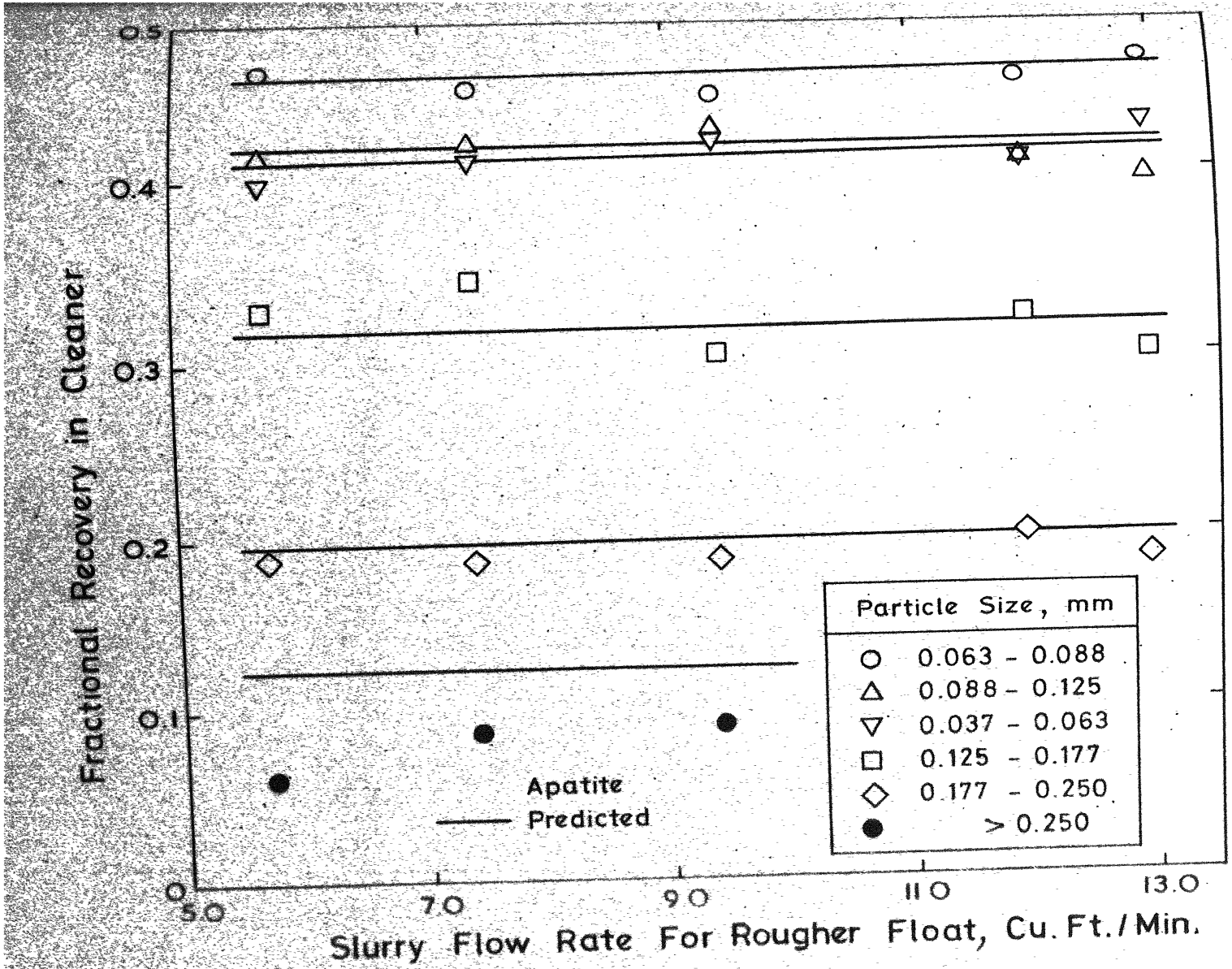

Fig.7.10 Predicted and experimental fractional recoveries of apatite for six particle size groups in a cleaner float using rougher concentrate as feed resulting from different slurry flow rates in rougher cell. Slurry flow rate in cleaner is 9.4 cu. ft/min.

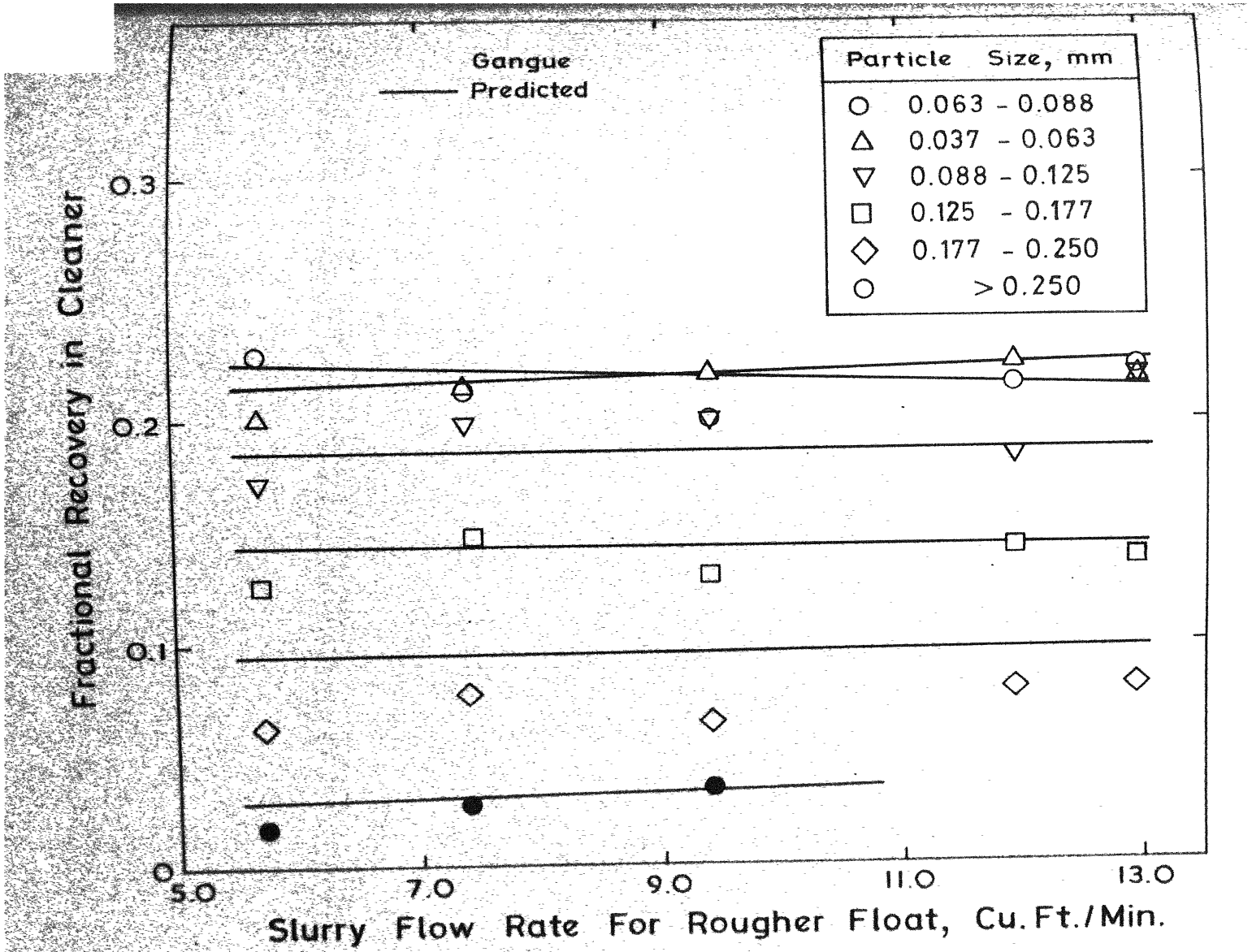

Fig. 7.11 Predicted and experimental fractional recoveries of gangue for six particle size groups in a cleaner float using rougher concentrate as a feed resulting from different slurry flow rates in rougher cells. Slurry flow rate in cleaner is 9.4 cu ft/min.

where Ka(0.5,L) is the median apparent flotation rate constant for particles of size L. As discussed in the last chapter (equation 6.22), $\bar{\eta}(L)$ is proportional to Ka(0.5,L) and the constant of proportionality $K^{o}(0.5)$, is, by definition, independent of particle size. Therefore, equation (6.14) becomes

$$\frac{Ka(L)}{Ka(0.5,L)} = \frac{K^{o}}{K^{o}(0.5)} \qquad (7.23)$$

This implies that plots of $R_F(Ka,L)$ as a function of dimensionless flotation rate constant Ka(L)/Ka(0.5,L) should be independent of particle size, provided the hydrophobicity of the species (i.e., K^{o}) remains unchanged with particle size. A mathematically rigorous derivation of this result is given in previous chapter. Figs. 7.12 and 7.13 show the collapsed distributions for apatite and gangue. The values of the median flotation rate constants were read off from smooth curves in Figs. 7.3 and 7.4. Apatite results are remarkably good, some deviation in gangue data points pertaining to particle size > 0.25 mm could be due to either experimental and computational errors or change in hydrophobocity of large particles. The collapsibility of the flotation rate distributions has a significant implication, namely, other things equal, the apparent rate constants in a distribution are modified to the same extent with change in particle size.

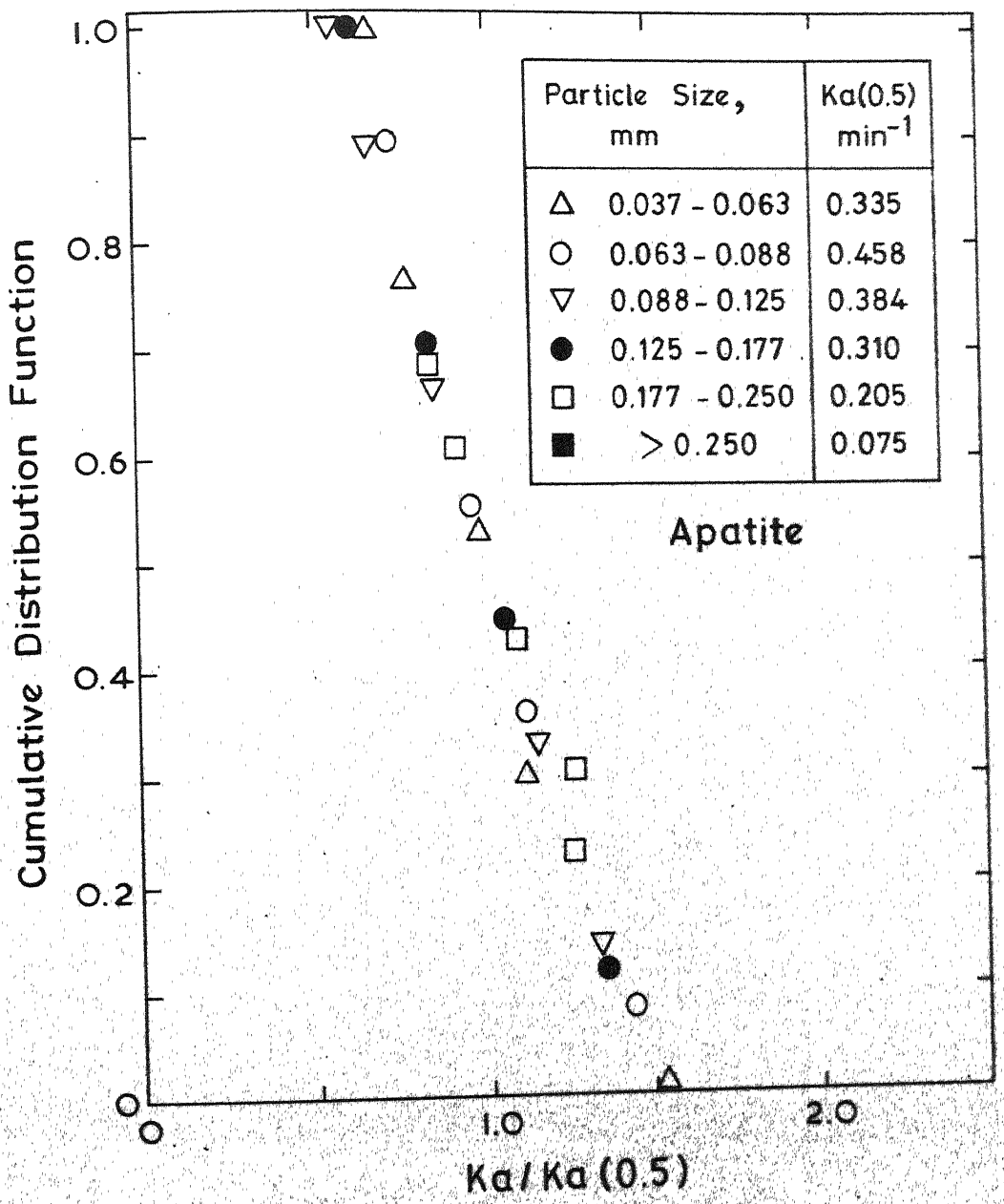

Fig.7.12 Self-similar form of cumulative flotation rate distributions of apatite as a function of the dimensionless flotation rate constant Ka / Ka(0.5) for six particle size groups.

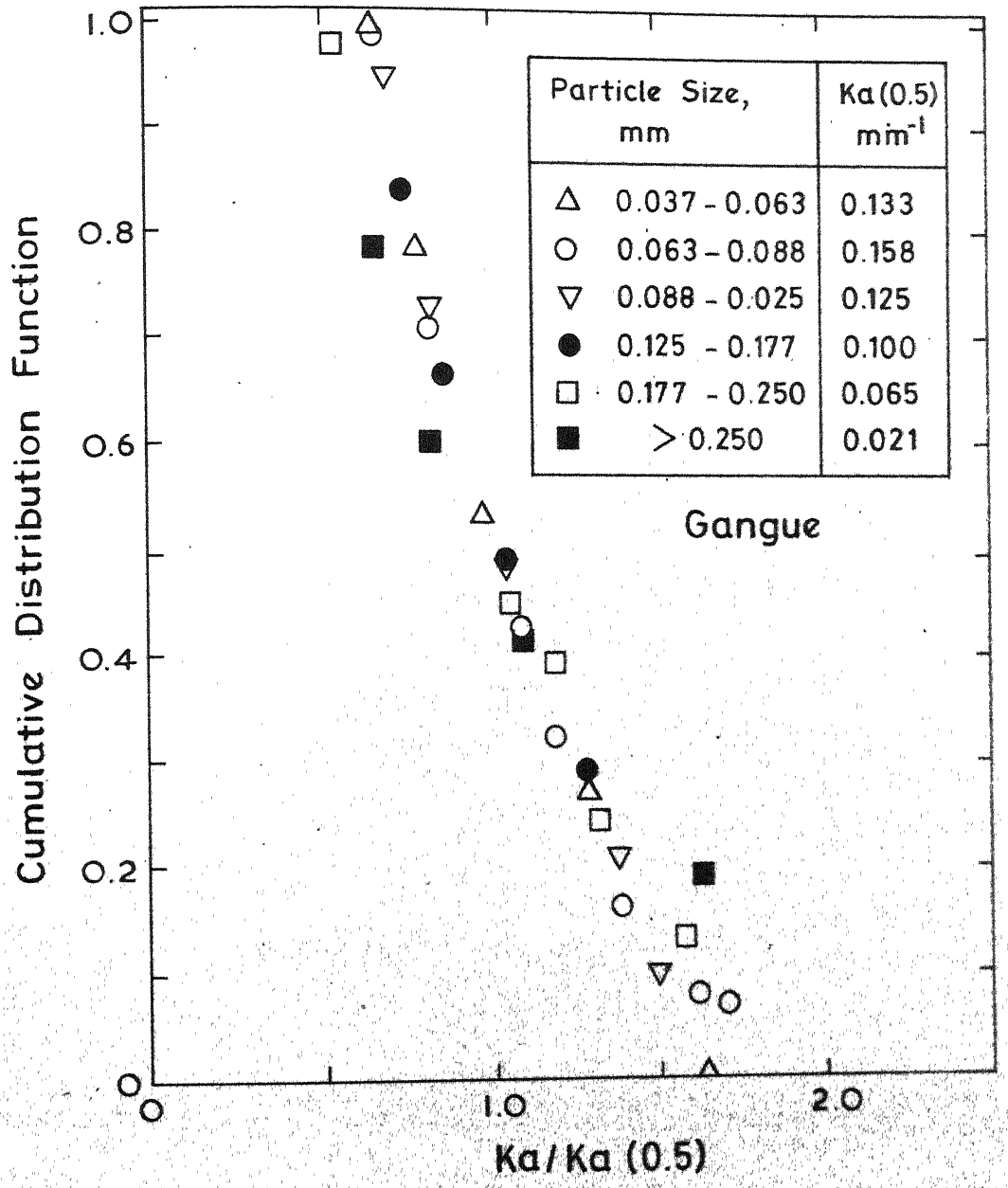

Fig.7.13 Self-similar form of cumulative flotation rate distributions of gangue as a function of the dimensionless flotation rate constant Ka/Ka(0.5) for six particle size groups.

Since the median rate constant Ka(0.5,L) is proportional to the function $\bar{\eta}(L)$, it is now possible to determine the relationship between the latter function and the mean particle size with an uncertainty of a constant of proportionality. Fig. 7.14 shows Ka(0.5,L) as a function of the mean particle size for both apatite and gangue. As expected, in both the cases, there exist characteristic peaks at intermediate size range where the flotation rate is maximum. These curves, moreover, show that optimal separation between apatite and gangue would occur when the particle size is about 0.075 mm and negligible flotation is to be expected when it exceeds about 0.45 mm. From equation (6.14), it follows that the ratio of the median flotation rate constants of apatite and gangue is invariant of particle size. Consequently, if the ordinate of the gangue curve in Fig. 7.14 is approximately rescaled, the resulting curve should match the apatite curve. The broken curve in this figure, scaled by a factor of 3, is in fair agreement with that of apatite except in fine particle size range. Due to possible flocculation and agglomeration of fines the actual situation is perhaps more complicated than what is allowed for in an admittedly highly simple expression in equation (6.14).

COMPUTATION OF FLOTATION RATE DISTRIBUTIONS IN IMPULSE CASE:

The method used here for determining the flotation rate distribution from steady state flotation kinetics pertaining to different slurry flow rates was dictated by availability of

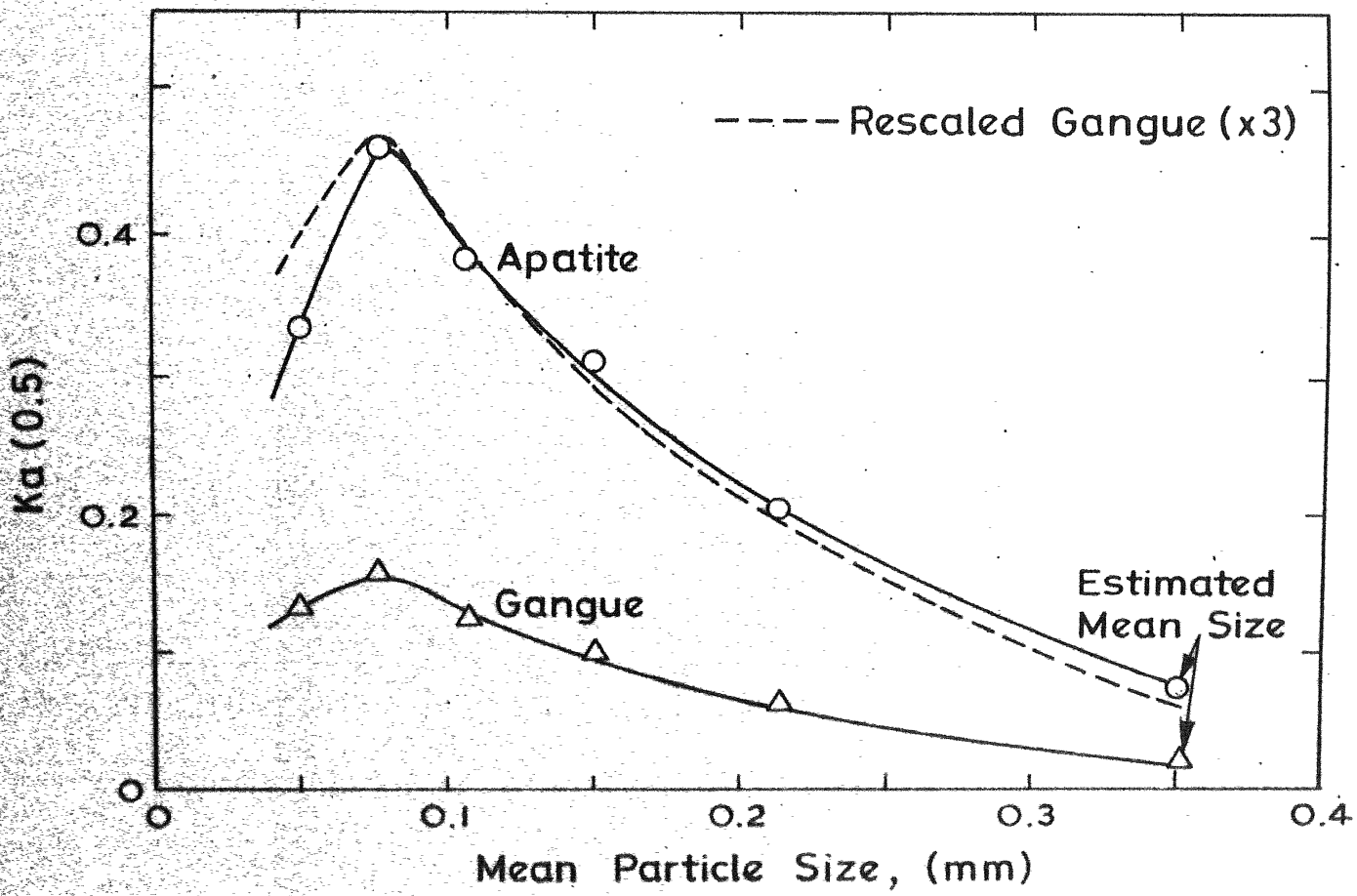

Fig. 7.14 Median apparent flotation rate constant for apatite and gangue as a function of mean particle size.

extensive data in the literature. With slight modification, this technique may be readily applied for response data to a tracer impulse in a continuous cell which would be more convenient provided a suitable tracer is available. As far as the final results are concerned Woodburn et al have already demonstrated the equivalence of steady state and dynamic tests. Briefly, the computation of algorithm in the impulse case is as follows: In response to a tracer impulse, the mass flow rate in tailings stream time t later is

$$M_T(Ka,L,t) = E(t)\, M_F(Ka,L) \exp\left[-Ka\ t\right] \qquad (7.24)$$

or

$$M_T(L,t) = E(t) \int_0^\infty M_F(Ka,L) \exp\left[-Ka\ t\right] dKa \qquad (7.25)$$

Substitution of equation (7.3) leads to

$$M_T(L,t) = E(t) \int_0^\infty - \frac{\partial R_F(Ka,L)}{\partial Ka} \exp\left[-Ka\ t\right] dKa \qquad (7.26)$$

Integrating by parts

$$M_T(L,t) = E(t) \left[1-t \int_0^\infty R_F(Ka,L) \exp\left[-Ka\ t\right] dKa\right] \qquad (7.27)$$

Change in variable from Ka to x leads to

$$M_T(L,t) = E(t) \left[1- \frac{st}{2^{st}} \int_{-1}^{1} F(x)\ (x+1)^{st-1}\ dx\right] \qquad (7.28)$$

where the transformation variable x is same as defined in equation (5.9), viz.,

$$x = 2 \exp\left[-\frac{Ka}{s}\right] - 1 \qquad (7.29)$$

and

$$F(x) = R\left(s \ln\left[\frac{2}{x+1}\right], L\right) \qquad (7.30)$$

Discretization of the integral term in equation (7.28) by n-point Lobatto quadrature formula gives

$$M_T(L,t) = E(t)\left\{1 - st\left[\frac{1}{n(n-1)} + \frac{1}{2^{st}} \sum_{i=2}^{n-1} w_i F(x_i)(x_i+1)^{st-1}\right]\right\} \qquad (7.31)$$

It is now possible to set up the least squares objective function using data at different times which may then be optimized with suitable choice of unknown F(x). Although, the impulse technique is experimentally more efficient, steady state approach may have to be used if suitable radioactive tracer is not available.

DISCUSSION AND CONCLUSIONS:

Given a flotation cell, suitable experiments can be designed to determine the residence time distribution of particles and the apparent flotation rate distribution by either dynamic testing with a tracer impulse or by monitoring the steady state output at different slurry flow rates. The apparent flotation rate distribution turns out to be independent of the slurry flow rate, results, which to a first approximation and at least for modelling purposes, are intuitively valid provided, of course, the hydrodynamic regime is not drastically altered with the slurry flow rate.

The effect of particle size on the apparent flotation rate constant is similar to that in semi-batch case and hence the analysis of flotation kinetics in semi-batch case can be extended to a continuous configuration. Although suitable data is not available, the effect of the aeration rate in continuous cell may also turn out to be the same as in semi-batch cell, in view of the results shown in Chapter 6. More significantly, the kinetic model for continuous cell has been demonstrated to possess sufficiently accurate predictive power and is deemed suitable for modelling, control and optimization purposes. The latter aspect is discussed in the next chapter.

PART II

CHAPTER 8

OPTIMAL AND SUBOPTIMAL SYNTHESIS AND DESIGN OF FLOTATION CIRCUITS

The importance of synthesis and design of chemical reactor units for optimization of the efficiency of the process has been touched upon and some of the generalized techniques, developed so far, have been discussed in the literature review in Chapter 2. Whenever, two or more reactor units are to be interconnected to perform a task, the problem of synthesis of reactor units comes into play. For simple systems trial and error approach to synthesis can be applied, but it becomes progressively cumbersome and eventually impossible as the number of reactor units in the assembly increases.

In this chapter we have carried out tentative investigation of the feasibility of synthesizing and designing optimal and suboptimal multicell flotation circuits, employing a number of appropriate objective functions of recovery and grade, and profit, by a direct optimization approach due to Umeda, Hirai and Ichikawa[149]. First, a flotation circuit with two cells and feed comprising of two species of known overall rate constants is synthesized and designed, and the results are then compared with the real optimum circuit

obtained by using the trial and error technique. Second, the approach is extended to a flotation circuit with four cells and for batteries of cells for a feed comprising of three species. It will be seen that the direct optimization technique seems to be quite promising for synthesis and design of the industrial flotation circuits with large number of interconnected cells and feed comprising of a number of species which can lead to better performance and efficiency of the flotation process.

STATEMENT OF THE PROBLEM:

For illustration purposes, consider two interconnected cells. Fig. 8.1 shows six possible intuitively meaningful configurations in which, for the time being, split streams are excluded. In the trial and error approach the problem is broken into two parts. First, all possible configurations are enumerated, then the best design parameters are determined for each structure, and the optimum configuration is selected by comparing the values of the objective functions. In general, a flotation circuit comprises of many cells, performing rougher, cleaner and scavanger functions and it is quite tedious to enumerate all meaningful structures. Moreover, there is no a priori justification for ignoring split streams and the enumeration problem thus becomes even more complex. In the integral approach, proposed by Umeda, Hirai and Ichikawa[149], enumerations are totally circumvented and

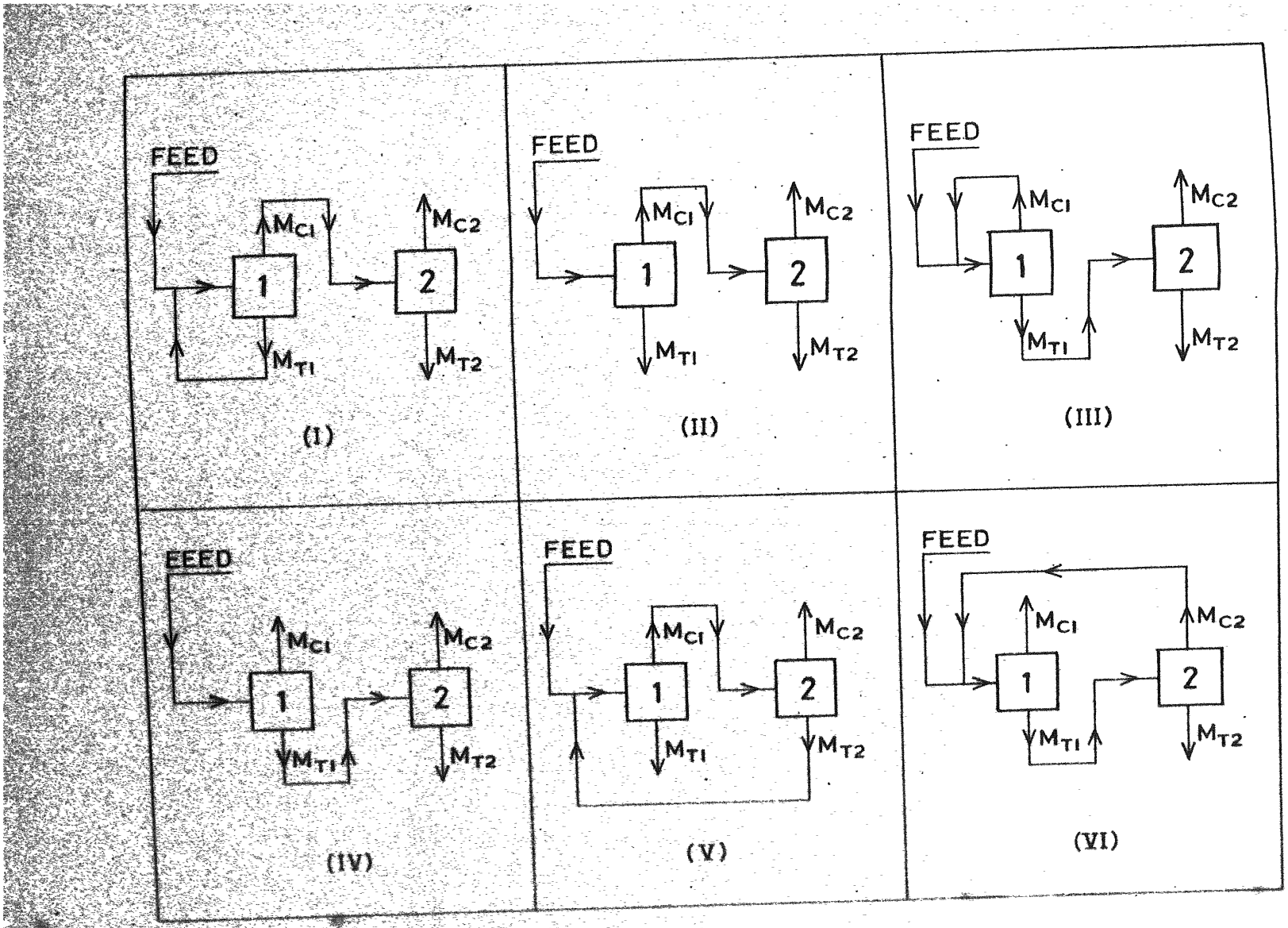

Fig. 8.1 Six possible configurations for a circuit with two flotation cells.

the optimal structure and design parameters are extracted simultaneously from a generalized circuit by direct search. This technique has been applied to solve linkage (including split streams) problem and to determine the optimal residence time distribution of particles in each cell. The residence time distribution, as a design parameter, is an automatic engineering choice since, as pointed out by Woodburn et al[91], only the holding time is at present capable of being included into a quantitative description of the flotation kinetics. These authors had also earlier determined the optimal residence times in perfectly mixed cells but for an assumed circuit configuration.

FLOTATION KINETIC MODEL:

From the literature reviewed in Chapter 2, it is evident that for all practical purposes the kinetics of flotation can be approximately described by a first order expression with distributed flotation rate constant. For industrial modelling purposes it is also known from data of Woodburn et al[53] that the cell behaves like, more or less, a perfect mixer and the mean residence time is a function of particle size and density. Thus, if $M_F(Ka)$ is mass flow rate of particles of overall flotation rate constant Ka to the cell, as defined earlier, and $\bar{t}$ is the mean residence time in the pulp, the mass flow rates in concentrate and tailings stream at steady state are

$$M_C(Ka) = M_F(Ka) \left[\frac{Ka\ \bar{t}}{1+Ka\ \bar{t}} \right] \qquad (8.1)$$

and

$$M_T(Ka) = M_F(Ka) \left[\frac{1}{1+Ka\ \bar{t}} \right] \qquad (8.2)$$

Using these relationships it is now possible to construct a steady state mathematical model for n_s particulate species (discretized apparent flotation rate distribution) of same size and density in a flotation circuit with n_c cells. For simplicity, the treatment is restricted to single size particles, or more correctly to particles of same value of $\bar{t}$. Relaxation of this constraint is discussed later. It will be noted that water balance of circuit, while important, is not really germane to the problem, as each cell is normally equipped with arrangement for addition of water (and surfactant) to bring the pulp to required consistency and level. A constraint, given in the sequel, will assure that the pulp density never exceeds a limiting value, say 20 percent.

Let the specific flotation rate constant of the j-th species be Ka_j and f_j be its fractional valuable mineral content, and $\bar{t}_i$ be the mean residence time of solid particles in i-th cell. In the generalized configuration, the feed is split into n_c streams and fed to each cell. Similarly, each concentrate and tailings stream is split into (n_c+1) streams and connected as feed to every other cell as well as short circuited back to the cell from which it originated. The

(n_c+1)-th split leaves the circuit as concentrate or tailings output, as the case may be. The generalized configuration for 2 cells is shown in Fig. 8.2. Consider now the i-th cell. The total feed flow rate of j-th species to this cell is

$$F_{ji} = M_{Fj}\,\delta_{fi} + \sum_{k=1}^{n_c} M_{Tjk}\,\delta_{ki} + \sum_{k=1}^{n_c} M_{Cjk}\,\beta_{ki} \qquad (8.3)$$

where M_{Fj} is flow rate of j-th component in new feed, δ_{fi} is fraction of this feed going to i-th cell, M_{Tjk} is tailings flow rate of j-th species from k-th cell, δ_{ki} is split fraction of this flow going to i-th cell, M_{Cjk} is concentrate flow rate of j-th species originating from k-th cell and β_{ki} is split fractio of concentrate flow from k to i-th cell. Let in equations (8.1 and (8.2)

$$\alpha_{ji} = \frac{1}{1+Ka_j\,\bar{t}_i} \qquad (8.4)$$

Therefore, equations for flow rates of j-th species from i-th cell in concentrate and tailings streams can be rewritten as

$$M_{Cji} = F_{ji}\,[1-\alpha_{ji}] \qquad (8.5)$$

and

$$M_{Tji} = F_{ji}\,\alpha_{ji} \qquad (8.6)$$

Combining equations (8.5) and (8.6)

$$M_{Cji} = M_{Tji}\left[\frac{1-\alpha_{ji}}{\alpha_{ji}}\right] \qquad (8.7)$$

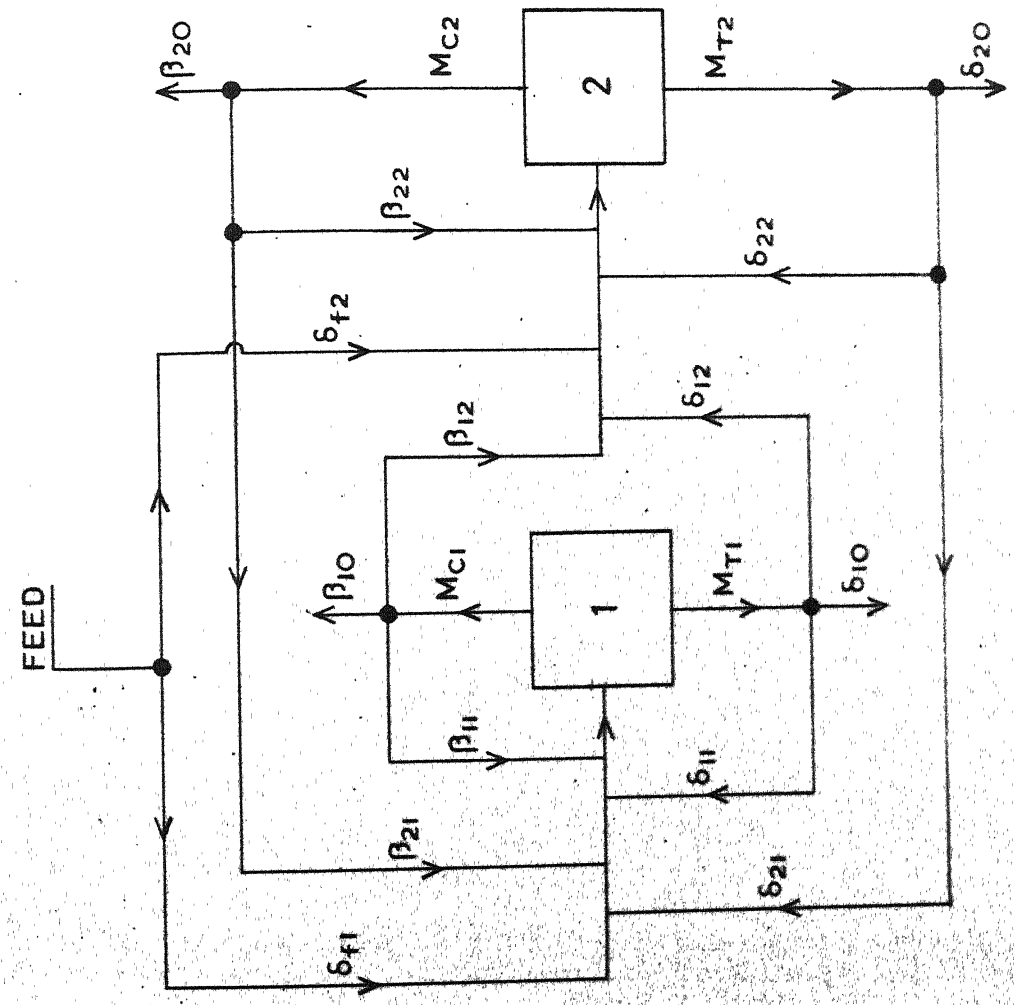

Fig. 8.2 Generalized configuration for two flotation cells.

Substitution in equation (8.3) gives

$$F_{ji} = M_{Fj}\,\delta_{fi} + \sum_{k=1}^{n_c} M_{Tjk}\left\{\left[\frac{1-\alpha_{jk}}{\alpha_{jk}}\right]\beta_{ki} + \delta_{ki}\right\} \quad (8.8)$$

Substitution in equation (8.6) results in

$$M_{Tji} = M_{Fj}\,\delta_{fi}\,\alpha_{ji} + \alpha_{ji}\sum_{k=1}^{n_c} M_{Tjk}\left\{\left[\frac{1-\alpha_{jk}}{\alpha_{jk}}\right]\beta_{ki}+\delta_{ki}\right\},$$

$$j = 1,2,\ldots, n_s$$

$$i = 1,2,\ldots, n_c \quad (8.9)$$

These (n_s+n_c) linear algebraic equations can be solved for M_{Tji} in terms of linkage and design parameters. The formal solution can be written as

$$M_{Tji} = \phi_{ji}\,(M_{Fj},\ \delta\text{'s},\ \beta\text{'s},\ \alpha\text{'s}) \quad (8.10)$$

Similarly from equation (8.7)

$$M_{Cji} = \phi_{ji}\left[\frac{1-\alpha_{ji}}{\alpha_{ji}}\right] \quad (8.11)$$

Let δ_{io} and β_{io} be the fractions of tailings and concentrate from i-th cell, respectively, leaving the circuit, then, by definition (fraction of concentrate/feed flow rate.), the percentage overall recovery is,

$$R_c = \frac{\sum_{i=1}^{n_c}\sum_{j=1}^{n_s} M_{Cji}\,\beta_{io}}{\sum_{j=1}^{n_s} M_{Fj}} \times 100 \quad (8.12)$$

of overloading of bubbles and loss of flotation selectivity, the pulp density D_p (Percent mass of solid in slurry) should not exceed a prescribed value d_p in any cell. By definition of the mean residence time the hold up of solids in i-th cell is

$$H_i = \bar{t}_i \sum_{j=1}^{n_s} M_{Tji} \tag{8.19}$$

Therefore, the lower bound on volume of the i-th cell is

$$v_i \geq H_i \left[\frac{1}{D_s} + \frac{100-d_p}{d_p} \right] \tag{8.20}$$

where D_s is solid density. Moreover, the overall size of the plant is also restricted to some reasonable volume V_T of all cells combined, hence

$$V_T = \sum_{i=1}^{n_c} v_i \tag{8.21}$$

Following the suggestion of Woodburn et al, for convenience in computation, personal judgement is used to impose a quite liberal upper constraint $\bar{t}'$ on $\bar{t}$, i.e.,

$$0 \leq \bar{t}_i \leq \bar{t}'; \quad i = 1,2,\ldots, n_c \tag{8.22}$$

To be acceptable, it is necessary that the grade of the concentrate does not drop below a minimum level g, which gives rise to

$$G \geq g \tag{8.23}$$

An obvious objective is to maximize recovery given in equation (8.12), subject to above constraints. In view of the fact that as $Ka_1 > Ka_2 \ldots, > Ka_{n_s}$ in general, $f_1 > f_2 > \ldots, > f_{n_s}$,

we may infer from physical nature of the problem that the optimum lies on boundary of constant G = g. This, however, may not be necessarily true for more complicated objective functions as illustrated subsequently.

COMPUTATIONAL ASPECTS:

The integral approach used here requires search through a rather large parameter space. This gives rise to well known difficulties in matter of slow rate of convergence and false optima. An allied problem is of deciding whether a split stream is, in fact, missing or not when linkage parameters δ's and β's are near one or zero. On the otherhand, realization of a large number of suboptima is not necessarily a disadvantage, since some configurations may turn out to be simpler to design with lower capital investment and more economical to operate than the global optimum structure with only a marginal loss in performance.

The set of algebraic equations in (8.9) were solved by Gauss Jordan technique[161]. A systematic evaluation of the best optimization algorithm was beyond the scope of this investigation. However, modified complex[162,163] and Random search[160] methods were employed (See Appendix B). Success with the first algorithm, used by Umeda et al[149] also, was found to be highly sensitive to initial guess, the latter method although slow, was quite reliable. In every case a number of

different initial guesses were tried in order to assure, as far as possible, a true optimum. The optimization was carried out in two or more stages. In course of computation it was observed that eventually the improvement in the objective function became rather slow. The search was stopped at this stage and linkage ratios which were less than or greater than prespecified values were taken as zero and one, respectively. Starting with the reduced generalized configuration, the search was renewed in the smaller parameter space. This stage wise search procedure was continued as long as the successive reduced configuration resulted in an improvement in the objective function. As pointed out by Hendry, Rudd and Seader[150], this integral approach with direct stage wise search may not necessarily lead to the global optimum although for two cell case treated in the sequel the convergence has been verified by independent means.

TWO SPECIES, TWO CELL PROBLEM:

For demonstration, consider first the case $n_s = n_c = 2$. This will permit evaluation of the efficacy of the integral method by comparison with the enumerated structures, in Fig.8.1, optimized individually with respect to the mean residence time in cells I and II. Table 8.1 lists the numeric values of feed characteristics and the constraints on the process design variables employed for this exercise. Expansion of equation (8.9) for this particular case, and rearrangement of terms leads to

Table 8.1: Numeric Values Used in Computation of Design Parameters in Two Cell Circuit Problem.

Feed composition percent	Constraints on variables	Values of the parameters
Valuable = 22	$V_T \leq 20$ cuft	$Ka_{val} = 1\ min^{-1}$
Gangue = 78	$d_p \leq 20$ percent	$Ka_{gang} = 0.1\ min^{-1}$
	$0 \leq \bar{t}_1, \bar{t}_2 \leq 20$	$M_F = 25$ lbs/min
		$p_F = 10.0$ units
		$p_G = 1.00$ units

following two equations.

$$M_{Tj1}\,(\delta_{11}\,\alpha_{j1} + \beta_{11}\,(1-\alpha_{j1})-1) + M_{Tj2}\,[\delta_{21} + \beta_{21}(\frac{1-\alpha_{j2}}{\alpha_{j2}})]\,\alpha_{j1} + M_{Fj}\,\delta_{f1}\,\alpha_{j1} = 0,$$

$$j = 1,2,\ldots, n_s \quad (8.24)$$

and

$$M_{Tj1}\,(\delta_{12} + \beta_{12}\,(1-\frac{\alpha_{j1}}{\alpha_{j1}}))\,\delta_{j2} + M_{Tj2}\,[\delta_{22}\,\alpha_{j2} + \beta_{22}\,(1-\alpha_{j2})-1] + M_{Fj}\,\delta_{f2}\,\alpha_{j2} = 0$$

$$j = 1,2,\ldots, n_s \quad (8.25)$$

Equations (8.24) and (8.25) can be solved simultaneously for M_{Tj1} and M_{Tj2} in terms of M_{Fj}, δ's, β's and α's to give ϕ_{ji} which, then can be substituted in equation (8.11) to give M_{Cji}. Once M_{Cji} are known, explicit expression for recovery R_c and grade G in terms of linkage parameters δ's and β's and design parameters α's can be obtained from equations (8.12) and (8.13), as follows

$$R_c = \frac{(M_{C11} + M_{C21})\,\beta_{10} + (M_{C12} + M_{C22})\,\beta_{20}}{M_{F1} + M_{F2}} \times 100 \quad (8.26)$$

and

$$G = \frac{(M_{C11}\,f_1 + M_{C21}\,f_2)\,\beta_{10} + (M_{C12}\,f_1 + M_{C22}\,f_2)\,\beta_{20}}{(M_{C11} + M_{C21})\,\beta_{10} + (M_{C12} + M_{C22})\,\beta_{20}} \times 100 \quad (8.27)$$

where

$$M_{Cj1} = \frac{(1-\alpha_{j1})}{\alpha_{j1}\Delta_j} M_{Fj} \left\{ \delta_{f1}\alpha_{j1} \left[1-\delta_{22}\alpha_{j2} - \beta_{22}(1-\alpha_{j2})\right] + \delta_{f2}\delta_{j2} \left[\delta_{21} + \beta_{21} \left(\frac{1-\alpha_{j2}}{\alpha_{j2}}\right)\right] \alpha_{j1} \right\}, \quad j = 1,2 \qquad (8.28)$$

$$M_{Cj2} = \frac{(1-\alpha_{j2})}{\alpha_{j2}\Delta_j} M_{Fj} \left\{ \delta_{f2}\alpha_{j2} \left[1-\delta_{11}\alpha_{j1} - \beta_{11}(1-\alpha_{j1})\right] + \delta_{f1}\delta_{j1} \left[\delta_{12} + \beta_{12} \left(\frac{1-\alpha_{j1}}{\alpha_{j1}}\right)\right] \alpha_{j2} \right\}, \quad j = 1,2 \qquad (8.29)$$

and

$$\Delta_j = \begin{vmatrix} \left[\delta_{11}\alpha_{j1} + \beta_{11}(1-\alpha_{j1})-1\right] & \left[\delta_{21}\alpha_{j1} + \beta_{21} \left(\frac{1-\alpha_{j2}}{\alpha_{j2}}\right) \alpha_{j1}\right] \\ \left[\delta_{12}\alpha_{j2} + \beta_{12}\left(\frac{1-\alpha_{j1}}{\alpha_{j1}}\right)\alpha_{j2}\right] & \left[\delta_{22}\alpha_{j2} + \beta_{22}(1-\alpha_{j2})-1\right] \end{vmatrix}$$

$$j = 1,2 \qquad (8.30)$$

Two objective functions used were, maximize recovery subject to constraint that grade does not fall below (A) 35 and (B) 75 percent respectively. In addition, a profit objective function (C), given below, was also formulated.

$$(C) = p_F + (G - G_F)\, p_G \qquad (8.31)$$

where p_F is price of feed ore of grade G_F and p_G is the increase in price of the concentrate for every one percent improvement in the grade.

Results are presented in Tables 8.2(A), 8.2(B) and 8.2 (C), where initial guess, optimal configuration at first

Table 8.2(A): Values of Designed Parameters for Stage Wise Optimization for 2 Cell 2 Species Problem in Case of Objective A.

Parameters	Initial Value	Stage I	Stage II	Optimal Value
δ_{10}	0.525	0.764	1.00	1.00
δ_{11}	0.150	0.067	0.00	0.00
δ_{12}	0.325	0.169	0.00	0.00
δ_{20}	0.717	0.00	0.00	0.00
δ_{21}	0.101	0.494	1.00	1.00
δ_{22}	0.182	0.506	0.00	0.00
β_{10}	0.346	0.184	0.00	0.00
β_{11}	0.185	0.122	0.00	0.00
β_{12}	0.469	0.694	1.00	1.00
β_{20}	0.661	0.900	1.00	1.00
β_{21}	0.152	0.00	0.00	0.00
β_{22}	0.187	0.100	0.00	0.00
δ_{f1}	0.254	0.00	0.00	0.00
δ_{f2}	0.746	1.00	1.00	1.00
$\bar{t}_1$	6.84	9.100	18.545	18.700
$\bar{t}_2$	5.238	2.015	3.945	3.730
v_1	-	8.08	11.90	12.51
v_2	-	6.59	7.48	7.48
Recovery	-	61.49	61.99	62.01
Grade	-	35.00	35.00	35.00

Table 8.2(B): Values of Designed Parameters for Stage-Wise Optimization for 2 Cell 2 Species Problem in Case of Objective B.

Parameter	Initial value	Stage I	Stage II	Optimal value
δ_{10}	0.352	0.00	0.00	0.00
δ_{11}	0.320	0.522	0.00	0.00
δ_{12}	0.328	0.478	1.00	1.00
δ_{20}	0.840	0.973	1.00	1.00
δ_{21}	0.088	0.012	0.00	0.00
δ_{22}	0.072	0.015	0.00	0.00
β_{10}	0.643	0.783	1.00	1.00
β_{11}	0.144	0.141	0.00	0.00
β_{12}	0.213	0.076	0.00	0.00
β_{20}	0.025	0.002	0.00	0.00
β_{21}	0.485	0.619	1.00	1.00
β_{22}	0.490	0.379	0.00	0.00
δ_{f1}	0.078	0.00	0.00	0.00
δ_{f2}	0.912	1.00	1.00	1.00
$\bar{t}_1$	1.093	0.996	0.658	0.658
$\bar{t}_2$	2.527	3.650	14.032	14.032
v_1	--	1.612	1.420	1.420
v_2	--	12.170	18.580	18.580
Recovery	-	22.350	24.867	24.867
Grade	-	35.00	35.00	35.00

Table 8.2(C): Values of Designed Parameters for Stage-Wise Optimization for 2 Cell 2 Species Problem in case of Objective C.

Parameters	Initial value	Stage I	Stage II	Optimal value
δ_{10}	0.518	0.908	1.00	1.00
δ_{11}	0.377	0.088	0.00	0.00
δ_{12}	0.105	0.004	0.00	0.00
δ_{20}	0.285	0.006	0.00	0.00
δ_{21}	0.237	0.443	1.00	1.00
δ_{22}	0.478	0.551	0.00	0.00
β_{10}	0.651	0.001	0.00	0.00
β_{11}	0.236	0.325	0.00	0.00
β_{12}	0.113	0.674	1.00	1.00
β_{20}	0.670	0.880	1.00	1.00
β_{21}	0.049	0.002	0.00	0.00
β_{22}	0.281	0.118	0.00	0.00
δ_{f1}	0.246	0.271	0.00	0.00
δ_{f2}	0.754	0.729	1.00	1.00
$\bar{t}_1$	8.948	13.460	14.816	14.806
$\bar{t}_2$	4.353	0.715	0.822	0.822
v_1	-	16.65	17.31	17.31
v_2	-	3.33	2.69	2.69
Recovery	-	34.69	33.630	33.645
Grade	-	57.60	60.70	60.70
Price	-	395.70	409.76	409.78

stage and the final optimal structures synthesized from the reduced configuration for three objective functions (A), (B) and (C), respectively, are shown. The reduction was carried out by equating large and small linkage parameters (> 0.8 and < 0.2) with one and zero, respectively. As expected, in first two cases optimum occurs at grade constraint boundary, but, interestingly, depending on the grade stipulation, the structures of the optimal circuits are quite different. For objective (A) and (B) the resulting configurations are equivalent to configuration No. (VI) and (V) in Fig. 8.1(Cell number 1 in the computed configuration refers to cell number 2 in Fig. 8.1 and vice-versa). The last column under each of the three objectives presents results of trial and error approach obtained by optimizing individually the six configurations in Fig. 8.1 with respect to residence times only. The agreement provides a partial check that it is possible, at least in this case, to derive an optimal circuit starting from the generalized configuration in Fig. 8.2.

The two optimal circuits are intuitively reasonable. Thus, when recovery is to be increased at some sacrifice of the grade, as in objective (A), it is obvious that one of the cells must act as a scavanger (Cell II, Fig. 8.1(vi)). On the other hand in objective (B) high grade restriction makes it necessary that the rougher concentrate be refloated in cleaner cell (Cell I, in Fig. 8.1 (V)).

THREE SPECIES FOUR CELL PROBLEM:

From industrial flotation point of view, this is a more meaningful problem. The additional particulate species, considered in this case, is middlings in which valuable mineral is locked in gangue matrix. Table 8.3 gives the numeric values used for maximizing the recovery subject to a minimum of 35 percent grade. As shown in Fig. 8.3, the generalized structure has a rather large number of parameters and attainment of convergence in a reasonable time is doubtful. Therefore, optimization was carried out in four stages. At the end of a stage, all split stream ratios ≤ 0.05 were set zero and those ≥ 0.95 were equated with one. Each stage resulted in improvement in recovery. The optimal structure is shown in Fig. 8.4, the linkage parameters are given in the paranthesis. Table 8.4 gives stage-wise progress of the linkages and design parameters and the objective function.

It will be noted in Fig. 8.4 that in the optimal configuration there is one split stream of value 0.17 only. In order to simplify the structure, it was decided to remove this stream and seek new parameters for best recovery. Results of this stage of computation, in column 7 in Table 8.4, show that the recovery has now fallen somewhat. Further reduction was carried out in stage 6 by eliminating cell 4 altogether from the circuit, since its computed volume was comparatively small as

Table 8.3: Numeric Values Used in Computation of Design Parameters in 4 Cell 3 Species Problem.

Feed Composition, percent	Constraints	Values of the parameters
Valuable = 15	$g = 35$	$Ka_{val} = 1\ min^{-1}$
Middling = 20	$0 \leq t_j \leq 20$	$Ka_{mid} = 0.1\ min^{-1}$
	$j = 1,2,\ldots,4$	
Gangue = 65	$d_p = 20$	$Ka_{gang} = 0.01\ min^{-1}$
	$V_T = 80$ cuft	$M_F = 25$ lbs/min.

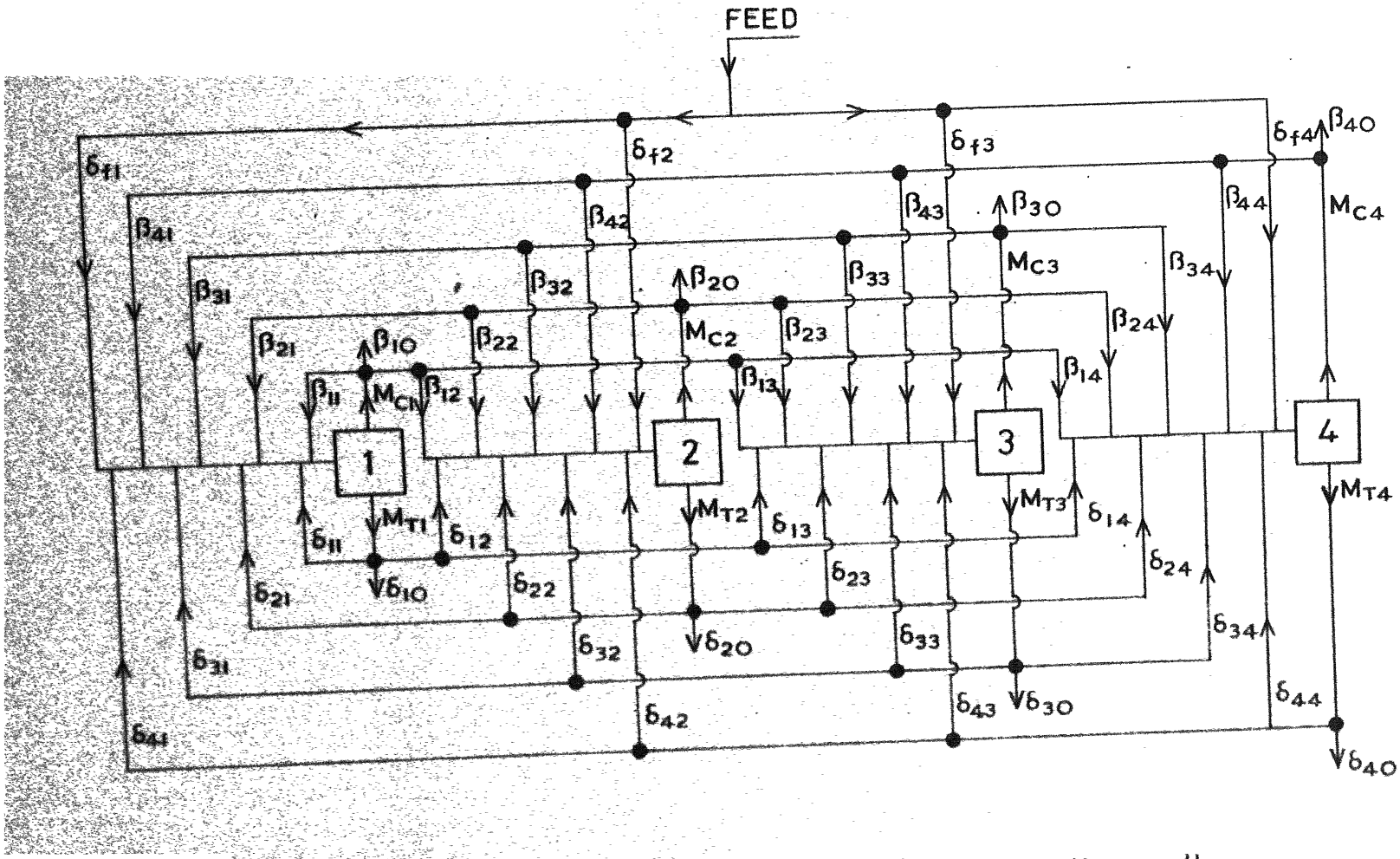

Fig. 8. 3 Generalized configuration for four flotation cells.

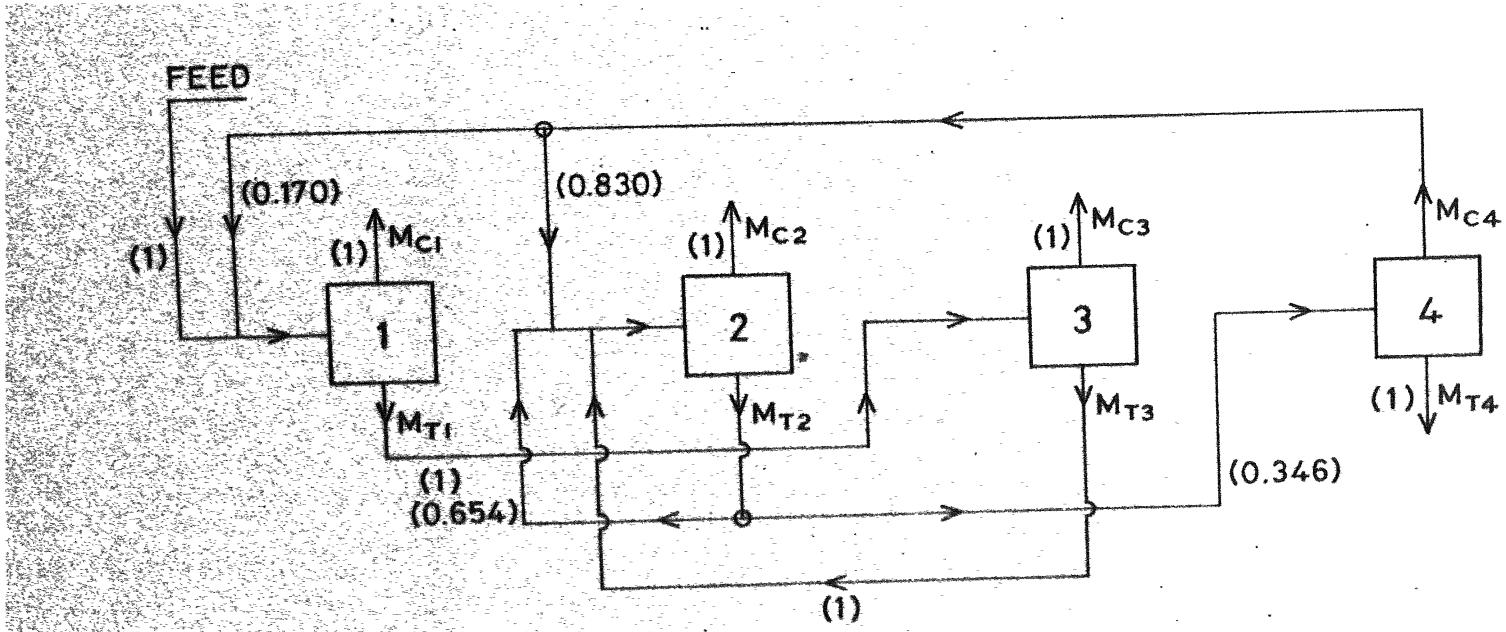

Fig. 8.4 Optimal configuration for three species four cells problem.

Table 8.4: Values of Designed Parameters for Stage-Wise Optimization for 4 Cell 3 Species Problem in Case of Objective A.

Parameters	Initial value	Stage I	Stage II	Stage III	Stage IV	Stage V	Stage VI
δ_{10}	0.484	0.031	0.002	0.000	0.000	0.000	0.000
δ_{11}	0.046	0.068	0.031	0.000	0.000	0.000	0.000
δ_{12}	0.180	0.389	0.352	0.000	0.000	0.000	0.000
δ_{13}	0.166	0.403	0.615	1.000	1.000	1.000	1.000
δ_{14}	0.124	0.109	0.000	0.000	0.000	0.000	-
δ_{20}	0.541	0.049	0.016	0.002	0.000	0.000	0.298
δ_{21}	0.250	0.251	0.014	0.000	0.000	0.000	0.000
δ_{22}	0.130	0.367	0.238	0.743	0.654	0.680	0.702
δ_{23}	0.036	0.165	0.423	0.000	0.000	0.000	0.000
δ_{24}	0.043	0.168	0.309	0.255	0.346	0.320	-
δ_{30}	0.285	0.019	0.020	0.000	0.000	0.000	0.000
δ_{31}	0.183	0.000	0.000	0.000	0.000	0.000	0.000
δ_{32}	0.207	0.800	0.945	1.000	1.000	1.000	1.000
δ_{33}	0.099	0.143	0.035	0.000	0.000	0.000	0.000
δ_{34}	0.226	0.038	0.000	0.000	0.000	0.000	-
δ_{40}	0.507	0.403	0.543	0.982	1.000	1.000	-
δ_{41}	0.220	0.045	0.000	0.000	0.000	0.000	-
δ_{42}	0.033	0.072	0.000	0.000	0.000	0.000	-
δ_{43}	0.219	0.407	0.457	0.018	0.000	0.000	-
δ_{44}	0.021	0.073	0.000	0.000	0.000	0.000	-

contd...

contd...

Parameters	Initial value	Stage I	Stage II	Stage III	Stage IV	Stage V	Stage VI
β_{10}	0.371	0.736	0.658	1.000	1.000	1.000	1.000
β_{11}	0.156	0.003	0.000	0.000	0.000	0.000	0.000
β_{12}	0.244	0.018	0.000	0.000	0.000	0.000	0.000
β_{13}	0.061	0.239	0.342	0.000	0.000	0.000	0.000
β_{14}	0.168	0.004	0.000	0.000	0.000	0.000	-
β_{20}	0.414	0.990	1.000	1.000	1.000	1.000	1.000
β_{21}	0.210	0.007	0.000	0.000	0.000	0.000	0.000
β_{22}	0.245	0.000	0.000	0.000	0.000	0.000	0.000
β_{23}	0.084	0.000	0.000	0.000	0.000	0.000	0.000
β_{24}	0.047	0.003	0.000	0.000	0.000	0.000	-
β_{30}	0.551	0.582	1.000	1.000	1.000	1.000	1.000
β_{31}	0.021	0.077	0.000	0.000	0.000	0.000	0.000
β_{32}	0.205	0.194	0.000	0.000	0.000	0.000	0.000
β_{33}	0.406	0.014	0.000	0.000	0.000	0.000	0.000
β_{34}	0.177	0.133	0.000	0.000	0.000	0.000	-
β_{40}	0.323	0.105	0.811	0.030	0.000	0.000	-
β_{41}	0.150	0.359	0.090	0.702	0.170	0.000	-
β_{42}	0.058	0.227	0.089	0.268	0.830	1.000	-
β_{43}	0.249	0.308	0.000	0.000	0.000	0.000	-
β_{44}	0.220	0.001	0.010	0.000	0.000	0.000	-

Contd...

Contd...

Parameters	Initial value	Stage I	Stage II	Stage III	Stage IV	Stage V	Stage VI
δ_{f1}	0.080	0.279	0.637	0.577	1.000	1.000	1.000
δ_{f2}	0.004	0.550	0.362	0.423	0.000	0.000	0.000
δ_{f3}	0.045	0.170	0.000	0.000	0.000	0.000	0.000
δ_{f4}	0.871	0.001	0.000	0.000	0.000	0.000	-
$\bar{t}_1$	4.580	13.015	11.707	14.88	18.090	19.890	20.000
$\bar{t}_2$	4.390	15.028	14.206	19.98	19.420	18.810	18.290
$\bar{t}_3$	0.196	5.077	7.107	15.19	19.020	16.540	16.880
$\bar{t}_4$	1.610	4.332	14.803	14.88	8.410	5.920	-
v_1	-	20.42	10.23	10.67	20.18	21.60	21.69
v_2	-	45.73	42.96	47.95	31.14	31.84	31.42
v_3	-	9.78	14.99	8.85	16.43	14.31	14.54
v_4	-	3.41	11.80	7.77	4.28	3.02	-
Recovery	12.80	69.08	70.27	70.72	71.13	71.08	70.93
Grade	79.40	35.00	35.01	35.00	35.00	35.00	35.00

compared to other cells. It will be seen from column 8 of Table 8.4 that the recovery has further decreased somewhat but the final circuit is now considerably simpler. The last two structures are shown in Fig. 8.5, stage 5 structure in broken and stage 6 in solid lines. This example illustrates, given the necessary data, it should be possible to incorporate capital investment and operation cost also in a more comprehensive profit function for an objective decision on choice of the most efficient circuit. It is reiterated that the final structure shown here may not necessarily be optimal in the global sense. Nontheless, in view of the very large number of possibilities, even the suboptimal or near optimal configuration is very difficult to synthesize based on only plant experience, intuitive feeling or even test results of a single flotation cell.

THREE SPECIES AND BATTERIES OF FLOTATION CELLS:

Batteries of flotation cells, frequently used in industry, can also be synthesized and designed using the integral approach. A battery consists of flotation cells arranged in series so that the tailings of one cell goes to the next cell in series. While the parallel concentrate streams from each cell combine together to form concentrate stream from the battery, the tailings of the last cell in series constitute the tailings stream. A typical battery with four flotation cells is shown in Fig. 8.6. A generalized circuit with four batteries will be

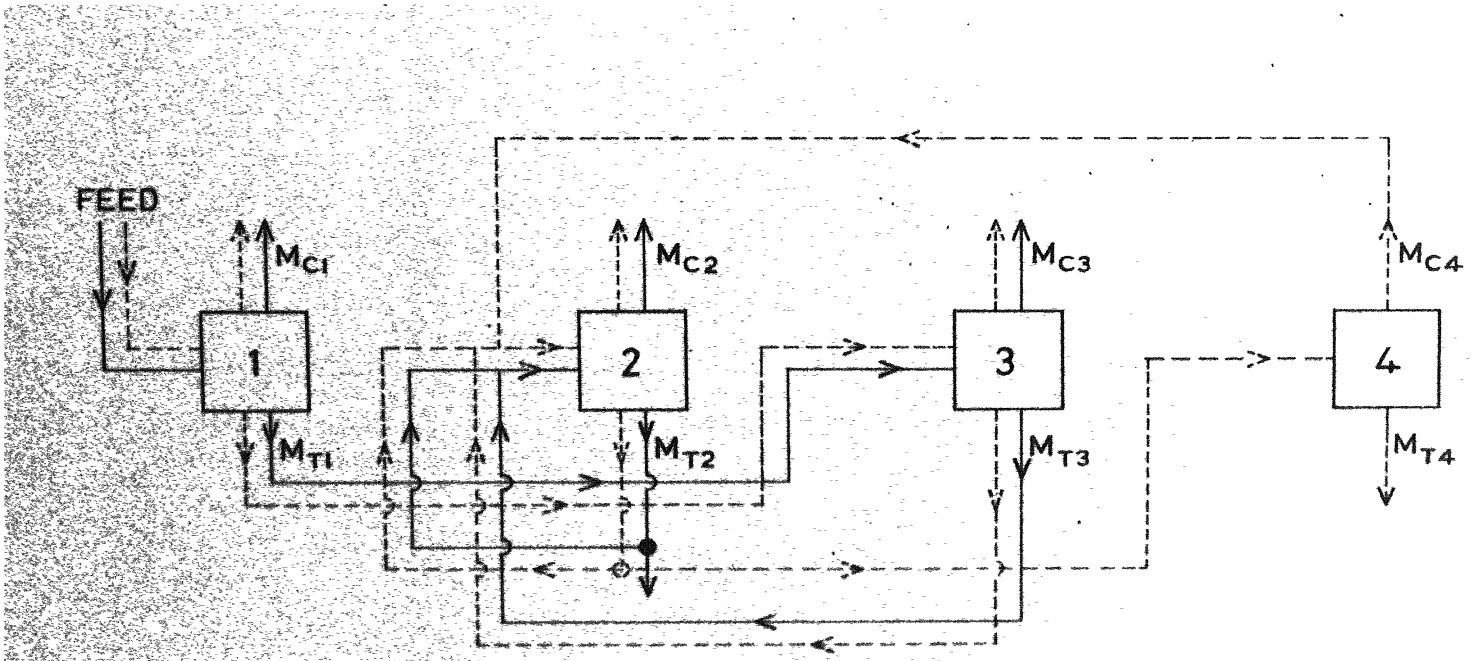

Fig. 8.5 Suboptimal configuration for three species four cells problem.

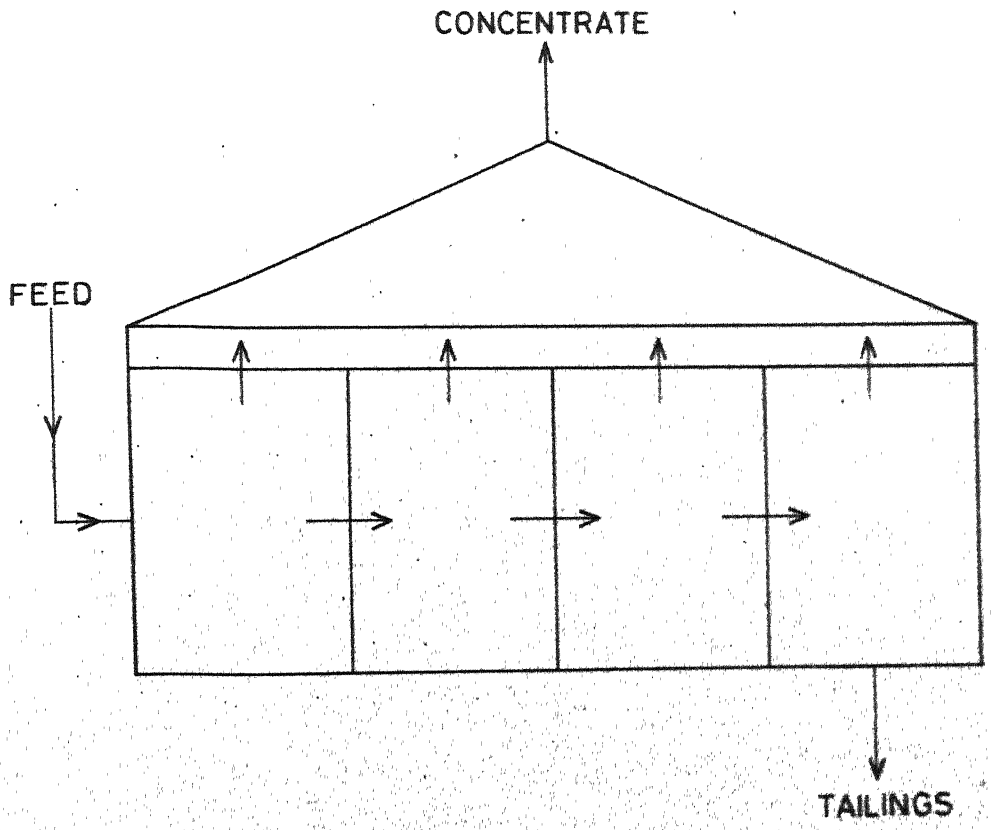

Fig.8.6 A battery of four flotation cells.

identical to the one given in Fig. 8.3. However, it should be recognized that each block (1 to 4) in this figure now represents a battery similar to one shown in Fig. 8.6 rather than individual flotation cell. If a single battery consists of n_c flotation cells each of which is a perfect mixture, and if the mean residence time of each cell is equal to $\bar{t}$, it can be shown (See Appendix C) that the mass flow rate of j-th species in tailings is

$$M_{Tj} = M_{Fj} \left[\frac{1}{1+Ka_j \bar{t}} \right]^{n_c} \qquad (8.32)$$

If α_{ji} is redefined as

$$\alpha_{ji} = \left[\frac{1}{1+Ka_j \bar{t}_i} \right]^{n_c} \qquad (8.33)$$

it follows that the analysis of the circuit is identical to the case discussed above. For illustration purpose a flotation circuit with four batteries and a feed consisting of three species with same characteristics as discussed in the preceding section, is considered. Each battery in the circuit consists of four flotation cells. In this case, instead of defining the upper bound for the total volume V_T, the volume of each cell was predefined (25 cu ft). This problem was analyzed for the same objective, as in the preceding section, for a mass flow rate of solid feed equal to 100 lbs/min. Table 8.5 gives stage wise progress of linkage and design parameters and objective function. The optimal structure is shown in Fig.8.7.

Table 8.5: Values of Designed Parameters for Stage-Wise Optimization for Flotation Cell Batteries 3 Species Problem in Case of Objective A.

Parameters	Initial value	Stage I	Stage II	Stage III	Stage IV
δ_{10}	0.678	0.098	0.043	0.781	1.000
δ_{11}	0.000	0.000	0.000	0.000	0.000
δ_{12}	0.159	0.442	0.398	0.092	0.000
δ_{13}	0.156	0.269	0.300	0.070	0.000
δ_{14}	0.007	0.191	0.258	0.057	0.000
δ_{20}	0.660	0.630	0.719	0.709	1.000
δ_{21}	0.140	0.341	0.281	0.291	0.000
δ_{22}	0.031	0.000	0.000	0.000	0.000
δ_{23}	0.168	0.029	0.000	0.000	0.000
δ_{24}	0.000	0.000	0.000	0.000	0.000
δ_{30}	0.468	0.036	0.037	0.036	0.020
δ_{31}	0.100	0.242	0.333	0.216	0.277
δ_{32}	0.000	0.000	0.000	0.000	0.000
δ_{33}	0.209	0.114	0.010	0.000	0.000
δ_{34}	0.223	0.608	0.619	0.748	0.702
δ_{40}	0.219	0.059	0.001	0.000	0.000
δ_{41}	0.203	0.488	0.741	0.341	0.141
δ_{42}	0.209	0.175	0.110	0.370	0.545
δ_{43}	0.179	0.097	0.000	0.000	0.000
δ_{44}	0.190	0.180	0.148	0.289	0.313
β_{10}	0.784	0.789	0.981	1.000	1.000
β_{11}	0.000	0.000	0.000	0.000	0.000
β_{12}	0.212	0.291	0.016	0.000	0.000
β_{13}	0.001	0.000	0.000	0.000	0.000
β_{14}	0.003	0.000	0.000	0.000	0.000

Contd...

Contd...

Pagameters	Initial value	Stage I	Stage II	Stage III	Stage IV
β_{20}	0.765	1.000	1.000	1.000	1.000
β_{21}	0.003	0.000	0.000	0.000	0.000
β_{22}	0.008	0.000	0.000	0.000	0.000
β_{23}	0.224	0.000	0.000	0.000	0.000
β_{24}	0.000	0.000	0.000	0.000	0.000
β_{30}	0.718	0.741	0.688	0.825	1.000
β_{31}	0.012	0.007	0.000	0.000	0.000
β_{32}	0.000	0.000	0.000	0.000	0.000
β_{33}	0.079	0.051	0.000	0.000	0.000
β_{34}	0.191	0.201	0.312	0.175	0.000
β_{40}	0.952	1.000	1.000	1.000	1.000
β_{41}	0.005	0.000	0.000	0.000	0.000
β_{42}	0.010	0.000	0.000	0.000	0.000
β_{43}	0.010	0.000	0.000	0.000	0.000
β_{44}	0.023	0.000	0.000	0.000	0.000
δ_{f1}	0.106	0.031	0.000	0.000	0.000
δ_{f2}	0.181	0.164	0.017	0.000	0.000
δ_{f3}	0.129	0.117	0.129	0.448	0.495
δ_{f4}	0.584	0.688	0.853	0.552	0.504
$\bar{t}_1$	2.981	3.613	4.203	9.681	8.574
$\bar{t}_2$	4.274	8.190	3.187	10.624	12.732
$\bar{t}_3$	4.360	12.885	12.660	9.220	9.54
$\bar{t}_4$	2.694	4.012	3.000	4.387	4.976
Recovery	45.33	70.57	70.76	71.23	71.27
Grade	51.22	35.00	35.00	35.00	35.00

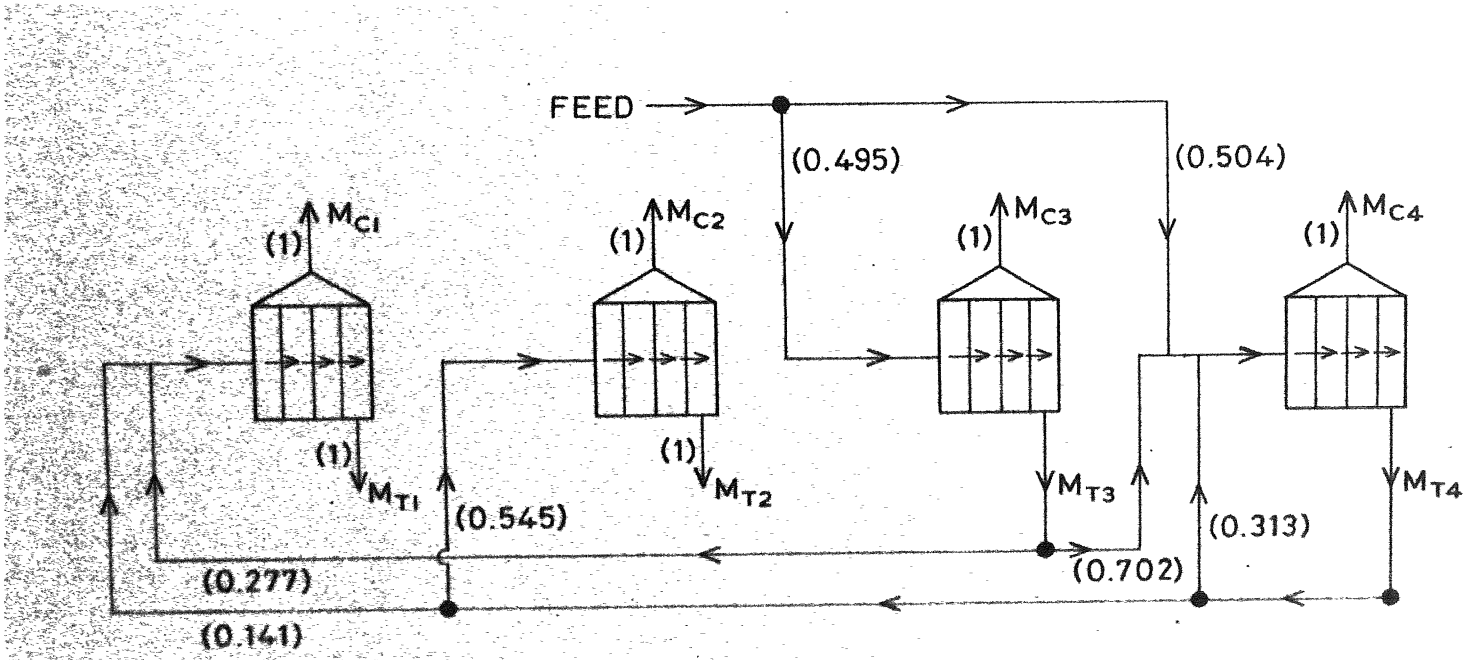

Fig. 8.7 Optimum configuration for batteries of flotation cells and three species problem.

is independent of particulate environment in the suspension. Equation (8.2) for particles of size L can then be written as

$$M_T(L) = M_F(L) \left[\frac{1}{1+Ka(L)\ \bar{t}(L)} \right] \qquad (8.35)$$

Now the design parameters to be optimized are the constants C_1, C_2, ... in an empirical expression relating $\bar{t}$ to size L

$$\bar{t}(L) = \bar{t}(L, c_1, c_2, \ldots) \qquad (8.36)$$

Experimental data of Woodburn et al[83] shows that the following relationship is perhaps sufficient for this purpose

$$\bar{t}(L) = c_1 + c_2 L + \ldots \qquad (8.37)$$

The main drawback in the integral approach, as indicated earlier, is in the optimization step which becomes more acute as the parameter space increases. After this work was completed the author has come across a more efficient hyperconical random search[164] method which may prove to be better for this kind of problem.

Using the algorithm developed in Chapter 7, the apparent rate distribution can be determined and then discretized in two or more groups of species. This may be incorporated in a generalized circuit in order to synthesize either the optimal or a number of near optimal circuits with residence times as the design parameters which play a central role in the kinetics of flotation and separability of species. The optimal circuits

were found to be strongly dependent on the objective function which in industrial practice changes frequently with availability of ore, market price and demand trend. Consequently, the procedure enumerated here provides a rational and objective method for design of new and adaptation of existing circuits. Even a marginal improvement in the performance can make significant economical impact in view of the very large tonnage treated in typical flotation circuits.

CHAPTER 9

SUMMARY

In the first part of this investigation some quantitative aspects of flotation kinetics have been studied. These include (1) a phenomenological model for flotation kinetics in distributed flotation rate constants (2) an algorithm for numerical inversion of the Laplace transform for estimation of the apparent flotation rate distribution; (3) the effects of aeration rate, particle size and pulp density on the flotation rate distributions; (4) the effects of particle size and feed rate on the flotation rate distributions in a continuous cell. The second part deals with (5) the synthesis and design of a flotation circuit.

1. A Phenomenological Model for Flotation Kinetics:

Equations (4.18), (4.23) and (4.25) describe the kinetics of flotation under assumption of a rate distributed first order particle-bubble attachment sub-process. The quasi-steady state conditions have been stipulated, which are necessary to reduce these equations to a first order distributed apparent flotation rate kinetics form, which has been postulated by many previous workers. The relationship between the apparent flotation rate constant and the particle-bubble

attachment detachment rate constants is given in equation (4.37) The apparent flotation rate and the attachment rate distributions are related to each other in equation (4.41). When the detachment probability of the particle is high, such as for coarse particles, the first order distributed apparent flotation rate kinetics is valid for single size particles only. However, when λ predominates, the relationship between the apparent and attachment rates is given in equation (4.43) and the apparent first order kinetics prevails even for a dispersed particle size spectrum. For a given size, a distribution of valuable mineral in attachment rate constant is introduced starting from a trivariate density function in surface reactivity, particle size and grade. It has been pointed out that the flotation kinetics can be formulated concurrently for distribution in total mass and valuable mineral using the apparent flotation rate constant as the common attribute. These two distributions are related to each other through the cumulative grade as shown in equation (4.49).

2. Estimation of Apparent Flotation Rate Distribution by Numerical Inversion of the Laplace Transform:

The problem of estimation of the distribution function of the apparent rate constant is equivalent to the inversion of the Laplace transform from $M_s(t)$ to $M_s(Ka)$. It was found that the estimation of the rate constant distribution in cumulative mode was easier and more reliable as compared to that in the

frequency function because the former is smoother and less prone to influence of errors. Moreover, the cumulative distribution provides a number of constraints which not only constrict the region of numerical search but also prevent possible wild fluctuations in the computed distribution. Approximation of the integral in equation (5.12) by the Lobatto quadrature formula automatically satisfies the constraints at the end points of the cumulative distribution. The cumulative distribution has been evaluated at discrete points by optimization of a least squares objective function with inequality constraints using univariant search with Fibonacci search technique, and Rosenbrock's method of optimization. The proposed algorithm has been tested for synthetic data generated from different distribution functions. It has been shown that by using this algorithm it is possible to extract back the distribution which is used to generate the data. Data accurate to two decimal places in range 0.01 to 1 has been inverted satisfactorily by the proposed method. The success of the method does not seem to depend on the initial guess values in the optimization step. Off starting points also give accurate results but at the expense of efficiency with respect to computation time. For a 8-point Lobatto quadrature formula, as small as seven number of well spaced data points lead to reasonable results. With appropriate modification, data pertaining to feed with non-floatable component can also be inverted satisfactorily.

3. The Effects of Aeration Rate, Particle Size and Pulp Density on the Flotation Rate Distributions:

Published flotation kinetic data has been employed for computation of the flotation rate distribution by numerical inversion of the Laplace transform, using the algorithm developed in the preceding section. These distributions and corresponding apparent flotation rate constants, have been analyzed as a function of aeration rate, particle size and initial pulp density. Thus, it has been possible, for the first time, to scrutinize the distribution as a whole for the effects of these variables. The principal conclusion is that the nature of the function R(Ka) does not change with variation in aeration rate and particle size. Only the argument of the function, Ka, is altered or rescaled as in equation (4.43) and (6.14), and the scaling parameters may be determined from the appropriate data. The scaling factor increases rapidly with the rate of aeration and exhibits a characteristic maximum for intermediate particle size. The evaluated distributions are independent of initial pulp density when dilute, but show marked divergence for concentrated pulp. In this manner it has been possible to develop useful correlation for the structure of the apparent flotation rate constant Ka and to check the validity of the conclusions derived from model in part (1).

4. The Effects of Particle Size and Feed Rate on the Flotation Rate Distribution in a Continuous Cell:

The approach used for analysis of flotation kinetic data for semi-batch flotation operation has been extended to the analysis of the flotation kinetic data for continuous steady state operation. The cumulative rate constant distribution, $R_F(Ka,L)$, in equation (7.5) has been evaluated by using a method similar to numerical inversion of the Laplace transform. The integral term in equation (7.5), after appropriate transformation, has been discretized by a Lobatto quadrature formula and the distribution at discrete points is evaluated by optimizing a least squares objective function by univariant, Rosenbrock and Random search methods of optimization. The method is again not restricted to any a priori assumption concerning the mathematical form of the distribution function. Using the tabulated data of Woodburn et al.,[83] the effects of particle size and feed rate on rate distribution have been examined. It is observed that these distributions are independent of the slurry flow rates and the effect of particle size on the distribution was similar to that in the semi-batch process. The estimated rate distribution has been employed to predict quite accurately the kinetics of a cleaner cell whose feed comprises of the rougher concentrate. Similar results have been obtained for gangue component. An algorithm, given in equation (7.31), for analyzing the kinetic data in the impulse case has also been outlined.

5. Optimal-Suboptimal Synthesis and Design of Flotation Circuit:

The optimal structure and design parameters are extracted simultaneously from a generalized circuit. This technique has been applied to solve the linkage (including split streams) problem and to determine the optimal mean residence time of particles in each cell. First, a flotation circuit with two cells and feed comprising of two species of known overall rate constants is synthesized and designed for three objective functions: (1) maximize recovery such that concentrate grade $\geq$ 35 percent; (2) maximize recovery such that concentrate grade $\geq$ 75 percent; and (3) maximize profit, which is defined as the difference between the prices of concentrate and ore. Modified complex method and Random search techniques were used for optimizing the objective function but Random search seems to be more reliable. The results obtained by using this approach have been compared with the real optimum circuit obtained by using the trial and error technique in which all possible meaningful configurations are enumerated (Fig. 8.1) and each configuration is then examined separately. The optimum configurations for above three objective functions are identical to those shown in Figs. 8.1(vi), 8.1(v) and 8.1(vi), respectively. This approach has been extended to a flotation circuit with four cells and for batteries of cells for a feed comprising of valuable, gangue and middlings. The optimal configuration

for these two cases for objective (1) are shown in Figs. 8.4 and 8.7, respectively. Simplification in the configurations which result in somewhat smaller values of the objective function have been obtained by using engineering guesses, for four cells, and resulting simplified configurations are shown in Fig. 8.5.

CHAPTER 10

SUGGESTIONS FOR FUTURE WORK

The continuation of the present work may be carried out in thefollowing directions.

1. The importance of the study of the effect of process variables on flotation kinetics has been duly emphasized in the previous chapters. In Chapter 6, the effects of aeration rate, particle size and initial pulp densities on the flotation rate distributions have been studied. The effects of some of the other important variables such as chemical reagents, e.g. collector and frother etc., agitation (which is related to the turbulence in the cell) and froth level etc. may be studied. This will give further insight into the structure of the flotation rate constant which may be important from the view point of the control of the process and for eventual derivation of the flotation rate constant from first principles.

2. As discussed in Chapter 6, the assumed structure of apparent rate constant Ka in equation (6.14) is somewhat similar to the model proposed by Woodburn et al and given by equation (6.25). When only one variable is changed, either aeration rate or particle size, both models require self-similar distribution in scaled apparent flotation rates. However, in

equation (6.25) parameter θ, which is a function of particle size and a hydrodynamic parameter, does not permit separation of particle size effect as in the model proposed in the present study. To discriminate between these two structures of the apparent flotation rate constant, experiments, at the laboratory scale, with particles of different sizes and at different aeration rates for each of these particle sizes may be carried out. The data thus obtained can be analyzed as follows:

First a plot of $\bar{R}(K)$ versus $Ka/Ka(0.5)$ for different particle sizes is obtained which is expected to result in number of curves of the type shown in Fig.6.2, each curve corresponding to a particular particle size. If these self similar forms of distribution collapse on to a single curve, similar to the curves shown in Fig. 6.8 to Fig. 6.11, the validity of equation (6.14) is established.

3. The problem of synthesis and design of optimal-suboptimal multicell flotation circuits, discussed in Chapter 8, is rather simple. A more comprehensive profit function can be formulated incorporating the capital investment, operation cost and price of the products etc. The analysis can be extended to particles of various sizes and densities as suggested in Chapter 8. The random search technique of optimization is perhaps not the best technique of optimization. Faster and more reliable techniques

of optimization would be more desirable. Directional random search techniques seem to be more appropriate for this type of optimization problems involving large number of constrained variables. One such technique is the hyperconical random search.

4. Recently, a number of techniques of synthesis of chemical reactors have been proposed which take care of some of the draw backs of direct search technique of synthesis, used in the present study. A new method of synthesis proposed by Ichikawa and Fan and a multilevel technique proposed by Osakada and Fan seem to be encouraging and feasibility of these techniques for synthesis and design of a multicell flotation circuit may be investigated.

5. In formulating the kinetic model in Chapter 8, it is assumed that the mean residence time of water and solid partic in the cell is same. A more sophisticated model, incorporating different values of mean residence time for different species, can be formulated and this model then can be used for synthesis and design problem, discussed in Chapter 8.

REFERENCES

1. Hines P.R. and Vincent J.D.: " The Early Days of Froth Flotation", Froth Flotation 50th Anniversary Vol. (Ed. D.W. Fuerstenau), AIME, New York, 1968, 11-38.

2. Rose E.H.: " The Controversial Art of Flotation", Trans. AIME, 1946, 169, 240-47.

3. Sutherland K.L. and Wark I.W.: " Principles of Flotation", Aust. Inst. Min. Met., 1955, 13-23.

4. Arbiter N. and Harris C.C.: " Flotation Kinetics", Froth Flotation 50th Anniversary Vol. (Ed. D.W.Fuerstenau), AIME, New York, 1968, 215-46.

5. Gracia-Zuniga H.: " Flotation Recovery is an Exponential Function of Time", Bol. Soc. Mac. Min. Santigo, 1935, 47, 83-86.

6. Beloglazov K.F.: " Kinetics of Flotation Process", Tsvet. Metal, 1939, 9, 70-76.

7. Grunder W. and Kadur E.:" Relation Between Foam Surface and Volume in Flotation Cell", Metall. U. Erz., 1940, 37, 367-72.

8. Plaksin I.N., Klassen V.I. and Berger G.S.: " Kinetic Equation of Flotation Processes", Tsvet. Metal., 1956, 4, 20-24.

9. Schuhmann R.: " Flotation Kinetics I: Methods for Steady State Study of Flotation Problems", J. Phys. Chem., 1942, 46, 891-902.

10. Mika T.S.: D. Eng. Thesis, University of California, Berkeley, 1969.

11. Sutherland K.L.: " Physical Chemistry of Flotation Part II: Kinetics of Flotation Process", J. Phys. Chem., 1948, 52, 394-424.

12. Volkova Z.V.: " The Laws Governing the Process Separation of Solids of Different Floatabilities", Acta Physicochim., 1946, 21, 1105-13.

13. Morris T.M.: "Flotation Rates and Flotation Efficiency", Trans. AIME, 1951, 190, 991-92.

14. Brown D.E. and Smith H.G.: "The Flotation of Coal as a Rate Process", Trans. Inst. Min. Engrs., 1953, 113, 1001-17.

15. Jowett A. and Safvi S.M.M.: "Refinement in Methods of Determining Flotation Rates", Trans. AIME, 1960, 217, 351-57.

16. Modi H.J. and Fuerstenau D.W.: "Flotation of Corrundum: An Electrochemical Interpretation", Trans. AIME, 1960, 217, 381-87.

17. Imaizumi T. and Inoue T.: "Flotation as a Rate Process", Nippon Kogyo Kaishi, 1961, 77, 987-94.

18. Chi J.W.H. and Yound E.F.: "Kinetics of Flotation Conditioning of a Hematite Ore", Trans. Inst. Min. Metal., 1962, 72, 169-80.

19. Arbiter N.: "Flotation Rate and Flotation Efficiency", Trans. AIME, 1951, 190, 791-96.

20. Bennett A.J.R., Chapman W.R. and Dell C.C.: "Froth Flotation of Coal", 3rd Inst. Coal Prep. Cong., Brushell, Liege, 1958, E2, 452-62.

21. Hukki R.T.: "Measurements and Evaluations of the Rate of Flotation as a Function of Particle Size", Trans. AIME, 1953, 196, 1122-24.

22. Mitrofanov S.I.: "Rate of Flotation", Tsvet. Metal., 1953, 26,

23. Mitrofanov S.I.: "Second Order Equation for the Rate of Flotation", Tsvet Metal, 1954, 27.

24. Suwanasing P. and Salman T.: "Particle Size in Flotation Kinetics", Cand. Min. J., 1970, 55-62.

25. Bogdanov O.S. and Khainman V.Ya.: "Relationship Between Rate of Flotation of Size of Mineral Particles", Tsvet. Metal., 1953, 26, 22-26.

26. Bogdanov O.S., Kizevalter B.V. and Khainman V.Ya.: "Equation for Rate of Flotation", Tsvet. Meta., 1954, 27.

27. Horst W.E., " Scale up Relationships in Spodumene Flotation", Trans. AIME, 1958, 211, 1182-85.

28. Horst W.E. and Morris T.M.: " Can Flotation Rate be Improved", Eng. Min. J., 1956, 157, 81-84.

29. deBruyn P.L. and Modi H.J.: " Particle Size and Flotation Rates of Quartz", Trans. AIME, 1956, 205, 415-20.

30. Volin M.E. and Swami D.V.: " Flotation Rates of Iron Oxides", 7th Int. Min. Proc. Cong. Vol. I, New York (1964), Gordon and Breach Sci. Pub., 1965, 193-206.

31. Krokhin S.I.; " Rate of Flotation", Concentration and Metallurgy of Non-Ferrous Metals (Papers), Severo-Kaukazska Min. Metal. Inst., 1955, 13.

32. Kakovskii I.A.: " On the Rate of Flotation", Tsvet.Metal., 1954.

33. Pogorely A.D.: " Limits of the Use of the Kinetic Equation Proposed by K.F. Beloglazov", Invest. Uysshikh Usheb. Zavendenii, Tsvet. Metal., 1962, 5, 33-40.

34. Tomlinson H.S. and Fleming M.G.: " Flotation Rate Studies" 6th Int. Min. Proc. Cong., Cannes (1963), Pergamon, 1965, 563-79.

35. Morris T.M.: " Measurement and Evaluation of the Rate of Flotation as a Function of Particle Size", Trans. AIME, 1952, 193, 794-98.

36. Bushell C.H.G.:" Kinetics of Flotation", Trans. AIME, 1962, 223, 266-78.

37. Cooper H.R.:" Feed Back Process Control of Mineral Flotation Part I: Development of a Model Equation for Froth Flotation", Trans. AIME, 1966, 235, 439-46.

38. Bogdanov O.S. and Kizevalter B.V.: " Some Results of Physical Studies of the Flotation Process", Rep. 2nd Conf. Mekhanobr Ins. (Papers), Metallurgidat, 1952.

39. Bogdanov O.S., Kizevalter B.V., Forsh O.B. and Maslova S.G.: " Explanation of Basic Relationships Between Physical Factors Determining Mineralization of Dispersed Air and Efficiency of the Flotation Process", Mekhanobr Inst., 1948.

40. Bogdanov O.S., Hainman V.J. and Maximov I.I.: " On Certain Physical Mechanical Factors Determining the Rate of Flotation", 7th Int. Min. Proc. Cong., Vol. I, New York (1964), Gordon and Breach Sci. Pub., 1965, 169-74.

41. Kelsall D.F.: " Application of Probability in the Assessment of Flotation Systems", Trans. Inst. Min. Metal., 1960/61, 70, 191-204; Discussion, 1960/61, 70, 491-502, 741-42.

42. Davis W.J.N.:" The Development of a Mathematical Model of the Lead Flotation Circuit at the Zinc. Corp. Ltd., Aust. Inst. Min. Met., 1964, 42, 61-89.

43. Woodburn E.T.: " Mathematical Modelling of Flotation Processes", Mineral Sci. and Eng., 1970, 2, 3-17.

44. Bodzinoy J.: " On the Analogy Between a Deterministic and Stochastic Model of the Kinetics of Flotation", Acad. Pol. Des. Sci. Bol-Ser dis Sci. Tech., 1965, 13, 485-90.

45. Katz S. and Shinnar R.: " Particulate Methods in Probability Systems", Ind. Eng. Chem., 1969, 61, 60-73.

46. Bharucha-Reid A.T.: " Elements of the Theory of Markov Processes and Their Applications", McGraw Hill Book Co., New York, 1960.

47. Harris C.C. and Rimmer H.W.: " Study of a Two Phase Model of the Flotation Process", Trans. Inst. Min. Met., Sec. C, 1966, 77, C 153-62.

48. Harris C.C., Jowett A. and Ghosh S.K.:" Analysis of Data From Flotation Tests", Trans. AIME, 1963, 226, 444-48.

49. Bogdanov O.S. and Emel'yanov M.F.:" Development of Ideas About the Kinetics of Flotation", Obogashch Rud., 1970, 15, 33-37.

50. Bull W.R.:" The Rates of Flotation of Mineral Particles in Sulfide Ores", Aust. Inst. Min. Met. Proc., 1966, 220, 69-78.

51. Ball B., Kapur P.C. and Fuerstenau D.W.: " Prediction of Grade Recovery Curves From a Flotation Kinetic Model", Trans. AIME, 1970, 247 , 263-69.

52. Niemi A.:" Dynamics of Flotation", Acta Polytech. Scand., Chem. Met. Series, 1966, No. 48, 18-52.

53. Woodburn E.T. and Loveday B.K.:" The Effect of Variable Residence Time on the Performance of a Flotation System", J. South Afr. Inst. Min. Metal., 1965, 65, 612-28, Discussion, 1966, 66, 649-54.

54. Imaizumi T. and Inoue T.:" Kinetics Consideration of Froth Flotation", 6th Int. Min. Proc. Cong., Canes (1963), Pergamon, 1965, 581-93.

55. Maksimov I.I. and Khainman V. Ya.: " Effect of Processes Occurring in the Froth Layer on the Rate and Selectivity of Flotation", Tsvet. Metal., 1965, 38, 8-10.

56. Taggart A.F.:" Hand Book of Mineral Dressing", John Wiley and Sons, Inc., New York, 1948.

57. Bogdanov O.S. and Filanovski M.Sh.:" Adhesion of Mineral Particles to an Air Bubble", J. Phy. Chem., 1940, 14, 244-47.

58. Gaudin A.M.:" Flotation", McGraw Hill Book Co., Inc., New York, 1932, 88-98.

59. Malozemoff P. and Ramsey R.H.: " Operating Characteristics of Mechanical Flotation Machines", Eng. Min. J., 1941, 142, 45-49.

60. Plante E.C. and Sutherland K.L.: " The Physical Chemistry of Flotation X: The Separation of Ergot From Rye", J. Phys. Chem., 1944, 48, 203-23.

61. Spedden H.R. and Hannan W.S.:" Attachment of Mineral Particles to Air Bubbles in Flotation", Am. Inst. Min.Met. Engrs., Min. Tech. 12, No. 2, Tech. Publ. No.2354, 1948,6.

62. Whelan P.F. and Brown,D.I.: " Particle Bubble Attachment In Froth Flotation", Bull Inst. Min. Metal., 1956, 591.

63. Kirchberg H. and Topfer E.:" The Mineralization of Air Bubbles in Flotation", 7th Int. Min. Proc. Cong., New York (1964), Gordon and Breach Sci. Publ., 1965, 157-68.

64. Klassen V.I.;" Theoretical Premises for Intensification of the Flotation Process", Min. J., 1945, 4.

65. Smith H.G., Abbott J. and Frangiskos A.Z.:" Particle-Bubble Attachment in Coal Flotation", 2nd Sym. on Coal Prep., Leads, 1957, 329-49.

66. Klassen V.I.: " Theoretical Basis of Flotation by Gas Precipitation", Proc. Int. Min. Proc. Cong., Inst. Min. Met., London, 1960, 309-21.

67. Philippoff W.:" Some Dynamic Phenomena in Flotation", Trans. AIME, 1952, 193, 386-90.

68. Evans L.F.: " Bubble Mineral Attachment in Flotation", Ind. Eng. Chem., 1954, 46,2420-24.

69. Langmuir I.:" The Production of Rain by a Chain Reaction in Cumulus Clouds at Temperatures Above Freezing", J. Meteorology, 1948, 5, 175-92.

70. Herne H.:" The Classical Computation of the Aerodynamic Capture of Particles by Spheres", Int. J. Air Pollu., 1960, 3, 26.

71. Ranz W.E. and Wong J.B.: " Impaction of Dust and Smoke Particles on Surface and Body Collectors", Ind. Eng. Chem., 1952, 44, 137-81.

72. Flint L.R. and Howarth W.J.: " The Collision Efficiency of Small Particles with Spherical Air Bubbles", Chem. Eng. Sci., 1971, 26, 1155-68.

73. Matveeko N.V.: " Kinetics of Flotation on the Basis of Similarity Between Adsorption and Mineralization of Air Bubbles", Tsvet. Metal., 1957, 30, 5-8.

74. Derjaguin B.V. and Dukhin S.S.:" Theory of Flotation of Small and Medium Size Particles", Trans. Inst. Min. Metal., 1960, 70, 221-46.

75. Eigeles M.A.: " Kinetics and Adhesion of Mineral Particles to Air Bubbles in Flotation Suspension", Comp. Rend. Acad. Sci. (U.R.S.S.), 1939, 24, 340-44.

76. Eigeles M.A.: " Kinetics of Mineralization of Air Bubbles in Flotation Suspensions", Tsvet. Metal., 1940, 2, 39-45.

77. Volkova Z.V.: " The Adhesion of Mineral Particles to the Surface of Air Bubbles During Flotation", J. Phys. Chem. (U.R.S.S.), 1940, 14, 789-800.

78. Volkova Z.V.: " The Laws of Adhesion in Flotation. The Process of Bubble Mineralization", Acta Physics Chem. (U.R.S.S.), 1946, 21, 171-86.

79. Morris T.M.: " Measurement of Equilibrium Forces Between an Air Bubble and an Attached Solid in Water", Trans. AIME, 1950, 187, 91-95.

80. Zaidenberg I.S.: " Evaluation of the Probability of Air Bubble Mineralization During Flotation", Obogashch Rud., 1969, 14, 21-25.

81. Glembotskii V.A., Solozhenkin P.M. and Giatsintova K.V.: " Kinetics of Physico-chemical Processes Taking Place on the Liquid Gas Phase Separation Surface", Fiz. Khim. Osn Kompleks Pererab Rud. Srednei, Azu (Ed.Glembotskii V.A.), 1970, 5-10.

82. Mika T.S. and Fuerstenau D.W.: " A Microscopic Model for Flotation Kinetics", 8th Int. Min. Proc. Cong., Leningrad, 1968.

83. Woodburn E.T., King R.P. and Colborn R.P.:" The Effect of Particle Size Distribution on the Performance of a Phosphate Flotation Process", Metal. Trans., 1971, 2, 3163-74.

84. Pogorely A.D.: " Flotation Properties of Industrial Pulp", Invest. Uysshikh, Usheb, Zavedenii, Tsvet. Metal., 1961, 5, 59-68.

85. Huber-Panu I.:" A Note on the Theory of Flotation Kinetics", Freiberger Forschhft, 1965, 335, 159-69.

86. Inoue T. and Imaizumi T.: " Some Aspects of Flotation Kinetics", 8th Int. Min. Proc. Cong., Leningrad, 1968.

87. Loveday B.K.: " Analysis of Froth Flotation Kinetics", Trans. Inst. Min. Met., Sec. C, 1966, 75, C219-225.

88. Harris C.C. and Chakravarti A.: " Semi-Batch Froth Flotation Kinetics: Species Distribution Analysis", Trans. SME, AIME, 1970, 247, 162-72.

89. Huber-Panu I.:" The Preparation of Ore and Auxiliary Materials: Some Equations Concerning the Kinetics of Flotation", Acad. Rep. Populare Rom. Study I Cercetari Met., 1964, 9, 17-28.

90. Black K.G. and Faulkner B.P.:" Evaluation of Batch Flotation Results by Multiple Linear Regression", Trans. SME, AIME, 1972, 252, 19-21.

91. Woodburn E.T., King R.P., Buchalter L.M. and Piper S.E.: " Integrated Grinding and Flotation Control Computational Problems in an Optimum Decision Making Model", A Decade of Digital Computing in the Mineral Industry, (Ed.Alfred W.), AIME, 1970, 695-728.

92. Huber-Panu I.: " Equations and Methods of Calculating Flotation Results", Rudy, 1970, 18, 121-32.

93. Tille R. and Panou G.:" Kinetics of Flotation", Obogashch Rud., 1968, 13, 5-13.

94. Cuttris R.H.: " Kinetic Model Fitted to Batch Flotation Data", Tech. Report, Dept. of Min. Met., Univ. of Queensland, Submitted by Lynch A.J., July 1-Dec.31,1971,58.

95. Krylov V.I. and Skoblya N.S.: " Handbook of Numerical Inversion of the Laplace Transform", (Translated from Russian by Louvish D.), IPST Press, Wiener Bindey Ltd., 1969, 1-44.

96. Bellman R.E., Kalaba R.E. and Lockett J.A.: " Numerical Inversion of Laplace Transform: Application to Biology, Economics, Engineering and Physics", Am. Elsevier, New York, 1966.

97. Zaidenberg I.Sh., Lisvoskii D.I. and Burovoi I.A.:" One Approach to the Construction of a Mathematical Model for Flotation Process", Tsvet. Metal., 1965,5,26-32.

98. King R.P.: " Model for Design and Control of Flotation Plants", 10th Int. Symp. on Application of Computer Methods in the Mineral Industry, 1972.

99. Jowett A.: " Investigation of Residence Time of Fluid in Froth Flotation Cells", Brit. Chem. Eng., 1961, 6, 254-58.

100. Niemi A. and Paakkinen U.:" Simulation and Control of Flotation Circuits", Automation, 1969, 5, 551-61.

101. Gaudin A.M.:" Flotation", McGraw Hill Book Co., Inc., New York, 1957, 369.

102. Johnson R.W.: " Mixing Characteristics of Pilot Plant Flotation", Automatic Control Gr. Rept., Dept. Min. Metal. Eng., Univ. of Queensland, Submitted by A.J.Lynch, Jan. 1-June 30, 1970, 58-74.

103. Smith H.W. and Bjerring A.K.: " A Preliminary Dynamic Model for a Flotation Circuit", A Decade of Digital Computing in the Mineral Industry, (Ed. Alfred W.), AIME, 1970, 867-87.

104. Bogdanov O.S., Kizevalter B.V. and Khainman V.Ya.: " The Influence of Pulp Flow Rate in Flotation Machines on Flotation Time", Tsvet. Metal., 1961, 2, 3-10.

105. Zakhvatkin V.K., Kulimin S.G., Georgiviev K.T. and Veselinov S.K.: " Increasing Flotation Machine Output in Bulgarian Concentrate Plants", Tsvet. Metal., 1965, 6, 17-24.

106. Kidd R.L. and Wall W.A.: " Effect of Particle Size on Flotation of Sphalerite", Mining and Metallurgy, 1933, 14, 421-22.

107. Shio-Chuan S. and Zimmerman R.E.: " The Mechanism of Coarse Coal and Mineral Froth Flotation", Trans. AIME, 1950, 187, 612-22.

108. Gaudin A.M., Schumann R. and Schlechten A.W.: " Froth Flotation Kinetics II: The Effect of Size on the Behaviou of Galena Particles", J. Phys. Chem., 1942, 46,902-10.

109. Eigeles M.A. and Leviush I.T.: " Rate of Flotation of Sizes of Particles", Proc. 2nd Sci. Tech. Sess., Mekhanob Inst. (Papers) Metallurgizdat, 1952.

110. Brown D.J.: " Coal Flotation", Froth Flotation, 50th Anniversary Vol. (Ed. Fuerstenau D.W.), AIME, New York, 1968, 518-38.

111. Krokhin S.I.: " Flotation Activity of Mineral Particles", Izv. Vysshikh Uchebrykh Zavednii, Tsvet. Metal, 1963, 6, 41-50.

112. Mackenzie J. M.W. and Matheson G.H.: " Kinetic and Dynamic Relationships in Coal Flotation", Trans. AIME, 1963, 226, 68-74.

113. Huber-Panu I.: " The Kinetic Study of Flotation", Comun. Acad. Rep. Rom. 1956, 6, 115-22.

114. Huber-Panu I., Pandelescu C. and Protopopescu A.: " Effect of Aeration Rate on the Flotation of Very Fine Ground Ores", Acad. Rep.Pop. Rom. Studii Cer. Met., 1963,8, 297-330.

115. Huber-Panu I. and Pandelescu. C.:" Flotation of Very Fine Ores", Rev. Minelor, 1966, 17, 65-70.

116. Heinrich S.and Walter S.:" Coarse Grain Flotation of Syloite", Freiberg Forschungsh A., 1968, 436, 99-107.

117. Ek C.:" Contribution A L'etude De La Cinetique De La Flottation", Extrait de la Collection des de l' universit de Liege, 1968.

118. Tewari S.N. and Biswas A.K.:" Flotation Kinetics for Calcite in a Semi-Batch System", J. Appl. Chem., 1969, 19, 173-77.

119. Clement M., Harms H. and Troendle H.M.:" Flotation Behaviour of Various Minerals in Relation to Particle Size", 9th Proc. Int. Min. Proc. Cong., 1970, 178-87.

120. Huber-Panu I. and Georgescu B.:" The effect of Aeration on Flotation Kinetics", Acad. Rep. Pop. Rom. Studii Cer. Met., 1961, 6, 67-83.

121. Lynch A.J.: " Automatic Control of Flotation Process: Possibilities for Continuous Feed Back Control of an Open Air Circuit Rougher-Scavanger Bank", Tech.Rept., Dept. of Min. Met. Eng., Univ. of Queensland, Jan. 1-June 30, 1970, 1-10.

122. Edward G.E.:" Assessment of the Froth Flotation Characteristics of Coal", J. Inst. Fuel, 1972, 514-21.

123. Burdon R.G.:" Some Factors Influencing the Rate of Flotation of Coal", Paper D6, 4th Int.Coal. Prep. Cong., 1962.

124. King R.P.;" Flotation Research Work of the N.I.M. Researc Group, and the Department of Chemical Engineering, University of Natal, J. South Afr. Inst. Min. Metal, 197 72, 135-45.

125. Newton J. and Ipsen A.C.:" Pulp Density as a Factor in Flotation", Eng. Min. J., 1938, 139, 42-45.

126. Gutsalyuk T.G.:" The Effect of Pulp Density and Grade on the Recovery of Mineral Particles of Different Sizes", Bull. Tech. Inf. Dept. Non-Ferr. Metal Kaz, S.S.R., Alma-Ata, 1956.

127. Klassen V.I.:" Influence of Pulp Density on the Speed of Flotation", Tsvet. Metal, 1939, 66-72.

128. Grunder W., Siemes W. and Kauffman J.F.:" Measurement of Aeration of Flotation Cells", Erz. Metall, 1956, 9, 559-63.

129. Woodburn E.T. and King R.P.:" Computer-Controlled Flotation Plants in Canada and Finland", Rept. No. 1517, Chem. Eng. Research Gr., Dept. of Chem.Eng., Univ. Natal, 1973.

130. Eerola P.I. and Paakkinen U.E.:" Introduction of Theoretical Aspects into the Computer Control of a Flotation Process", A Decade of Digital Computing in the Mineral Industry (Ed. Alfred W.), AIME, 1970, 827-52.

131. Cibulka J., Kaspar J. and Rotter R.:" Control and the Automation of the Flotation Process", 7th Int. Min.Proc. Cong. Vol. I, New York (1964), Gordon and Breach Sci. Pub., 1965, 471-91.

132. Nixon J.C. and Moir D.N.:" The Assessment of Flotation Results", Trans. Inst. Min. Metal., 1956/57, 66,453-69.

133. Jowett A. and Ghosh S.K.:" Flotation Kinetics: Investigation Leading to Process Optimization", 7th Int. Min. Proc. Cong. Vol. I, New York (1964), Gordon and Breach Sci. Pub., 1965, 175-84.

134. Sergeev V.P. and Smirnov A.:" A Comparison of an Algorith for Controlling Flotation of Phosphate Ores", Khim. Prom 1968, 362-65.

135. Rudd D.F.:" The Synthesis of System Designs: I.Elementary Decomposition Theory", AICh E J., 1968, 14, 343, 49.

136. Nishida N., Kobayashi S. and Ichikawa A.:" Optimal Synthe of Heat Exchanger Systems, Necessary Conditions for Minimum Heat Transfer Area and Their Application to System Synthesis", Chem. Eng. Sci., 1971, 26, 1841-49.

137. Kobayashi S., Umeda T. and Ichikawa A.:" Synthesis of Optimal Heat Exchange Systems. An Approach by the Optimal Assignment Problem in Linear Programming", Chem. Eng. Sci., 1971, 26, 1367-80.

138. Menzies A. and Johnson A.I.:" Synthesis of Optimal Energy Recovery Networks Using Discrete Methods", Cand. J. Chem. Eng., 1972, 50, 290-96.

139. Umeda T. and Ichikawa A.:" Synthesis of Optimal Processing Systems by a Method of Decomposition", Paper Presented at Am. Inst. Chem. Engrs. Meeting, Dallas, Texas, 1972.

140. Masso A.H. and Rudd D.F.:" The Synthesis of System Designs: II. Heuristic Structuring", AIChE J., 1969,15, 10-17.

141. Siirola J.J., Powers G.J. and Rudd D.F.:" Synthesis of System Designs: III. Towards a Process Concept Generator", AIChE J., 1971, 17, 677-82.

142. Nishimura H., Hiraizumi Y. and Suzuki E.:" The Optimal Synthesis Pattern of Heat Exchanger System", Chem.Eng. Japan, 1971, 4, 107.

143. King C.J., Gantz D.W. and Barnes F.J.:" Systematic Evolutionary Processes Synthesis", Paper Presented to Am. Chem. Soc. Annual Meeting, Los Angeles (March 1971).

144. Ichikawa A. and Fan L.T.:" Optimal Synthesis of Process Systems. Necessary Conditions for Optimal System and its Use in Synthesis of Systems", Chem. Eng. Sci, 1973,28,357-74

145. McGalliard R.L. and Westerberg A.W.: " Structural Sensitivity Analysis in Design Synthesis", Paper Presented at Am. Inst. Chem. Engrs. Meeting, Dallas, Taxas (1972).

146. Lasdon L.S.:" Optimization Theory for Large Systems", McMillan (1970).

147. Watanabe N., Nishimura Y. and Matsubara M.:" Optimal Design of Chemical Processes Involving Parameter Uncertainty, Chem. Eng. Sci., 1973, 28, 905-13.

148. Lee K.F., Masso A.H. and Rudd D.F.:" Branch and Bound Synthesis of Integrated Process Design", Ind. Eng.Chem. Fundls,, 1970, 9, 48-58.

149. Umeda T., Hirai A. and Ichikawa A.:" Synthesis of Optimal Processing System by an Integrated Approach", Chem. Eng. Sci., 1972, 27, 795-804.

150. Hendry J.E., Rudd D.F. and Seader J.D.:" Synthesis in the Design of Chemical Processes", AIChE J. 1973,19, 1-15.

151. Osakada K. and Fan L.T.:" Synthesis of an Optimal Large Scale Interconnected System by Structural Parameter Model Computed with Multilevel Technique", The Cand. J.Chem.Eng., 1973, 51, 94-101.

152. Sastry K.V.S. and Fuerstenau D.W.:" Theoretical Analysis of a Counter Current Flotation Column", Trans. Soc. Min. Eng., AIME, 1970, 247, 46-52.

153. Holdbrook J.G.: " Laplace Transformation for Electrical Engineers", Pergamon Press, New York, 1959, 108-10.

154. Andersson A.S. and White E.T.:" The Analysis of Residence Time Distribution Measurements Using Laguerre Functions", The Canad. J. Chem. Eng., 1969, 47, 288-95.

155. Hilderband F.B.:" Introduction to Numerical Analysis", McGraw Hill Book Co., New York, 1956, 338-45.

156. Kopal Z.:" Numerical Analysis", Wiley, New York, 1961, 573-75.

157. Beveridge G.S.G. and Schechter R.S.:" Optimization: Theory and Practice", McGraw Hill Book Co., New York, 1970, 363-67, 180-93.

158. Wilde D.J.:" Optimum Seeking Methods", Prentice Hall Inc., New Jersey, 1964, 24-30.

159. Rosenbrock H.H.:" An Automatic Method of Finding the Greatest or Least Value of a Function", Comp. J., 1960, 175-84.

160. Lee E.S.:" Random Search Technique", Quasilinearization and Invariant Imbedding (Mathematics in Science and Engineering, Vol. 41), Acad. Press, New York, 1968, 95-100.

161. K.S. Kunz:" Numerical Analysis", McGraw Hill Book Co., New York, 1957, 221-22.

162. Guin J.A.:" Modification of Complex Method of Constrained Optimization", Comp. J., 1967, 10, 416-17.

163. Umeda T. and Ichikawa A.:" A Modified Complex Method for Optimization", Ind. Eng. Chem. Process Des. Dev., 1971, 10, 229-36.

164. Wozny M.J. and Heydt G.T.:" Hyperconical Random Search", Trans. AIME,J. Dynamic Systems, Measurements and Control, 1972, Ser. G, 94, 71-78.

165. Ralston A.:" A First Course in Numerical Analysis", McGraw Hill Book Co., N.Y., 1965, 97-98.

166. Erdelyi A.:" Inversion Formula for the Laplace Transformation ", Philos. Mag., 1943, 34, 533-37.

167. Erdelyi A.:" Note on an Inversion Formula for the Laplace Transformation", J. Lond. Math. Sci., 1943, 18/19, 72-77.

168. Popoulis A.:" A New Method of Inversion of the Laplace Transform", Quart. Appl. Math., 1957, 14, 405-16.

169. Miller M.X. and Guy W.T.:" Numerical Inversion of the Laplace Transform by Use of Jacobi Polynomial", SIAM J. Numerical Analysis, 1966, 3, 625-35.

170. Felix M., Sajalsli C. and Kuntzman J.:" Une Variant de la Methode de Tricomi-Picone Pour l' Inversion de la Transformation de Carson", Chiffers, 1958, 1, 63-74.

171. Nugeyre J.B.:" Etude de Procedes d' Inversion Numerique de la Transformation de Laplace", Chiffers, 1960, 3, 101-06.

172. Bellman R.E. and Kalaba R.E.:" Numerical Inversion of Laplace Transform ", Trans. IEEE, Aut. Cont., 1967, 12, 624-25.

173. Piessens R.:" A New Method for the Inversion of the Laplace Transform", J. Inst. of Math. and Its Application 1972, 10, 185-92.

174. Lanczos C.:" Applied Analysis", Prentice Hall, New Jersey, 1956.

175. Fletcher R.:" Function Evaluation Without Evaluating Derivatives: A Review", Comp. J., 1965, 8, 33-41.

176. Box M.J.: " A New Method of Constrained Optimization and a Comparison with Other Methods", Comp. J., 1965, 8, 42-52.

177. Brooks S.H.:" A Discussion of Random Methods for Seeking Maxima", Operation Res., 1958, 6, 244-51.

178. Gurin L.S. and Rastrigin L.A.:" Convergence of the Random Search Method in the Presence of Noise", Automatika i Telem., 1965, 26, 1505-11.

179. Karnopp D.:" Random Search Techniques for Optimization Problems", Automatika, 1963, 1, 111-21.

180. Gurin L.S.:" Random Search in the Presence of Noise, Engrg. Cybernetics, 1966, 752-60.

181. Rastrigin L.:" The Convergence of the Random Search Method in the External Control of a Many Parameter System", Automatika i Telem., 1963, 24, 1467-73.

182. White R.C.:" A Survey of Random Methods for Parameter Optimization", Simulation, 1971, 17, 197-204.

183. Betrami E.J. and Indusi J.P.:" An Adaptive Random Search Algorithm for Constrained Minimization;" Trans. IEEE Comp., 1972, 1004-08.

APPENDIX A

ALGORITHMS FOR NUMERICAL INVERSION OF THE LAPLACE TRANSFORM

As pointed out in the text, if

$$M_s(t) = \int_0^\infty \bar{M}_s(Ka) \exp[-Ka\ t]\ dKa \qquad (A-1)$$

$M_s(t)$ is known as the Laplace transform of function $\bar{M}_s(Ka)$, and $\bar{M}_s(Ka)$ is the inverse of the Laplace transform. For equation (A-1) to be valid $\bar{M}_s(Ka)$ must be defined for all positive values of Ka and in our problem it can not take negative values.

One of the commonly used methods for inversion of the Laplace transform consists of approximating $\bar{M}_s(Ka)$ by Jacobi polynomial[165] after carrying out suitable transformation to change the limits of the integral, in equation (A-1), to -1 to 1 (see Chapter 5). Thus $\bar{M}_s(Ka)$, which after transforming Ka to x is denoted by M'(x), is given by

$$M'(x) = (1-x)^{\mu} (1+x)^{\nu} \sum_{n=0}^{\infty} b_n P_n^{(\alpha', \beta')}(x) \qquad (A-2)$$

where μ, ν, α', and β' are the unknown parameters, $b_n (n = 0, 1, \ldots)$ are coefficients in series and P_n is the Jacobi polynomial. Coefficients b_n can be analytically determined once the series is truncated using some suitable criterion and values of parameters μ, ν, α' and β' are suitably chosen. Different values of these parameters and techniques for evaluating the

coefficients b_n have resulted in various algorithms, documented in literature. Erdelyi[166,167] has given explicit forms for b_n but in the method proposed by Papoulis[168], and Miller and Guy[169] b_n are embedded in a system of linear equations, whose coefficient matrix is triangular. Numerical examples based on these approaches have been given by Felix, Sajalsli and Kuntzman[170], and Nugeyre[171]. Erdelyi obtained a general inversion formula analogous to equation (A-2) by use of an orthogonal set of functions over the interval $(0,\infty)$.

Bellman, Kalaba and Lockett[96,172] have discussed the numerical methods of inversion in which integral in equation (A-1) can be approximated by either Laguerre, Legendre or shifted Legendre quadrature formula after carrying out proper transformation of the variables. This leads to an equation of the following form

$$M_s(t) = \sum_{i=1}^{n} f(x_i,t) \; F_u(x_i) \; w_i \qquad (A-3)$$

where the quantities $F_u(x_i)$, $i = 1,2,\ldots, n$ are unknown function of x_i and $f(x_i,t)$ is some known function of x_i and t, the form of which will depend on the quadrature formula used for discretizing the integral in equation (A-1), x_i and w_i, as defined earlier, are the i-th abscissa and weight, respectively, of the quadrature formula. Now allowing the variable t to assume n different values, $i = 1,2,\ldots, n$, one can obtain a

system of n equations in n unknowns. Recently Piessens[173] has modified Bellman's method to avoid the loss of significant figures inherent in earlier methods. He has shown that his, as well as, Bellman's method are theoretically equivalent to a more generalized method proposed by Lanczos[174]. None of the methods are suitable for noise corrupted data.

APPENDIX B

OPTIMIZATION TECHNIQUES

During the last two decades, a large number of algorithms have been proposed for maximizing or minimizing nonlinear functions with or without equality and inequality constraints, using numerical techniques. Only those optimization techniques which have been employed in the present study are discussed in this Appendix. These are univariant, Fibonacci, Rosenbrock, modified complex and random search methods of optimization.

UNIVARIANT SEARCH:

This method, also known as one-at-a-time, or sectioning method, has been basically developed for unconstrained objective functions. However, due to the special feature of our problem in Chapter 5 this method was found to be quite suitable for optimization of the objective function in equation (5.21). For the sake of clarity the objective function can be rewritten as,

$$E = E(X_2, X_3, \ldots X_{n-1}) \qquad (B-1)$$

subject to constraint

$$0 \leq X_2 \leq X_3 \ldots \leq X_{n-1} \leq 1 \qquad (B-2)$$

where X_i now corresponds to $F(x_i)$ in equation (5.15). The univariant search used in this work is similar to Friedman and Savage method and is as follows:

Step 1: Choose $(X_2^{(o)}, X_3^{(o)}, \ldots, X_{n-1}^{(o)})$ as initial base point such that the constraints in equation (B-2) are satisfied.

Step 2: The objective function is now minimized with respect to one variable only, say, X_2, keeping all other variables constant. Fibonacci search technique (to be discussed in the following section) in range 0 to $X_3^{(0)}$ is used for this search. If $X_2^{(1)}$ is the optimal point, the new base point now becomes $(X_2^{(1)}, X_3^{(0)}, \ldots, X_{n-1}^{(0)})$. Next, the objective function is minimized with respect to X_3 keeping all other variables constant. The search is restricted in range $X_2^{(1)}$ to $X_4^{(0)}$ rather than $X_2^{(0)}$ and $X_4^{(0)}$. This procedure is continued until the objective function is optimized with respect to all the variables once, to give a new vector $(X_2^{(1)}, X_3^{(1)}, \ldots, X_{n-1}^{(1)})$. This completes the first stage of computations.

Step 3: The whole cycle is repeated until there is no significant change in the objective function, or until the change is within a preselected value.

A flow chart used for computer programming is given in Fig. (B-1).

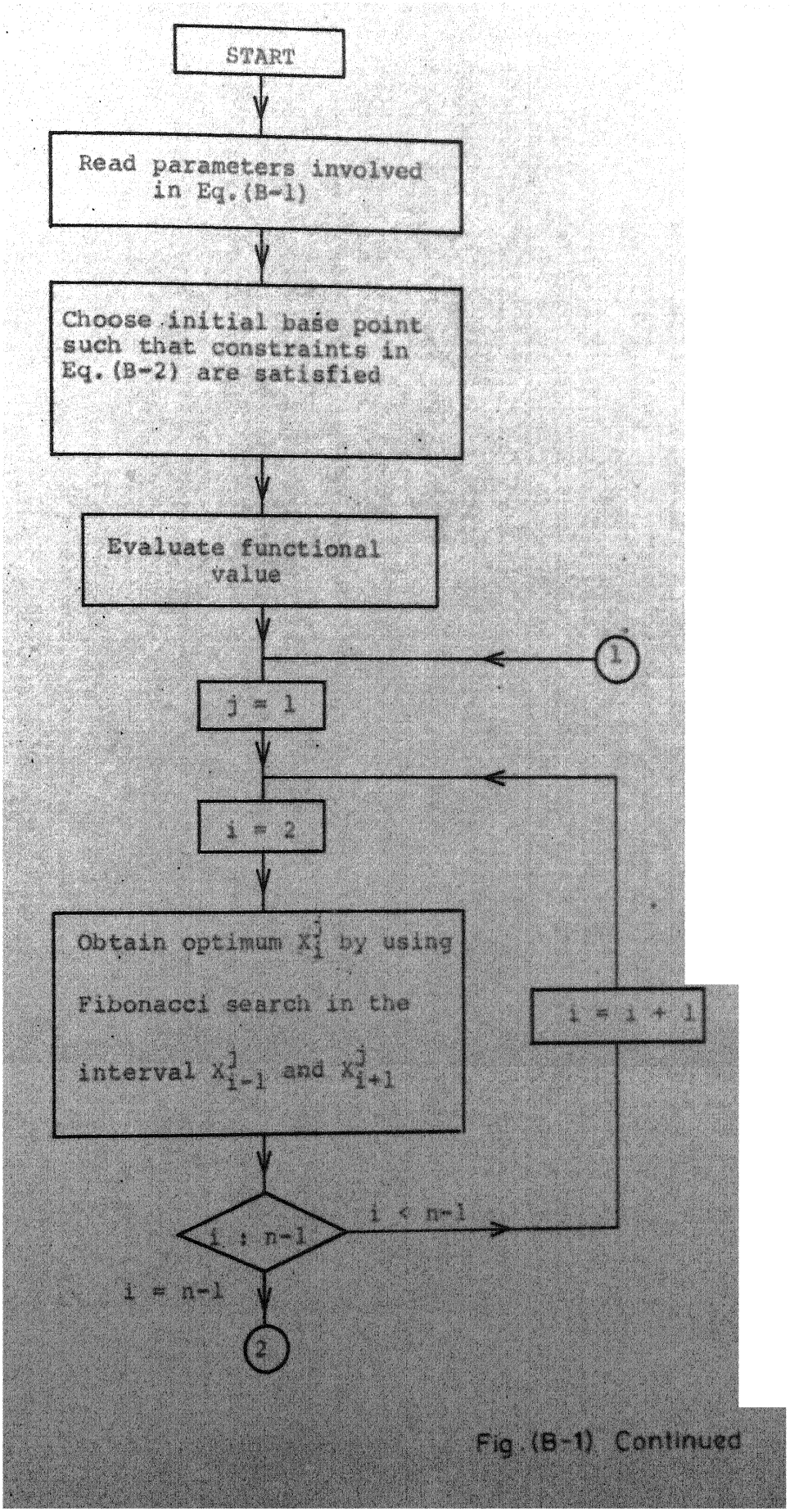

Fig. (B-1) Continued

Fig. (B-1) Continued

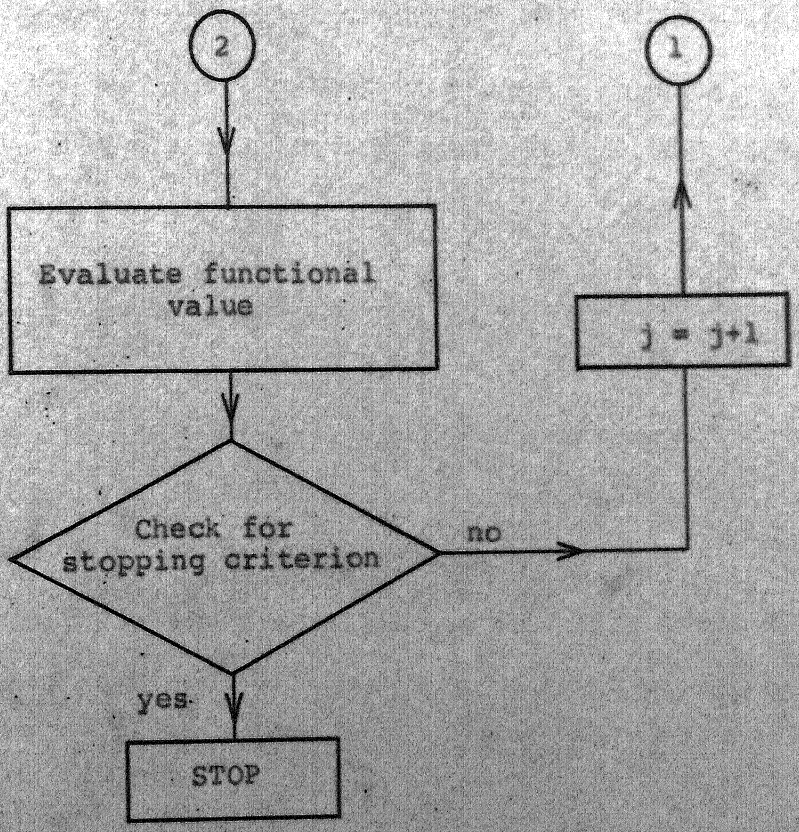

Fig. B-1 Flow chart for univariant search technique of optimization.

FIBONACCI SEARCH:

This technique is used for optimizing objective functions with a single variable. The steps are as follows:[157,158]

Step 1: Placing the First Two Experiments: First two trial points x_1 and x_2 ($x_2 > x_1$) are placed at a distance l_1, from each end of the original search interval L_1. The distance l_1 is defined as

$$l_1 = \left(\frac{F_{n'-2}}{F_{n'}} - \frac{(-1)^{n'}\varepsilon}{F_{n'}}\right) L_1 \qquad (B-3)$$

where ε is arbitrarily predefined small number (say, 0.005) which defines the distance between the last two trial points, $F_{n'}$ defines the n'-th number in the sequence of Fibonacci numbers and n' is the total number of trials finally required. The sequence of Fibonacci numbers is defined as follows:

$$F_o = F_1 = 1$$
$$F_j = F_{j-1} + F_{j-2} \quad , j = 2,3,\ldots, n' \qquad (B-4)$$

The values of the objective function at the two trial points are compared and one of the three sub intervals containing the worse trial point is rejected such that the rejected trial point forms one of the two end points of the remaining subinterval and the other trial point lies in this subinterval.

Step 2: The new reduced interval of search $\bar{L}_2$, remaining after first two trials, is

$$\bar{L}_2 = \bar{L}_1 - l_1 = \frac{F_{n'-1}}{F_{n'}} \bar{L}_1 + \frac{(-1)^{n'} \varepsilon}{F_{n'}} \bar{L}_1 \qquad (B-5)$$

Now, two trials in this region are placed at a distance l_2 from each end of the interval such that

$$l_2 = \bar{L}_2 - \bar{L}_3 \qquad (B-6)$$

where $\bar{L}_3$ is defined by following equation

$$\bar{L}_{j+2} = \bar{L}_j - \bar{L}_{j+1} \qquad (B-7)$$

It can be shown that one of the two new trial points will exactly coincide with the trial point remaining from the previous search cycle. Thus, in second cycle, only one new trial point is necessary to determine the third search interval. The new trial point is placed such that the new point and the old point are symmetrically placed in the new subinterval of search. This holds for subsequent cycles also. Thus, only one trial point is to be added in each cycle. Again the values of objective function at these two points are compared and the subinterval with the worse point is rejected.

Step 3: The search is carried out in this manner, placing new trial point symmetrically with respect to the trial point remaining from the previous cycle in the subinterval $\bar{L}_j$, until all but one trial point are placed.

Step 4: The last trial point is placed, in the subinterval $\bar{L}_{n-1}$, according to dichotomous search plan, that is, new point is placed symmetrically with respect to old point at an arbitrarily small distance $\bar{\epsilon}$ from it. Again the subinterval with worse point is rejected and the subinterval $\bar{L}_n$, remaining after this trial, becomes the final region of uncertainty.

In Fibonacci search, the number of trial points is to be predefined. Larger the number of trials, smaller is the region of uncertainty. In order to accelerate the univariant search, in Laplace inversion problem, in first stage only three trials were prescribed. After every additional stage the number of trials was increased by one to maximum 12 trials in 10 stages. This results in a maximum possible final region of uncertainty of only 0.5 percent. This procedure, which is computationally more efficient, begins with coarse adjustment initially with progressively fine 'tuning' of the vector $X_2, X_3, \ldots, X_{n-1}$ at the final stages. Flow chart for Fibonacci search is given in Fig. (B-2).

ROSENBROCK METHOD:

This method incorporates a direct search strategy which gives acceleration in both direction and distance. The computational algorithm is illustrated for minimizing the following objective function

$$E = E(X_1, X_2, \ldots, X_n) \qquad \text{(B-8)}$$

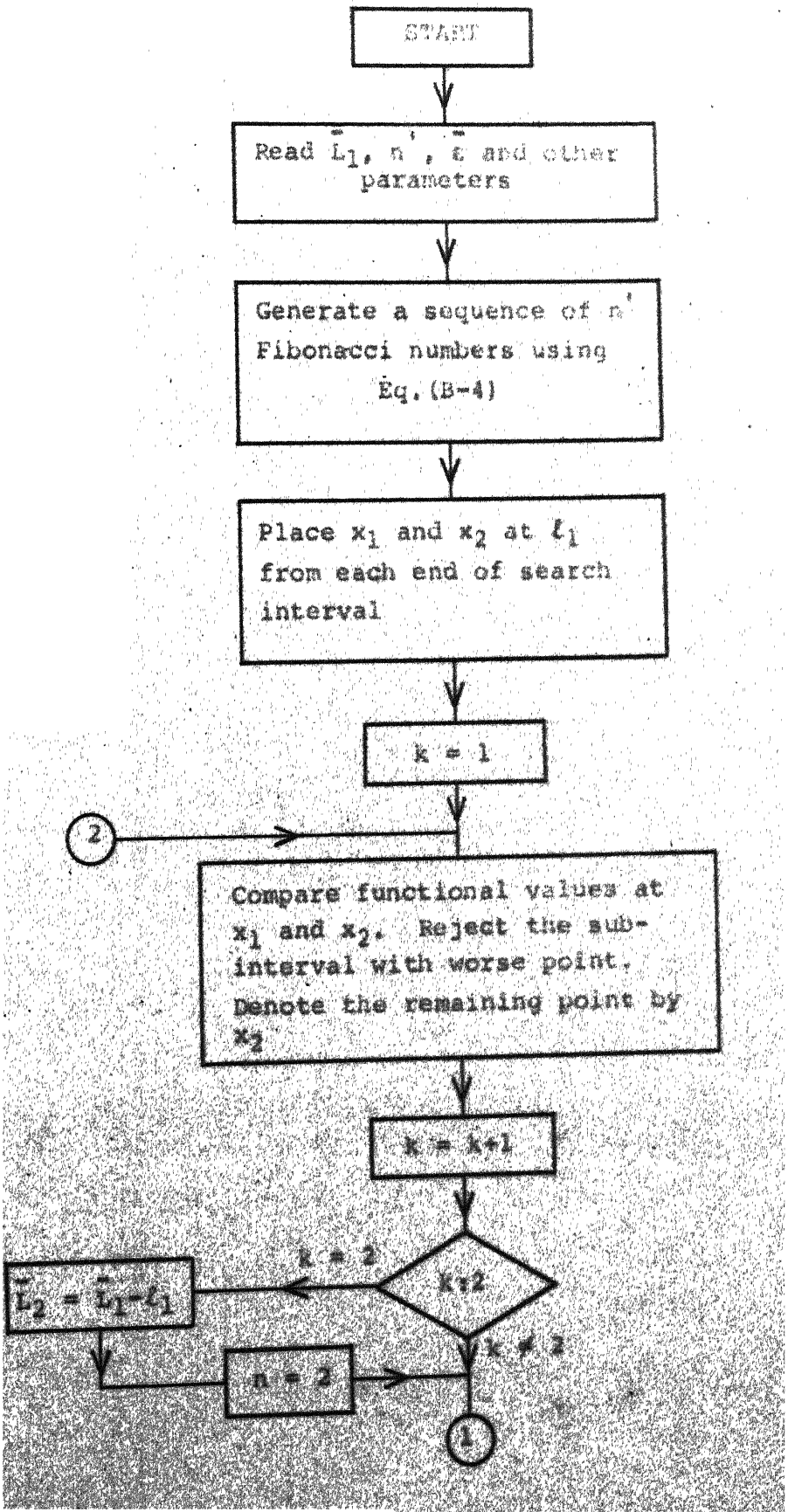

Fig. (B-2) Continued

Fig.(B-2) Continued

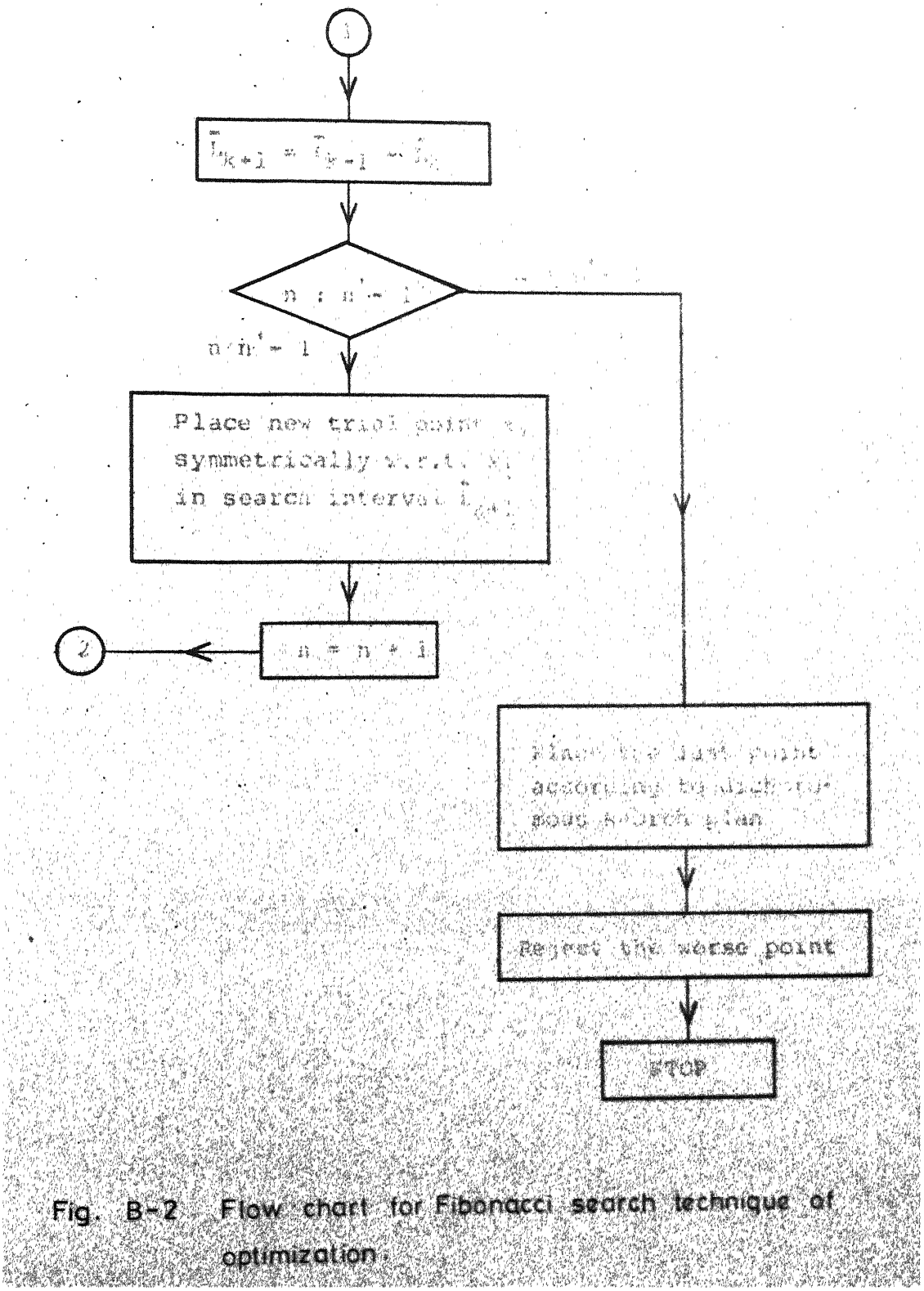

Fig. B-2 Flow chart for Fibonacci search technique of optimization.

Although, basically the original method was developed for unconstrained variables only, it has been modified to incorporate the constraints also. The modified method is summarized as follows[159]:

Step 1: Select a set of n mutually orthogonal directions coinciding initially with the coordinate directions (although not necessary). Let this set be

$$\begin{aligned} \xi_1^{(0)} &= (1,0,\ldots 0) \\ \xi_2^{(0)} &= (0,1,\ldots 0) \\ &\vdots \\ \xi_n^{(0)} &= (0,0,\ldots 1) \end{aligned} \qquad \text{(B-9)}$$

Let $e_1, e_2, \ldots, e_n$ be the set of step sizes and $(x_1^{(0)}, x_2^{(0)}, \ldots x_n^{(0)})$ be the starting point which satisfies all constraints.

Step 2: A new trial point $(x_1^{(0)} + e_1, x_2^{(0)}, \ldots, x_n^{(0)})$ is obtained and the value of the objective function at this point is compared with the functional value at the starting base point. If the trial is a success, i.e., the functional value at the new trial point is smaller than that at the base point, the step size is increased by a factor $\bar{\alpha}$ ($\bar{\alpha} > 1$). However, in the case of failure the step size is reduced by a factor $\bar{\beta}$ ($0 < \bar{\beta} < 1$) and the old base point is retained. This procedure is repeated until one success and one failure is recorded in $\xi_1^{(0)}$

direction[175]. Rosenbrock recommended $\alpha = 3$ and $\beta = 0.5$. If the functional values at the trial point and the base point are same, the trial is considered as a success. This ensures that there will be atleast one success and one failure because if there is no success, the reduction of step size will ultimately bring the trial point to original base point.

The search is now carried out along $\xi_2^{(0)}, \xi_3^{(0)}, \ldots, \xi_n^{(0)}$ directions sequentially using the same criterion of one success and one failure in each direction. The set of trials made with one set of directions and the subsequent change of these directions is called a stage.

Step 3: Once a stage of computations is over, a new set of orthogonal directions is generated by using Gram Schmidt orthogonalization method which is as follows.

Let $d_1, d_2, \ldots, d_n$ be the algebraic sum of all the successful steps in direction $\xi_1^{(j)}, \xi_2^{(j)}, \ldots, \xi_n^{(j)}$ and a set of n independent vector be defined as

$$\begin{aligned} u_1 &= d_1 \xi_1^{(j)} + d_2 \xi_2^{(j)} + \ldots + d_n \xi_n^{(j)} \\ u_2 &= d_2 \xi_2^{(j)} + \ldots + d_n \xi_n^{(j)} \\ u_n &= d_n \xi_n^{(j)} \end{aligned} \qquad \text{(B-10)}$$

Orthogonal unit vectors $\xi_1^{(j+1)}, \xi_2^{(j+1)}, \ldots, \xi_n^{(j+1)}$ are now obtained in the following manner

$$
\begin{aligned}
\bar{u}_1 &= u_1 \\
\xi_1^{(j+1)} &= \bar{u}_1/|\bar{u}_1| \\
\bar{u}_2 &= u_1 - u_2\, \xi_1^{(j+1)}\, \xi_1^{(j+1)} \\
\xi_2^{(j+1)} &= \bar{u}_2/|\bar{u}_2| \\
&\cdot \\
&\cdot \\
&\cdot \\
\bar{u}_n &= u_n - \sum_{i=1}^{n-1} u_n\, \xi_i^{(j+1)}\, \xi_i^{(j+1)} \qquad \text{(B-11)} \\
\xi_n^{(j+1)} &= \bar{u}_n/|\bar{u}_n|
\end{aligned}
$$

where $\bar{u}_1, \bar{u}_2, \ldots, \bar{u}_n$ refer to a set of orthogonal vectors which is normalized to give a set of orthonormal vectors

$$\xi_1^{(j+1)}, \xi_2^{(j+1)}, \ldots, \xi_n^{(j+1)} .$$

Step 4: The process of generating the set of orthonormal directions and then searching along these directions is continued until a predefined convergence criterion is satisfied.

If there are some constraints to be satisfied, at each trial point variables are tested for constraints. If a particular trial point violates the constraint, the trial is considered as a failure. A flow chart describing the computer program used in the present study is given in Fig. (B-3).

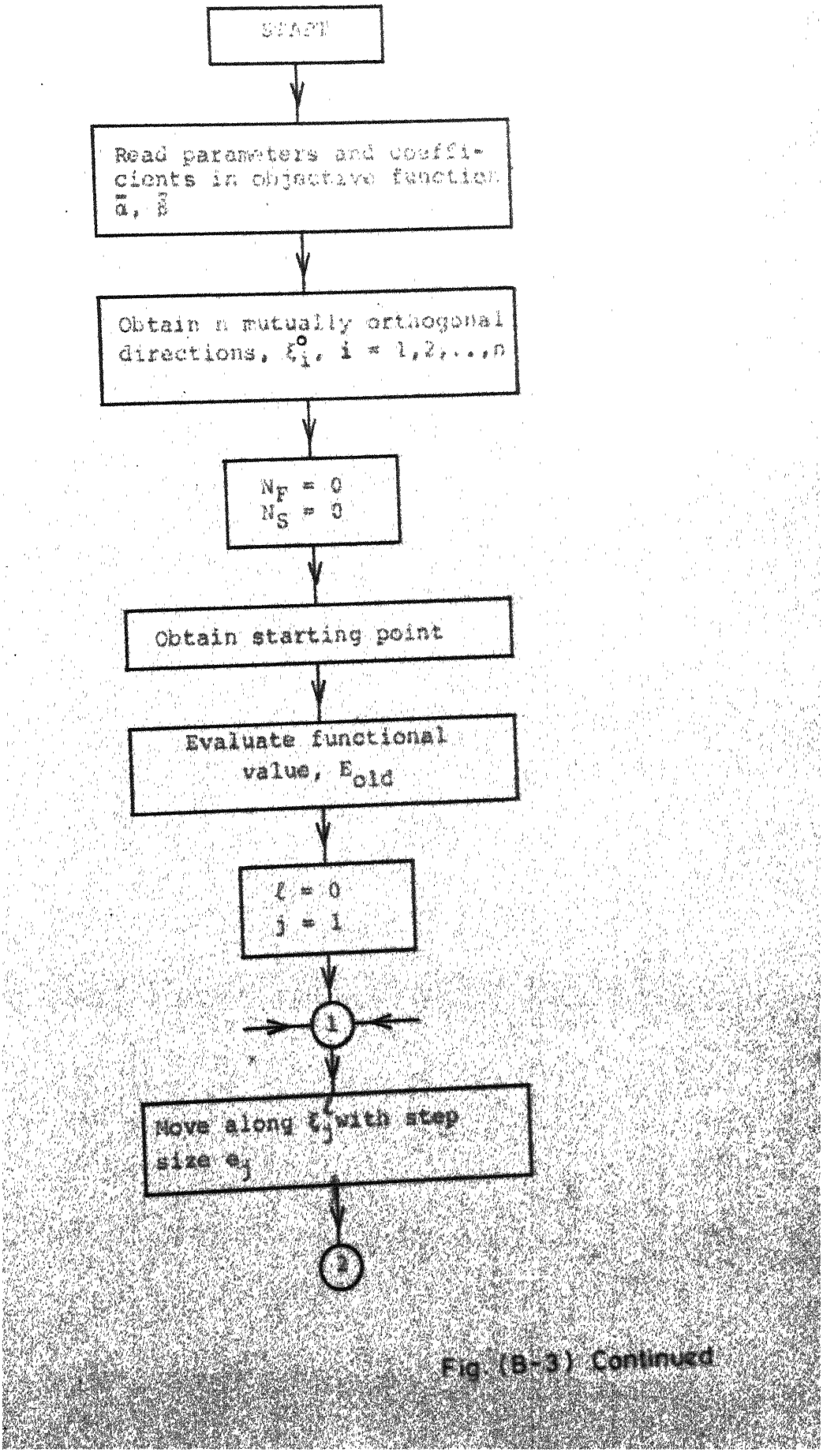

Fig. (B-3) Continued

Fig.(B-3) Continued

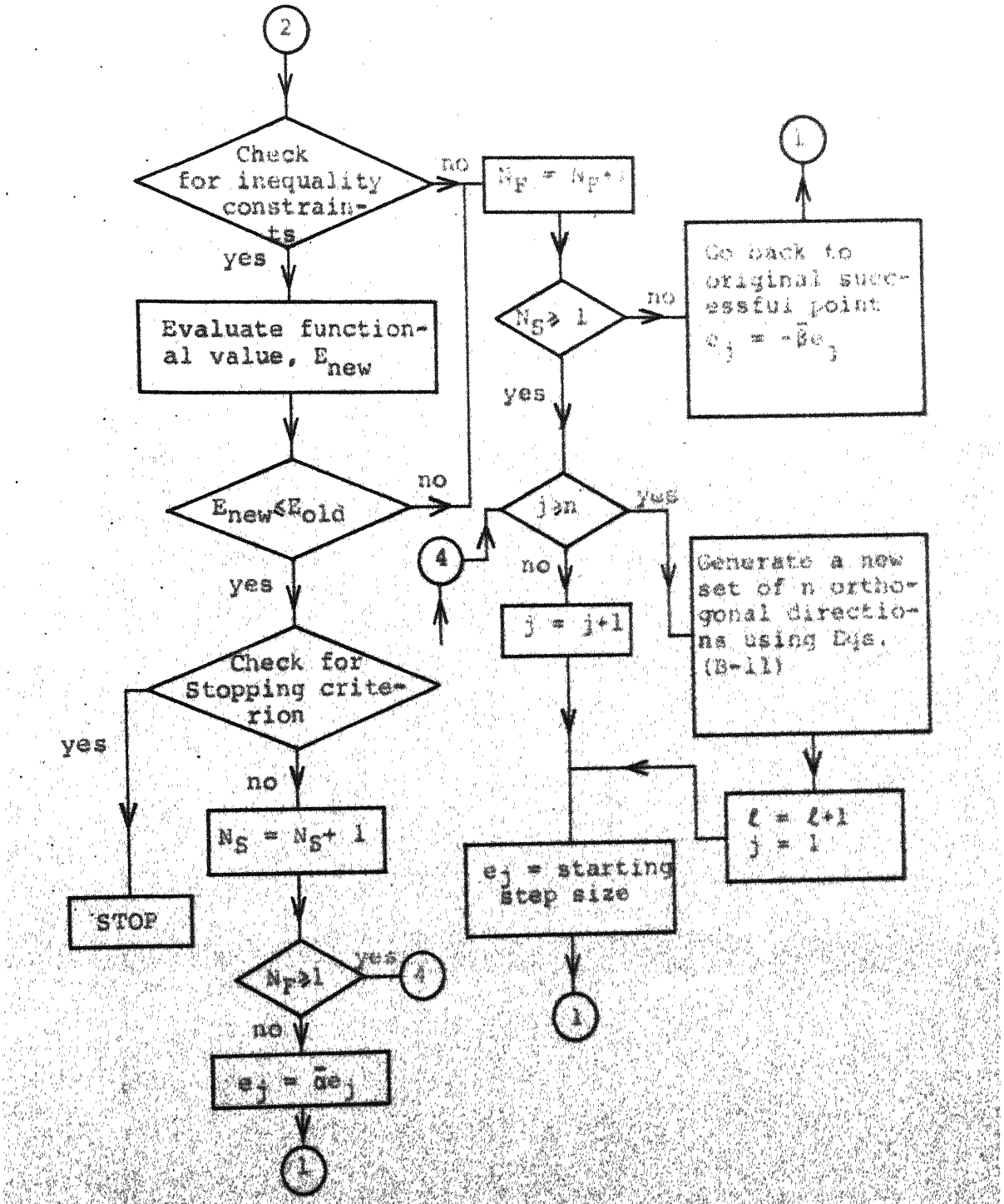

Fig. B-3 Flow chart for Rosenbrock's method of optimization.

COMPLEX METHOD:

The complex method of Box[176] differs from the well known Simplex method in two respects. Firstly, the complex is not regular and secondly, it can be used to solve implicitly and/or explicitly constrained optimization problems. The method is more useful if the variables are bounded, i.e., $X_{iL} \leq X_i \leq X_i^L$ where X_{iL} and X_i^L refer to Lower and upper limits of X_i, respectively. Even if the bounds of variables are not defined in the problem, some guess can always be made. The algorithm for complex method for an optimization problem with n variables is as follows:

Step 1: Generate a complex with k vertices where $k \geq n+1$. Box suggested that for n upto 5, $k = 2n$ but for $n > 5$, k can be less than 2n. To generate a complex, first a base point which satisfies all the constraints is obtained. The remaining of the k-1 vertices are obtained by using the following equation,

$$X_{ij} = X_{iL} + r'_{ij} (X_i^L - X_{iL}) \quad \begin{matrix} i = 1,2,\ldots,n \\ j = 1,2,\ldots,k-1 \end{matrix} \qquad (B-12)$$

where X_{ij} refers to i-th coordinate of j-th vertex and r'_{ij} is a random number usually between 0 to 1, but this range can be modified depending on the type of constraints on the variables.

Step 2: If any of the vertices, so determined, violates any of the constraints, move half way in towards the centroid of the already chosen vertices. The base point which satisfies all constraints ensures the generation of the complex whose vertices satisfy all constraints.

Step 3: Comparing the functional values, E_j, $j = 1,2,\ldots, k$, at the vertices find the worst point and its position in space. A new complex is formed by replacing the worst point by a point $\bar{\alpha}$ times as far from the centroid of the remaining points as the reflection of the worst point in the centroid. The coordinate of this new point, X_N, are

$$X_{iN} = \frac{\bar{\alpha}+1}{(k-1)} \left[\sum_{j=1}^{k} X_{ij} - X_{iR} \right] - \bar{\alpha} X_{iR}$$

$$i = 1,2,\ldots, n \qquad \text{(B-13)}$$

where X_{iR} is the i-th coordinate of the worst point to be rejected.

Step 4: If the new point is still a worst point or violates some constraint, a new trial point is obtained by moving half way towards the centroid.

Step 5: This cycle is repeated until a prespecified stopping criterion is satisfied.

To improve the reliability of the method some modifications have been proposed by Umeda and Ichikawa[163], and Guin[162] and are discussed below:

1. While evaluating the centroid of the remaining points the functional values at vertices of the complex should also be given weightage. Thus, the modified coordinates of the centroid are

$$X_{iC} = \frac{\sum_{\substack{j=1 \\ \neq R}}^{k} (\Delta E_j)^{m'} X_{ij}}{\sum_{\substack{j=1 \\ \neq R}}^{k} (\Delta E_j)^{m'}}, \quad i = 1,2,\ldots, n \qquad \text{(B-14)}$$

where m' is a positive number, and

$$\Delta E_j = \frac{E_{max} - E_j}{E_{max} - E_{min}} \quad \text{for minimization problem}$$

$$= \frac{E_j - E_{min}}{E_{max} - E_{min}} \quad \text{for maximization problem} \qquad \text{(B-15)}$$

where E_{max} and E_{min} are respectively, maximum and minimum functional values. Now the new trial point becomes

$$X_{iN} = (1+\bar{\alpha}) \frac{\sum_{\substack{j=1 \\ \neq R}}^{k} (\Delta E_j)^{m'} X_{ij}}{\sum_{\substack{j=1 \\ \neq R}}^{k} (\Delta E_j)^{m'}} - \bar{\alpha} X_{iR}; \quad i = 1,2,\ldots,n \qquad \text{(B-16)}$$

2. Above modification should be used as long as

$$[(E_{max} - E_{min})/E_{max}] > 0.5 \qquad \text{(B-17)}$$

When this inequality does not hold, original complex method should be applied by taking $m' = 0$.

3. In the case of violation of inequality constraints, instead of moving half way towards the centroid of the remaining points a more general way of moving is defined as,

$$X_{iN'} = \bar{\alpha}' X_{iN} + (1-\bar{\alpha}') X_{iR}; \; i = 1,2,\ldots,n \qquad (B-18)$$

where $\bar{\alpha}'$, the reflection factor, is obtained in such a way that the functional value is optimum with respect to X_{iN}.

4. The method may fail if all points lying on the line joining the worst point and the centroid of the remaining points are worse than the original point because eventually the projected point will coincide with the original point. To avoid this situation Guin suggested that if $\bar{\alpha}$ falls below a certain value (Say, $< 10^{-5}$) without obtaining a better functional value this point should be replaced by its original unprojected position and the second worst point be rejected.

5. In the case of non-convex curves, centroid itself may violate the constraints. If this happens at some stage, all but the best point of the complex are discarded and a new complex is generated according to

$$X_{ij} = X_{ib} + r'_{ij} (X_{iC} - X_{ib}) \quad \begin{matrix} i = 1,2,\ldots,n \\ j = 1,2,\ldots,k-1 \end{matrix} \qquad (B-19)$$

where X_{iC} and X_{ib} refer to i-th coordinates of the unfeasible centroid and the best vertex in the old complex.

Generation of the Initial Base Point:

Although, a few methods are available in literature to evaluate the initial base point, it was found that the nature of constraints in the present study was such that equation (B-11) itself could be used to generate the base point. A set of n random numbers was generated and initial base point was obtained by using this equation. If this point violated some of the constraints, a new set of random numbers was generated and the procedure was repeated until a point, which satisfied all the constraints, was obtained. Although this method of obtaining the base point is not the most efficient, it is conceptually very simple and easy to apply.

A flow chart of the complex method used in the present study is given in Fig. (B-4).

RANDOM SEARCH:

One of the main drawbacks of Rosenbrock and complex methods is that the solution obtained may not be the global optimum. Even large number of initial guesses donot guarantee the global solution. This problem becomes even more acute with increasing number of variables. However, this problem is taken care of to a great extent by using a random search technique. Basically, the method consists of specifying each of the variables, to be investigated, in a random manner within the region of interest. Each variable is assumed to be

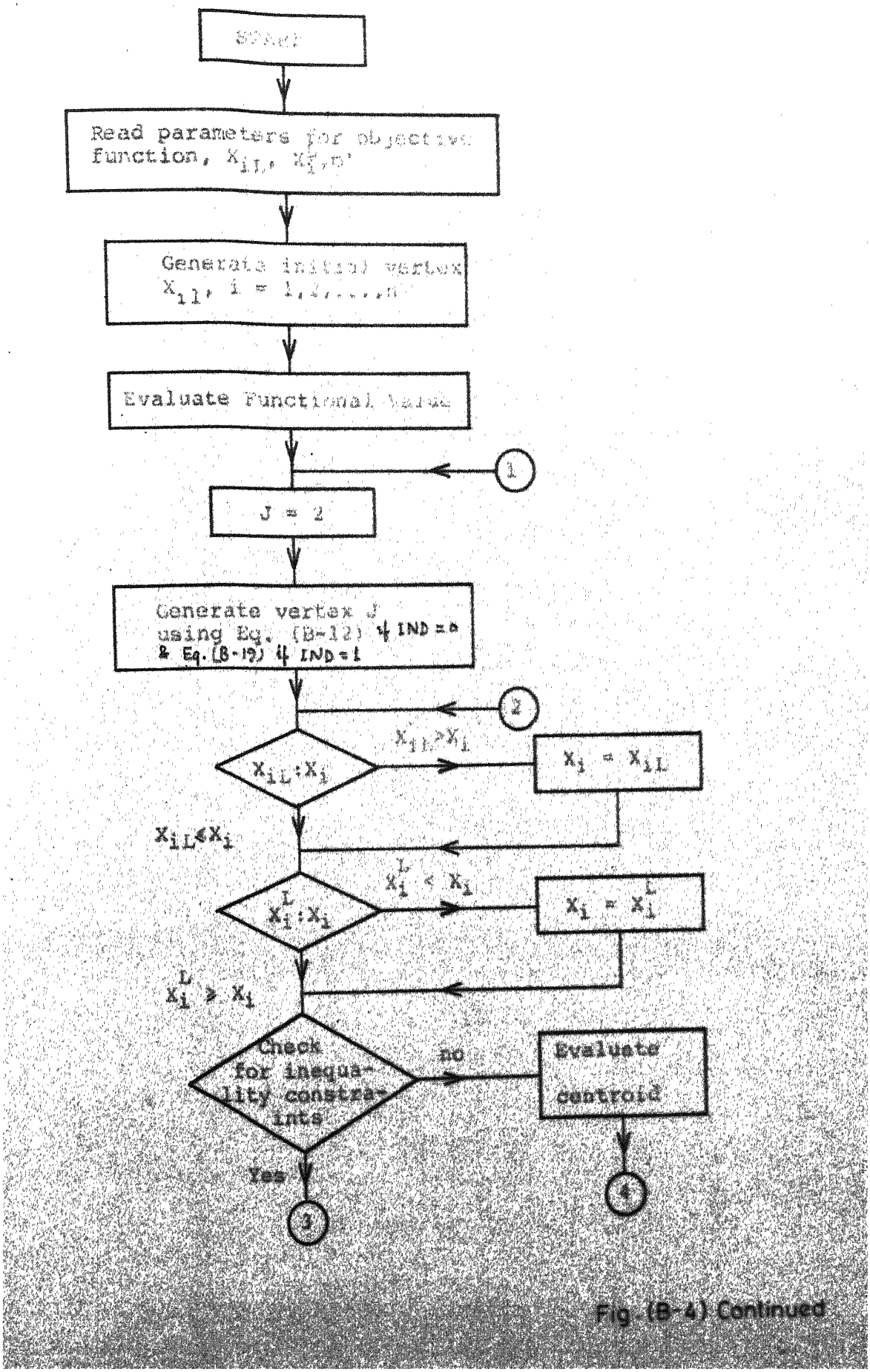

Fig. (B-4) Continued

Fig.(B-4) Continued

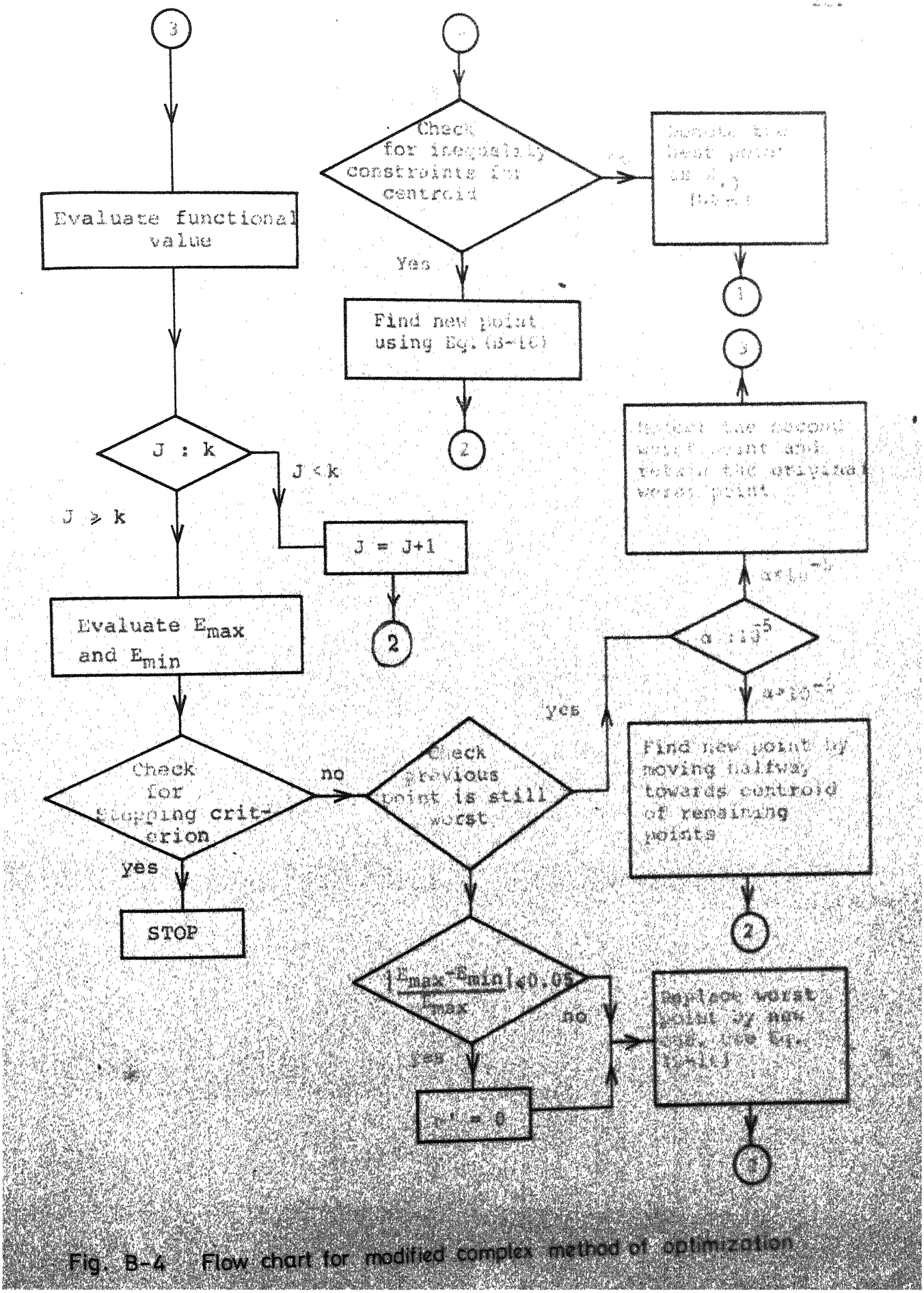

Fig. B-4 Flow chart for modified complex method of optimization

independent of others. Some of other attractive features of this technique are: (1) ease in computer programming; (2) freedom from mathematical restriction on functional form, and (3) convergence in noisy environment. Details of these features and various random search schemes are extensively documented in literature[160,164,177-183]. The steps involved in the algorithm used in the present study are listed below[160]. The problem considered here is same as discussed above, namely

Minimize,

$$E = E(X_1, X_2, \ldots, X_n) \qquad \text{(B-20)}$$

Subject to constraint

$$X_{iL} \leq X_i \leq X_i^L \qquad i = 1,2,\ldots, n \qquad \text{(B-21)}$$

Step 1: Denote the initial base point which satisfies all constraints by $X_{i,old}$ $(i = 1,2,\ldots,n)$ and the functional value at this point by E_{old}.

Step 2: Generate a set of n random numbers, r_i' $(i = 1,2,\ldots,n)$, by using some suitable subroutine and then evaluate a new trial point by using following equation.

$$X_{i,new} = X_{i,old} + \Delta X_i, \quad i = 1,2,\ldots,n \qquad \text{(B-22)}$$

where

$$\Delta X_i = \frac{r_i'(X_i^L - X_{iL})}{\bar{w}'\left(\sum_{i=1}^{n} r_i^2\right)^{1/2}} \qquad \text{(B-23)}$$

where $\bar{w}'$ is a weighting factor.

Step 3: Test the new trial point for constraints. If all constraints are satisfied, function E_{new}, corresponding to new trial point, is obtained and is compared with E_{old}. If $E_{new} < E_{old}$, original E_{old} and $X_{i,old}$ are discarded and E_{new} and $X_{i,new}$ are stored and, respectively, become E_{old} and $X_{i,old}$. A new trial point is obtained by using equation (B-22) using the same value of ΔX_i as in the previous stage.

Step 4: The whole procedure is repeated, if $E_{new} > E_{old}$, or any of the constraints, other than those defined by (B-21), is violated. The old trial point is retained and the new trial point is discarded and a new trial point is obtained by using a new set of random numbers and equations (B-22) and (B-23). However, if constraints given by equation (B-21) are violated, X_i is replaced by corresponding limiting value, i.e., if $X_i > X_i^L$, it is replaced by X_i^L and if $X_i < X_{iL}$, it is replaced by X_{iL}.

Step 5: The search is continued until a prespecified convergence criterion is satisfied.

Detailed computational procedure is given in flow chart in Fig. (B-5). The number I_2 in the flow diagram refers to the maximum number of successful trials allowed with same ΔX_i. This is used to prevent situation such as only a very small improvement is made on E in each successful trial. I_1 is the number of successive unsuccessful trials after which computation

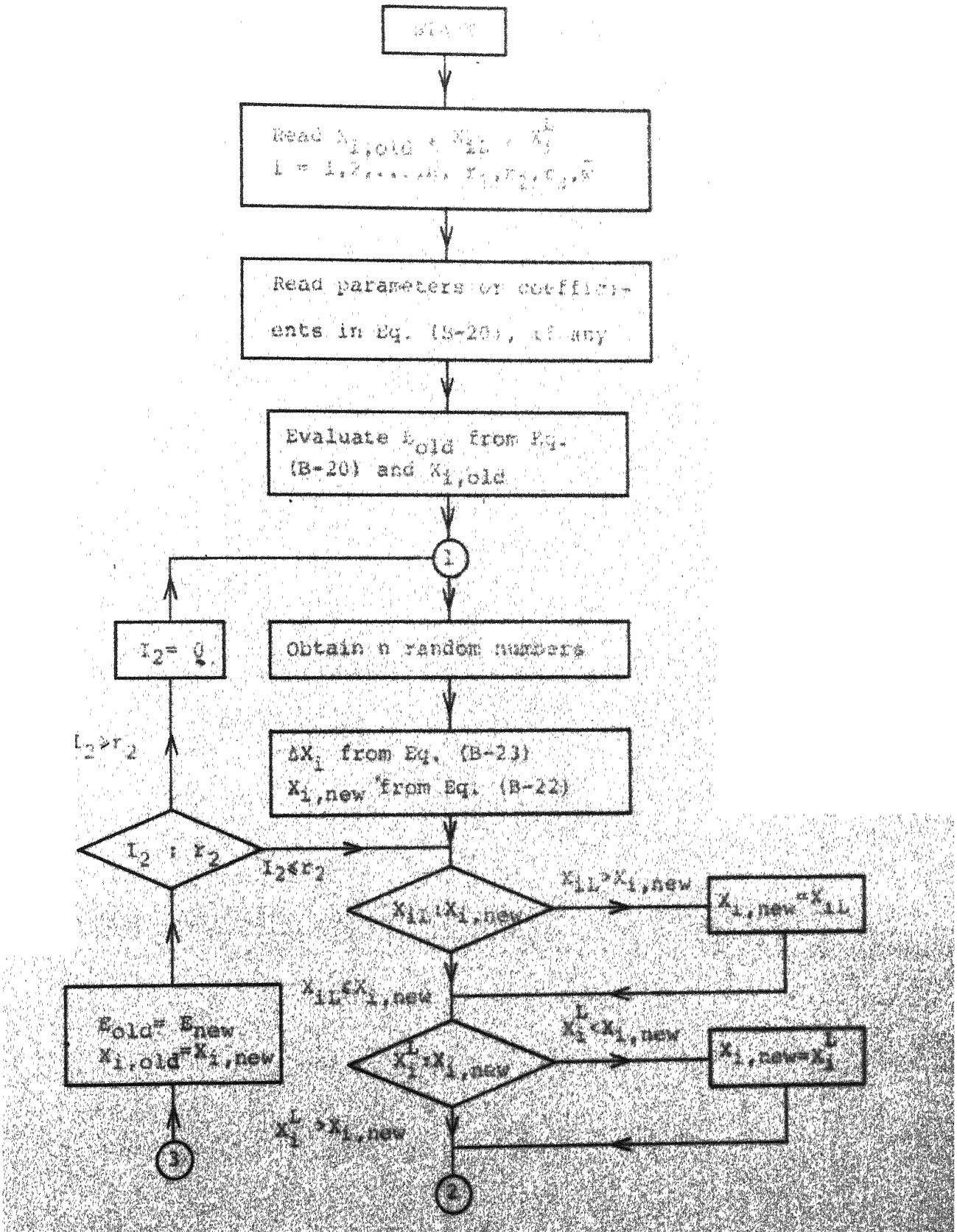

Fig (B-5) Continued

Fig. (B-5) Continued

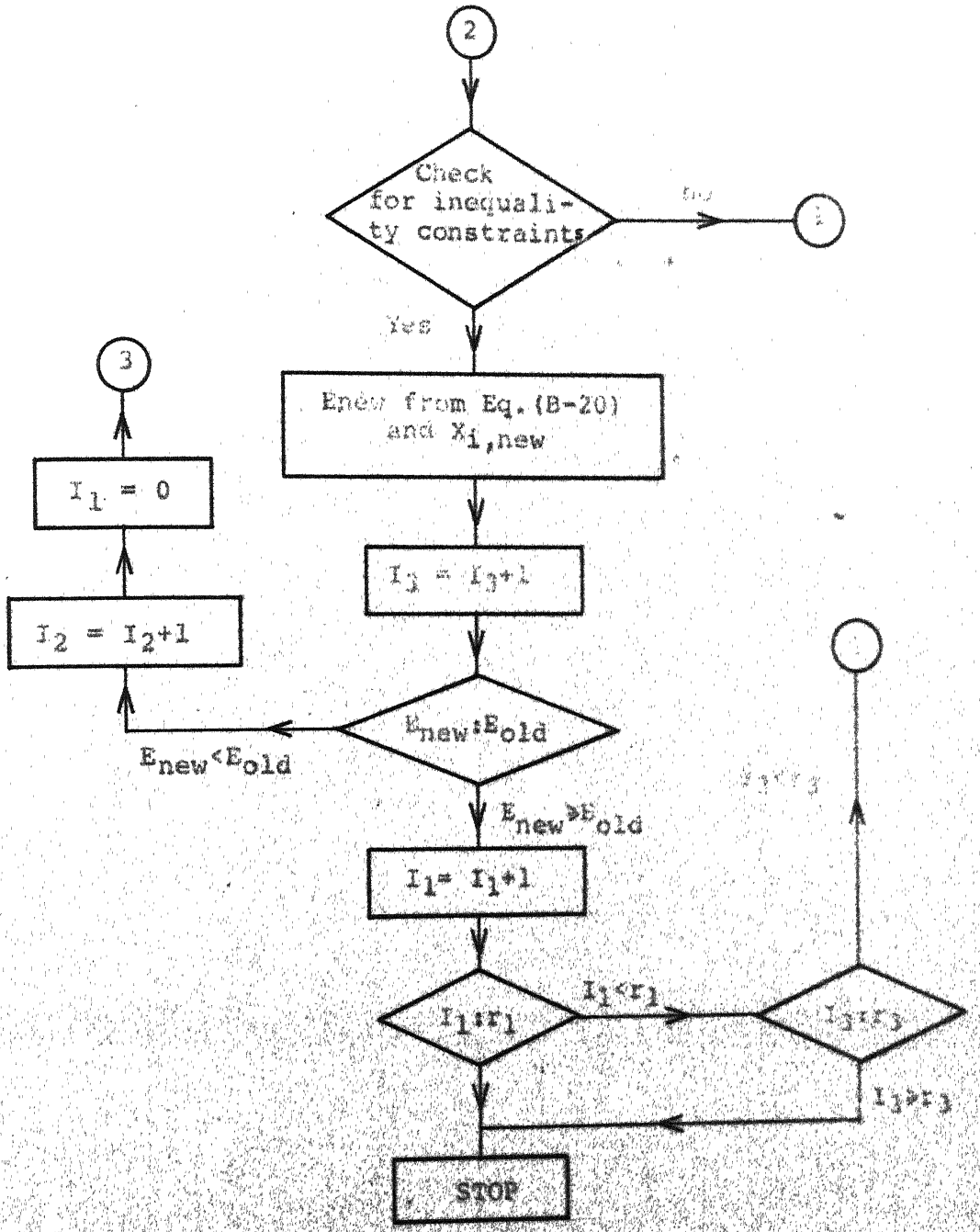

Fig. B-5 Flow chart for random search technique of optimization

is stopped. The assumption here is that I_1 successive unsuccessful trials mean that E has attained the optimum value. The number I_3 defines the total number of trials that are allowed whether they are successful or not.

APPENDIX C

MASS BALANCE EQUATION IN CASE OF A BATTERY OF FLOTATION CELLS

Consider a battery of n_c identical flotation cells arranged in series in such a way that tailings from one cell becomes feed for the next cell in series whereas concentrate from each cell is collected in parallel. A battery of four cells is shown in Fig. 8.6. Consider cell 1 in the battery using the same notations as in Chapter 8, the mass flow rate of j-th species in tailings and concentrate streams, respectively, are

$$M_{T_1}(Ka) = M_F(Ka) \left[\frac{1}{1+Ka\ \bar{t}} \right] \qquad (C-1)$$

and

$$M_{C_1}(Ka) = M_F(Ka) \left[\frac{Ka\ \bar{t}}{1+Ka\ \bar{t}} \right] \qquad (C-2)$$

It should be noted here that subscript j used in Chapter 8 to denote j-th species has been removed for simplicity in notation but with the understanding that these are applicable for any particular species, say j-th. Now for cell 2 in the battery M_{T_1} becomes the mass flow rate in feed. Therefore, tailings and concentrate flow rates for cell 2 are, respectively,

$$M_{T2}(Ka) = M_{T1}(Ka) \left[\frac{1}{1+Ka\ \bar{t}} \right] \qquad (C-3)$$

and

$$M_{C2}(Ka) = M_{T1}(Ka) \left[\frac{Ka\ \bar{t}}{1+Ka\ \bar{t}} \right] \qquad (C-4)$$

Substitution of equations (C-1) in (C-3) and (C-4) results in

$$M_{T2}(Ka) = M_F(Ka) \left[\frac{1}{1+Ka\ \bar{t}} \right]^2 \qquad (C-5)$$

and

$$M_{C2}(Ka) = M_F(Ka) \left[\frac{Ka\ \bar{t}}{1+Ka\ \bar{t}} \right] \left[\frac{1}{1+Ka\ \bar{t}} \right] \qquad (C-6)$$

This argument can be extended to n_c-th cell to give

$$M_{Tn_c}(Ka) = M_F(Ka) \left[\frac{1}{1+Ka\ \bar{t}} \right]^{n_c} \qquad (C-7)$$

and

$$M_{Cn_c}(Ka) = M_F(Ka) \left[\frac{Ka\ \bar{t}}{1+Ka\ \bar{t}} \right] \left[\frac{1}{1+Ka\ \bar{t}} \right]^{n_c-1} \qquad (C-8)$$

It should be recognized that tailings flow rate for the battery as a whole ($M_T(Ka)$) is same as that for n_c-th cell, whereas the concentrate flow rate ($M_C(Ka)$) is the summation of concentrate flow rate of individual cells in battery. Thus,

$$M_T(Ka) = M_{Tn_c}(Ka)$$

$$= M_F(Ka) \left[\frac{1}{1+Ka\ \bar{t}} \right]^{n_c} \qquad (C-9)$$

and

$$M_C(Ka) = \sum_{i=1}^{n_c} M_{Ci}(Ka)$$

$$= \sum_{i=1}^{n_c} M_F(Ka) \left[\frac{Ka\ \bar{t}}{1+Ka\ \bar{t}} \right] \left[\frac{1}{1+Ka\ \bar{t}} \right]^{i-1}$$

$$= M_F(Ka) \left[1-\left(\frac{1}{1+Ka\ \bar{t}} \right)^{n_i}\right] \qquad (C-10)$$

Thus, if we redefine α_{ji} in equation (8.4) as

$$\alpha = \left(\frac{1}{1+Ka\ \bar{t}} \right)^{n_c} \qquad (C-11)$$

substitution of equation (C-11) in (C-9) and (C-10) leads to

$$M_T(Ka) = M_F(Ka)\ \alpha \qquad (C-12)$$

and

$$M_C(Ka) = M_T(Ka)\ (1-\alpha) \qquad (C-13)$$

Thus, the basic form of equation (C-12) and (C-13) is same as of equations for a single cell (equations (8.5) and (8.6)).